Hadronic Electroweak Processes in a Finite Volume

Dissertation
zur
Erlangung des Doktorgrades (Dr. rer. nat.)
der
Mathematisch-Naturwissenschaftlichen Fakultät
der
Rheinischen Friedrich-Wilhelms-Universität Bonn

von
Andria Agadjanov
aus
Tiflis, Georgien

Bonn, 2017

Dieser Forschungsbericht wurde als Dissertation von der Mathematisch-Naturwissenschaftlichen Fakultät der Universität Bonn angenommen und ist auf dem Hochschulschriftenserver der ULB Bonn `http://hss.ulb.uni-bonn.de/diss_online` elektronisch publiziert.

1. Gutachter:	PD. Dr. Akaki Rusetsky
2. Gutachter:	Prof. Dr. Ulf-G. Meißner
Tag der Promotion:	07.11.2017
Erscheinungsjahr:	2017

Acknowledgements

First of all, I would like to thank my supervisor PD. Dr. Akaki Rusetsky. Over the last few years, our scientific collaboration has been very fruitful, and it will continue in the future. I am grateful to Prof. Dr. Ulf-G. Meißner for sharing his vast expertise and knowledge in the field. Also, I thank Prof. Dr. Anzor Khelashvili for giving many important insights into the elementary particle physics.

Further, I thank Prof. Dr. Michael Döring, Dr. Jambul Gegelia, Prof Dr. Jose Antonio Oller, and other colleagues in the Institute for useful discussions. I acknowledge the financial support from German Research Foundation, Bonn-Cologne Graduate School, Volkswagen Foundation and Shota Rustaveli National Science Foundation. Their generosity allowed me to attended many interesting conferences and schools around the world. I am also grateful to the Dr. Klaus Erkelenz Foundation and its founder, Dr. Gabriele Erkelenz.

Finally, I express my gratitude to my parents and brother for their help and support.

Abstract

In the present cumulative thesis, we study a number of hadronic electroweak processes in a finite volume. Our work is motivated by the ongoing and future lattice simulations of the strong interaction theory called quantum chromodynamics. According to the available computational resources, the numerical calculations are necessarily performed on lattices with a finite spatial extension.

The first part of the thesis is based on the finite volume formalism which is a standard method to investigate the processes with the final state interactions, and in particular, the elastic hadron resonances, on the lattice. Throughout the work, we systematically apply the non-relativistic effective field theory. The great merit of this approach is that it encodes the low-energy dynamics directly in terms of the effective range expansion parameters. After a brief introduction into the subject in Chapter 1, we formulate a framework for the extraction of the $\Delta N\gamma^*$ (Chapter 2) as well as the $B \to K^*$ (Chapter 3) transition form factors from lattice data. Both processes are of substantial phenomenological interest, including the search for physics beyond the Standard Model. Moreover, we provide a proper field-theoretical definition of the resonance matrix elements, and advocate it in comparison to the one based on the infinitely narrow width approximation.

In the second part, which includes Chapter 4, we consider certain aspects of the doubly virtual nucleon Compton scattering. The main objective of the work is to answer the question whether there is, in the Regge language, a so-called fixed pole in the process. To answer this question, the unknown subtraction function, which enters one of the dispersion relations for the invariant amplitudes, has to be determined. The external field method provides a feasible approach to tackle this problem on the lattice. Considering the nucleon in a periodic magnetic field, we derive a simple relation for the ground state energy shift up to a second order in the field strength. The obtained result encodes the value of the subtraction function at nonzero photon virtuality. The knowledge of the latter is also important to constrain the two-photon exchange contribution to the Lamb shift in a muonic hydrogen.

Contents

CHAPTER 1

Hadronic Electroweak Processes in a Finite Volume

1.1 Introduction

Nowadays, the Standard Model (SM) is regarded as an extremely successful theory of the elementary particles (leptons, quarks, gauge bosons and Higgs particle), which unites the electromagnetic, weak and strong interactions in a mathematically elegant way [1–6]. The recent LHC discovery of the last missing building block, the Higgs boson, is a definite triumph of the theory [7, 8].

The SM is a quantum gauge field theory, which has the invariance property under a continuous group of local transformations. The symmetry group has a non-abelian structure:

$$SU(2) \times U(1) \times SU(3). \tag{1.1}$$

Here, the $SU(2) \times U(1)$ part (the Weinberg-Salam model) is responsible for the electromagnetic and weak interactions, mediated by the photons (γ) and weak bosons (W^+, W^-, Z), respectively (see Fig. 1.1). The remaining gauge group $SU(3)$ underlies the modern theory of the strong interaction, called quantum chromodynamics (QCD) [9]. It describes the interaction between quarks and gluons, both of which carry in addition three different color charges. The fact that one should have three colors guarantees the absence of the chiral anomalies in the SM and thus its renormalizability [10].

The SM is experimentally confirmed with high precision. Nevertheless, there are currently several experimental tensions, which are problematic to explain within the SM. These deviations are seen in the following cases:

- Proton radius puzzle. The proton radius determined from the precise measurement of the Lamb shift in the muonic hydrogen atom has significantly smaller values than the ones obtained from the electron-proton scattering and hydrogen spectroscopy [11, 12]. At the same time, a proper dispersive analysis of ep data gives a small radius [13, 14].
- Anomalous magnetic moment of muon. The measurement of muon's $g-2$ at Brookhaven leads to the discrepancy between experiment and the theoretical prediction [15, 16].
- Anomalies in rare B meson decays. The LHCb, Belle and BaBar collaborations have observed interesting patterns of deviations in several decay modes, in particular, in $B \to K^* \mu^+ \mu^-$ [17–20].

These experimental results have triggered a lot of activity on the theoretical side. The proposed explanations fall into one of two categories: physics beyond the SM (BSM) or the strong sector of SM, described

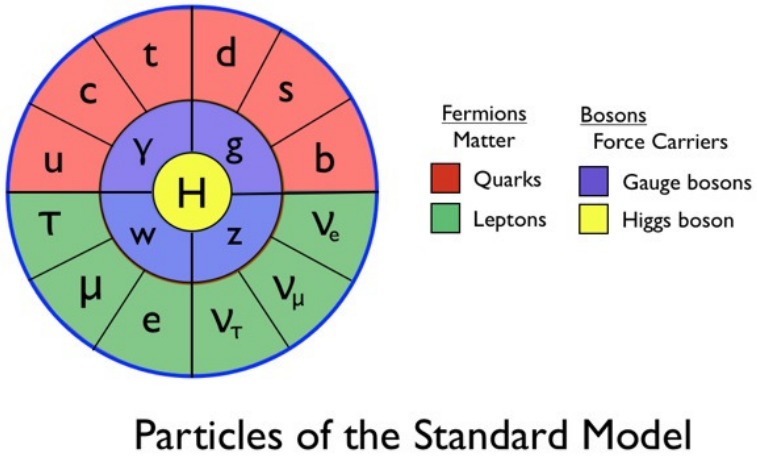

Figure 1.1: Elementary particles of the Standard Model [21].

by QCD. It is important to keep in mind that all measured observables are sensitive to the hadronic uncertainties. The latter arise due to the non-perturbative contributions of QCD. In order to quantify these uncertainties, the strong sector of the SM should be better understood. In particular, Chapter 3 deals with the form factors which enter the analysis of the experimental data on the $B \to K^* \mu^+ \mu^-$ process. Also, the work presented in Chapter 4 is related to the study of the two-photon exchange contribution to the Lamb shift.

1.2 Strong interaction

Historically, it took many years until it was finally realized that the strong interaction can be described by a Yang-Mills theory [22]. The turning point was the discovery of asymptotic freedom in this class of non-abelian gauge theories by Gross, Wilczek and Politzer [23, 24]. The existence of the quantum field theories, in which the coupling constant becomes small at high energies ($\sim 100 - 1000$ GeV), opened a possibility to perform the systematic calculations of different observables in pertubation theory. Moreover, QCD exhibits the so-called confinement property at the hadronic scale (~ 1 GeV), although it cannot be analytically proven. Nevertheless, this property qualitatively explains, why the quarks cannot be directly observed, but rather form color singlet states (proton, neutron, pion, etc.) . At the same time, perturbation theory breaks down at this energy scale, since the coupling constant becomes large. In order to obtain the meaningful results, alternative methods should be applied, as discussed below.

The quarks were first introduced in an attempt to classify the plethora of observed hadrons. The developed scheme, called Eightfold Way (or the quark model), provided the classification of the strongly interacting particles according to the representations of the vectorial $SU(3)_V$ group [25]. From the modern perspective, this global (flavor) symmetry is encoded in the mathematical structure of QCD. This symmetry is, however, approximate, since the masses of the light quarks u, d, s are not equal.

The Lagrangian of QCD has the so-called chiral symmetry in the limit of vanishing quark masses $m_q \to 0$. It is associated with the independent rotations of the left (L)- and right (R)-chiral components of the quark fields in the flavor space. This symmetry, is, however, *spontaneously* broken due to the low-energy QCD dynamics (the formation of the quark condensate). In other words, it ceases to be a symmetry of the QCD vacuum. The relevant scale $\Lambda_\chi \approx 1$ GeV distinguishes the light quarks $m_f < \Lambda_\chi$

(u, d, s) and heavy quarks $m_f > \Lambda_\chi$ (c, b, t). Retaining only the light quarks, the QCD Lagrangian is classicaly invariant under flavor symmetry group transformations

$$SU(N_f)_L \times SU(N_f)_R \times U(1)_V \times U(1)_A\,, \tag{1.2}$$

where $N_f = 2, 3$. Here, the vector symmetry $U(1)_V$ corresponds to the baryon number conservation (B=0 for mesons and B=1 for baryons). It is an exact symmetry of QCD. In contrast, the axial symmetry $U(1)_A$ is violated in the quantum theory, due to anomalies [26–28]. Further, the symmetry breaking pattern reads

$$SU(N_f)_L \times SU(N_f)_R \longrightarrow SU(N_f)_V. \tag{1.3}$$

i.e. the remaining flavor group coincides with the one in the quark model. The result Eq. (1.3) further implies the existence of the octet of the massless modes (the Goldstone bosons): the π's, K's and η [29, 30]. These mesons, however, acquire masses due to the *explicit* breaking of chiral symmetry by the mass term in the QCD Lagrangian. Thus it is seen that the quark model is naturally incorporated in QCD.

As is well known, perturbative calculations in quantum field theories lead to ultraviolet divergences - the loop integrals, corresponding to the Feynman diagrams, become infinite. The infinities occur due to the ultraviolet behaviour of the integrands (large momentum, short distances). The procedure to get rid of (subtract) them is called renormalization. At the first step, one introduces some regularization which makes the integrals finite. At present, dimensional regularization [31] is widely used since it preserves the underlying symmetries of the theory. In case of the renormalizable theories, all possible divergences are eliminated by the redefinition of the bare parameters in the Lagrangian. The subtraction is performed at some scale μ, so that the renormalized parameters (the quark masses and strong coupling constant) become dependent on this scale and on the renormalization scheme (in QCD, it is usually the $\overline{\text{MS}}$ scheme). Moreover, the requirement that the physical quantities (e.g., the cross sections) have to be independent of the scale μ, leads to the notion of the running parameters. The dependence of the parameters on μ is not arbitrary, but it is governed by the renormalization group equations. In particular, this means that the value of the renormalized QCD coupling constant $g = g(\mu)$ (or equivalently $\alpha_s = \frac{g^2}{4\pi}$) depends on the characteristic energy scale in a given process (see Fig. 1.2). Applying the Feynman rules for QCD [32, 33], one obtains the famous one-loop result:

$$\mu\frac{d\alpha_s}{d\mu} = -b_0\alpha_s^2 + \ldots, \quad b_0 = \frac{33 - 2N_f}{12\pi}, \tag{1.4}$$

where the parameter b_0 is positive for $N_f < 16$. The crucial minus sign in this formula explains, why the coupling becomes small at high energies. This fact also justifies the success of the parton model (the predecessor of QCD) [34, 35].

1.3 Lattice gauge theory

The other distinct feature of QCD is confinement. In this case, the perturbation theory is not reliable any more and non-perturbative methods are thus required. At present, the lattice regularized QCD (lattice QCD, LQCD) is the only approach, which allows one to investigate the low-energy properties of strong interaction directly from the underlying theory (QCD). It was formulated by K. Wilson in an attempt to solve the confinement problem [39]. Moreover, he considered the limit $g \to \infty$ in pure Yang-Mills theory, and showed analytically that the confinement manifests itself as a linearly rising potential between heavy

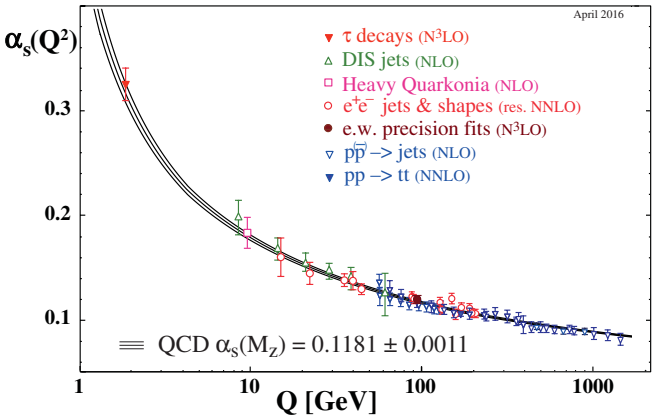

Figure 1.2: Summary of measurements of the strong coupling constant α_s as a function of the energy scale Q (a momentum transfer in a given process) [36].

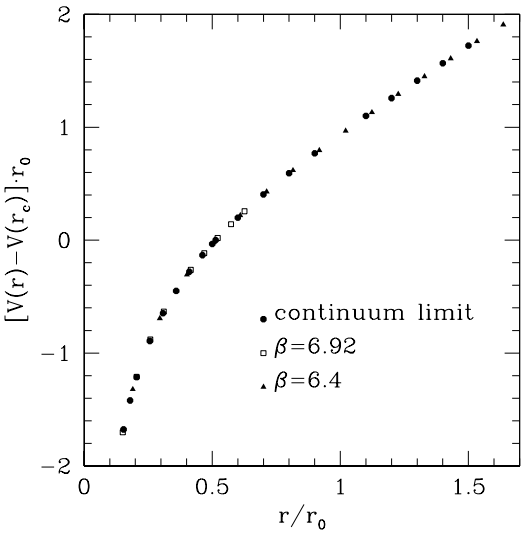

Figure 1.3: Lattice calculation of the heavy quark potential in SU(3) Yang-Mills theory [37]. The parameter $\beta = 6/g^2$ and $r_c \approx 0.51 r_0$, where $r_0 \approx 0.5$ fm is the so-called Sommer scale [38].

quark and anti-quark. Some years later, M. Creutz performed the first numerical study of the confinement in pure SU(2) gauge theory[40]. Since this pioneering work, LQCD has become a vast and important field of research. The results of the lattice calculations and their averages are reviewed by the "Flavour Lattice Averaging Group" (FLAG) [41]. As an example, Fig. 1.3 shows the lattice measurement of a static potential in pure SU(3) Yang-Mills theory [37, 42].

LQCD is based on the path integral formulation of the theory in the discretized Euclidean spacetime. At the first step, one writes down the lattice version of the gauge and fermion actions. In the continuum, they read

$$S_g = \frac{1}{4g^2}\int d^4x \mathrm{Tr}[F_{\mu\nu}^2], \quad F_{\mu\nu} = \partial_\mu A_\nu - \partial_\nu A_\mu + i[A_\mu, A_\nu], \tag{1.5}$$

$$S_f = \sum_f \int d^4x \bar{q}_f [D_\mu \gamma_\mu + m_f] q_f, \quad D_\mu = \partial_\mu + A_\mu, \tag{1.6}$$

where $q_f(x)$ are the quark fields and the gluon field $A_\mu(x)$ takes the values in the $su(3)$ Lie algebra. Further, the Euclidean spacetime is replaced by a finite grid, as shown in Fig. 1.4. The shortest distance between the neighbouring points, called a lattice spacing, provides a natural ultraviolet cutoff $\Lambda \sim 1/a$, so that the theory becomes well defined and finite. Accordingly, the derivatives in Eq. (1.5) and (1.6) are replaced by finite differences, while a sum over all lattice points is taken instead of the integration (the Riemann sum).

In order to preserve the gauge invariance on the lattice, one introduces the gluon field $U_\mu(x)$ as an element of the $SU(3)$ group. The field $U_\mu(x)$ can be considered geometrically as a gauge link connecting the points x and $x + a\hat{\mu}$, where a is the lattice spacing and $\hat{\mu}$ is a unit vector in the μ-direction (see Fig. 1.4). Then the gauge transformations of the quark fields $q(x)$ and $U_\mu(x)$ take the form

$$q(x) \to V(x)q(x), \quad \bar{q}(x) \to \bar{q}(x)V^\dagger(x), \quad U_\mu(x) \to V(x)U_\mu(x)V(x + a\hat{\mu}), \tag{1.7}$$

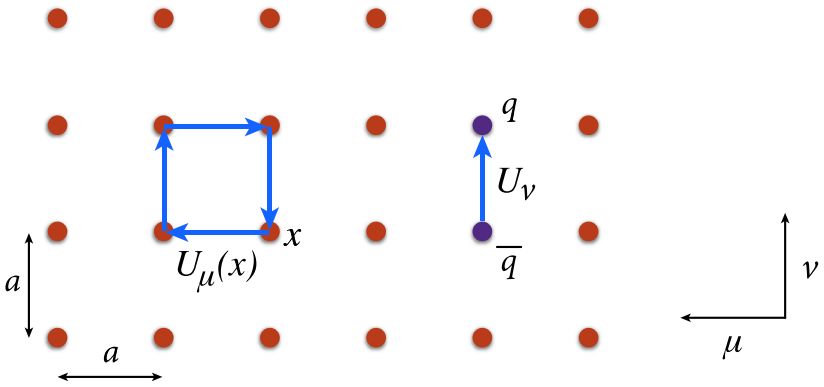

Figure 1.4: Gluon and quark fields on the lattice [36].

where $V(x) \in \mathrm{SU}(3)$ denotes an element of the gauge group.

The suitable lattice gauge action, proposed by Wilson, is given by

$$S_g = \beta \sum_{x,\mu<\nu} \left\{ 1 - \frac{1}{3}\mathrm{ReTr}[U_\mu(x)U_\nu(x+a\hat{\mu})U_\mu^\dagger(x+a\hat{\nu})U_\nu^\dagger(x)] \right\}. \tag{1.8}$$

Here, $\beta = 6/g_{\mathrm{lat}}^2$, where g_{lat} is a bare coupling constant in the lattice scheme. Setting $U_\mu(x) = e^{iaA_\mu(x)}$, the continuum form of the S_g, Eq. (1.5), is easily reproduced.

In practice, however, the non-zero values of the lattice spacing lead to the discretization errors. In case of the gauge action Eq. (1.8), they are of order $O(a^2)$. To reduce the cut-off dependence, one applies the so-called Symanzik improvement program [43, 44]. One starts with the modified (or effective) gauge action

$$S_g \to S_g + a^2 \sum_k c_k O_6^{(k)}, \tag{1.9}$$

where $O_6^{(k)}$ are dimension-six operators, which are allowed by lattice symmetries (the Euclidean rotational invariance is broken, since the lattice has a finite size). By tuning the coefficients c_k, it is possible to eliminate these operators in the effective action. In this way, one arrives at $O(a^2)$ improved action [45]

The case of the lattice fermions is more complicated. The simplest discretization of the covariant derivative $D_\mu q(x)$ leads to a so-called naive fermion action. In the continuum limit, this action, however, describes $2^4 = 16$ fermion fields. The extra doubler fermions appear always whenever the action has a continuum-like chiral symmetry. This fact is expressed in the Nielsen-Ninomiya theorem [46]. Also, the chiral anomaly is absent in the theory, since it is cancelled among the doublers. One way to avoid the doubling problem is the introduction of the additional terms in the Lagrangian, which explicitly break the chiral symmetry. This leads to the so-called Wilson-type fermions with the action [47]

$$S_f = a^4 \sum_x \bar{q}(x)\frac{1}{2}[\nabla_\mu + \nabla_\mu^* + 2m]q(x) - a^5 \sum_x \bar{q}(x)\frac{1}{2}\nabla_\mu\nabla_\mu^* q(x) + a^5 \sum_x c_{\mathrm{sw}}\bar{q}(x)\frac{i}{4}\sigma_{\mu\nu}\hat{F}_{\mu\nu}q(x), \tag{1.10}$$

where

$$\nabla_\mu q(x) = \frac{1}{a}[U_\mu(x)q(x+a\hat{\mu}) - q(x)], \quad \nabla_\mu^* q(x) = \frac{1}{a}[q(x) - U_\mu(x-a\hat{\mu})q(x-a\hat{\mu})]. \tag{1.11}$$

Here, $\sigma_{\mu\nu} = \frac{i}{2}[\gamma_\mu, \gamma_\nu]$, and $\hat{F}_{\mu\nu}$ is a lattice-site centered discretization of the gluon field strength tensor $F_{\mu\nu}$ [47]. The first term in Eq. (1.10) represents the naive action, which takes the form Eq. (1.6) in the continuum limit. The second term, introduced by Wilson, solves the doubling problem: the doublers acquire the mass of order $O(1/a)$, become heavy in the limit $a \to 0$ and hence decouple from a theory. This term introduces, however, the discretization errors linear in a. The improvement is achieved by adding the third term in Eq. (1.10) and tuning the coefficient $c_{\rm sw}$ to eliminate the $O(a)$ effects [48, 49]. Finally, there are alternative formulations of the lattice fermions, which are used in practice [36].

Further, the quantum theory is defined through the Euclidean-space partition function

$$Z = \int \mathcal{D}U \prod_f \mathcal{D}q_f \mathcal{D}\bar{q}_f \, e^{-S_g[U] - \sum_f \bar{q}_f (D[U] + m_f) q_f}, \tag{1.12}$$

where f denotes a quark flavour and $\mathcal{D}q_f = \prod_x dq_f(x)$, $\mathcal{D}\bar{q}_f = \prod_x d\bar{q}_f(x)$. The lattice Dirac operator $D[U]$ can be read off, e.g., from Eq, (1.10). The $\mathcal{D}U = \prod_{x,\mu} dU_\mu(x)$ is the (gauge-invariant) Haar measure. The physical information is contained in the *correlation functions* (or Green's functions), which are the vacuum expectation values of the multi-local gauge-invariant operators

$$\langle 0|\mathcal{O}(U, q, \bar{q})|0\rangle = \frac{1}{Z} \int \mathcal{D}U \prod_f \mathcal{D}q_f \mathcal{D}\bar{q}_f \, \mathcal{O}(U, q, \bar{q}) e^{-S_g[U] - \sum_f \bar{q}_f (D[U] + m_f) q_f}, \tag{1.13}$$

It is important to mention that link variables are integrated over the SU(3) manifold. The latter is compact, and thus gauge fixing (the Faddeev-Popov procedure) is not required. This is, however, not the case, if one wants to extract the information from the gauge-dependent correlation functions (e.g., the gluon propagator) [50]. The integration over quark and antiquark fields (the Grassmann variables) in Eq. (1.13) leads to the product of the fermion determinants $\prod_f \det(D[U] + m_f)$. According to Wick's theorem, one also gets a series of quark propagators $(D[U] + m_f)^{-1}$, which connect the quark fields in $\mathcal{O}(U, q, \bar{q})$. Hence, one ends up with an integral over $N_s^3 \times N_t \times 4 \times 9$ variables U, where N_s/N_t are the number of lattice points in the spatial/temporal direction.

The direct integration in Eq. (1.13) is not feasible due to the large number of variables, and one resorts to the Monte Carlo method [51]. The idea of the method is to generate a Markov chain of gauge configurations $U^{(i)}$, $i = 1, \ldots N$ with a probability distribution $P(U) \propto e^{-S_g[U]} \prod_f \det(D[U] + m_f)$ (the importance sampling, [52]). Then the expectation value $\langle 0|\mathcal{O}(U, q, \bar{q})|0\rangle$ is given as an average over these configurations

$$\langle 0|\mathcal{O}(U, q, \bar{q})|0\rangle = \frac{1}{N} \sum_{i=1}^{N} \mathcal{O}(U^{(i)}) + O(N^{-1/2}), \tag{1.14}$$

where the error of the result decreases as $1/\sqrt{N}$. Here, the variable $\mathcal{O}(U)$ is obtained after performing the Wick contractions in Eq. (1.13).

As an example, let us consider the two-point function of quark bilinears $A(x) = \bar{u}(x)\Gamma u(x)$ and $B(x) = \bar{u}(x)\Gamma' u(x)$, where the Γ, Γ' matrices act on the spin indices. The following expression has to be evaluated on the lattice

$$\begin{aligned} \langle 0|A(x)B(y)|0\rangle \;=\; & \frac{1}{N} \sum_{i=1}^{N} \Big(-\mathrm{Tr}\left\{\Gamma D_u^{-1}[U^{(i)}; x, y] \Gamma' D_u^{-1}[U^{(i)}; y, x]\right\} \\ & + \mathrm{Tr}\left\{\Gamma D_u^{-1}[U^{(i)}; x, x]\right\} \mathrm{Tr}\left\{\Gamma' D_u^{-1}[U^{(i)}; y, y]\right\} \Big) + O(N^{-1/2}), \end{aligned} \tag{1.15}$$

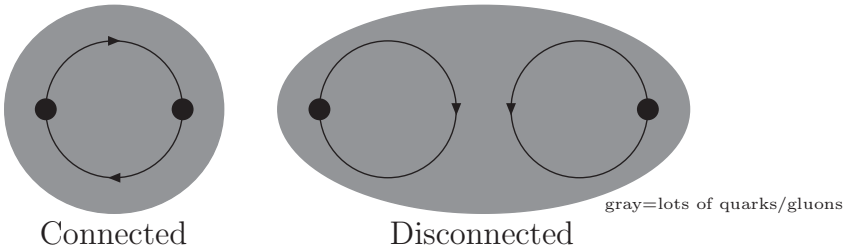

Figure 1.5: Connected and disconnected contributions for a two-point function Eq. (1.15). The quark lines depict the propagators obtained after Wick contractions [53].

where $D_u \equiv D[U] + m_u$, and the trace is taken over color and spin indices.

In general, the first and second term in Eq. (1.15) is referred to as a connected and a disconnected contribution to a given correlation function, respectively (see Fig. 1.5). The latter is computationally much more demanding to determine on the lattice since it requires the inversion of the Dirac operator D_u in *all* lattice points. It is either neglected, or estimated in an effective field theory, such as the partially quenched chiral perturbation theory (discussed in Subsection 1.4.1).

The gauge configurations are generated for different values of a, lattice sizes and quark masses. Also, they are stored and can be used for various purposes. Some of them are publicly available through the International Lattice Data Grid (ILDG) [54]. To reduce the statistical errors, one generates an ensemble of $N \sim 10^3$ statistically independent configurations. This is done at fixed values of quark masses and parameters of the lattice. The computational cost of an ensemble generation, however, increases with a lattice volume. It is also inversely proportional to the quark masses, which makes the simulations at physical pion mass to be a challenging task.

The results obtained from lattice simulations are additionally affected by systematic uncertainties. As mentioned above, there are discretization errors, which are of order $O(a^2\Lambda^2)$. Here, Λ is a typical momentum scale for a given quantity. In practice, this puts a limit on the momenta of the involving particles ($\Lambda \lesssim 300$ MeV). Another subtle issue regards the finite-volume effects. These are inevitable, since lattice calculations are performed in a finite space-time boxes $L^3 \times L_t$, where $L = aN$ and $L_t = aN_t$. The finite temporal direction leads to the excited-stated contamination, which could be, however, neglected for $L_t \gtrsim 2L$. The effects due to the finite spatial volume are of two kinds. For the matrix elements, involving a single hadron in the initial and final states, they are exponentially suppressed, $e^{-M_\pi L}$, where M_π is the pion mass and $L > 2$ fm [55, 56]. Hence, the finite-volume corrections are small, if the condition $M_\pi L \gtrsim 4$ is satisfied. But the quantities, containing mutli-hadron states, acquire a non-trivial power-law dependence on the volume: the finite-volume effects fall off only as an inverse powers of the volume. The reason behind this is the strong interaction of hadrons in the initial/final state. Moreover, the precise knowledge of this dependence allows one to determine the scattering observables, such as phase shifts and electroweak amplitudes, from lattice data. This topic will be considered in Section 1.5.

1.3.1 Stable hadrons

The stable hadrons are the ones, which do not decay due to the strong interaction. For instance, these are the light pseudoscalar (π, K, η) and baryon (N, Σ, Λ, Ξ) octets. Their properties can be determined on the lattice in a straightforward manner. Let us consider how the masses of particles are extracted. Taking a

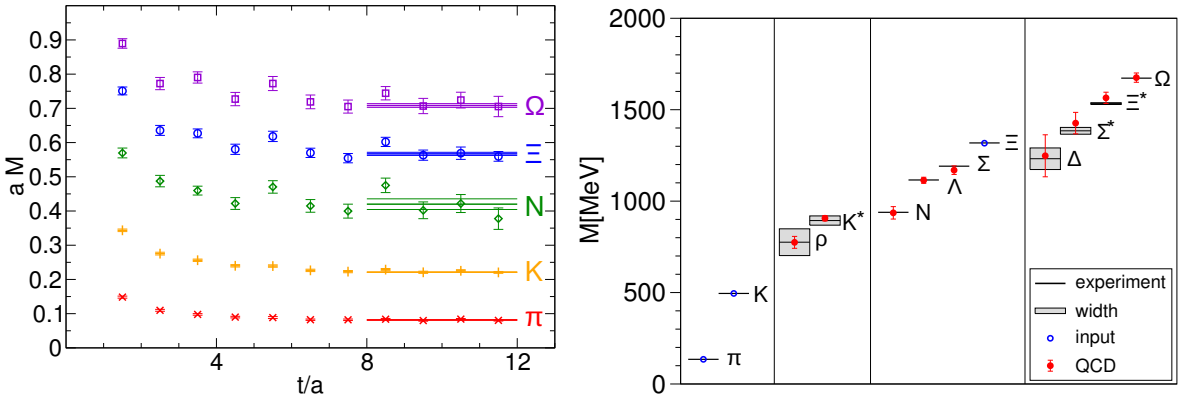

Figure 1.6: The left plot is a lattice calculation of the effective masses for π, K, N, Ξ and Ω. The right plot shows the light hadron spectrum of QCD obtained by BMW Collaboration [59].

pion as an example, one computes a two-point correlation function

$$C(t) = \sum_{\mathbf{x}} \langle 0|O_\pi(\mathbf{x}, t)O_\pi^\dagger(\mathbf{0}, 0)|0\rangle. \tag{1.16}$$

Here, $O_\pi(\boldsymbol{x}, \tau)$ is a field operator, which couples to the charged pion state $|\pi^+\rangle$: $\langle 0|O_\pi(\boldsymbol{x}, t)|\pi^+\rangle \neq 0$. It is usually taken in the form $O_\pi = \bar{d}\gamma_4\gamma_5 u$. On the other hand, by inserting a completeness relation in Eq. (1.16), one gets the spectral decomposition of $C(t)$

$$C(t) = Z\frac{e^{-M_\pi t}}{2M_\pi}\left[1 + \sum_n Z_n e^{-\Delta E_n t}\right], \tag{1.17}$$

where M_π is the pion mass and the factors Z, Z_n quantify the overlap of the pion field operator with a given state. For instance, $Z = |\langle 0|O_\pi(0)|\pi^+\rangle|^2$ gives a probability to create the pion by acting the operator O_π on the vacuum. Further, $\Delta E_n = E_n - M_\pi > 0$, where E_n denotes the energy of the n-th excited state. The index n is an integer since the lattice Hamiltonian has discrete eigenvalues in a cubic box. In particular, the energy of a free pion with 3-momentum $\mathbf{k}$ is given by

$$E_\pi(\mathbf{k}) = \sqrt{M_\pi^2 + \mathbf{k}^2}, \qquad \mathbf{k} = \frac{2\pi}{L}\mathbf{n}, \quad \mathbf{n} \in \mathbb{Z}^3. \tag{1.18}$$

Here, the periodic boundary conditions on the (anti)quark fields are imposed in spatial directions:

$$q(\mathbf{x} + \mathbf{n}L) = q(\mathbf{x}), \quad \forall \mathbf{n} \in \mathbb{Z}^3. \tag{1.19}$$

One can also impose more general twisted boundary conditions [57, 58], in which an additional phase factor appears on the right-hand side of Eq. (1.19)

As it is seen from Eq. (1.17), after sufficiently long time t, only the ground state contributes to the exponential decay of the correlation function $C(t)$. To extract the hadron masses, one determines the so-called effective mass

$$M = \frac{1}{a}\log\left(\frac{C(t)}{C(t+a)}\right). \tag{1.20}$$

The left plot in Fig. 1.6 shows the lattice calculation of this quantity corresponding to the different

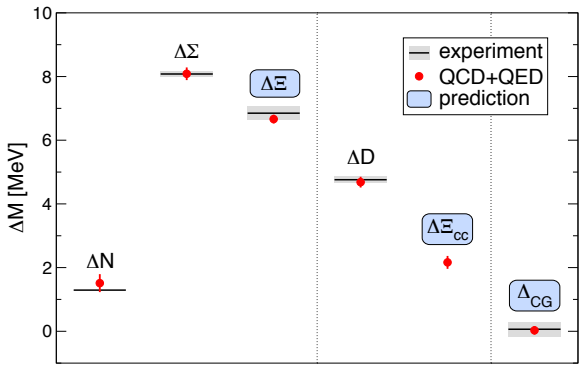

Figure 1.7: Lattice QCD+QED calculation of mass splittings [70].

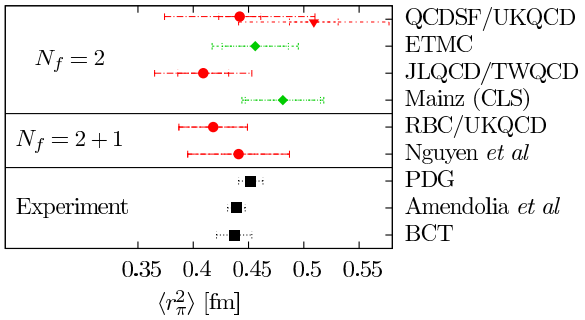

Figure 1.8: Summary of the results for the pion charge radius. It is seen an overall agreement with the PDG value $\langle r_\pi^2 \rangle = 0.45$ fm^2 [71]

.

stable hadrons. The excited-state contamination is clearly visible at small times. But later the plateau is eventually reached, which indicates that only the ground state survives. In this way, one obtains the spectrum of the light hadrons. The respective lattice calculations at almost physical pion masses were performed by several lattice groups [59–61]. The result of BMW Collaboration is shown in Fig. 1.6.

It is much more complicated to determine the masses of excited states. In practice, a large basis of the field operators and subsequent application of the variational methods are required [62]. The anisotropic lattices, which have different (smaller) values of the lattice spacing in the time direction, are also used. They allow one to substantially improve the resolution of the energy levels. By applying these and other techniques, the rich excited-state spectra has been recently obtained [63–65]. These predictions will be confronted by upcoming GlueX and PANDA experiments [66, 67].

Nowadays, the lattice calculations have reached such a level of accuracy [41], that the isospin-breaking effects have to be taken into account. The light quarks are electrically charged and the mass difference $m_d - m_u$ in the QCD Lagrangian Eq. (1.10) is non-zero. The electromagnetic effects, described by quantum electrodynamics (QED), also change the hadron masses. The respective shifts in the values are of order $O(\alpha_{\rm em})$, where $\alpha_{\rm em} \approx 1/137$ is the fine-structure constant. This leads to the violation of the isospin symmetry. Moreover, these two different sources of violation can be disentangled on the lattice. Since the pioneering work [68], lattice QCD+QED simulations have become increasingly important over the last years. For instance, the BMW Collaboration has recently performed the full lattice calculation of the neutron-proton mass difference as well as a number of other quantities sensitive to the isospin breaking, including a test of the Coleman-Glashow relation [69] (see Fig. 1.7).

Further, one is interested in the matrix elements of the electromagnetic and weak operators. They are parametrized in terms of the *form factors*. As an example, the electromagnetic pion form factor is defined through the current matrix element:

$$\langle \pi^+(p')|J_\mu(0)|\pi^+(p)\rangle = (p+p')_\mu F_\pi(Q^2). \tag{1.21}$$

Here, $Q^2 = -(p'-p)^2 > 0$ is the spacelike momentum transfer, where p and p' are the 4-momenta of the initial and final pions, respectively. J_μ denotes the electromagnetic current, which for $N_f = 2$ can be taken in the form $J_\mu = \frac{2}{3}\bar{u}\gamma_\mu u - \frac{1}{3}\bar{d}\gamma_\mu d$. The form factor $F_\pi(Q^2)$ obeys a polynomial expansion near $Q^2 = 0$

$$F_\pi(Q^2) = 1 - \frac{1}{6}\langle r_\pi^2 \rangle Q^2 + O(Q^4), \tag{1.22}$$

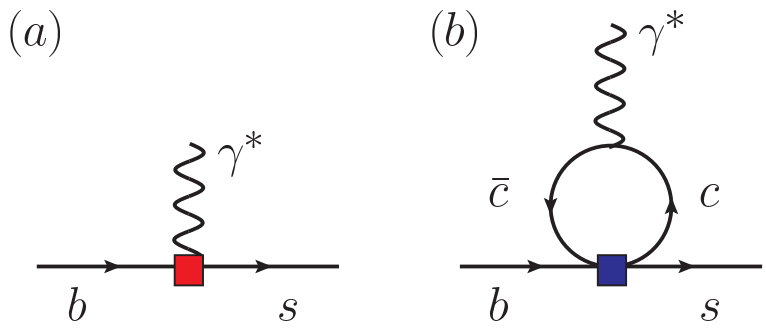

Figure 1.9: Effective theory of the $b \to s$ transition. *a*) Short distance operator. The respective contribution to the decay amplitude is parametrised by form factors. *b*) Long distance contribution from charmonium resonances.

where $\langle r_\pi^2 \rangle$ denotes the mean-square pion charge radius. This quantity has been measured both in experiment and on the lattice. The compilation of the results is presented in Fig. 1.8. The large-Q^2 kinematic region is amenable to perturbative QCD treatment [72]. However, for the intermediate values of Q^2, e.g., $0 < Q^2 < 6$ GeV^2, lattice calculations play an important role [73, 74].

In order to determine the matrix elements of type Eq. (1.21), the three-point correlation functions have to be evaluated:

$$C(t', t; \boldsymbol{p'}, \boldsymbol{p}) = \sum_{\boldsymbol{x},\boldsymbol{y}} \langle 0|O_\pi(\boldsymbol{y}, t') J_\mu(0) O_\pi^\dagger(\boldsymbol{x}, t)|0\rangle \, e^{-i\boldsymbol{p'y}+i\boldsymbol{px}}. \tag{1.23}$$

Next, one studies the limit of large time separation between the three operators in this expression: $t' \to +\infty$, $t \to -\infty$. Inserting complete set of states into Eq. (1.23), the spectral decomposition of $C(t', t; \boldsymbol{p'}, \boldsymbol{p})$ takes the form

$$C(t', t; \boldsymbol{p'}, \boldsymbol{p}) = \frac{Z}{2E_\pi(\mathbf{p'})2E_\pi(\mathbf{p})} e^{-E_\pi(\mathbf{p'})t' + E_\pi(\mathbf{p})t} \langle \pi^+(p')|J_\mu(0)|\pi^+(p)\rangle \, . \tag{1.24}$$

The desired matrix element $\langle \pi^+(p')|J_\mu(0)|\pi^+(p)\rangle$ can hence be extracted, because other quantities can be determined from the two-point function.

There are more complicated matrix elements, which might contribute to the amplitude of a given electroweak process. In particular, for the decays of type $A \to A'\gamma^*$, the long-distance effects lead to the non-local matrix elements of the form

$$T_\mu \propto i \int d^4x e^{iqx} \langle A'(p')|T J_\mu(x) O_{4q}(0)|A(p)\rangle, \tag{1.25}$$

where $q = p - p'$ denotes the four-momentum of the virtual photon γ^*. Here, O_{4q} is a four-quark operator, which is contained in the effective weak Hamiltonian relevant to a given transition. As seen from Eq. (1.25), one has to calculate the four-point correlation function. This is a straightforward but computationally demanding task. Recently, this approach has been applied in the exploratory lattice study of the rare kaon decays $K \to \pi l^+ l^-$ and $K \to \pi\nu\bar{\nu}$ [75, 76]. However, the processes involving heavy mesons, such as $B \to K l^+ l^-$ and $B \to K^* l^+ l^-$, are more complicated (see Fig. 1.9). Here, further progress is needed [77, 78].

If the operator O_{4q} is replaced by electromagnetic current J^ν, it is possible to infer the matrix element Eq. (1.25) from the behavior of the two point function $\langle A'(p')|A(p)\rangle$ in the presence of a weak *external* electromagnetic field. This method will be discussed in Section 1.6 in the context of Compton scattering.

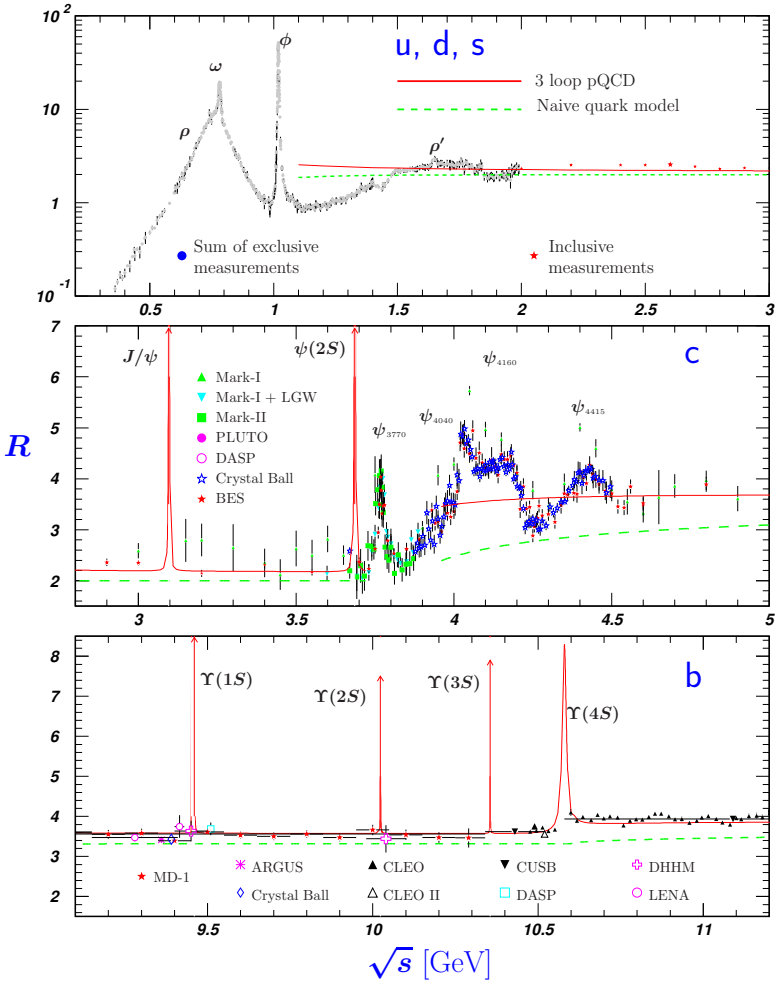

Figure 1.10: World data on the ratio $R = \sigma(e^+e^- \to hadrons)/\sigma(e^+e^- \to \mu^+\mu^-)$ in the light-flavor, charm, and beauty threshold regions [36]. Breit-Wigner parameterizations of $J/\psi, \psi(2S)$, and $\Upsilon(nS), n = 1, 2, 3, 4$, are also shown .

1.3.2 Hadron resonances

The lattice methods, described above, are straightforward as long as one deals with the matrix elements involving one-particle initial and final states. However, most of the hadrons in nature are resonances - they eventually decay into multiple strongly interacting particles. The classical examples include the $\rho(770)$, $K^*(892)$ and $\Delta(1232)$ resonances:

$$\rho \to \pi\pi, \quad K^* \to K\pi, \quad \Delta \to N\pi. \tag{1.26}$$

The resonance is sometimes seen as a peak in the cross section. Depending on the width of the peak, the narrow and wide resonances are distinguished. This is observed nicely in the e^+e^- collisions, where one measures the total cross section $\sigma(e^+e^- \to hadrons)$ as a function of the center-of-mass (CM) energy $E_{\rm CM} = \sqrt{s}$. In practice, one plots the branching ratio $R = \sigma(e^+e^- \to hadrons)/\sigma(e^+e^- \to \mu^+\mu^-)$ shown in Fig. 1.10.

A resonance behaviour can be largely understood by considering two-body scattering processes, such

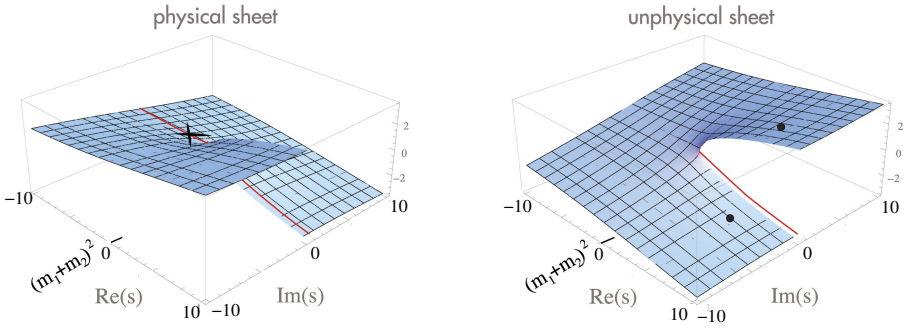

Figure 1.11: Riemann sheets of a one–channel scattering amplitude in the s-plane. The complex poles are located on the second Riemann sheet, whereas the bound states (the cross) on the physical one [36].

as $\pi\pi \to \pi\pi$, $\pi N \to \pi N$ and so on. For a general process $p_1 + p_2 \to p_3 + p_4$, the corresponding T-matrix is a function of two Mandelstam variables $s = (p_1 + p_2)^2$ and $t = (p_1 - p_3)^2$: $\mathcal{T} = \mathcal{T}(s,t)$. It is convenient to consider the process in the CM frame: $\mathbf{p}_1 + \mathbf{p}_2 = 0$. The scattering amplitude is expanded in partial waves

$$\mathcal{T}(s,t) = 4\pi \sum_{l=0}^{\infty} \sum_{m=-l}^{l} T_l(s) \mathcal{Y}_{lm}(\mathbf{p}') \mathcal{Y}^*_{lm}(\mathbf{p}) \,, \tag{1.27}$$

Here, l denotes the angular momentum; $l = 0$ correspond to the S-wave, $l = 1$ to the P-wave, and so on. The quantity $\mathcal{Y}_{lm}(\mathbf{p})$ is defined as $\mathcal{Y}_{lm}(\mathbf{p}) = |\mathbf{p}|^l Y_{lm}(\hat{\mathbf{p}})$, where Y_{lm} are the usual spherical harmonics and $\hat{\mathbf{p}} = \mathbf{p}/|\mathbf{p}|$. The relative 3-momenta are given by $|\mathbf{p}| = |\mathbf{p}'| = \lambda^{1/2}(m_1^2, m_2^2, s)/2\sqrt{s}$, where $\lambda(x,y,z) \equiv x^2 + y^2 + z^2 - 2xy - 2yz - 2zx$ is the Källen function, and m_1, m_2 are the masses of the hadrons in the scattering process. The label l will be dropped for brevity.

The partial-wave amplitude $T(s)$ depends only on s. It might be also a matrix in the channel space. According to the properties of $T = T(s)$, it is a double-valued function of s which is analytic on the whole s-plane except for cuts and poles (Fig. 1.11). The resonances are associated with complex poles of the scattering amplitude on unphysical Riemann sheets

$$E_R = M_R - i\,\Gamma_R/2, \quad s_R = E_R^2, \tag{1.28}$$

where M_R and Γ_R are mass and width of the resonance, respectively. The experimental values of these parameters can be found in PDG review [36].

The scattering amplitude T is normally split into the background (non-resonant) part and the pole part: $T = T^{\mathrm{b}} + T^{\mathrm{pole}}$. This splitting is, however, not unique and process-dependent. The background term T^{b} is taken as a smooth function of s. In the vicinity of $s = s_R$, the pole part T^{pole} takes the form

$$T^{\mathrm{pole}}_{\alpha\beta} = \frac{g_\alpha g_\beta}{s_R - s}, \tag{1.29}$$

where g_α denotes a coupling of the resonance to a given channel $\alpha = 1, 2, \ldots$. The pole position s_R and couplings g_α characterize the properties of the resonance, i.e. they are process-independent quantities.

If observed resonance structure is narrow, the Breit-Wigner (BW) parametrization is commonly used [79, 80]:

$$T^{\mathrm{pole}}_{\alpha\beta} = \frac{b_\alpha b_\beta}{M^2_{\mathrm{BW}} - i M_{\mathrm{BW}}\,\Gamma_{\mathrm{BW}} - s}. \tag{1.30}$$

Here, the couplings b_α are related to the BW parameters of a resonance: $b_\alpha = \sqrt{8\pi M_{BW}^2 \Gamma_\alpha / p_\alpha}$, where p_α and Γ_α are the relative three-momentum and partial width in the channel α, respectively. Obviously, the total width is given by $\Gamma_{\rm BW} = \sum_\alpha \Gamma_\alpha$. Contrary to the amplitude defined in Eq. (1.29), the BW formula is valid only near $s = M_{\rm BW}^2$ in a range governed by the width $\Gamma_{\rm BW}$. Indeed, the amplitude in Eq. (1.30) should not have a complex pole because it is defined on the physical sheet.

The presence of a resonance can be also interpreted as a rapid change of the *phase shift* near the BW pole. The unitarity of the S-matrix allows one define the scattering amplitude T as

$$T = \frac{8\pi\sqrt{s}}{\eta(p\cot\delta(p) - ip)}, \tag{1.31}$$

where the one-channel case $\alpha = 1$ is taken for simplicity. The coefficient η denotes the symmetry factor; $\eta = \frac{1}{2}$ for identical particles and otherwise $\eta = 1$. Here, $\delta(p)$ stands for the phase shift. It is a function of the CM energy $E = \sqrt{s}$, since $p = \lambda^{1/2}(m_1^2, m_2^2, s)/2\sqrt{s}$. The expression Eq. (1.31) clearly satisfies the unitarity condition

$$i(T^\dagger - T) = k\, T^\dagger T\,, \tag{1.32}$$

where k is a kinematic factor which should be properly chosen. Neglecting the background term $T^{\rm b}$, a comparison of Eq. (1.31) with the BW formula gives

$$\cot\delta(E) = \frac{E_{\rm BW} - E}{\Gamma_{\rm BW}/2}\,, \quad b = \sqrt{\frac{8\pi M_{\rm BW}^2 \Gamma}{\eta p}}\,. \tag{1.33}$$

It is seen that the phase shift passes through $\pi/2$ at energy $E = E_{\rm BW}$. The total change of the phase is $\delta(E > E_{\rm BW}) - \delta(E < E_{\rm BW}) = \pi$.

The resonance might be not sufficiently narrow, e.g., such as the ρ meson. In this case one should search for a complex pole $p = p_R$ of the amplitude Eq. (1.31) on the unphysical sheet:

$$p_R \cot\delta(p_R) + i p_R = 0. \tag{1.34}$$

In practice, the effective range expansion is used to solve this equation analytically [80, 81]

$$p\cot\delta(p) = -\frac{1}{a} + \frac{1}{2} r_0 p^2 + O(p^4), \tag{1.35}$$

where the parameters a and r_0 are called the scattering length and effective range, respectively. These quantities are fixed by fitting the data to the phase shift. The expansion Eq. (1.35) is assumed to be valid up to the resonance region. It is written for S-wave scattering but can be generalized to higher partial waves and multiple channels. One has to keep in mind that resonance parameters determined from a BW parametrization are, generally, process- and model-dependent, since the background term is unknown. On the other hand, the pole parameters defined by Eq. (1.29) are free of these ambiguities. A similar conclusion can be drawn for the matrix elements involving resonances. In particular, the corresponding form factors can only be defined at the resonance pole.

There are a number of electromagnetic and weak processes, which involve resonances. For instance, the electroexcitation $\gamma^* N \to \pi N$ allows for a study of the nucleon resonances [82]. To disentangle the resonance effects in experimental data, one is interested in the resonant contributions to the corresponding amplitude. For a general electroweak transition $\gamma^* P \to P_1 P_2$ or $P \to P_1 P_2 \gamma^*$, shown in Fig. 1.12, the amplitude $\mathcal{A}_\alpha$, $\alpha = 1, 2, \ldots$, can be expressed through the matrix element F_R of the electromagnetic

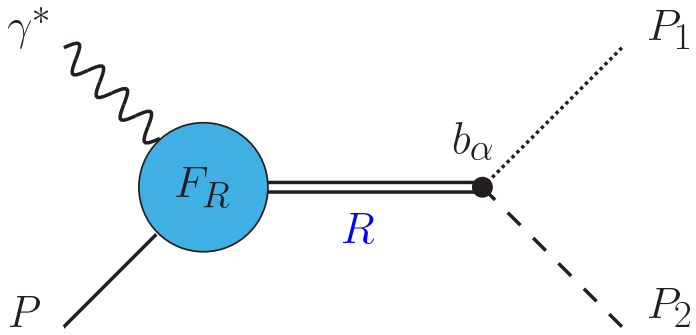

Figure 1.12: Schematic representation of the electroweak amplitude in the vicinity of a narrow resonance R.

current [82]. Assuming that the resonance R has a Breit-Wigner form near $E = M_{\mathrm{BW}}$, one gets

$$\mathcal{A}_\alpha(E) = \frac{b_\alpha F_R(E)}{M_{\mathrm{BW}}^2 - E^2 - iM_{\mathrm{BW}}\Gamma_{\mathrm{BW}}} + \cdots , \tag{1.36}$$

Here, the ellipses stand for the terms that are regular in the limit $\Gamma_{\mathrm{BW}} \to 0$. The current matrix element F_R describes the $RP\gamma^*$ vertex. It can be written in terms of the gauge-invariant structures containing the form factors, similarly to Eq. (1.21). Setting $E = M_{\mathrm{BW}}$, the imaginary part of electroweak amplitude takes the form

$$\mathrm{Im}\mathcal{A}_\alpha(M_{\mathrm{BW}}) = \sqrt{\frac{8\pi\Gamma_\alpha}{p_\alpha \Gamma_{\mathrm{BW}}^2}}\, F_R(E)\Big|_{E=M_{BW}} , \tag{1.37}$$

where all quantities are evaluated at $E = M_{\mathrm{BW}}$. This formula can be also understood as a definition of the resonance matrix elements. Such a definition, however, is applicable only if the resonance is infinitely narrow, so that the background can be neglected. A more rigorous way is to define matrix element at the resonance pole position $E = E_R$. Both definitions should, of course, converge for infinitely narrow resonances. The field-theoretical study of a similar problem for the matrix elements between bound states was first done by Mandelstam [83].

1.4 Effective field theories

The alternative description of the low-energy behaviour of QCD is based on chiral effective field theories (chiral EFTs). The classical examples of EFT are the Fermi theory of beta decay [84] and the Euler-Heisenberg Lagrangian [85]. In general, EFT is an approximation of a full underlying theory valid at a given low-energy (soft) scale. In order to set up EFT, one first disentangles light and heavy degrees of freedom in a full theory. As long as such separation of scales exists, the decoupling theorem [86] states that the effects of heavy particles can be included into the parameters of the EFT. It means that low-energy physics is insensitive to the physics at short distances (high energy). In other words, the heavy particles are integrated out from the full theory. This leads to an effective field theory which contains only the degrees of freedom relevant to a given soft scale.

The described concept can be nicely illustrated by the Euler-Heisenberg approach to light-by-light scattering. In the full theory (QED), which contains electrons and photons, the lowest order contribution to this process is given by the electron loop, as shown in Fig. 1.13. However, at photon energies E_γ much below the mass of the electron $E_\gamma \ll m_e$, the electromagnetic field will be the only degree of freedom in the EFT. Imposing Lorentz invariance, $U(1)$ gauge invariance and the other symmetries of QED, the

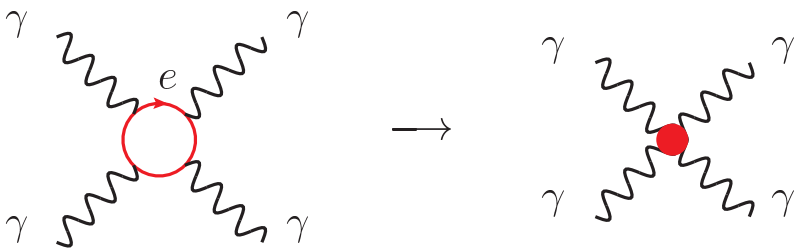

Figure 1.13: Effective field theory of the light-by-light scattering for low-frequency photons $E_\gamma \ll m_e$. The electrons are integrated out from the full theory (QED).

effective Lagrangian takes the form

$$L_{\text{eff}}(A_\mu) = -\frac{1}{4}F_{\mu\nu}F^{\mu\nu} + \frac{\alpha^2}{m_e^4}\left\{c_1(F_{\mu\nu}F^{\mu\nu})^2 + c_2(F_{\mu\nu}\tilde{F}^{\mu\nu})^2\right\} + O(m_e^{-6}), \tag{1.38}$$

where, $\tilde{F}^{\mu\nu} = \frac{1}{2}\epsilon^{\mu\nu\alpha\beta}F_{\alpha\beta}$, and $F_{\mu\nu} = \partial_\nu A_\mu - \partial_\mu A_\nu$ denotes the electromagnetic field tensor. Further, $\alpha = e^2/4\pi$ is the fine-structure constant and the factor m_e^{-4} is added on dimensional grounds. The $O(m_e^{-6})$ term contains an infinite tower of higher-dimensional operators. They are, however, suppressed by the inverse powers of the electron mass m_e. The parameter which controls the convergence of the perturbation expansion is the ratio E_γ/m_e. This is an example of the *power counting*. The scattering amplitude behaves as $\sim \alpha E_\gamma^4/m^4$. This formula is valid only for low-energy photons, since otherwise it would violate the unitarity of the S-matrix.

In order to determine the constants c_1, c_2, one calculates the tree-level amplitude of the process with Lagrangian Eq. (1.38). Then it is equated to the one-loop QED result. The constants are found to be $c_1 = 1/90$ and $c_2 = 7/360$. This procedure of fixing the low-energy constants in the effective Lagrangian is called *matching*.

1.4.1 Chiral perturbation theory

The effective field theory of QCD, called chiral perturbation theory (χPT), is based on the chiral symmetry. The building blocks of the theory are hadrons, which are the appropriate degrees of freedom at low energies. As seen from Fig. 1.6, there is a large gap between the masses of the pions and the masses of the vector mesons, such as the $\rho(770)$. It is accordingly possible to generate an expansion in terms of the ratio Q/Λ_χ, where $Q \sim M_\pi \approx 140$ MeV is a soft scale in a process, and $\Lambda_\chi \sim M_\rho \sim 1$ GeV is the chiral-symmetry breaking scale. Further, EFT should have all symmetries of underlying theory, including the chiral one. This establishes a genuine connection with QCD, in accordance with the “folk theorem" of Weinberg [87]:

> If one writes down the most general possible Lagrangian, including all terms consistent with assumed symmetry principles, and then calculates matrix elements with this Lagrangian to any given order of perturbation theory, the result will simply be the most general possible S-matrix consistent with analyticity, perturbative unitarity, cluster decomposition, and the assumed symmetry principles.

The pions interact weakly since they are pseudo-Goldstone bosons. This feature is implemented in the non-linear realization of the chiral symmetry [88–92]. A general method for the construction of Lagrangians consistent with broken symmetries was developed by Callan, Coleman, Wess, and Zumino

[93, 94]. According to the pattern of chiral-symmetry breaking in QCD Eq. (1.3), the pion fields $\boldsymbol{\pi} = (\pi_1, \pi_2, \pi_3)$ represent the coordinates of the coset space $SU(2) \times SU(2)/SU(2)$. One introduces the $SU(2)$ matrix U which collects the pions. It is usually taken in the exponential form $U = \exp(i\boldsymbol{\sigma} \cdot \boldsymbol{\pi}/F_\pi)$, where $\boldsymbol{\sigma} = (\sigma_1, \sigma_2, \sigma_3)$ are Pauli matrices and $F_\pi \approx 92$ MeV is the pion decay constant ($\pi^+ \to \mu^+\nu_\mu$). The matrix U transforms under the global chiral rotations as

$$U \to RUL^\dagger, \qquad L \in SU(2)_L, \quad R \in SU(2)_R \tag{1.39}$$

The effective Lagrangian $\mathcal{L}_{\text{eff}}$ consists of chirally-invariant part, as well as a part which explicitly breaks the chiral symmetry. The power counting allows one to organize the $\mathcal{L}_{\text{eff}}$ in the form

$$\mathcal{L}_{\text{eff}} = \mathcal{L}^{(2)} + \mathcal{L}^{(4)} + \cdots, \tag{1.40}$$

where the superscript refers to the number of derivatives or pion mass insertions. The leading order Lagrangian is given by

$$\mathcal{L}^{(2)} = \frac{F^2}{4}\text{Tr}\left\{\partial_\mu U \partial^\mu U^\dagger + M^2(U + U^\dagger)\right\}. \tag{1.41}$$

Here, the trace Tr is taken in flavor space. Further, $F = F_\pi|_{m_u, m_d \to 0}$ and the pion mass M satisfies the Gell-Mann-Oakes-Renner relation [95]

$$M^2 = (m_u + m_d)B, \qquad B = \left.\frac{|\langle 0|\bar{u}u|0\rangle|}{F_\pi^2}\right|_{m_u, m_d \to 0}, \tag{1.42}$$

where the constant B is proportional to the quark condensate $\langle 0|\bar{u}u|0\rangle \approx (-270 \text{ MeV})^3$. The second term in Eq. (1.41) breaks the chiral symmetry. On the other hand, it gives a proper mass to the pions:

$$\begin{aligned}\mathcal{L}^{(2)}_{\pi\pi} &= \frac{1}{2}\partial_\mu\boldsymbol{\pi} \cdot \partial^\mu\boldsymbol{\pi} - \frac{1}{2}M^2\boldsymbol{\pi}^2 \\ &\quad + \frac{1}{6F^2}(\boldsymbol{\pi} \cdot \partial_\mu\boldsymbol{\pi})(\boldsymbol{\pi} \cdot \partial^\mu\boldsymbol{\pi}) - \frac{1}{6F^2}\boldsymbol{\pi}^2\partial_\mu\boldsymbol{\pi} \cdot \partial^\mu\boldsymbol{\pi} + \frac{1}{24F^2}M^2\boldsymbol{\pi}^4 + O(\boldsymbol{\pi}^6),\end{aligned} \tag{1.43}$$

where the constant F^2M^2 was dropped.

The terms with four pion fields describe the elastic $\pi\pi$ scattering. The respective tree level scattering amplitude for the generic process $\pi^a(p_1)\pi^b(p_2) \to \pi^c(p_3)\pi^d(p_4)$ reads

$$T^{ab,cd} = \delta^{ab}\delta^{cd}\frac{s - M_\pi^2}{F_\pi^2} + \delta^{ac}\delta^{bd}\frac{t - M_\pi^2}{F_\pi^2} + \delta^{ad}\delta^{bc}\frac{u - M_\pi^2}{F_\pi^2}, \tag{1.44}$$

where $s = (p_1 + p_2)^2$, $t = (p_1 - p_3)^2$ and $u = (p_1 - p_4)^2$ are the Mandelstam variables satisfying the condition $s + t + u = 4M^2$. The result Eq. (1.44) is in complete agreement with earlier calculation of Weinberg [96] based on the pion pole dominance [97] and the current algebra framework [98]. In particular, one can infer the values of the scattering length a_l^I for a given partial wave with angular momentum l and isospin I. Denoting the corresponding amplitude as $t_l^I(s)$, one has $a_l^I = t_l^I(s = 4M_\pi^2)$. Indeed, the insertion of the effective range expansion Eq. (1.35) into Eq. (1.31) shows that the scattering length is proportional to the value of the T-matrix at threshold $s = 4M_\pi^2$. In particular, the S-wave ($l = 0$) scattering lengths take the values

$$a_0^0 \overset{\text{LO}}{=} \frac{7M^2}{32\pi F^2}, \quad a_0^2 \overset{\text{LO}}{=} -\frac{M^2}{16\pi F^2}, \tag{1.45}$$

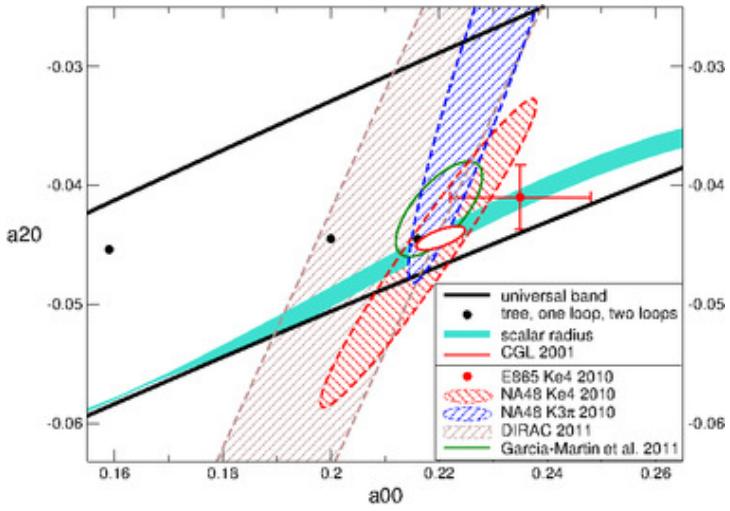

Figure 1.14: Experimental data on the S-wave scattering lengths (in fm). The black dots denote the χPT predictions at LO, NLO and NNLO. The small ellipse indicates the result obtained on the basis of the Roy equations [99].

where LO denones the leading order.

The next-to leading order Lagrangian $\mathcal{L}^{(4)}$ was worked out by Gasser and Leutwyler in their seminal works [100, 101]. For $N_f = 2$, it contains 7 low-energy constants l_i, $i = 1, \dots 7$, and 3 contact terms. At order $O(p^4)$, the purpose of these constants is to absorb *all* one-loop divergences generated by $\mathcal{L}^{(2)}$. The values of the renormalized couplings $l_i^{(r)}$, however, remain arbitrary,

$$l_i^{(r)}(\mu) = \frac{\gamma_i}{16\pi^2} \ln \frac{\mu^2}{\Lambda_i^2}, \qquad i = 1, \dots 7, \tag{1.46}$$

where γ_i are known coefficients, which are obtained from the cancellation of the one-loop divergences. The parameter μ is a running scale in dimensional regularization, whereas the scales Λ_i are RG-invariant. The values of $l_i^{(r)}(\mu)$ are either estimated theoretically or determined on the lattice [41]. In general, they should be of a natural size, provided $\mu \sim M_\pi$. For instance, $\bar{l}_3 \equiv \ln \frac{M_\pi^2}{\Lambda_3^2} = 3.16 \pm 0.31$ and $\bar{l}_4 \equiv \ln \frac{M_\pi^2}{\Lambda_4^2} = 4.03 \pm 0.16$ [41, 102]. If the values of the low-energy constants are large, this would be an indication of substantial resonance contributions to the scattering amplitude. In this case the low-lying meson resonances should be included as explicit degrees of freedom in the chiral EFT [103].

The scattering lengths get corrections at next-to-leading order (NLO):

$$a_0^0 \overset{\text{NLO}}{=} \frac{7M_\pi^2}{32\pi F_\pi^2} \left\{ 1 + \frac{9M_\pi^2}{32\pi F_\pi^2} \log \frac{\lambda_0^2}{M_\pi^2} \right\}, \quad a_0^2 \overset{\text{NLO}}{=} -\frac{M_\pi^2}{16\pi F_\pi^2} \left\{ 1 - \frac{M_\pi^2}{32\pi F_\pi^2} \log \frac{\lambda_2^2}{M_\pi^2} \right\}, \tag{1.47}$$

where λ_0, λ_2 can be expressed in terms of the scales $\Lambda_1, \dots \Lambda_4$ [100, 101]. The appearance of chiral logarithms $M_\pi^2 \log M_\pi^2$ is a typical feature of higher-order calculations in χPT. The two-loop (NNLO) result for the scattering lengths was also derived [104, 105]. The further theoretical improvement was achieved by applying Roy equations [106], which are dispersive relations for $\pi\pi$ scattering [107]. These theoretical predictions are shown in Fig . 1.14. Altogether, they are confirmed by experiment to high degree of accuracy.

The methods of chiral EFT can be extended to the $N_f = 3$ sector, which includes strange mesons. The

structure of the effective Lagrangian is essentially the same, except that the pseudo-Goldstone bosons are collected into $SU(3)$ matrix, and there are more operators at NLO, NNLO, and so on. Finally, it is also possible to include baryons into the chiral EFT framework. This opened, e.g., the possibility to perform a systematic study of the nuclear forces devoid of any model dependence [108, 109].

The other aspect of χPT concerns its application to lattice QCD simulations. It is useful to analyse the dependence of the results on the quark masses, lattice spacing and spatial volume. Depending on the formulation of the lattice action, there are different versions of χPT that should be used. A particular example of interest is a partially quenched χPT (PQχPT) [110–112]. It allows one to estimate the quark-disconnected contributions to the correlation functions.

The partial quenching is easily understood by considering again the vacuum expectation value of a general operator given by Eq. (1.13). After integration over Grassmann fields, one has schematically

$$\langle 0|\mathcal{O}(q,\bar{q})|0\rangle \propto \int \mathcal{D}A_\mu \det(D+m_{\rm sea}) e^{-S_g[A]} \frac{1}{D+m_{\rm valence}} \dots \frac{1}{D+m_{\rm valence}} \tag{1.48}$$

If the masses of the sea quarks $m_{\rm sea}$ are chosen to be different from the masses of the valence quarks $m_{\rm valence}$, then the underlying theory is called partially quenched QCD (PQQCD). The matrix elements in QCD are reproduced by setting $m_{\rm sea} = m_{\rm valence}$.

In order to disentangle the effects of sea and valence quarks, PQQCD has an extended quark content. The fermionic QCD Lagrangian in Eq. (1.6) is supplemented by similar kinetic terms, corresponding to a certain number N of the valence quarks q_v and ghost fields $\tilde{q}$. The number N depends on the choice of the correlation function. The purpose of the ghosts is to exactly cancel the effects of valence quarks so that the QCD partition function is reproduced. In the chiral limit the Lagrangian of PQQCD has an extended chiral symmetry which is spontaneously broken:

$$SU(N_f+N|N)_L \times SU(N_f+N|N)_R \longrightarrow SU(N_f+N|N)_V\,, \tag{1.49}$$

where $SU(N_f+N|N)$ denotes a graded group.

For illustration of the method, let us consider a two-point function of type Eq. (1.15), which contains the flavour-diagonal field operators. Introducing one mass-degenerate valence quark q_v, it can be rewritten in PQQCD identically as

$$\langle 0|\bar{q}(y)\Gamma' q(y)\bar{q}(x)\Gamma q(x)|0\rangle_{\rm QCD} \equiv \underbrace{\langle 0|\bar{q}(y)\Gamma' q_v(y)\bar{q}_v(x)\Gamma q(x)0|\rangle_{\rm PQQCD}}_{\text{connected}} + \underbrace{\langle 0|\bar{q}(y)\Gamma' q(y)\bar{q}_v(x)\Gamma q_v(x)|0\rangle_{\rm PQQCD}}_{\text{disconnected}}. \tag{1.50}$$

It is seen that the connected and disconnected pieces are completely disentangled – they appear in different correlators on the right-hand side of this equation.

At the next step, the correlators are estimated in PQχPT. If $m_{\rm sea} = m_{\rm valence}$, the latter is identical with χPT, as shown in Fig. 1.15. According to the pattern of the chiral symmetry breaking, the Goldstone fields parametrize the $SU(N_f+N|N)$ group elements. There are $(N_f+2N)^2-1$ such fields. The leading order effective Lagrangian has a form similar to the one in the ordinary χPT, while the trace is replaced by a supertrace. But there are additional operators at higher orders because the Cayley-Hamilton theorem does not apply for graded groups [113, 114]. For instance, there is a new four-derivative operator in the $N_f = 3$ case. Its contribution to the physical quantities, however, starts only at next-to-next-to-leading order. Nevertheless, the additional constants have to be accounted for in lattice fits.

The described framework has been applied to estimate the disconnected pieces in the hadronic vacuum polarisation. The precise theoretical knowledge of the latter is important to resolve the muon $g-2$ problem. It was found that the ratio of disconnected to connected contributions amounts to a few percent in magnitude [53, 115]. This result is in qualitative agreement with the lattice determination of the

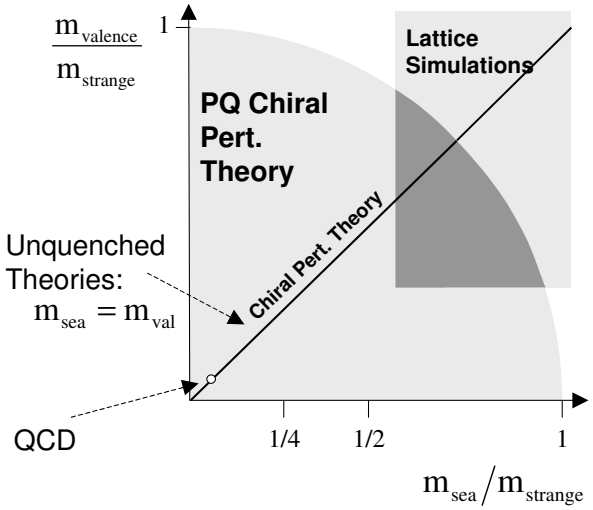

Figure 1.15: The space of PQχPT in comparison to χPT. PQχPT provides more flexibility to perform the chiral extrapolation of lattice data [112].

disconnected piece [116]. More recently, the disconnected diagrams in the isoscalar and isovector channels of the $\pi\pi$ scattering have been also studied [117, 118].

1.4.2 Non-relativistic EFT

There are systems, in which the matter fields are non-relativistic. Typical examples include shallow bound states or low-energy scattering. The non-relativistic nature of the problem allows one to introduce a small expansion parameter $|\mathbf{p}|/M$, where $\mathbf{p}$ is a typical 3-momentum in the system (soft scale), and M is a mass of a non-relativistic particle (hard scale). The field-theoretical approach which provides a systematic expansion of the S-matrix in this parameter is called a non-relativistic EFT. This development was started by Caswell and Lepage, who formulated the non-relativistic QED [119]. In contrary to the relativistic Bethe-Salpeter approach [120, 121], the framework proved to be very useful in study of the non-relativistic two-body bound states, such as muonic hydrogen and hadronic atoms [122, 123].

Let us consider a single scalar field $\Phi(x)$ which describes the particle of mass M such as pion. The non-relativistic effective Lagrangian reads

$$\mathcal{L}_{NR} = \Phi^\dagger\left(i\partial_t - M + \frac{\triangle}{2M}\right)\Phi + \frac{g_1}{M^2}\,(\Phi^\dagger\Phi^\dagger)(\Phi\Phi) + \cdots \tag{1.51}$$

where the ellipses denote the terms with higher spatial derivatives. Here, $\partial_t \equiv \partial/\partial t$ and Δ is the Laplacian. There are in general infinite number of coupling constants g_i, $i = 1, \ldots$. The important feature of the Lagrangian Eq. (1.51) is that the number of heavy particles is conserved in any vertex. In particular, the two-particle sector of the non-relativistic EFT does not mix with sectors containing different numbers of massive particles. In contrary to the relativistic theory, the non-relativistic Lagrangian does not contain the antiparticle degrees of freedom. The effects of antiparticles are included in the low-energy constants. This property drastically simplifies the actual calculations.

The values of the couplings g_i are determined by matching to the relativistic theory, such as χPT. According to Eq. (1.51), the free propagator has a pole at $p^0 = M + \mathbf{p}^2/2M$. It is a non-relativistic dispersion law, and thus results are Lorentz-invariant only approximately, up to a given order in the expansion in $1/M$. Another point concerns the normalization of one–particle states in the non–relativistic

theory. It is different from the relativistic one:

$$\langle \mathbf{k}|\mathbf{p}\rangle = (2\pi)^3\,\delta^3(\mathbf{k}-\mathbf{p}) \quad \text{(non–relativistic)}, \qquad \langle \mathbf{k}|\mathbf{q}\rangle = (2\pi)^3\,2w(\mathbf{p})\,\delta^3(\mathbf{k}-\mathbf{p}) \quad \text{(relativistic)}\,, \tag{1.52}$$

where $w(\mathbf{p}) = \sqrt{M^2+\mathbf{p}^2}$. Considering a generic two-body scattering $p_1 + p_2 \to p_3 + p_4$ (e.g., $\pi\pi$ scattering), the matching condition for the scattering amplitude reads

$$\prod_{i=1}^{4}(2w(\mathbf{p}_i))^{1/2} T_{NR}(\mathbf{p}_3,\mathbf{p}_4;\mathbf{p}_1,\mathbf{p}_2) = T_R(\mathbf{p}_3,\mathbf{p}_4;\mathbf{p}_1,\mathbf{p}_2)\,. \tag{1.53}$$

Here, the additional kinematic factors appear because of the different normalizations in Eq. (1.52). For instance, the matching can be done at threshold $s = 4M^2$. The relativistic amplitude becomes a constant $T_R = a$, where a is given essentially by the scattering length. However, the value of the non-relativistic counterpart T_{NR} is not Lorentz-invariant, but rather depends on the reference frame: $T_{NR} = \frac{a}{4M^2} - \frac{a}{16M^4}\mathbf{P}^2 + \cdots$, where $\mathbf{P}$ is a total 3-momentum.

In order to preserve the invariance of the non-relativistic amplitudes, a modified covariant framework was proposed [124, 125]. In this approach, one rescales the field $\Phi(x) \to \sqrt{2W}\,\Phi(x)$, where $W = \sqrt{M^2-\Delta}$. The normalization of the one-particle states in this theory becomes the same as in the relativistic case. The effective Lagrangian takes the form

$$\mathcal{L} = \Phi^\dagger 2W(i\partial_t - W)\Phi + \frac{c_1}{4}\,(\Phi^\dagger\Phi^\dagger)(\Phi\Phi) + \cdots\,, \tag{1.54}$$

where the ellipses stand for all possible *Lorentz-invariant* four-particle operators containing space derivatives. To set up a power counting scheme, it is convenient to introduce a small parameter v, which is the velocity of the massive particle. The mass M is counted as $O(1)$, whereas all 3-momenta $|\mathbf{p}_i|$ and space derivatives ∇ as $O(v)$. The kinetic energies $T_i = w(\mathbf{p}_i) - M$ are of order $O(v^2)$. Also, the coupling constant $c_1 \sim O(1)$. The matching at tree level gives $T_{NR} = c_1 = a$. This result is independent of the reference frame since the kinematic factors in Eq. (1.53) are absent in the modified theory.

The non-relativistic Lagrangian Eq. (1.54) can be used beyond the leading order. The free propagator is given by

$$i\langle 0|T\Phi(x)\Phi^\dagger(y)|0\rangle = \int \frac{d^4p}{(2\pi)^4}\,\frac{\mathrm{e}^{-ip(x-y)}}{2w(\mathbf{p})(w(\mathbf{p})-p_0-i\epsilon)} \tag{1.55}$$

The scattering amplitude has a simple diagrammatic structure in the non-relativistic theory, shown in Fig. 1.16. It is given as a sum of the bubble-chain diagrams:

$$T_{NR}(\mathbf{p}_3,\mathbf{p}_4;\mathbf{p}_1,\mathbf{p}_2) = c_1 + c_1^2\eta G(P^0,\mathbf{P}) + c_1^3\eta^2 G(P^0,\mathbf{P})^2 + \ldots\,, \tag{1.56}$$

where η denotes the symmetry factor introduced in Eq. (1.31). Here, G is a one-loop integral in a moving frame with total 4-momentum $P^\mu = (P^0,\mathbf{P})$:

$$G(P^0,\mathbf{P}) = \int \frac{d^dl}{(2\pi)^d}\,\frac{1}{4w(\mathbf{l})w(\mathbf{P}-\mathbf{l})(w(\mathbf{l})+w(\mathbf{P}-\mathbf{l})-P^0)}\,, \tag{1.57}$$

where d is a number of space dimensions in dimensional regularization.

To preserve the predictive power of the non-relativistic EFT, it is important that the radiative corrections do not violate the counting rules. For instance, this is a case in the meson χPT since the masses of the pseudo-Goldstone bosons are treated as small parameters. In the non-relativistic EFT, however, the power counting is destroyed by the presence of a heavy mass scale M; similarly, it is the nucleon mass

Figure 1.16: Diagrammatic representation of the scattering amplitude in the non-relativistic EFT.

in the baryon χPT. Indeed, the integrand in Eq. (1.57) contains such a heavy mass. The resolution of this problem consists in using a certain prescription called the threshold expansion [125, 126]. As a first step, the integrand is expanded in inverse powers of M. Then one integrates the obtained series by taking into account the fact that regular momentum integrals vanish in dimensional regularization: $\int \frac{d^d l}{(2\pi)^d} l^n = 0$. The final result takes a Lorentz-invariant form ($d = 3$):

$$G(s) = \frac{i}{16\pi}\left(1 - \frac{4M^2}{s}\right)^{1/2} = \frac{i\,|\mathbf{p}|}{8\pi\sqrt{s}}, \qquad s = P^2, \tag{1.58}$$

where $|\mathbf{p}| = \lambda^{1/2}(M^2, M^2, s)/2\sqrt{s}$ is the relative 3-momentum in the CM frame. Now, this expression is counted as $O(v)$, so that the naive power counting remains valid. It also correctly reproduces the imaginary part of the relativistic one-loop integral in the vicinity of the elastic threshold $s = 4M^2$.

The result Eq. (1.58) implies that the non-relativistic amplitude is Lorentz-invariant at any given order of the expansion parameter v. Also, the low-energy constant A is proportional to the scattering length to all orders in perturbation theory, since $G(4M^2) = 0$. Further, the amplitude T_{NR} contains the non-analytic terms given by the odd powers of the relative 3-momentum p (the right-hand cut $s > 4M^2$). In fact, the relativistic amplitude has the same non-analytic structure near threshold $s = 4M^2$, $t = u = 0$ — the contributions from $t-$ and $u-$channels are polynomials in p^2 in this kinematic region [123].

After summation to all orders in Eq. (1.56), it straightforward to check that the non-relativistic amplitude T_{NR} satisfies the Lippmann-Schwinger equation [127]:

$$T_{NR} = V + V\eta G(s) T_{NR}, \tag{1.59}$$

where the potential is the $V = c$. This shows that the non-relativistic EFT is useful not only in perturbation theory, but also for study of bound states and resonances in the vicinity of the elastic threshold. This conclusion is not affected by the presence of the derivative couplings in the effective Lagrangian, Eq. (1.54).

The form of the terms with derivative couplings is dictated by the effective-range expansion of the relativistic amplitude near threshold. At order $O(v^2)$, one gets

$$\mathcal{L}_2 = c_2\left[(\Phi^\dagger)^\mu(\Phi^\dagger)_\mu\Phi\Phi - M^2\Phi^\dagger\Phi\Phi^\dagger\Phi + \text{h.c.}\right] + c_3\left[\Phi^\dagger(\Phi^\dagger)^\mu - (\Phi^\dagger)^\mu\Phi^\dagger\right]\left[(\Phi)_\mu\Phi - \Phi(\Phi)_\mu\right], \tag{1.60}$$

where h.c. stands for hermitian conjugate, and

$$(\Phi)_\mu = (\mathcal{P})_\mu\Phi\,, \quad (\Phi^\dagger)_\mu = (\mathcal{P}^\dagger)_\mu\Phi^\dagger\,, \qquad (\mathcal{P})_\mu = (W, -i\nabla)\,, \quad (\mathcal{P}^\dagger)_\mu = (W, i\nabla)\,. \tag{1.61}$$

The constant c_2 is related to the S-wave scattering parameters, while c_3 is proportional to the P-wave scattering volume. The operators of higher order can be constructed in a similar manner.

The Lippmann-Schwinger (LS) equation for the partial-wave scattering amplitude takes the form

$$T_l(s) = V_l(s) + V_l(s)|\mathbf{p}|^{2l}G(s)T_l(s), \tag{1.62}$$

where the subscript 'NR' is omitted for brevity. The quantities $V_l(s)$ are coefficients in the partial-wave expansion of the potential, similar to Eq. (1.27). The latter can be read off from the effective Lagrangian, Eqs. (1.54,1.60). The unitarity condition for the partial-wave amplitudes, similar to Eq. (1.32), gives

$$T_l(s) = \frac{8\pi\sqrt{s}}{\eta|\mathbf{p}|^{2l+1}} \frac{1}{\cot\delta_l(s) - i}, \qquad V_l(s) = \frac{8\pi\sqrt{s}}{\eta|\mathbf{p}|^{2l+1}} \tan\delta_l(s), \tag{1.63}$$

where $\delta_l(s)$ is the scattering phase.

The main advantage of the non-relativistic framework as compared to a relativistic theory is following. The results in the relativistic theory, e.g., in χPT, are given in terms of the renormalized parameters that have no direct relevance to experimental data. On the other hand, the low-energy constants in the non-relativistic EFT can be expressed directly through the parameters of the effective range expansion (scattering length, effective range, etc.). The latter are observables that completely characterize the low-energy properties of the hadrons. Once the matching is done, one can proceed with the Lippmann-Schwinger equation.

1.5 Finite volume formalism

According to the discussion in Subsection 1.3.2, the resonances are not eigenstates of the QCD Hamiltonian. It means that the energy levels determined on the lattice do not correspond to any resonance. What one needs are the lattice data of the phase shifts. This implies the calculation of a suitable four-point correlation function corresponding to the two-body scattering. In order to put the external particles on their mass-shells, one has to perform an analytic continuation of the result from Euclidean to Minkowski momenta. In principle, such a procedure is guaranteed by the reconstruction theorem [128, 129]. However, the analytic continuation becomes an issue in a finite volume since the lattice data are obtained only at a discrete and a finite set of three-momenta. It is consequently important to have an alternative possibility to reach the timelike kinematic region directly from the *Euclidean* correlation functions.

In case of matrix elements between one-particle states, the solution is to separate the terms with leading exponential fall-off for large Euclidean times. That is how the masses of stable hadrons and transition form factors are determined. But the problems start to appear when trying to extract the physical quantities in the presence of a final state interaction. Suppose one aims at computing, e.g., the timelike pion form factor. For that purpose the three-point correlation function, defined similar to Eq. (1.23), should be studied in the limit $t' \to +\infty$, $t \to +\infty$, $t' \gg t$. One would naively get the desired matrix element. But the latter is real on the lattice, while the pion form factor is complex in the timelike region. The complex phase is acquired because of the $\pi\pi$ final state interaction. In the elastic region, Watson's theorem states [130]:

$$F_\pi(s) = |F_\pi(s)|e^{i\delta(s)}, \tag{1.64}$$

where $\delta(s)$ is the elastic $\pi\pi$ phase shift. Moreover, the authors of [131] arrived at the following conclusion (the Maiani-Testa no-go theorem): in the infinite volume, the three-point correlation function in the timelike region involves the off-shell quantities that do not vanish in the Euclidean spacetime. This result will be discussed in Subsection 1.5.2.

The no-go theorem, however, is not relevant to the actual lattice simulations in which the observed energy spectrum is not a continuous, but a discrete one. For instance, the energy of two non-interacting pions in the CM frame is given by

$$E(\mathbf{p}) = 2\sqrt{M_\pi^2 + \mathbf{p}^2}, \qquad \mathbf{p} = \frac{2\pi}{L}\mathbf{n}, \quad \mathbf{n} \in \mathbb{Z}^3. \tag{1.65}$$

For a physical pion mass $M_\pi \approx 140$ MeV and lattice size $L \gtrsim 3$ fm, the level spacing is sizable. It means that each energy level can be clearly disentangled on the lattice.

The actual spectrum of the $\pi\pi$ system will deviate from the free one because of the meson interaction. It is a specific finite volume effect – there is a non-zero probability that two particles in a box are within the interaction range. These corrections where studied many years ago in the context of the non-ideal Bose gas [132]. In particular, for the ground state $\mathbf{p} = 0$, one finds

$$E = 2M_\pi - \frac{4\pi a_0}{M_\pi L^3}\left\{1 + d_1\frac{a_0}{L} + d_2\frac{a_0^2}{L^2}\right\} + O(L^{-6}), \tag{1.66}$$

where $a_0 = \lim\limits_{p\to 0} \tan\delta_0(p)/p$ is the S-wave scattering length in the channel with isospin $I = 0$ or $I = 2$. The coefficients d_1, d_2 take the values $d_1 \approx -2.83$, $d_2 \approx 6.38$. The crucial importance of this result is that the energy shift is determined entirely by the low-energy parameters of the two-body scattering amplitude. The final expression does not depend on the explicit form of the interaction potential. This fact can be explained as follows. The derivation of the formula assumes the large-L expansion. Since the meson interaction is short-ranged, the wave function describing the $\pi\pi$ scattering takes the asymptotic form inside the box. Its value is expressed through the phase shifts away from the interaction region. The periodic boundary conditions lead to the eigenvalue equation for the energy. This equation provides a relation between the on-shell quantities.

1.5.1 Lüscher's method

A general method to extract the partial-wave phase shifts from the volume dependence of the two-body energy spectrum was developed by Lüscher [133, 134]. The original derivation was based on the Schrödinger equation. Lüscher also proved that the result remains valid in quantum field theory. The non-relativistic EFT framework introduced above is equally well suited for the discussion of the method.

Let us first discuss the problem in 1+1 dimensions. Consider a non-relativistic model which describes the scattering of two identical, spinless particles of mass M. The asymptotic value of the wave function is given by

$$\psi(x) \propto e^{-ip|x|} + e^{2i\delta(p)}e^{ip|x|}\,, \tag{1.67}$$

where x denotes the relative distance between particles, and p is the relative 3-momentum, so that the total energy is $E = 2M + p^2/m$. The periodic boundary condition $\psi(0) = \psi(L)$ leads to a simple exact relation between the finite-volume energy value and the phase shift at this energy:

$$pL + 2\delta(p) = 2\pi n\,, \quad n \in \mathbb{Z}. \tag{1.68}$$

This equation is a one-dimensional analogue of the so-called Lüscher formula. By setting $\delta \equiv 0$, the spectrum of the free theory, $p_n = \frac{2\pi n}{L}$, is reproduced.

In contrast to Eq. (1.66), the formula Eq. (1.68) represents a non-perturbative result. It is also applicable in the vicinity of a resonance. If the resonance is narrow, the energy levels exbibit a peculiar behaviour referred to as the avoided level crossing. This is illustrated in Fig. 1.17. The curves reach a plateau at a certain energy $E = E_R$ which corresponds to the resonance mass. According to Eq. (1.33), the width of the resonance is given by the slope: $d\delta(p)/dE\Big|_{E=E_R} = 2/\Gamma_R$. In other words, for small volumes the ground state energy might agree well with the resonance mass. This fact explains, why the masses of the light resonances, such as ρ and K^*, determined by standard methods were in good agreement with experiment (Fig. 1.6). However, in large volumes the ground state energy will eventually

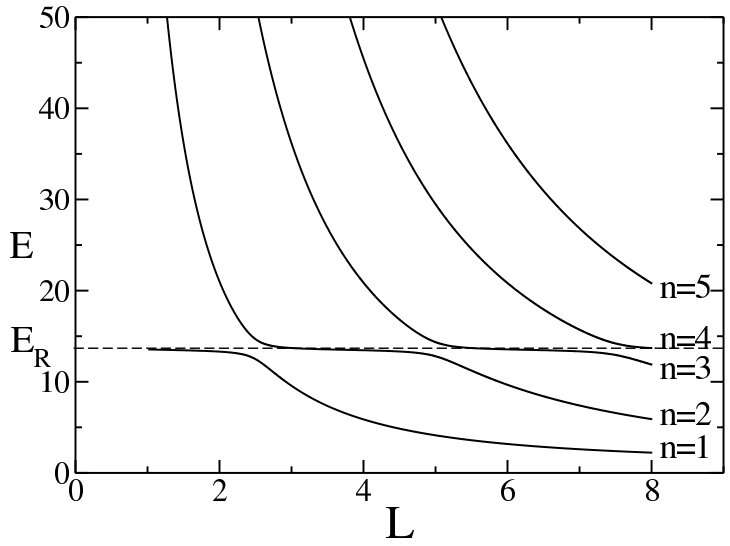

Figure 1.17: Energy levels of an interacting two-body system in the vicinity of a narrow resonance. The position of a plateau gives the resonance mass $E = E_R$ [135].

approach the free particle energy level.

Before proceeding to the three-dimensional problem, it is useful to derive the quantization condition, Eq. (1.68), in the non-relativistic EFT. The starting point is the LS equation given by Eq. (1.62). The partial wave index l can be omitted, and the scattering amplitude takes the form

$$T = \frac{1}{V_0^{-1}\cot\delta(p) - J(p)} \tag{1.69}$$

where the parameter V_0 is fixed by unitarity. Further, $J(p)$ denotes a one-loop integral [125]

$$J(p) = \int_{-\infty}^{\infty} \frac{dl}{2\pi} \frac{1}{2\sqrt{s}} \frac{1}{l^2 - p^2}\,. \tag{1.70}$$

which is related to the Green's function for the one-dimensional Schrödinger equation [136]. Performing the contour integration, one obtains

$$J(p) = \frac{i}{4\sqrt{s}p}\,, \qquad V_0 = 4\sqrt{s}p. \tag{1.71}$$

When the system is considered in a finite volume, the integral over 3-momentum has to be replaced by a discrete sum

$$J(p) \to J_L(p) = \frac{1}{2\sqrt{s}} \frac{1}{L} \sum_{n\in\mathbb{Z}} \frac{1}{\left(\frac{2\pi n}{L}\right)^2 - p^2}. \tag{1.72}$$

The interaction potential is not affected by the presence of a box since it contains the short-distance physics. There are also polarisation effects associated with the propagation of the virtual particles. The respective contributions, which are of order $O(e^{-M_\pi L})$, are assumed to be suppressed; as a rule of

thumb the condition $M_\pi L \gtrsim 4$ is usually applied. In fact, they are absent in the non-relativistic EFT since the respective momentum integrals vanish in dimensional regularization. The non-trivial volume dependence arises only when all particles in the intermediate states go on their mass-shells. Accordingly, the scattering amplitude in a finite volume T_L reads

$$T_L = \frac{4\sqrt{s}p}{\cot\delta(p) - 4\sqrt{s}p\, J_L(p)}\,. \tag{1.73}$$

It has simple poles which are the eigenvalues of the finite-volume Hamiltonian. These energy eigenvalues satisfy the equation

$$\delta(p) + \phi(q) = \pi n\,, \quad n \in \mathbb{Z}\,, \qquad \cot\phi(q) = -\frac{q}{\pi}\sum_{m\in\mathbb{Z}}\frac{1}{m^2-q^2}, \quad q = \frac{pL}{2\pi}\,. \tag{1.74}$$

The quantity $\cot\phi(q)$ has a certain relation to the Riemann zeta function $\zeta(n) = \sum_{k=1}^{\infty}\frac{1}{k^n}$. Indeed, it can be easily verified that $\sum_{m=1}^{\infty}\frac{1}{m^2-q^2} = -\sum_{n=0}^{\infty}\zeta(2n+2)q^{2n}$. The result of summation can be expressed through the trigonometric function: $\sum_{m\in\mathbb{Z}}\frac{1}{m^2-q^2} = -\frac{\pi}{q}\cot(\pi q)$. Accordingly, the quantization condition, Eq. (1.68), is reproduced within the non-relativistic EFT framework.

The transition to 3+1 dimensions is complicated by the lack of rotational symmetry. As a result, the admixture of the partial waves is inevitable. The partial-wave expansion of the scattering amplitude has to be modified:

$$\mathcal{T}(\mathbf{p}_3,\mathbf{p}_4;\mathbf{p}_1,\mathbf{p}_2) = 4\pi\sum_{lm,l'm'} T_{lm,l'm'}(s;\mathbf{P})\mathcal{Y}_{lm}(\mathbf{p}')\mathcal{Y}^*_{l'm'}(\mathbf{p})\,, \tag{1.75}$$

where $\mathbf{P}$ is a total 3-momentum which is quantized $\mathbf{P} = \frac{2\pi}{L}\mathbf{d}$, $\mathbf{d}\in\mathbb{Z}^3$. The LS equation becomes

$$T_{lm,l'm'}(s;\mathbf{P}) = -\delta_{lm,l'm'}V_l(s) - 4\pi\sum_{l''m''}V_l(s)\mathcal{X}_{lm,l''m''}T_{l''m'',l'm'}(s;\mathbf{P})\,. \tag{1.76}$$

The quantity $\mathcal{X}_{lm,l''m''}$ is a certain finite-volume counterpart of the one-loop integral Eq. (1.58). It can be brought to the form [137]

$$\mathcal{X}_{lm,l'm'} = \frac{|\mathbf{p}|^{l+l'+1}}{32\pi^2\sqrt{s}}\,i^{l-l'}\,M_{lm,l'm'}\,, \quad M_{lm,l'm'} = \frac{(-1)^l}{\pi^{3/2}\gamma}\sum_{j=|l-l'|}^{l+l'}\sum_{s=-j}^{j}\frac{i^j}{q^{j+1}}\,Z^{\mathbf{d}}_{js}(1;q^2)C_{lm,js,l'm'}\,, \tag{1.77}$$

with the Lorentz factor $\gamma = \sqrt{1+\mathbf{P}^2/s}$ and the dimensionless parameter $q = |\mathbf{p}|L/2\pi$. The coefficients $C_{lm,js,l'm'}$ are given in terms of Wigner $3j$-symbols

$$C_{lm,js,l'm'} = (-)^{m'}i^{l-j+l'}\sqrt{(2l+1)(2j+1)(2l'+1)}\begin{pmatrix} l & j & l' \\ m & s & -m'\end{pmatrix}\begin{pmatrix} l & j & l' \\ 0 & 0 & 0\end{pmatrix}. \tag{1.78}$$

The function $Z^{\mathbf{d}}_{js}(1;q^2)$ is defined as a sum

$$Z^{\mathbf{d}}_{js}(1,q^2) = \sum_{\mathbf{z}\in P_{\mathbf{d}}}\frac{\mathcal{Y}_{js}(\mathbf{z})}{\mathbf{z}^2-q^2}, \quad P_{\mathbf{d}} = \left\{\mathbf{z}\,\middle|\,\mathbf{z} = \gamma^{-1}\left(\mathbf{n}-\frac{1}{2}\,\boldsymbol{\Delta}\right),\,\mathbf{n}\in\mathbb{Z}^3\right\}, \quad \boldsymbol{\Delta} = \mathbf{d}\left(1+\frac{m_1^2-m_2^2}{s}\right). \tag{1.79}$$

It should be properly regularized for the numerical evaluation.

The scattering amplitude has simple poles which are the eigenvalues of the QCD Hamiltonian in a

finite volume. The system of linear equations Eq. (1.76) has singular solutions if the corresponding determinant vanishes. Using Eqs. (1.63,1.77), the determinant equation for the energy spectrum is given by

$$\det\left(M_{lm,l'm'} - \delta_{ll'}\delta_{mm'}\cot\delta_l\right) = 0. \tag{1.80}$$

This is the Lüscher formula for the spinless particles of unequal masses in a moving frame [138].

The obtained result is further simplified by studying the symmetry properties of the system. One has to classify all transformations which leave the spatial volume invariant. In general, the Lorentz boost deforms the cubic box to a rectangular parallelepiped. Accordingly, the symmetry group reduces to certain subgroups of the cubic group. The full group-theoretical analysis of the problem can be found in [139]. The partial diagonalization of the matrix M is achieved in the basis of a given irreducible representation (irrep) Γ of the symmetry group (Schur's lemma)

$$D^l:\ |lm\rangle \quad \longrightarrow \quad \Gamma:\ |\Gamma\alpha ln\rangle = \sum_m c_{lm}^{\Gamma\alpha n}|lm\rangle\,, \tag{1.81}$$

where $|lm\rangle$ are the basis vectors of an irreducible representation D^l of the rotation group of total angular momentum l. Further, α runs from 1 to the dimension of Γ, and n runs from 1 to $N(\Gamma, l)$, the number of occurrences of the irreducible representation Γ in D^l. The coefficients $c_{lm}^{\Gamma\alpha n}$ can be inferred from the tables in [139]. The Lüscher formula takes the form

$$\det\left(M^{\Gamma}_{ln,l'n'} - \delta_{ll'}\delta_{nn'}\ \cot\delta_l\right) = 0\,, \quad M^{\Gamma}_{ln,l'n'} = \sum_{mm'} c_{lm}^{\Gamma\alpha n\,*}\, c_{l'm'}^{\Gamma\alpha n'}\ M_{lm,l'm'}\,. \tag{1.82}$$

To apply Lüscher's method in practice, one has to set a cut-off on the angular momentum. If resonances are seen in the S- or P-waves, then it is plausible to neglect D- and higher partial waves. The justification of this is that the phase shifts $\delta_l(p)$ behave as $\delta_l(p) \sim p^{2l+1}$ in the vicinity of the elastic threshold. In general, however, it is impossible to avoid the admixture of the remaining partial waves. There are still particular cases, where the matrices M^{Γ} become diagonal. For instance, let us consider the irrep $\Gamma = A_1$ and the total momentum $\mathbf{d} = (0, 0, 1)$. For $l \le 1$, the matrix M^{A_1} reads [139]

$$M^{A_1} = \begin{pmatrix} w_{00} & \sqrt{3}iw_{10} \\ -\sqrt{3}iw_{10} & w_{00} + 2w_{20} \end{pmatrix}, \quad w_{lm} = \frac{1}{\pi^{3/2}\sqrt{2l+1}}\gamma^{-1}q^{-l-1}\,Z^{\mathbf{d}}_{lm}(1, q^2). \tag{1.83}$$

According to Eq. (1.79), the non-diagonal element w_{10} vanishes if the masses are equal $m_1 = m_2$, and/or in the limit $\mathbf{d} \to 0$. Therefore, the S- and P-waves can be determined separately. Setting $l = 0$ and $\mathbf{d} = 0$, the phase shift $\delta_0(p)$ satisfies the equation

$$\delta_0(p) + \phi(q) = \pi n\,, \quad n \in \mathbb{Z}\,, \qquad \cot\phi(q) = -\frac{1}{2\pi^2 q}\sum_{\mathbf{r}\in\mathbb{Z}^3}\frac{1}{\mathbf{r}^2 - q^2}\,. \tag{1.84}$$

It looks very similar to the one-dimensional formula Eq. (1.68), except that the sum can only be calculated only numerically.

The large-L limit of Eq. (1.84) reproduces the ground state energy of the two-particle system in a finite volume given by Eq. (1.66). The leading correction can be obtained as follows. Having in mind the S-wave $\pi\pi$ scattering, the free energy level $E = 2M_\pi$ corresponds to the limit $q \to 0$. Then, $\cot\phi(q) \approx \frac{1}{2\pi^2 q^3}$ to a good approximation. Using the effective-range expansion for the phase shift,

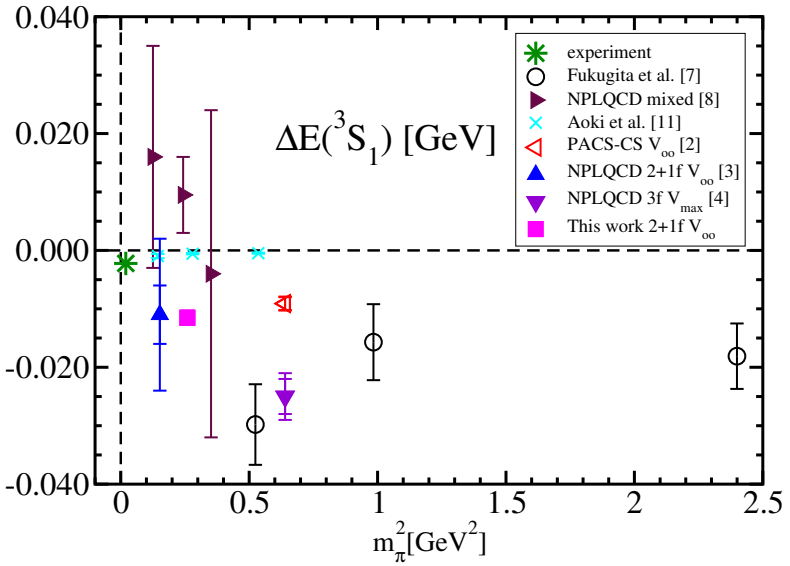

Figure 1.18: Binding energy of the deuteron at different values of the pion mass [140].

$p \cot \delta_0(p) \approx 1/a_0 + O(p^2)$, the Lüscher formula can be easily solved:

$$\frac{1}{pa_0} + \frac{1}{2\pi^2 q^3} = 0 \quad \Rightarrow \quad p^2 = -\frac{4\pi a_0}{L^3}\,. \tag{1.85}$$

Since $E = 2\sqrt{M_\pi^2 + p^2} = 2M_\pi + p^2/M_\pi + O(p^4)$, the leading term in the $1/L$ expansion, Eq. (1.66), is indeed reproduced. It is not difficult to obtain the sub-leading corrections as well [134]. The fact that the $\pi\pi$-system has energy below threshold is a final-volume effect. This has nothing to do with a two-body bound state which is observed in the infinite volume.

An interesting aspect of the Lüscher formula concerns its application to the study of the bound states in a finite volume. Such a possibility follows from the analytic properties of the scattering amplitude in the complex s-plane. The energy E_B of the S-wave two-body bound state in the infinite volume is a solution of the equation

$$i \cot \delta(p)\Big|_{p=i\gamma} = -1\,, \tag{1.86}$$

where γ denotes the binding momentum of the system, so that $E_B = 2\sqrt{M^2 - \gamma^2}$ in case of equal masses. In a finite volume, it is convenient to rewrite Eq. (1.84) using an alternative representation of the sum for imaginary values of the argument q:

$$i \cot \delta(p)\Big|_{p=i\kappa} = -1 + \sum_{\mathbf{m}\neq 0} \frac{1}{|\mathbf{m}|\kappa L}\, e^{-|\mathbf{m}|\kappa L}\,, \tag{1.87}$$

where κ is related to the finite-volume binding energy $E_B^{(L)} = 2\sqrt{M^2 - \kappa^2}$. To get this formula, the sum is transformed by first applying Poisson's resummation formula $\sum_{\mathbf{r}\in\mathbb{Z}^3} \delta^{(3)}(\mathbf{x} - \mathbf{r}) = \sum_{\mathbf{m}\in\mathbb{Z}^3} e^{i2\pi\mathbf{m}\cdot\mathbf{x}}$, and then performing the contour integration over the variable $\mathbf{x}$ for all $\mathbf{m} \neq 0$.

The shallow bound states are of particular interest. They have very small binding energy $|E_B - 2M|$ and binding momentum γ. A classical example is a deuteron consisting of a neutron and a proton. It has a

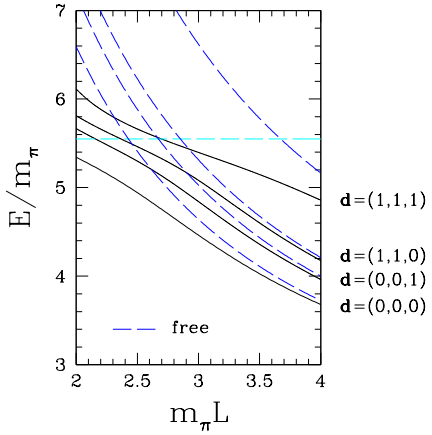

Figure 1.19: Energy levels of the $\pi\pi$-system from Lüscher formula with input experimental phase shift [139].

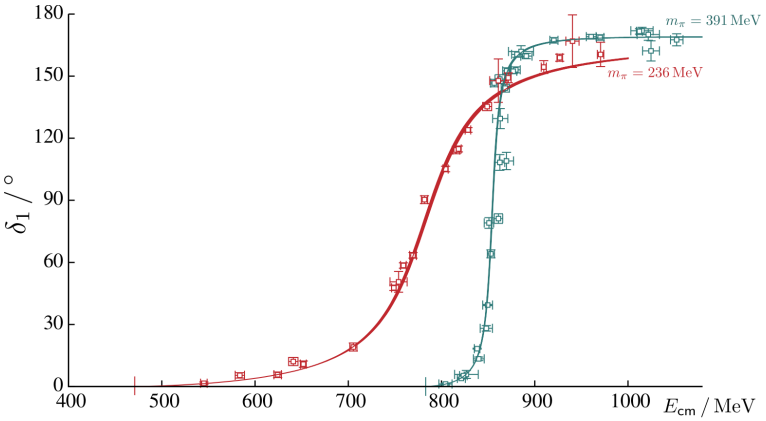

Figure 1.20: Lattice calculation of the elastic $I = 1, P = 1$ $\pi\pi$ phase shift for two different pion masses [146].

binding energy of 2.2 MeV and $\gamma_d \sim 40$ MeV. For such systems, Eq. (1.87) has an approximate solution

$$E_B^{(L)} = E_B - \frac{12\gamma}{ML(1 - r_0\gamma)} e^{-\gamma L} + O(e^{-\sqrt{2}\gamma L}), \tag{1.88}$$

This is precisely the result derived by Lüscher in the non-relativistic quantum mechanics [55]. It can be also expressed through asymptotic normalization coefficient A of the bound state wave function $\psi_B(r)$

$$\psi_B(r) = A\frac{e^{-\gamma r}}{\sqrt{4\pi}r}, \; r \to \infty\,, \qquad |A|^2 \approx \frac{2\gamma}{1 - r_0\gamma}\,. \tag{1.89}$$

As it is seen, while the polarization effects $\sim e^{-M_\pi L}$ are negligible, the finite-volume correction to the binding energy E_B is not suppressed since $\gamma \ll M$. This makes difficult to investigate the bound states with current lattices. Nevertheless, such calculations were performed [140–143], although at large pion masses $\sim 400 - 1000$ MeV. The results for the deuteron are summarized in Fig. 1.18.

Returning to the study of the resonances on the lattice, the $\rho(770)$ meson, which is a P-wave resonance, provides a testing ground of Lüscher's method [144]. Fig. 1.19 shows the finite-volume ground state energy levels of the $\pi\pi$-system for various total momenta $\mathbf{P}$ predicted by Lüscher formula with the experimental phase shift as input. The advantage of using moving frames becomes evident: many data points can be obtained at the same value of L [145]. To disentangle these energy levels, different types of interpolating fields are required, including the two-pion operators. Moreover, these operators have to transform according to a given irrep as discussed in [139].

Further, it is seen in Fig. 1.19 that the avoided level crossing is washed out, partly because the ρ is not narrow. Accordingly, the use of Lüscher's method becomes a necessity. The respective lattice calculations were done by many groups. The recent works include [147–150]. Many studies concentrate on the isospin $I = 1$ and $I = 2$ $\pi\pi$ scattering. In these channels the disconnected pieces are absent, at least in the isospin limit. The values of the $I = 1$ phase shift δ_1 obtained by Hadron Spectrum Collaboration are shown in Fig. 1.20. The curves exhibit a typical behaviour in the vicinity of the resonance. The latter is associated with the $\rho(770)$ meson. To determine the resonance parameters, the data is fitted, e.g., by effective range expansion or BW formula. The recent lattice data on the ρ meson mass m_ρ and the coupling constant $g_{\rho\pi\pi}$ are summarized in Fig. 1.21. The width can be found from the equation

$\Gamma = \frac{g^2_{\rho\pi\pi}}{48\pi m^2_\rho}(m^2_\rho - 4m^2_\pi)^{3/2}$.

Lüscher's method was subsequently generalized for an arbitrary number of open two-body channels, with arbitrary masses, spin and total momenta. The respective quantisation conditions which are valid for CM energy below the three-body inelastic threshold can be found in [151] and references therein.

The application of the method to baryon resonances, such as the $\Delta(1232)$, is more complicated, partly because of the signal-to-noise issues in the baryon correlation functions. One also has to make sure that available lattice volumes are suitable to cover the resonance region. Nevertheless, such calculations are underway and first results are expected in the near future [152]. At the same time, there is a progress in the study of the baryon-baryon systems, such as the low-energy nucleon-nucleon scattering [153, 154].

Until now, the discussion was confined to the finite volume formalism for two-body systems below inelastic thresholds. The latter can be understood as a limitation of Lüscher's method. For instance, the Roper resonance $N^*(1140)$ is genuinely inelastic – it decays to $N\pi\pi$ with a branching ratio 30 – 40%. The recent lattice study [155] indicates that this resonance should be generated in the coupled-channel scattering including the three-body process. Accordingly, it becomes mandatory to have a similar framework for the three-body problem in a finite volume.

The study of the three-body bound states seems to be a tractable problem. At least, this appears in a so-called unitary limit in which the two-body scattering length is much larger then the effective range $a \gg r_0$. Such systems are common in atomic physics, such as ^{4}He atoms. They exhibit interesting universal low-energy properties [156, 157]. In particular, three identical bosons form a sequence of bound states called Efimov states [158]. In the limit $a \to \infty$ the energy shift of a given bound state has a simple analytic form [159, 160], similar to Eq. (1.88),

$$\Delta E_B = -\frac{c\kappa^2|A|^2}{M(\kappa L)^{-3/2}} e^{-2\kappa L/\sqrt{3}} + \cdots , \tag{1.90}$$

where the ellipses stand for suppressed terms and the numerical constant $c \approx -96.4$. The quantity A denotes a three-body analogue of the asymptotic normalization coefficient and κ is the binding momentum. The infinite-volume three-body binding energy reads $E_B = \kappa^2/M$. It is worth mentioning that the presence of three-body interaction is encoded solely in the constant A.

The first step towards the formulation of the method was done in [161, 162]. It was shown that the three-body finite-volume spectrum is completely determined by the infinite volume scattering amplitude.

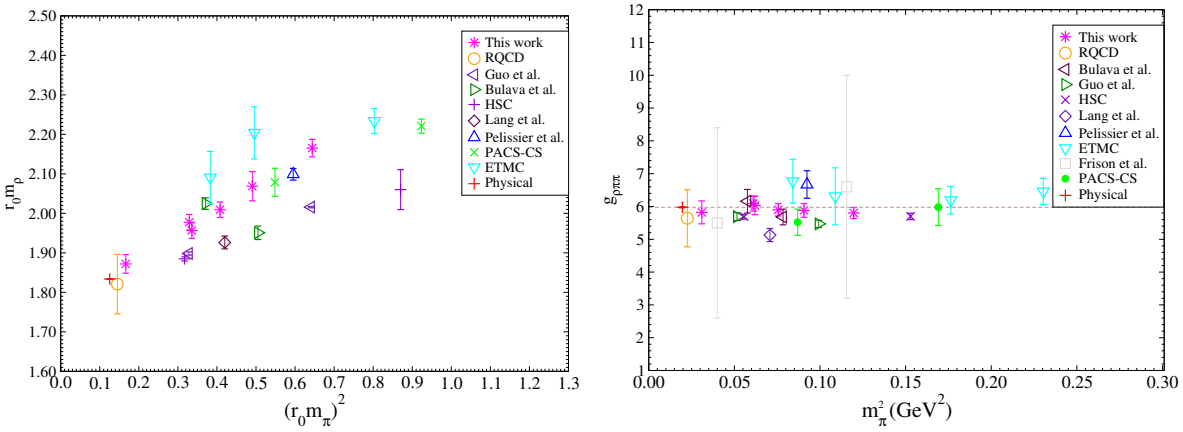

Figure 1.21: Summary of the recent work on the ρ meson parameters [147]. The masses m_π and m_ρ are scaled with the Sommer scale.

Despite further progress [163], it is still unclear how to apply the three-body quantisation condition for the analysis of the lattice data.

More recently, the authors of [164, 165] have proposed an equivalent, but simpler framework that is based on the non-relativistic EFT in the particle-dimer picture. They essentially follow a bottom-up approach: only a necessary number of the low-energy constants are included in the Lagrangian. The idea is that one fits this minimal set of the couplings to the finite-volume energy spectrum. At the next step, the three-body scattering amplitude can be determined numerically in the same non-relativistic EFT. This research direction should be further explored.

1.5.2 Electroweak processes

Lüscher's method provides a basis for the lattice study of the electroweak processes involving resonances. More generally, one has to investigate the consequence of the final-state interaction. Before proceeding with this topic, let us consider the content of the no-go theorem in more detail.

Having in mind the timelike form factor, one starts with the three-point correlation function in the *infinite volume*

$$C(t', t; \mathbf{k}) = \langle 0 \,|\, \Pi(\mathbf{k}, t)\, \Pi(-\mathbf{k}, t')\, J(0) \,|\, 0 \rangle \,, \tag{1.91}$$

where $t' > t > 0$ and the operator J has a non-zero overlap with two-pion states in S-wave. Also, $\Pi(\mathbf{k}, t)$ is a Fourier transform of the pion field operator:

$$\Pi(\mathbf{k}, t) = \int d^3x\, e^{-i\mathbf{k}\cdot\mathbf{x}}\, O_\pi(\mathbf{x}, t) \,. \tag{1.92}$$

Using the LSZ reduction formulas [166], it can be shown that in the limit $t' \gg t \gg 0$ the correlator $C(t', t; \mathbf{k})$ takes the form [131, 167]

$$C(t', t; \mathbf{k}) = \frac{Z\, e^{-E_\mathbf{k}(t+t')}}{(2E_\mathbf{k})^2} \left\{ \frac{1}{2} \Big[{}_{\text{out}}\langle \pi(\mathbf{k})\pi(-\mathbf{k}) \,|\, J(0) \,|0\rangle \;+\; {}_{\text{in}}\langle \pi(\mathbf{k})\pi(-\mathbf{k}) \,|\, J(0) \,|0\rangle \Big] + \; 2E_\mathbf{k} \mathcal{P}_\mathbf{k}(t') \right\}, \tag{1.93}$$

where *in* and *out* two-pion states are distinguished, and $E_\mathbf{k} = \sqrt{M_\pi^2 + \mathbf{k}^2}$. The quantity $\mathcal{P}_\mathbf{k}(t')$ can be written as follows:

$$\mathcal{P}_\mathbf{k}(t') = -\sum_n \mathcal{P} \left(\frac{1}{E_n(E_n - 2E_\mathbf{k} - i\varepsilon)} \right) {}_{\text{out}}\langle\, n \,|\, J(0) \,|0\rangle\, T^*\, e^{-(E_n - 2\,E_\mathbf{k})t'} \,, \tag{1.94}$$

where the summation/integral is performed over two-pion intermediate states. Here, $\mathcal{P}$ stands for the principal value,

$$\frac{1}{x - i\varepsilon} = i\pi\delta(x) + \mathcal{P}\frac{1}{x}. \tag{1.95}$$

The quantity T is an off-shell matrix element; in the on-shell limit $E_n \to 2E_\mathbf{k}$ it reduces to the S-wave scattering amplitude of the process $\pi(k_1) + \pi(k_2) \to n(p_n)$,

$$(2\pi)^4 \delta^{(4)}(p_n - k_1 - k_2)\, (iT(\mathbf{k}, -\mathbf{k}; n)) = {}_{\text{out}}\langle m \,|\pi(\mathbf{k})\pi(-\mathbf{k})\,\rangle_{\text{in}} - {}_{\text{out}}\langle m \,|\pi(\mathbf{k})\pi(-\mathbf{k})\,\rangle_{\text{out}} \,. \tag{1.96}$$

In Minkowski space the correlation function is obtained by replacing $t \to it$ in the exponentials. Using Eq. (1.95), the quantity $\mathcal{P}_\mathbf{k}(t')$ is split into two terms. The first term can be evaluated by contour integration after expanding the integration range to $(-\infty, \infty)$. Indeed for positive and large t, one can close the contour in the lower-half plane. Since the pole $E_n = 2E_\mathbf{k} + i\varepsilon$ is located outside this contour,

the integral becomes zero. The remaining contribution from $\delta(E_n - 2E_{\mathbf{k}})$ gives the expected result for the correlator

$$C(t', t; \mathbf{k}) = \frac{Z\, e^{-E_{\mathbf{k}}(t+t')}}{(2E_{\mathbf{k}})^2}\ {}_{\text{out}}\langle \pi(\mathbf{k})\pi(-\mathbf{k}) \,|\, J(0)\,|0\rangle \quad \text{(Minkowski)}\,. \tag{1.97}$$

In Euclidean space, however, the exponent $\exp(-E_n t')$ does not allow one to integrate by contours. Accordingly, there is a non-zero contribution from the off-shell amplitude. Moreover, $\mathcal{P}_{\mathbf{k}}(t')$ will dominate the correlator since its leading behaviour for $t' \to \infty$ is governed by the divergent factor $\sim \exp(2(E_{\mathbf{k}} - M_\pi)t')$. Finally, the matrix element ${}_{\text{out}}\langle \pi(\mathbf{k})\pi(-\mathbf{k}) \,|\, J(0)\,|0\rangle$ can not be determined on the lattice since the energy spectrum is continuous.

The problem drastically simplifies in a finite volume, where the energy levels are discrete. The spectrum E_n, $n = 0, 1, \ldots$, satisfies the Lüscher formula. In this case the matrix element $\langle E_n|\, J(0)\,|0\rangle$ is a well defined quantity on the lattice. The solution was given by Lellouch and Lüscher in their work on the weak $K \to \pi\pi$ decays [168]. They established a simple relation between the corresponding finite-volume matrix elements and the physical kaon-decay amplitudes. The heuristic derivation of the result proceeds as follows [167]. Instead of Eq. (1.91), it is convenient to consider a slightly different correlation function in a *finite volume*

$$C(t) = \int\limits_V d^3x\, \langle\, 0\,|J(\vec{x}, t)J(0)\,|\,0\,\rangle\,, \tag{1.98}$$

where the volume $V = L^3$ is taken to be asymptotically large. On the one hand, $C(t)$ obeys the spectral decomposition in terms of the infinite volume matrix elements

$$C(t) \xrightarrow{V\to\infty} \frac{\pi}{2(2\pi)^3} \int \frac{dE}{E} e^{-Et} |\langle 0|J(0)|\pi\pi, E\rangle|^2\, p(E)\,, \tag{1.99}$$

where $p(E) = \sqrt{\frac{E^2}{4} - M_\pi^2}$. On the other side, inserting the completeness relation $\sum_n |\pi\pi, n\rangle\langle\pi\pi, n| = 1$, one has

$$C(t) = V \sum_n |\langle 0|J(0)|\pi\pi, n\rangle_V|^2 e^{-E_n t} \xrightarrow{V\to\infty} V \int dE\, \rho_V(E)\, |\langle 0|J(0)|\pi\pi, E\rangle_V|^2 e^{-Et}\,, \tag{1.100}$$

where $|\pi\pi, n\rangle_V$ and $|\pi\pi, E\rangle_V$ denote the finite-volume two-pion states at fixed n and fixed energy E, respectively. The purpose of the function $\rho_V(E)$ is to provide the correspondence between finite volume sums and infinite volume integrals. This quantity can be naively interpreted as the density of states at energy E. It then follows from the Lüscher formula, Eq. (1.84), that

$$\rho_V(E) = \frac{dn}{dE} = \frac{\phi'(q) + \delta_0'(p)}{4\pi p} E\,, \tag{1.101}$$

where the derivatives are taken with respect to the variable p. The case of the operator J that has a non-zero overlap with one-particle states $|\mathbf{k}\rangle$ with mass M, can be considered along the same lines. A comparison of Eqs. (1.99) and (1.100) provides the following correspondence

$$|\pi\pi, E\rangle \Leftrightarrow 4\pi \sqrt{\frac{VE\rho_V(E)}{p(E)}}\, |\pi\pi, E\rangle_V\,, \quad |\mathbf{k} = 0\rangle \Leftrightarrow \sqrt{2MV}\, |\mathbf{k} = 0\rangle_V\,. \tag{1.102}$$

Next, these expressions can be used to obtain the matrix elements of any local operator. In particular the original Lellouch-Lüscher (LL) formula for the $K \to \pi\pi$ is reproduced. As discussed in [167], the

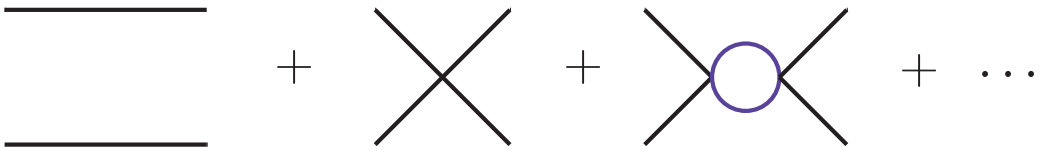

Figure 1.22: Diagrammatic representation of the two-point function in the non-relativistic EFT. The bubble integrals are evaluated in a finite volume.

obtained formula can be also applied in small volumes, in which there are only few energy levels below the inelastic thresholds. The polarization effects, however, still have to be exponentially suppressed. Having that in mind, the scalar form factor in the timelike region can be determined from the equation

$$|\langle \pi\pi, E_n|\, J(0)\,|0\rangle|^2 = \left.\frac{4\pi V E^2\,\{\delta_0'(p)+\phi'(q)\}}{p^2}\right|_{E=E_n} |\langle E_n|J(0)|0\rangle|^2\,. \tag{1.103}$$

where all quantities on the right-hand side are evaluated at $E = E_n$. The proportionality factor in Eq. (1.103) accounts for the different normalizations of the particle states in finite and infinite volume.

The non-relativistic EFT provides a more systematic method to obtain the LL formula for a given electroweak process. To simplify the discussion, it is convenient to consider again the scalar form factor in the timelike region. The effective Lagrangian in Eq. (1.54) has to be supplemented by the term which describes the interaction of the pions with the external scalar field $A(x)$,

$$\mathcal{L}_A = gA(x)J(x) = gA(x)\frac{1}{2}[\Phi^\dagger\Phi^\dagger + \Phi\Phi] + \cdots \tag{1.104}$$

where the ellipses stand for terms containing space derivatives. Further, one defines a two-pion operator,

$$O_n(x_0;\mathbf{k}) = \sum_{\mathbf{k}\in\Omega_n}\int_0^L d^3\mathbf{x}\, d^3\mathbf{y}\, e^{i\mathbf{k}(\mathbf{x}-\mathbf{y})}\,\Phi(x_0,\mathbf{x})\Phi(x_0,\mathbf{y})\,, \quad \Omega_n = \left\{\mathbf{k} = \frac{2\pi\mathbf{z}}{L}\,,\ \mathbf{z}^2 = n^2\right\}\,, \tag{1.105}$$

which creates the energy eigenstate $|\pi\pi, E_n\rangle$ from the vacuum. At the next step, suitable two- and three-point correlation functions are evaluated in perturbation theory. The calculation is performed in Euclidean space, so that the finite-volume free propagator is given by

$$0|T\Phi(x)\Phi^\dagger(y)|0\rangle = \int\frac{dp_0}{2\pi}\,\frac{1}{L^3}\sum_{\mathbf{p}}\frac{e^{ip_0(x_0-y_0)+i\mathbf{p}(\mathbf{x}-\mathbf{y})}}{2w(\mathbf{p})(w(\mathbf{p})+ip_0)}\,, \qquad w(\mathbf{p}) = \sqrt{M_\pi^2+\mathbf{p}^2}\,. \tag{1.106}$$

The two-point function has a spectral representation

$$D(x_0-y_0;\mathbf{k}) \equiv \langle 0|O_n(x_0;\mathbf{k})O_n^\dagger(y_0;\mathbf{k})|0\rangle = \sum_n |\langle 0|O_n(0;\mathbf{k})|E_n\rangle|^2 e^{-E_n(x_0-y_0)}\,, \quad x_0 > y_0 \tag{1.107}$$

On the other hand, the matrix element on the left-hand side of this equation can be calculated in perturbation theory. The relevant diagrams are shown in Fig. 1.22. After summing them up, the matrix element takes the form

$$D(x_0-y_0;\mathbf{k}) = \frac{\nu_n^2 L^3}{\eta}\int_{-\infty}^{\infty}\frac{dP_0}{2\pi}\,e^{iP_0(x_0-y_0)}\left\{\frac{-iL^3}{4w^2(\mathbf{k})(P_0-2iw(\mathbf{k}))} - \frac{T_L(P_0)}{(4w^2(\mathbf{k}))^2(P_0-2iw(\mathbf{k}))^2}\right\}, \tag{1.108}$$

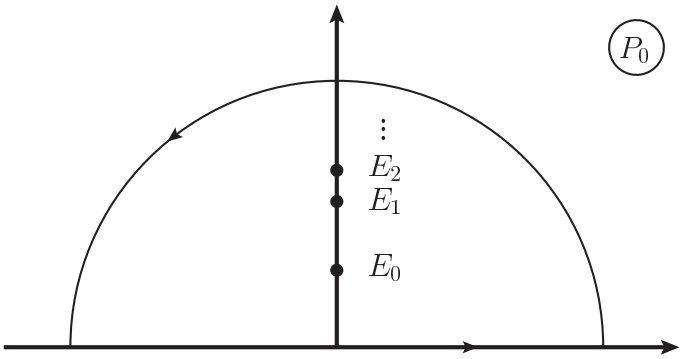

Figure 1.23: Integration contour for the two-point function in a finite volume.

where ν_n denotes the number of different vectors $\mathbf{z}$ which satisfy the condition $\mathbf{z}^2 = n^2$. The symmetry factor $\eta = \frac{1}{2}$ was pulled out. The first term in Eq. (1.108) corresponds to the free propagation of the pions. Further, $T_L(P_0)$ is the S-wave scattering amplitude in a finite volume,

$$T_L(P_0) = \frac{8\pi\sqrt{s}}{p\cot\delta(p) + p\cot\phi(q)}\,, \quad p = \sqrt{\frac{s}{4} - M_\pi^2}\,, \quad s = -P_0^2. \tag{1.109}$$

The form of the $T_L(P_0)$ in the vicinity of the simple pole $P_0 = iE_n$ can be easily found:

$$T_L(P_0) = \frac{32\pi\sin^2\delta(p_n)}{\delta'(p_n) + \phi'(q_n)}\,\frac{1}{E_n + iP_0} + \cdots\,, \tag{1.110}$$

where the Lüscher formula was used.

The integral in Eq. (1.108) is evaluated using Cauchy's theorem. The integration contour is shown in Fig. 1.23. It important that the free pole $P_0 = 2iw(\mathbf{k})$ does not contribute to the two-point function, but only the poles of the T-matrix do. Indeed, recall that $T_L(P_0)$ is a solution of the LS equation $T_L = V(1 + G_L T_L)$, where G_L denotes the finite-volume counterpart of the one-loop integral in Eq. (1.57). Obviously, the function G_L has a pole in the vicinity of $P_0 = 2iw(\mathbf{k})$. To satisfy the LS equation, the scattering amplitude has to vanish in the limit $P_0 \to 2iw(\mathbf{k})$,

$$T_L(P_0) = -iL^3 4w^2(\mathbf{k})(P_0 - 2iw(\mathbf{k})) + \cdots\,. \tag{1.111}$$

Accordingly, the free poles are exactly cancelled in the integrand of Eq. (1.108).

Performing the integration over P_0 and comparing the result with Eq. (1.107), one obtains

$$|\langle 0|\mathcal{O}_n(0;\mathbf{k})|E_n\rangle| = \left(\frac{64\pi V\sin^2\delta(p_n)}{\delta'(p_n) + \phi'(q_n)}\right)^{1/2}\frac{1}{4w^2(\mathbf{k})}\,\frac{1}{|E_n - 2w(\mathbf{k})|}\,. \tag{1.112}$$

The calculation of the three-point function proceeds along the same lines. The starting point is the matrix element

$$\langle 0|\mathcal{O}_n(x_0;\mathbf{k})\,\mathcal{L}_A(0)|0\rangle = gA(0)F_n(x_0;\mathbf{k})\,, \qquad x_0 > 0\,, \tag{1.113}$$

which has the spectral representation

$$\langle 0|\mathcal{O}_n(x_0;\mathbf{k})\,\mathcal{L}_A(0)|0\rangle = gA(0)\sum_n e^{-E_n x_0}\langle 0|\mathcal{O}_n(0;\mathbf{k})|E_n\rangle\langle E_n|J(0)|0\rangle\,. \tag{1.114}$$

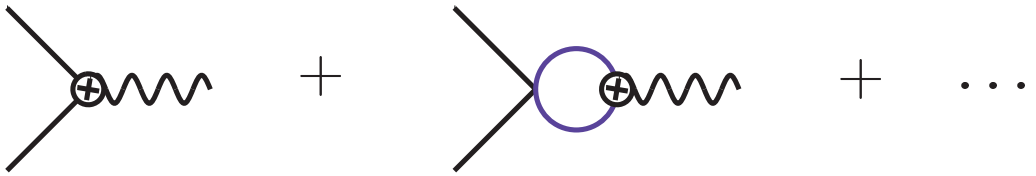

Figure 1.24: Three-point function in the non-relativistic EFT.

The diagrams which contribute to the quantity $F_n(x_0;\mathbf{k})$ are shown in Fig. 1.24. Summing up all bubbles yields

$$F_n(x_0;\mathbf{k}) = \nu_n \int_{-\infty}^{\infty} \frac{dP_0}{2\pi i}\, e^{iP_0 x_0}\, \frac{T_L(P_0)V_0^{-1}}{4w^2(\mathbf{k})(P_0 - 2iw(\mathbf{k}))}\, \bar{F}(P_0)\,, \tag{1.115}$$

where $V_0^{-1} = \frac{p}{8\pi\sqrt{s}} \cot\delta(p)$. The quantity $\bar{F}(s)$ denotes the sum of all two-particle irreducible diagrams. It is proportional to the amplitude of the pair creation from the vacuum in the presence of the field $A(x)$. The precise form of the relation is obtained after summing up all diagrams in Fig. 1.24, but in the *infinite* volume:

$${}_{\text{out}}\langle\pi\pi, E|J(0)|0\rangle \equiv F(E), \qquad F(E) = T(E)V_0^{-1}\bar{F}(E) = e^{i\delta_0(p)}\bar{F}(E)\cos\delta_0(p)\,. \tag{1.116}$$

This is nothing but the statement of the Watson theorem, Eq. (1.64).

The contour integration in Eq. (1.115) leads to the expression

$$F_n(x_0;\mathbf{k}) = \sum_n \frac{e^{-E_n x_0}}{4w^2(\mathbf{k})(2w(\mathbf{k}) - E_n)}\, \frac{4p\bar{F}(E_n)\cot\delta(p_n)\sin^2\delta(p_n)}{(\delta'(p_n) + \phi'(q_n))E_n}\,. \tag{1.117}$$

Using this result together with Eqs. (1.112), (1.116) and (1.114), one gets the analogue of the LL formula for the scalar form factor in the timelike region:

$$|F(E_n)| = \sqrt{\frac{4\pi V E_n^2\,\{\delta_0'(p_n) + \phi'(q_n)\}}{p_n^2}}\,|\langle E_n|J(0)|0\rangle|\,. \tag{1.118}$$

This expression coincides exactly with Eq. (1.103). It enables one do determine the absolute value of the scalar form factor in the timelike region from the finite-volume current matrix element $\langle E_n|J(0)|0\rangle$. The phase of the form factor is just the S-wave scattering phase shift $\delta_0(p)$.

The result of Lellouch and Lüscher was subsequently generalized to include multiple strongly-coupled decay channels [169–171] as well as the spin [172]. It was also applied in the lattice study of the direct CP violation in the $K \to \pi\pi$ decay [173]. The described approach can be also used in case of a resonant final-state interaction. In particular, Hadron Spectrum Collaboration performed the first exploratory lattice calculation of the resonant amplitude for $\pi\gamma^* \to \rho \to \pi\pi$ [174]. The respective value of the cross section is shown in Fig. 1.25.

A simple conclusion can be drawn in the approximation of an infinitely narrow resonance with a Breit-Wigner form. In this limit the derivative of the phase shift explodes, while the quantity $\phi'(q_n)$ stays finite and thus can be neglected. According to Eq. (1.37), the scalar form factor is proportional to the

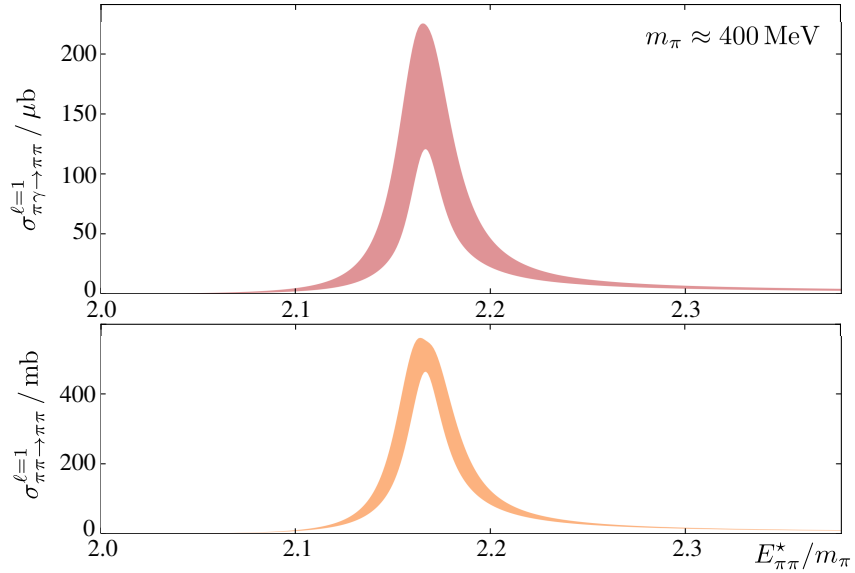

Figure 1.25: Lattice determination of the $\pi^+\gamma \to \pi^+\pi^0$ cross section as a function of the $\pi\pi$ CM energy. The lower panel shows the $l = 1$ elastic $\pi\pi$ scattering cross section [174].

resonance matrix element. Combining both expressions, one obtains

$$F_R(E_{\mathrm{BW}}) = 2E_{\mathrm{BW}}\, V\langle E_{\mathrm{BW}}|J(0)|0\rangle\,, \tag{1.119}$$

where E_{BW} denotes the mass of the BW resonance. The kinematic factor properly accounts for the normalization of states. This is precisely the result which is expected when the resonance becomes stable. A similar formula is applicable to the two-body bound state. However, the comment after Eq. (1.37) concerning the definition of the resonance matrix element should be kept in mind.

1.6 External field method

The finite volume formalism is a main tool to study the electroweak processes involving final-state interactions and resonances. At the same time, there are other types of hadronic processes which can be investigated on the lattice by using different approaches. An important case is Compton scattering.

The low-energy Compton scattering plays an indispensable role in probing the electromagnetic structure of hadrons [175]. The non-linear hadronic response to an applied electromagnetic field is quantified by the electric α, magnetic β as well as higher-order polarizabilities. In particular, the Euclidean space non-relativistic effective Lagrangian, which describes the gauge-invariant interaction of the nucleon $\Psi(\mathbf{x}, t)$ of mass M and charge q with an *external* electromagnetic field $A_\mu(x)$, is given by

$$\mathcal{L}_{\mathrm{eff}}(A) = \Psi^\dagger(\mathbf{x}, t)\left[\left(\frac{\partial}{\partial t} + i\,q\,A_4\right) + \frac{(-i\boldsymbol{\nabla} - q\,\mathbf{A})^2}{2M} - \mu\,\boldsymbol{\sigma}\cdot\mathbf{B} + 2\pi\left(\alpha\,\mathbf{E}^2 - \beta\,\mathbf{B}^2\right)\right]\Psi(\mathbf{x}, t) + \cdots\,, \tag{1.120}$$

where $\mathbf{B}$ and $\mathbf{E}$ denote the magnetic and electric field, respectively. Further, μ is the magnetic moment and the $\boldsymbol{\sigma}$ vector collects the Pauli matrices. The dots stand for the terms containing time derivatives of the external field and higher-order operators. The parameters of this Lagrangian can be directly related to the coefficients in the low-energy expansion of the real Compton scattering amplitude.

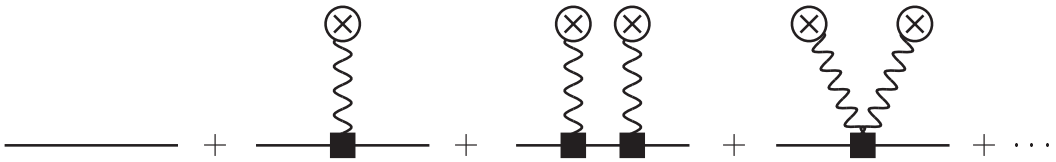

Figure 1.26: Expansion of the hadron two-point function in an external field [176].

The Lagrangian in Eq. (1.120) corresponds to the Schrödinger equation for the spin-1/2 particle in an external $U(1)$ field. In case of a time-independent uniform magnetic field, there are stationary solutions and the ground state energy takes the form

$$E_{j_z}(\mathbf{B}) = \left(n_L + \frac{1}{2}\right)\frac{|q\mathbf{B}|}{M} - \mu j_z |\mathbf{B}| - 2\pi\beta |\mathbf{B}|^2 + O(|\mathbf{B}|^3), \tag{1.121}$$

where $j_z = \pm 1/2$, $n_L \geq 0$ is the quantum number of the Landau level. The $\mathbf{B}$ field is chosen along the third axis. Accordingly, the lattice measurement of the nucleon ground state energy enables one to determine the low-energy structure of the Compton scattering amplitude.

The external field method is based on the observation that three- and four-point correlation functions can be determined by studying the behavior of the nucleon two-point function in a weak background electromagnetic field [177, 178]. In particular, the Compton tensor appears as a second-order term in the expansion in A, as illustrated in Fig. 1.26. The implementation of the external $U(1)$ field on the lattice is straightforward. In present lattice calculations the sea quarks do not couple to this field. Accordingly, it is sufficient to perform the following replacement of the SU(3) links after generation of the gauge configurations:

$$U_\mu(x) \to U_\mu(x) e^{iaA_\mu(x)}. \tag{1.122}$$

By a suitable choice of the external field, one can access different low-energy parameters of real Compton scattering. For instance, Fig. 1.27 shows the energy shift of the nucleon ground state in the presence of a constant magnetic field. Since the gauge links satisfy periodic boundary conditions, the magnetic field can take only the discrete values [180]:

$$\mathbf{B} = \frac{6\pi}{eL^2}\tilde{n}\mathbf{e}_z, \quad \tilde{n} \in \mathbb{Z}. \tag{1.123}$$

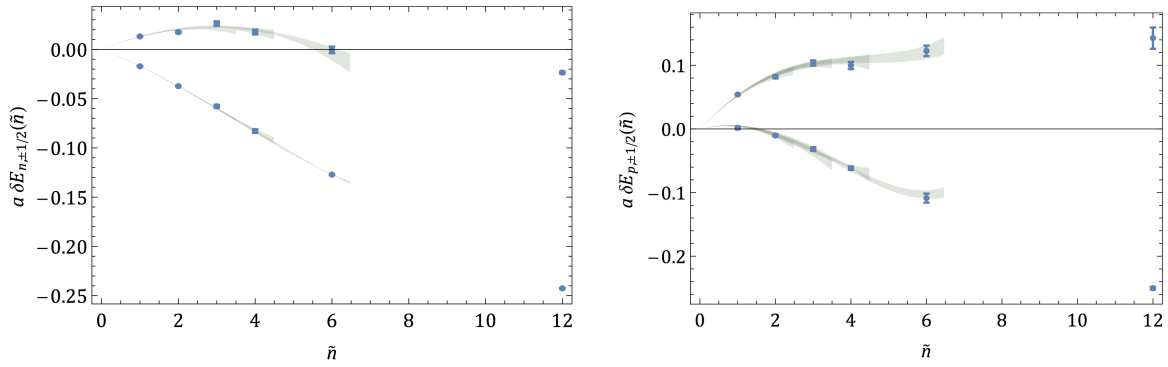

Figure 1.27: Energy shifts induced in each spin state of the neutron (left plot) and proton (right plot) by the uniform magnetic field [179].

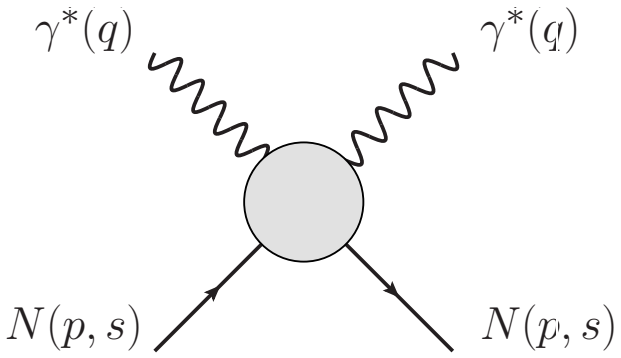

Figure 1.28: Doubly virtual nucleon Compton scattering

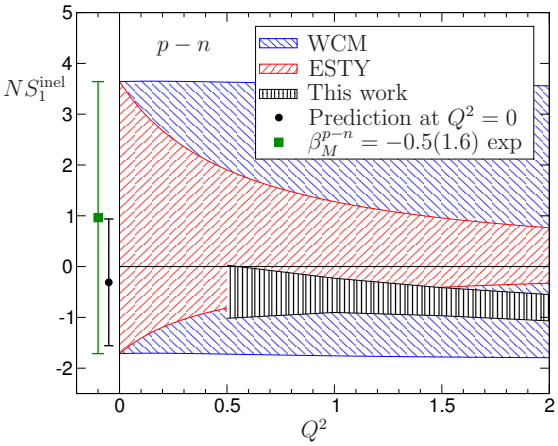

Figure 1.29: Momentum dependence of the subtraction function. The broad bands are obtained from the phenomenological parametrizations. The comparatively narrow grey band follows from the Reggeon dominance hypothesis [184].

The outlined method is applicable to a more general case of the doubly virtual Compton scattering $\gamma^* N \to \gamma^* N$. This process contributes to the Lamb shift in the muonic hydrogen [181] as well as to the electromagnetic piece of the neutron-proton mass difference [182]. In both cases one is interested in the spin-averaged forward scattering amplitude (Fig. 1.28). It is defined in terms of the two spin-independent amplitudes T_1, T_2,

$$\frac{1}{2}\sum_s \frac{i}{2}\int d^4x e^{iq\cdot x}\langle p,s|TJ^\mu(x)J^\nu(0)|p,s\rangle = T_1(\nu,q^2)K_1^{\mu\nu} + T_2(\nu,q^2)K_2^{\mu\nu}\,, \tag{1.124}$$

where q^2 denotes the photon virtuality, $\nu \equiv p\cdot q/m$ and $K_i^{\mu\nu}$, $i=1,2$, are known tensor structures [183].

The experimental data on the structure functions completely determine the amplitude T_2. The fixed-q^2 dispersion relation for the amplitude T_1, however, requires a subtraction. Moreover, the subtraction function $S_1 \equiv T_1(0,q^2)$ remains unknown. In principle, its elastic part is essentially given by the Born terms, but the inelastic piece is known only at the real photon point $q^2=0$ (low-energy theorem, [184]).

There are several approaches to fix the subtraction function, such as the chiral EFTs and phenomenological parametrizations [185, 186]. More recently, the authors of [184] have been able to determine its value by imposing the so-called Reggeon dominance hypothesis. They assume that the forward scattering amplitude does not contain any fixed pole, corresponding in the Regge language to the angular momentum $J=0$. In Regge theory, such a pole generates the energy-independent contribution to the amplitude.

The meaning of the $J=0$ fixed pole can be illustrated by a simple model [187]. The propagation of a spinless particle of mass M in the s-channel gives the following contribution to the amplitude

$$A(s,M) = \frac{M^2}{s-M^2}. \tag{1.125}$$

The factor M^2 ensures that in the limit of the point-like interaction $M\to\infty$ the amplitude remains finite The s-channel exchange can be represented as an infinite series of t-channel exchanges of different spins.

This duality is established by applying the Taylor expansion in Eq. (1.125); for $s < M^2$, one gets

$$A(s < M^2, M) = \sum_{J \geq 0} (-1)^J \left(-\frac{s^2}{M^2} \right)^J \tag{1.126}$$

The term of type s^{2J} is contained in the propagator of the spin-J particle in the t-channel, in accordance with the Feynman rules for particles of an arbitrary spin [188]. Hence, the point-like interaction, obtained in the limit $M^2 \to \infty$, corresponds to the exchange of an object with spin $J = 0$.

The results on the inelastic part of the subtraction function obtained in different approaches are shown in Fig. 1.29. In particular, the relatively narrow grey band indicates the calculation of [184]. Clearly, these determinations suffer from systematic uncertainties that are difficult to estimate.

In order to verify the Reggeon dominance hypothesis, lattice simulations provide a model-independent framework. The question whether there is a fixed pole in the Compton scattering is of conceptual interest. The subtraction function can be calculated within the external field method. For that purpose, a properly chosen external field configuration is required. The Compton scattering off pions might provide a good starting point to investigate the feasibility of the whole approach.

To summarize, lattice calculations of the two-point correlation function in the external (background) electromagnetic fields enable one to determine the electromagnetic properties of the nucleon and light nuclei. At the same time, the extracted quantities, such as the magnetic moments and polarizabilities, serve to parametrize the low-energy real Compton scattering. The freedom of choosing the external field configuration opens the possibility to investigate some important aspects of the doubly virtual Compton scattering as well.

List of publications

The present thesis is based on the following publications in international peer-reviewed journals:

- **A. Agadjanov**, V. Bernard, U.-G. Meißner and A. Rusetsky, “A framework for the calculation of the $\Delta N\gamma^*$ transition form factors on the lattice," Nucl. Phys. **B886**, 1199-1222 (2014).
- **A. Agadjanov**, V. Bernard, U.-G. Meißner and A. Rusetsky, “The $B \to K^*$ form factors on the lattice," Nucl. Phys. **B910**, 387-409 (2016).
- **A. Agadjanov**, U.-G. Meißner and A. Rusetsky, “Nucleon in a periodic magnetic field,” Phys. Rev. **D95**, 031502 (2017).

The third paper is supplemented by a section that contains an extended derivation of the main result.

Conference proceedings:

- A. Rusetsky, **A. Agadjanov**, V. Bernard and U.-G. Meißner, “The $\Delta N\gamma^*$ transition form factors on the lattice,” PoS LATTICE 2014, 169 (2014).
- **A. Agadjanov**, V. Bernard, U.-G. Meißner and A. Rusetsky, “Radiative decays of resonances on the lattice,” AIP Conf. Proc. 1701, 040001 (2016) .
- **A. Agadjanov**, V. Bernard, U.-G. Meißner and A. Rusetsky, “Resonance matrix elements on the lattice,” EPJ Web Conf. 112, 01001 (2016).
- A. Rusetsky, **A. Agadjanov**, V. Bernard and U.-G. Meißner, “$B \to K^*$ decays in a finite volume,” PoS LATTICE 2016, 313 (2016).
- **A. Agadjanov**, “Rare B meson decays on the lattice,” EPJ Web Conf. 137, 06001 (2017).

CHAPTER 2

Resonant pion production $\gamma^* N \to \pi N$

2.1 Summary

This work concerns the pion photo(electro)production in the vicinity of the $\Delta(1232)$ resonance. The knowledge on the respective $\Delta N\gamma^*$ transition form factors, in particular, is important to determine the quark transition charge density which could be visualized.

At present, the lattice data of these form factors are obtained at relatively large unphysical pion masses, so that the Δ is treated as a stable particle. Moreover, the applicability of the chiral EFTs to extrapolate the results down to the physical point is not guaranteed. Accordingly, it is timely to have a theoretical framework for the extraction of the form factors in case of the unstable Δ. The finite volume formalism is the right approach to tackle the problem.

The obtained results can be summarized as follows:

- The analogue of the Lellouch-Lüscher formula for the pion photo(electro)production amplitude is derived.
- The field-theoretical definition of the resonance matrix elements is formulated.
- The prescription for the pole extraction of the $\Delta N\gamma^*$ form factors is provided.
- The group-theoretical analysis of the problem is done (inclusion of spin, kinematics and partial-wave mixing).
- The limit of an infinitely narrow Δ resonance is considered. It is explicitly verified that the two definitions of the form factors converge into one.

Available online at www.sciencedirect.com

ScienceDirect

Nuclear Physics B 886 (2014) 1199–1222

www.elsevier.com/locate/nuclphysb

A framework for the calculation of the $\Delta N\gamma^*$ transition form factors on the lattice

Andria Agadjanov [a,b,*], Véronique Bernard [c], Ulf-G. Meißner [a,d], Akaki Rusetsky [a]

[a] *Helmholtz-Institut für Strahlen- und Kernphysik (Theorie) and Bethe Center for Theoretical Physics, Universität Bonn, D-53115 Bonn, Germany*

[b] *St. Andrew the First-Called Georgian University of the Patriarchate of Georgia, Chavchavadze Ave. 53a, 0162 Tbilisi, Georgia*

[c] *Institut de Physique Nucléaire, CNRS/Univ. Paris-Sud 11 (UMR 8608), F-91406 Orsay Cedex, France*

[d] *Institute for Advanced Simulation (IAS-4), Institut für Kernphysik (IKP-3) and Jülich Center for Hadron Physics, Forschungszentrum Jülich, D-52425 Jülich, Germany*

Received 20 May 2014; received in revised form 22 July 2014; accepted 25 July 2014

Available online 30 July 2014

Editor: Hong-Jian He

Abstract

Using the non-relativistic effective field theory framework in a finite volume, we discuss the extraction of the $\Delta N\gamma^*$ transition form factors from lattice data. A counterpart of the Lüscher approach for the *matrix elements* of unstable states is formulated. In particular, we thoroughly discuss various kinematic settings, which are used in the calculation of the above matrix element on the lattice. The emerging Lüscher–Lellouch factor and the analytic continuation of the matrix elements into the complex plane are also considered in detail. A full group-theoretical analysis of the problem is made, including the partial-wave mixing and projecting out the invariant form factors from data.

1. Introduction

In recent years, the calculation of the $\Delta N\gamma^*$ transition form factors on the lattice has been carried out, see Refs. [1–3]. The electromagnetic, axial and pseudoscalar form factors of the

* Corresponding author.

http://dx.doi.org/10.1016/j.nuclphysb.2014.07.023

Δ-resonance have been also studied [4,5]. It should be noted, however, that in these simulations the quark mass values are large enough so that the Δ is a stable particle and thus using the standard formalism for the analysis of the lattice data on these form factors is justified. On the other hand, lattice simulations with physical quark masses have already been performed. At such quark masses, the Δ is not stable anymore and the data should be analyzed properly to extract the parameters of the resonance (see, e.g., [6]).

It is well known that resonances cannot be identified with isolated energy levels in lattice QCD simulations which are necessarily performed in a finite volume. In order to determine the mass and width from the measured spectrum, one first extracts the scattering phase shift by using the Lüscher equation [7]. At the next step, using some parameterization for the K-matrix (e.g., the effective-range expansion), a continuation into the complex energy plane is performed. Resonances correspond to the poles of the scattering T-matrix on the second Riemann sheet, and the real and imaginary parts of the pole position define the mass and the width of a resonance. This is a pretty standard procedure that has been used in a number of recent papers [8–10]. A generalization of the approach to moving frames has been first proposed in Ref. [11], and a full group-theoretical analysis of the Lüscher equation in moving frames, including the issues related to the scattering of the spin-non-zero particles, has been carried out, e.g., in Refs. [12–18]. An alternative, albeit a closely related procedure consists in fitting the data to the energy spectrum by using unitarized ChPT in a finite volume [19–21]. The above approach qualitatively amounts to a parameterization of the K-matrix through the solution of the equations of the unitarized ChPT (in the infinite volume) that may *a priori* have a larger range of applicability than the effective-range expansion. Note also that the approach has been generalized to the multichannel scattering case [22–28]. An analysis of the two-channel case has been carried already out for the toy model in $1+1$ dimensions [29] and should now be applied in physically interesting cases. Further, using twisted boundary conditions [30–32] to facilitate the accurate extraction of the resonance parameters has been advocated, e.g., in Refs. [19,20,23], and the possibility of the partial twisting has been investigated in Refs. [31,33,34]. Last but not least, recently an extension of the Lüscher approach to the 3-particle case has been proposed by several groups [35–38], albeit there is still much more work required in this direction.

As one sees from the above discussion, up to date the framework for the extraction of the resonance parameters (the mass and the width) from lattice data is well established (at least, for the resonances that do not decay into three or more particles). For the calculation of the more complicated quantities, e.g., the resonance form factors, the old approach that treats the resonance as a stable state, is still widely used, albeit it is clear that the same problems arise also here. What one needs is a *generalization of the Lüscher finite-volume approach to the form factors.* In our recent papers [39,40], we have formulated such a generalization, considering the form factor of a spinless resonance. The procedure of extracting the resonance form factor from the *form factors of the eigenstates of the Hamiltonian*, which are actually measured on the lattice, closely resembles the procedure of extracting the resonance pole position and also implies the analytic continuation into the complex energy plane by using, e.g., the effective range expansion. There are, however, differences as well. Most notably, as was shown in Ref. [40], in $3+1$ dimensions, due to the presence of the so-called finite fixed points, the procedure of the analytic continuation and taking the infinite-volume limit is no more straightforward and measuring the form factor for at least two different energy levels is required, in order to achieve an unambiguous extraction of the resonance form factor.

The present paper is a continuation and the generalization of Refs. [39,40] in two aspects:

(i) In Refs. [39,40], an elastic resonance form factor (an example: the electromagnetic form factor $\Delta\Delta\gamma^*$) has been considered. In this paper, we address transition form factors, in particular, $\Delta N\gamma^*$ that is more interesting from the phenomenological point of view. It turns out that the presence of one stable particle in the out-state (here, the nucleon) leads to crucial simplifications. As we shall demonstrate, the finite fixed points do not exist in this case, so the measurement of a single energy level (albeit at several volumes) will suffice. We shall discuss in detail various lattice settings, which provide an access to the measurement of the form factor.
(ii) All particles and currents, considered in Refs. [39,40], were scalar. On the other hand, the particles, whose form factors we want to calculate, have spin. In this paper, we consider the inclusion of spin into the formalism and carry out a full group-theoretical analysis of the obtained equations along the lines described in Ref. [16].

The paper is organized as follows. In Section 2, we start from defining the resonance form factor in the infinite volume and discuss the analytic continuation into the complex plane. The projection of various scalar form factors will be considered. In Section 3 we consider the kinematics, which should be used for measuring the matrix elements of a current between the eigenstates of the Hamiltonian. This issue is very important for performing the analytic continuation of the above matrix element, *keeping the relative three-momentum of the photon and nucleon fixed*. Further, in Section 4, we calculate these matrix elements within the non-relativistic effective field theory (EFT) and demonstrate that the finite fixed points are absent, when one of the external particles is stable. The initial-state interactions, which manifest themselves in the Lüscher–Lellouch factor, should be properly included in order to take into account the difference in normalization of the matrix elements in the infinite and in a finite volume. In Section 5 we collect all bits and pieces and formulate a prescription for the extraction of the resonance transition form factor from data. Section 6 contains our conclusions. Finally, in Appendix A, the formulae for the partial-wave expansion of the photoproduction amplitudes are displayed.

2. Resonance form factor in the infinite volume

To the best of our knowledge, the procedure for calculating the matrix elements of operators between the bound state vectors in field theory has been first addressed in Ref. [41] (a very detailed and transparent discussion of the problem can be found in Ref. [42]). In short, the procedure boils down to the following. For simplicity, consider the scalar case first. Let $|P\rangle$ be a stable bound state moving with a four-momentum P_μ with $P_\mu P^\mu = M_B^2$. The fact that this is a bound state and not an elementary state is equivalent to the statement that $\langle 0|\phi(x)|P\rangle = 0$, where $\phi(x)$ stands for any field which is present in the Lagrangian. Consider now an operator $O(X)$ built from the elementary fields ϕ. The operator $O(X)$ can be either local or non-local. In the latter case, X denotes the center-of-mass coordinate of the fields entering in $O(X)$. The only requirement on this operator is that $\langle 0|O(X)|P\rangle \neq 0$. The Fourier-transform of the two-point function of the operators O has a pole at $P^2 = M_B^2$:

$$i\int d^4X e^{iPX}\langle 0|T\,O(X)\bar{O}(0)|0\rangle = \frac{Z_B}{M_B^2 - P^2} + \text{regular terms at } P^2 \to M_B^2, \tag{2.1}$$

where Z_B is the wave function renormalization constant of the bound state (for the scalar operators, considered here, the conjugated operator $\bar{O} = O^\dagger$).

Let us now consider the three-point function with any local operator J (the "current"). This function has a double pole

$$F(P,Q) = i^2 \int d^4X d^4Y e^{iPX - iQY} \langle 0|T\,O(X)J(0)\bar{O}(Y)|0\rangle = \frac{Z_B^{1/2}}{M_B^2 - P^2}\langle P|J(0)|Q\rangle \frac{Z_B^{1/2}}{M_B^2 - Q^2} + \cdots, \tag{2.2}$$

where the ellipses stand for the less singular terms. From this equation one immediately sees that the matrix element of a current J between the bound state vectors is defined through

$$\langle P|J(0)|Q\rangle = \lim_{P^2, Q^2 \to M_B^2} Z_B^{-1}\big(M_B^2 - P^2\big)\big(M_B^2 - Q^2\big)F(P,Q). \tag{2.3}$$

Due to the Lorenz-invariance, the matrix element in the l.h.s. of this equation is a function of a single scalar variable $t = (P-Q)^2$.

Note also that the expression given in Eq. (2.3) defines the matrix element between bound states. In a completely similar manner, it is possible to define the matrix elements between a bound state and an elementary state, or between two different bound states – all differences boil down to the proper choice of the operators O.

In case of a *resonance* rather than a bound system, no corresponding single-particle state exists in the Fock space. In the literature, one encounters two different approaches to the problem. One approach, which implies the definition of the form factor from the amplitudes measured at *real energies,* invokes the Breit–Wigner parameterization of the resonant amplitude and extracts the resonance formfactors at the energy where the scattering phase shift passes through 90°. Within the second approach, the resonance form factor is defined through the continuation to the resonance pole position in the complex plane, as described below. Let $O(X)$ be the operator with the quantum numbers of a resonance. The two-point function of the operators O develops a pole on the unphysical Riemann sheet in the complex plane

$$i \int d^4X e^{iPX} \langle 0|T\,O(X)\bar{O}(0)|0\rangle = \frac{Z_R}{s_R - P^2} + \text{regular terms at } P^2 \to s_R, \tag{2.4}$$

where the quantities s_R, Z_R are now complex. The real and imaginary parts of $E_R = \sqrt{s_R}$ give the mass and the half-width of the resonance, respectively.

Further, the three-point function develops a double pole in the complex plane, and the *resonance matrix element* of any current J is still defined by a formula similar to Eq. (2.3):

$$\langle P|J(0)|Q\rangle = \lim_{P^2, Q^2 \to s_R} Z_R^{-1}\big(s_R - P^2\big)\big(s_R - Q^2\big)F(P,Q). \tag{2.5}$$

We would like to stress that the quantity on the l.h.s. of Eq. (2.5) is a mere notation for the matrix element: there exists no isolated resonance state $|P\rangle$ in the spectrum. Again, due to the Lorentz-invariance, this quantity is a function of a single variable $t = (P-Q)^2$.

The following questions arise naturally in connection to the procedure described above:

(i) Is it not possible to avoid the analytic continuation into the complex energy plane?
(ii) Experiments can only be performed for real energies. How does one perform the analytic continuation of the experimental data?

In brief, answers to these question are:

(i) Relating the form factor to the measured scattering amplitudes by using, e.g., the Breit–Wigner parameterization, yields a model-dependent result, since the background is not known. Consequently, the form factor, extracted at the real energies, will be process-dependent. This problem does not arise, when an analytic continuation to the resonance pole is performed. The resonance matrix elements extracted through the analytic continuation, are the quantities that characterize the resonance itself and not the process where they were determined.

(ii) The analytic continuation of the experimental data (e.g., in order to extract the magnetic moment of a Δ-resonance) is, in general, a very difficult procedure and is severely limited by the experimental uncertainties. However, the goal is still worth trying, see the arguments above.

It should be mentioned that both definitions of the form factor: on the real axis (see, e.g., [43, 44]) as well as at the resonance pole [45], have been already used for the analysis of the experimental data (the latter work contains also the comparison of the resonance parameters, extracted by using different methods). In order to make it possible to compare lattice calculations with all existing experimental results, in this paper we provide the formulae which should be used on the real axis, as well as in the complex energy plane. Here we stress once more that only the definition, based on the analytic continuation, yields a resonance form factor that is devoid of any process-dependent ambiguities. Further, it will be explicitly demonstrated that both methods yield the same result in the limit of the infinitely small width.

Up to now, all particles and operators considered were scalars. In order to include the resonances of a generic spin, we follow closely the procedure of Ref. [46]. Let $O_\alpha(X)$ be the interpolating field for a resonance. Here, α denotes the collection of indices characterizing a resonance with spin (Dirac indices, vector indices). The two-point function in the vicinity of the resonance pole has the following behavior:

$$i\int d^4X e^{iPX}\langle 0|T\,O_\alpha(X)\bar{O}_\beta(0)|0\rangle = \frac{Z_R P_{\alpha\beta}(P,s_R)}{s_R - P^2} + \text{regular terms at } P^2 \to s_R, \qquad (2.6)$$

where $P_{\alpha\beta}$ denotes the projector on the positive energy "states"

$$P_{\alpha\beta} = \sum_\varepsilon u_\alpha(P,\varepsilon)\bar{u}_\beta(P,\varepsilon), \qquad (2.7)$$

where the sum runs over spin projections on the third axis (ε) and $u_\alpha(P,\varepsilon)$ denotes the solution of the free wave equation for a particle with a given spin.

Below, we shall give a construction of $u_\alpha(P,\varepsilon)$ in case of the spin-1/2 and spin-3/2 particles. In case of the spin-1/2 particle, this quantity is given by [46]:

$$u(P,1/2) = \sqrt{P^0 + E_R}\begin{pmatrix} 1 \\ 0 \\ \frac{P^3}{P^0+E_R} \\ \frac{P^1+iP^2}{P^0+E_R} \end{pmatrix},$$

$$u(P,-1/2)=\sqrt{P^0+E_R}\begin{pmatrix}0\\1\\\frac{P^1-iP^2}{P^0+E_R}\\\frac{-P^3}{P^0+E_R}\end{pmatrix},$$
$$\bar{u}(P,1/2)=\sqrt{P^0+E_R}\left(1,0,\frac{-P^3}{P^0+E_R},\frac{-(P^1-iP^2)}{P^0+E_R}\right),$$
$$\bar{u}(P,-1/2)=\sqrt{P^0+E_R}\left(0,1,\frac{-(P^1+iP^2)}{P^0+E_R},\frac{P^3}{P^0+E_R}\right). \tag{2.8}$$

These spinors obey the Dirac equations with the complex "mass" $P^2=s_R$

$$(\not{P}-E_R)u(P,\varepsilon)=0,\qquad \bar{u}(P,\varepsilon)(\not{P}-E_R)=0 \tag{2.9}$$

as well as the identities

$$\sum_{\varepsilon}u(P,\varepsilon)\bar{u}(P,\varepsilon)=(\not{P}+E_R),\qquad \bar{u}(P,\varepsilon)u\left(P,\varepsilon'\right)=2E_R\delta_{\varepsilon\varepsilon'}. \tag{2.10}$$

Note, however, that, if E_R and P_μ are complex quantities, then, in general,

$$\bar{u}(P,\varepsilon)\neq u(P,\varepsilon)^\dagger\gamma_0. \tag{2.11}$$

In case of a particle with a spin-3/2, one has to construct the solutions of the Rarita–Schwinger equation with a complex "mass". To this end, we define three vectors $\mathbf{e}_\omega$ with $\omega=\pm1,0$:

$$\mathbf{e}_{+1}=-\frac{1}{\sqrt{2}}\begin{pmatrix}1\\i\\0\end{pmatrix},\qquad \mathbf{e}_0=\begin{pmatrix}0\\0\\1\end{pmatrix},\qquad \mathbf{e}_{-1}=\frac{1}{\sqrt{2}}\begin{pmatrix}1\\-i\\0\end{pmatrix},$$
$$\bar{\mathbf{e}}_{+1}=-\frac{1}{\sqrt{2}}(1,-i,0),\qquad \bar{\mathbf{e}}_0=(0,0,1),\qquad \bar{\mathbf{e}}_{-1}=\frac{1}{\sqrt{2}}(1,i,0). \tag{2.12}$$

Further, define

$$f^\mu(P,\omega)=\left(\frac{\mathbf{e}_\omega\cdot\mathbf{P}}{E_R},\mathbf{e}_\omega+\frac{\mathbf{P}(\mathbf{e}_\omega\cdot\mathbf{P})}{E_R(P^0+E_R)}\right),$$
$$\bar{f}^\mu(P,\omega)=\left(\frac{\bar{\mathbf{e}}_\omega\cdot\mathbf{P}}{E_R},\bar{\mathbf{e}}_\omega+\frac{\mathbf{P}(\bar{\mathbf{e}}_\omega\cdot\mathbf{P})}{E_R(P^0+E_R)}\right). \tag{2.13}$$

The Rarita–Schwinger wave functions are given by group-theoretical expressions corresponding to the addition of spins 1 and 1/2:

$$u^\mu(P,\lambda)=\sum_{\omega,\varepsilon}\langle1\omega1/2\varepsilon|3/2\lambda\rangle f^\mu(P,\omega)u(P,\varepsilon),$$
$$\bar{u}^\mu(P,\lambda)=\sum_{\omega,\varepsilon}\langle1\omega1/2\varepsilon|3/2\lambda\rangle\bar{u}(P,\varepsilon)\bar{f}^\mu(P,\omega), \tag{2.14}$$

with $\langle\ldots\rangle$ the appropriate Clebsch–Gordan coefficients. These wave functions obey the equations

$$(\not{P}-E_R)u^\mu(P,\lambda)=0,\qquad P_\mu u^\mu(P,\lambda)=\gamma_\mu u^\mu(P,\lambda)=0,$$
$$\bar{u}^\mu(P,\lambda)(\not{P}-E_R)=0,\qquad \bar{u}^\mu(P,\lambda)P_\mu=\bar{u}^\mu(P,\lambda)\gamma_\mu=0, \tag{2.15}$$

and the identities

$$\sum_{\lambda} u^{\mu}(P,\lambda)\bar{u}^{\nu}(P,\lambda) = -\frac{\not{P}+E_R}{2E_R}\left(g^{\mu\nu} - \frac{1}{3}\gamma^{\mu}\gamma^{\nu} - \frac{2P^{\mu}P^{\nu}}{3E_R^2} + \frac{P^{\mu}\gamma^{\nu} - P^{\nu}\gamma^{\mu}}{3E_R}\right),$$
$$\sum_{\mu} \bar{u}^{\mu}(P,\lambda)u_{\mu}\left(P,\lambda'\right) = -2E_R\delta_{\lambda\lambda'}. \tag{2.16}$$

Below, we shall restrict ourselves to the case of the $\Delta N\gamma^*$ transition. However, the formalism can be directly generalized to particles with any spin. The three-point function for this transition takes the form

$$F^{\mu\rho}(P,Q) = i^2\int d^4X d^4Y e^{iPX - iQY}\langle 0|T\,O^{\mu}(X)J^{\rho}(0)\bar{\psi}(Y)|0\rangle$$
$$= \frac{Z_R^{1/2}}{s_R - P^2}\frac{Z_N^{1/2}}{m_N^2 - Q^2}\sum_{\lambda,\varepsilon} u^{\mu}(P,\lambda)\langle P,\lambda|J^{\rho}(0)|Q,\varepsilon\rangle\bar{u}(Q,\varepsilon) + \cdots. \tag{2.17}$$

Here, $O^{\mu}(X)$ and $\psi(Y)$ denote the Δ and nucleon interpolating field operators, respectively, J^{ρ} is the electromagnetic current, s_R is the Δ-resonance pole position in the complex plane, and m_N is the nucleon mass. The sum runs over the Δ and nucleon spin projections: $\lambda = -3/2, -1/2, 1/2, 3/2$ and $\varepsilon = -1/2, 1/2$. As already stated after Eq. (2.5), the matrix element that appears on the r.h.s. of the above equation is a mere notation: there is no stable Δ-state in the Fock space of the theory. We shall use this notation throughout the paper.

Projecting out the matrix element from Eq. (2.17), we get

$$\langle P,\lambda|J^{\rho}(0)|Q,\varepsilon\rangle = \lim_{P^2\to s_R,\, Q^2\to m_N^2}\frac{Z_R^{-1/2}}{2E_R}\frac{Z_N^{-1/2}}{2m_N}\left(s_R - P^2\right)\left(m_N^2 - Q^2\right)$$
$$\times\,\bar{u}_{\mu}(P,\lambda)F^{\mu\rho}(P,Q)u(Q,\varepsilon). \tag{2.18}$$

This matrix element can be expressed in terms of three scalar form factors (see, e.g., [47,48])

$$\langle P,\lambda|J^{\rho}(0)|Q,\varepsilon\rangle = \left(\frac{2}{3}\right)^{1/2}\bar{u}_{\mu}(P,\lambda)\left\{G_M(t)\mathcal{K}_M^{\mu\rho} + G_E(t)\mathcal{K}_E^{\mu\rho} + G_C(t)\mathcal{K}_C^{\mu\rho}\right\}$$
$$\times\,u(Q,\varepsilon), \tag{2.19}$$

where[1]

$$\mathcal{K}_M^{\mu\rho} = -\frac{3}{(E_R+m_N)^2 - t}\frac{E_R+m_N}{2m_N}\epsilon^{\mu\rho\alpha\nu}p_{\alpha}q_{\nu},$$
$$\mathcal{K}_E^{\mu\rho} = -\mathcal{K}_M^{\mu\rho} + 6i\Delta^{-1}(t)\frac{E_R+m_N}{m_N}\gamma_5\epsilon^{\mu\sigma\alpha\beta}p_{\alpha}q_{\beta}\epsilon^{\rho\omega\nu\delta}g_{\sigma\omega}p_{\nu}q_{\delta},$$
$$\mathcal{K}_C^{\mu\rho} = 3i\Delta^{-1}(t)\frac{E_R+m_N}{m_N}\gamma_5 q^{\mu}\left(q^2p^{\rho} - (q\cdot p)q^{\rho}\right), \tag{2.20}$$

and

$$p = \frac{1}{2}(P+Q), \qquad q = P - Q,$$
$$\Delta(t) = \left((E_R+m_N)^2 - t\right)\left((E_R-m_N)^2 - t\right). \tag{2.21}$$

[1] For the Dirac matrices, we use the conventions of Ref. [49].

$K_{M,E,C}$ are, respectively, the magnetic dipole, electric quadrupole and Coulomb (longitudinal) quadrupole covariants. In order to determine these three scalar form factors separately, it is convenient to work in a special kinematics. We choose both 3-momenta $\mathbf{P}$ and $\mathbf{Q}$ along the third axis. Further, the formulae simplify considerably in the rest-frame of the resonance $\mathbf{P} = 0$. Below, we shall adopt this choice.

Using Eqs. (2.19) and (2.20), it is straightforward to show that, in the rest-frame of the Δ-resonance,

$$\begin{aligned}
&\langle 1/2|J^3(0)|1/2\rangle = i\frac{E_R - Q^0}{E_R} A G_C(t),\\
&\langle 1/2|J^+(0)|-1/2\rangle = -i\sqrt{\frac{1}{2}} A\big(G_M(t) - 3G_E(t)\big),\\
&\langle 3/2|J^+(0)|1/2\rangle = -i\sqrt{\frac{3}{2}} A\big(G_M(t) + G_E(t)\big),
\end{aligned} \tag{2.22}$$

where

$$J^+(0) = \frac{J^1(0) + iJ^2(0)}{\sqrt{2}}, \qquad A = \frac{E_R + m_N}{2m_N}\sqrt{2E_R\big(Q^0 - m_N\big)}. \tag{2.23}$$

Further, it can be shown that the following field operators

$$\begin{aligned}
O_{3/2}(X) &= \frac{1}{2}(1+\Sigma_3)\frac{1}{2}(1+\gamma_0)\frac{1}{\sqrt{2}}\big(O^1(X) - i\Sigma_3 O^2(X)\big),\\
O_{1/2}(X) &= \frac{1}{2}(1-\Sigma_3)\frac{1}{2}(1+\gamma_0)\frac{1}{\sqrt{2}}\big(O^1(X) + i\Sigma_3 O^2(X)\big),\\
\tilde{O}_{1/2}(X) &= \frac{1}{2}(1+\Sigma_3)\frac{1}{2}(1+\gamma_0)O^3(X)
\end{aligned} \tag{2.24}$$

produce the Δ-particles with spin projection $\lambda = 3/2$ and $\lambda = 1/2$, respectively. Here, Σ_3 denotes the 4×4 matrix, describing the spin projection on the third axis. In terms of the Pauli matrices, it is given by $\Sigma_3 = \mathrm{diag}(\sigma_3, \sigma_3)$. Note also that the operators $O_{3/2}$ and $O_{1/2}$, $\tilde{O}_{1/2}$ belong to the different irreducible representations (irreps), G_2 and G_1, respectively, of the little group of the double cover of the cubic group, corresponding to the boost momentum along the third axis [16]. Moreover, there are two different operators that correspond to the spin projection $\lambda = 1/2$, whereas there exists only one operator for the projection $\lambda = 3/2$, see Eqs. (113) and (114) of Ref. [16].

The field operators, projecting onto the states with a given third component of the nucleon, are constructed trivially:

$$\bar{\psi}_{\pm 1/2}(Y) = \bar{\psi}(Y)\frac{1}{2}(1 \pm \Sigma_3)\frac{1}{2}(1+\gamma_0). \tag{2.25}$$

Using the above operators, we may construct the following three-point functions:

$$\begin{aligned}
\tilde{F}_{1/2}(P,Q) &= i^2\int d^4X d^4Y e^{iPX - iQY}\langle 0|T\,\tilde{O}_{1/2}(X)J^3(0)\bar{\psi}_{1/2}(Y)|0\rangle,\\
F_{1/2}(P,Q) &= i^2\int d^4X d^4Y e^{iPX - iQY}\langle 0|T\,O_{1/2}(X)J^+(0)\bar{\psi}_{-1/2}(Y)|0\rangle,\\
F_{3/2}(P,Q) &= i^2\int d^4X d^4Y e^{iPX - iQY}\langle 0|T\,O_{3/2}(X)J^+(0)\bar{\psi}_{1/2}(Y)|0\rangle.
\end{aligned} \tag{2.26}$$

In the vicinity of the double pole, these functions behave as

$$\begin{aligned}
\mathrm{Tr}\big(\tilde{F}_{1/2}(P,Q)\big) &= i\left(\frac{2}{3}\right)^{1/2}\frac{Z_R^{1/2}}{s_R-P^2}\,\frac{Z_N^{1/2}}{m_N^2-Q^2}\,\frac{E_R-Q^0}{E_R}\,BG_C(t)+\cdots,\\
\mathrm{Tr}\big(F_{1/2}(P,Q)\big) &= i\left(\frac{2}{3}\right)^{1/2}\frac{Z_R^{1/2}}{s_R-P^2}\,\frac{Z_N^{1/2}}{m_N^2-Q^2}\,\frac{1}{2}\,B\big(G_M(t)-3G_E(t)\big)+\cdots,\\
\mathrm{Tr}\big(F_{3/2}(P,Q)\big) &= i\left(\frac{2}{3}\right)^{1/2}\frac{Z_R^{1/2}}{s_R-P^2}\,\frac{Z_N^{1/2}}{m_N^2-Q^2}\,\frac{3}{2}\,B\big(G_M(t)+G_E(t)\big)+\cdots,
\end{aligned}\tag{2.27}$$

where the trace is performed over the Dirac indices, and

$$B=\frac{E_R(E_R+m_N)}{m_N}|\mathbf{Q}|.\tag{2.28}$$

So, with a special choice of the interpolating operators, the problem of a particle with spin boils down to the spinless case, considered in the beginning of this section. The three form factors G_C, G_M, G_E can be projected out individually.

3. Extracting the form factors on the lattice

Below, we adapt the formulae of the previous section and formulate the rules for projecting out the form factors G_C, G_M, G_E from the Euclidean Green functions on the lattice. Let us first restrict ourselves to the case when the Δ is stable and consider the following three-point functions at $t'>0$, $t<0$:

$$\begin{aligned}
\tilde{R}_{1/2}(t',t) &= \langle 0|\tilde{\mathcal{O}}_{1/2}(t')J^3(0)\bar{\psi}^{\mathbf{Q}}_{1/2}(t)|0\rangle,\\
R_{1/2}(t',t) &= \langle 0|\mathcal{O}_{1/2}(t')J^+(0)\bar{\psi}^{\mathbf{Q}}_{-1/2}(t)|0\rangle,\\
R_{3/2}(t',t) &= \langle 0|\mathcal{O}_{3/2}(t')J^+(0)\bar{\psi}^{\mathbf{Q}}_{1/2}(t)|0\rangle,
\end{aligned}\tag{3.1}$$

where

$$\begin{aligned}
\tilde{\mathcal{O}}_{1/2}(t') &= \sum_{\mathbf{X}}\tilde{O}_{1/2}(\mathbf{X},t'),\\
\mathcal{O}_{1/2}(t') &= \sum_{\mathbf{X}}O_{1/2}(\mathbf{X},t'),\\
\mathcal{O}_{3/2}(t') &= \sum_{\mathbf{X}}O_{3/2}(\mathbf{X},t'),\\
\bar{\psi}^{\mathbf{Q}}_{\pm1/2}(t) &= \sum_{\mathbf{X}}e^{i\mathbf{Q}\mathbf{X}}\bar{\psi}_{\pm1/2}(\mathbf{X},t).
\end{aligned}\tag{3.2}$$

The operators $\tilde{\mathcal{O}}_{1/2}(t')$, $\mathcal{O}_{1/2}(t')$, $\mathcal{O}_{3/2}(t')$ describe the Δ at rest, whereas $\bar{\psi}^{\mathbf{Q}}_{\pm1/2}(t)$ corresponds to the nucleon moving with the 3-momentum $\mathbf{Q}$. The operators on the r.h.s. of Eq. (3.2) are given in Eq. (2.24) with the substitution $\gamma_0\to\gamma_4$.

In the limit $t' \to +\infty$, $t \to -\infty$ only the one-particle Δ and nucleon states contribute:

$$\begin{aligned}
\tilde{R}_{1/2}(t',t) &\to \frac{e^{-E_\Delta t' + E_N t}}{4E_\Delta E_N}\langle 0|\tilde{\mathcal{O}}_{1/2}(0)|1/2\rangle\langle 1/2|J^3(0)|1/2\rangle\langle 1/2|\bar{\psi}^{\mathbf{Q}}_{1/2}(0)|0\rangle,\\
R_{1/2}(t',t) &\to \frac{e^{-E_\Delta t' + E_N t}}{4E_\Delta E_N}\langle 0|\mathcal{O}_{1/2}(0)|1/2\rangle\langle 1/2|J^+(0)|-1/2\rangle\langle -1/2|\bar{\psi}^{\mathbf{Q}}_{-1/2}(0)|0\rangle,\\
R_{3/2}(t',t) &\to \frac{e^{-E_\Delta t' + E_N t}}{4E_\Delta E_N}\langle 0|\mathcal{O}_{3/2}(0)|3/2\rangle\langle 3/2|J^+(0)|1/2\rangle\langle 1/2|\bar{\psi}^{\mathbf{Q}}_{1/2}(0)|0\rangle,
\end{aligned} \tag{3.3}$$

where $E_\Delta = m_\Delta$ in the rest-frame of the Δ and $E_N = \sqrt{m_N^2 + \mathbf{Q}^2}$ (here, m_Δ denotes the mass of a stable Δ). Further, we define the following 2-point functions

$$\begin{aligned}
\tilde{D}_{1/2}(t) &= \mathrm{Tr}\langle 0|\tilde{\mathcal{O}}_{1/2}(t)\bar{\tilde{\mathcal{O}}}_{1/2}(0)|0\rangle,\\
D_{1/2}(t) &= \mathrm{Tr}\langle 0|\mathcal{O}_{1/2}(t)\bar{\mathcal{O}}_{1/2}(0)|0\rangle,\\
D_{3/2}(t) &= \mathrm{Tr}\langle 0|\mathcal{O}_{3/2}(t)\bar{\mathcal{O}}_{3/2}(0)|0\rangle,\\
D^{\pm}_{\mathbf{Q}}(t) &= \mathrm{Tr}\langle 0|\psi^{\mathbf{Q}}_{\pm 1/2}(t)\bar{\psi}^{\mathbf{Q}}_{\pm 1/2}(0)|0\rangle.
\end{aligned} \tag{3.4}$$

It can be straightforwardly seen that, in the limit $t' \to +\infty$, $t \to -\infty$,

$$\begin{aligned}
&\mathcal{N}\frac{\mathrm{Tr}(\tilde{R}_{1/2}(t',t))}{\tilde{D}_{1/2}(t'-t)}\left(\frac{D^+_{\mathbf{Q}}(t')\tilde{D}_{1/2}(-t)\tilde{D}_{1/2}(t'-t)}{\tilde{D}_{1/2}(t')D^+_{\mathbf{Q}}(-t)D^+_{\mathbf{Q}}(t'-t)}\right)^{1/2} \to \langle 1/2|J^3(0)|1/2\rangle,\\
&-\mathcal{N}\frac{\mathrm{Tr}(R_{1/2}(t',t))}{D_{1/2}(t'-t)}\left(\frac{D^-_{\mathbf{Q}}(t')D_{1/2}(-t)D_{1/2}(t'-t)}{D_{1/2}(t')D^-_{\mathbf{Q}}(-t)D^-_{\mathbf{Q}}(t'-t)}\right)^{1/2} \to \langle 1/2|J^+(0)|-1/2\rangle,\\
&-\mathcal{N}\frac{\mathrm{Tr}(R_{3/2}(t',t))}{D_{3/2}(t'-t)}\left(\frac{D^+_{\mathbf{Q}}(t')D_{3/2}(-t)D_{3/2}(t'-t)}{D_{3/2}(t')D^+_{\mathbf{Q}}(-t)D^+_{\mathbf{Q}}(t'-t)}\right)^{1/2} \to \langle 3/2|J^+(0)|1/2\rangle,
\end{aligned} \tag{3.5}$$

where $\mathcal{N} = \sqrt{4E_\Delta E_N}$ and the Euclidean analogs of Eqs. (2.22) read (cf., e.g., with Ref. [3][2])

$$\begin{aligned}
\langle 1/2|J^3(0)|1/2\rangle &= \frac{E_\Delta - Q^0}{E_\Delta}AG_C(t)\\
\langle 1/2|J^+(0)|-1/2\rangle &= \sqrt{\frac{1}{2}}A\big(G_M(t) - 3G_E(t)\big),\\
\langle 3/2|J^+(0)|1/2\rangle &= \sqrt{\frac{3}{2}}A\big(G_M(t) + G_E(t)\big),
\end{aligned} \tag{3.6}$$

where $t = (E_\Delta - E_N)^2 - \mathbf{Q}^2$ and the quantity A is given by Eq. (2.23) with the replacement $E_R \to E_\Delta$. We would like to also mention that, in case of a stable Δ, the above relations hold up to the Lorentz-non-invariant terms exponentially suppressed in a box of size L.

When the Δ becomes unstable, the interpretation of the above equations changes. The ratios given in Eq. (3.5) can be still formed, but the functions that are extracted from these ratios are the matrix elements of the electromagnetic current calculated between a certain eigenstate of the Hamiltonian in a finite volume (with the volume-dependent energy E_Δ) and a one-nucleon state.

[2] Note the difference in sign and in a factor 2 with the third line of Eq. (4) of Ref. [3].

The normalization constant $\mathcal{N}$ in these equations also changes. Namely, $\mathcal{N} = \sqrt{8 w_{1\Delta} w_{2\Delta} E_N}$, where $w_{1\Delta}$ and $w_{2\Delta}$ are the energies of the nucleon and a pion in the CM system: $w_{1\Delta} = (E_\Delta^2 + m_N^2 - M_\pi^2)/(2E_\Delta)$, $w_{2\Delta} = (E_\Delta^2 - m_N^2 + M_\pi^2)/(2E_\Delta)$ and $w_{1\Delta} + w_{2\Delta} = E_\Delta$. In the infinite-volume limit, these matrix elements do not coincide with the resonance matrix elements defined in the previous section. Rather, the energy of any fixed level tends to the threshold value in this limit. Note also that, at a given energy, there may exist several eigenstates of the Hamiltonian in the vicinity of the resonance energy, and it is not clear, which of these matrix elements should be identified with the resonance matrix element we are looking for.

It is evident that the situation closely resembles the determination of the resonance pole position from the lattice data by using the Lüscher equation. As it is well known, in order to achieve the goal, one has to perform an analytic continuation into the complex energy plane. A detailed discussion of this procedure can be found, e.g., in Ref. [40]. Below, we give a short description of the procedure. One first extracts the scattering phase shift at different energies from the measured energy spectrum and fits the quantity $p^3 \cot\delta(p)$ by a polynomial in p^2, assuming the effective range expansion (here, p denotes the relative 3-momentum in the CM system). Then, one finds the poles of the T-matrix in the complex plane by finding the zeros of a polynomial with known coefficients. Below we shall prove the generalization of this procedure to the case of the matrix elements. Namely, the matrix elements given in Eq. (3.5) should be measured at several energies (corresponding to the measurement at several volumes), and the result should be fitted by some polynomial. Further, we shall show that, replacing p^2 by p_R^2 in this polynomial, where p_R denotes the value of the relative 3-momentum at the resonance pole, one obtains the resonance form factors defined in the previous section (up to the corrections that are exponentially suppressed in large volumes). This is the main result of our work. Note also that this prescription is much simpler than the one for the elastic Δ-form factor (see Ref. [40]) since, as we shall see below, no finite fixed points arise in the case of the transition form factor.

As it is clear from the previous discussion, in order to perform the fit, the matrix elements should be measured at several values of the relative 3-momentum p. These matrix elements depend on two kinematic variables: apart from p, there is the nucleon 3-momentum $|\mathbf{Q}|$ (alternatively, the variable t which at the resonance takes the complex value $t = (E_R - Q^0)^2 - \mathbf{Q}^2$). Note also that fixing $|\mathbf{Q}|$ is equivalent to fixing t because the (complex) resonance energy E_R, which is defined in the infinite volume, is also fixed. On the lattice, it is more convenient to fix the real quantity $|\mathbf{Q}|$, and we stick to this choice in the following.

According to the previous discussion, our goal is to find a way to "scan" the resonance region in the variable p, leaving the other variable $|\mathbf{Q}|$ fixed. There is, however, a problem, if one performs this scan by doing measurements at different volumes. Namely, the momentum on the lattice along any axis is quantized, and the smallest nonzero momentum available is equal to $2\pi/L$, where L denotes the box size. Consequently, if L is varied, the quantity $|\mathbf{Q}|$ will change along with p.

We can propose at least two strategies that help to circumvent this problem:

1. The use of asymmetric boxes. Consider the box with the geometry $L \times L \times L'$ and direct $\mathbf{Q}$ along the third axis. The Δ is in the rest frame. Changing L does not affect $\mathbf{Q}$ but affects p.
2. Using (partially) twisted boundary conditions. One may apply the twisting to a single quark in the nucleon, namely, the one that is attached to the photon (see Fig. 1). This gives an additional momentum to the nucleon along the third axis. The magnitude of this change is $|\mathbf{Q}_\theta| = \theta/L$. On the other hand, changing the cubic box size, we also change the magnitude of the nucleon momentum $|\mathbf{Q}|$. One may adjust the value of the twisting angle θ so that the

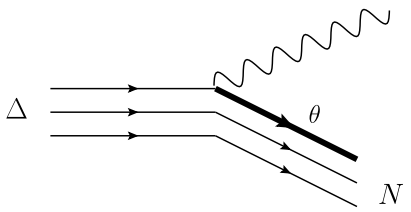

Fig. 1. Twisting a single quark in the nucleon.

sum of these two effects cancels and the nucleon momentum is kept fixed. It is important to stress that the value of θ can be determined prior to the simulations since it depends only on the box size. We also note that a similar technique of twisting has been already applied in the past for the calculation of nucleon form factors [50].

To summarize, on the lattice we have to measure the matrix elements given in Eq. (3.5). These matrix elements depend on two kinematic variables: the relative 3-momentum p in the Δ-channel and the 3-momentum $\mathbf{Q}$ of the nucleon (the three-momentum of the photon is $-\mathbf{Q}$). Using asymmetric boxes or twisted boundary conditions, we may scan the resonance region in p while keeping $\mathbf{Q}$ fixed. Let us now discuss how to perform the analytic continuation into the complex plane and extract the resonance form factors with the use of Eq. (3.6).

4. Matrix elements in a finite volume

4.1. Two-point function

In this section, we shall consider the resonance matrix elements by using the technique of the non-relativistic effective field theory in a finite volume. While doing so, we closely follow the path of Ref. [40], adapting the formulae given there, whenever necessary. To avoid problems, related to the mixing of the partial waves, the Δ-resonance is always considered in the CM frame. In this case, there is no S- and P-wave mixing. Neglecting the (small) P_{31} wave, the Lüscher equation [7] for the P_{33} wave is written as follows:

$$p\cot\delta(p) + p\cot\phi(q) = 0, \quad q = \frac{pL}{2\pi}, \tag{4.1}$$

where

$$p\cot\phi(q) = -\frac{2}{\sqrt{\pi}L}\left\{\hat{Z}_{00}\big(1;q^2\big) \pm \frac{1}{\sqrt{5}q^2}\hat{Z}_{20}\big(1;q^2\big)\right\}, \tag{4.2}$$

and $\delta(p)$ is the P_{33} phase shift in the infinite volume. Further, $\hat{Z}_{lm}(1;q^2)$ denotes the Lüscher zeta-function (for the asymmetric boxes, in general), and the signs $+$ and $-$ are chosen for the irreps G_1 and G_2 of the little group corresponding to $\mathbf{d} = (0,0,1)$, respectively (see Ref. [16]). In particular, for a symmetric box, $\hat{Z}_{lm}(1;q^2) = Z_{lm}(1;q^2)$ and $Z_{20}(1;q^2) = 0$ in the CM frame (there is no mixing to the P_{31} wave in this case). For an asymmetric box with $L' = xL$,

$$\hat{Z}_{lm}\big(1;q^2\big) = \frac{1}{x}\sum_{\mathbf{n}\in\mathbb{Z}^3}\frac{\mathcal{Y}_{lm}(\mathbf{r})}{\mathbf{r}^2 - q^2}, \quad r_{1,2} = n_{1,2},\ r_3 = \frac{1}{x}n_3, \qquad \hat{Z}_{20}\big(1;q^2\big) \neq 0. \tag{4.3}$$

The matrix element of an operator $\mathcal{O}_i$ between the vacuum and an eigenstate of a Hamiltonian $\langle 0|\mathcal{O}_i(0)|n\rangle$ contains two-particle reducible diagrams describing initial-state interactions, which

Fig. 2. Initial-state pion–nucleon interactions in the two-point function. The quantity X_i stands for the coupling of the operator $\mathcal{O}_i$ to the pion–nucleon pair in the intermediate state.

are volume-dependent (here, $\mathcal{O}_i$ stands for one of the operators $\tilde{\mathcal{O}}_{1/2}, \mathcal{O}_{1/2}, \mathcal{O}_{3/2}$). This matrix element is proportional to U_i even in case of an unstable Δ, where

$$\begin{aligned} U_{3/2} &= \frac{1}{2}(1+\Sigma_3)\frac{1}{2}(1+\gamma_4)\frac{1}{\sqrt{2}}\big(u^1(P,3/2) - i\,\Sigma_3 u^2(P,3/2)\big), \\ U_{1/2} &= \frac{1}{2}(1-\Sigma_3)\frac{1}{2}(1+\gamma_4)\frac{1}{\sqrt{2}}\big(u^1(P,1/2) + i\,\Sigma_3 u^2(P,1/2)\big), \\ \tilde{U}_{1/2} &= \frac{1}{2}(1+\Sigma_3)\frac{1}{2}(1+\gamma_4)u^3(P,1/2). \end{aligned} \tag{4.4}$$

This fact can be verified straightforwardly, since both the above matrix element as well as U_i are Dirac spinors with only one nonzero entry.

The calculation of the volume-dependent factor in the matrix element proceeds by using the same technique as in the derivation of Eq. (46) of Ref. [40]. Namely, we calculate the two-point function of the operators $\mathcal{O}_i, \bar{\mathcal{O}}_i$ in the non-relativistic effective field theory below the inelastic threshold. According to the discussion above, the coupling of the operator $\mathcal{O}_i$ to the pion–nucleon state in the effective theory is described by a local vertex $X_i U_i$, where the scalar function $X_i = X_i^{(0)} + X_i^{(1)}\mathbf{p}^2 + \cdots$ contains the terms with $0, 2, \ldots$ derivatives. Here, $\mathbf{p}^2$ stands for the relative momentum squared of the pion–nucleon pair in the CM system. Note that the X_i contain only short-range physics and are the same in a finite and in the infinite volume. Explicit values of $X_i^{(m)}$ are not important, because the X_i cancel in the final expressions.

Summing now up the pion–nucleon bubble diagrams as shown in Fig. 2, it is seen that the Euclidean two-point function takes the form

$$\begin{aligned} &\langle 0|\mathcal{O}_i(x_0)\bar{\mathcal{O}}_i(y_0)|0\rangle \\ &\quad = U_i X_i \left\{ \int_{-\infty}^{\infty} \frac{dP_0}{2\pi} e^{iP_0(x_0-y_0)} V\big(-i\,J(P_0) - J^2(P_0)T(P_0)\big) \right\} X_i \bar{U}_i, \end{aligned} \tag{4.5}$$

where

$$J(P_0) = \frac{1}{V}\sum_{\mathbf{k}} \frac{1}{2w_1(\mathbf{k})2w_2(\mathbf{k})} \frac{1}{P_0 - i(w_1(\mathbf{k}) + w_2(\mathbf{k}))}, \tag{4.6}$$

$w_1(\mathbf{k}) = \sqrt{m_N^2 + \mathbf{k}^2}$, $w_2(\mathbf{k}) = \sqrt{M_\pi^2 + \mathbf{k}^2}$, V is the lattice volume and $T(P_0)$ denotes the pion–nucleon scattering amplitude in a finite volume[3]

$$T(P_0) = \frac{8\pi\sqrt{s}}{p\cot\delta(p) + p\cot\phi(q)}, \quad s = -P_0^2, \tag{4.7}$$

and p is the relative momentum in the CM frame, corresponding to the total energy $\sqrt{s}$.

[3] Note that here we use a different normalization in the partial-wave expansion of the T-matrix than in Ref. [40].

Next, we perform the integration over the variable P_0, using Cauchy's theorem. It can be shown that only the poles of $T(P_0)$ contribute to this integral. In the vicinity of the n-th pole, this function is given by

$$T(P_0) = \frac{8\pi E_n^2}{w_{1n} w_{2n}} \frac{\sin^2 \delta(p_n)}{\delta'(p_n) + \phi'(q_n)} \frac{1}{E_n + i P_0} + \cdots, \tag{4.8}$$

where E_n are the eigenenergies in the box, p_n is the corresponding relative 3-momentum, $q_n = p_n L/(2\pi)$, and $w_{1n} = (E_n^2 + m_N^2 - M_\pi^2)/(2E_n)$, $w_{2n} = (E_n^2 - m_N^2 + M_\pi^2)/(2E_n)$. The derivatives are taken with respect to the variable p, so that $\phi'(q) = d\phi(q)/dp = (L/2\pi) d\phi(q)/dq$.

Performing the integration over p_0 and using the Lüscher equation

$$\frac{1}{V} \sum_{\mathbf{k}} \frac{1}{2w_1(\mathbf{k}) 2w_2(\mathbf{k})} \frac{1}{w_1(\mathbf{k}) + w_2(\mathbf{k}) - E_n} = \frac{p_n \cot \delta(p_n)}{8\pi E_n}, \tag{4.9}$$

we finally get

$$\begin{aligned} &\langle 0 | \mathcal{O}_i(x_0) \bar{\mathcal{O}}_i(y_0) | 0 \rangle \\ &\quad = U_i X_i \left\{ V \sum_n e^{-E_n (x_0 - y_0)} \frac{\cos^2 \delta(p_n)}{\delta'(p_n) + \phi'(q_n)} \frac{p_n^2}{8\pi w_{1n} w_{2n}} \right\} X_i \bar{U}_i. \end{aligned} \tag{4.10}$$

On the other hand,[4]

$$\langle 0 | \mathcal{O}_i(x_0) \bar{\mathcal{O}}_i(y_0) | 0 \rangle = \sum_n \frac{e^{-E_n (x_0 - y_0)}}{4 w_{1n} w_{2n}} \langle 0 | \mathcal{O}_i(0) | n \rangle \langle n | \bar{\mathcal{O}}_i(0) | 0 \rangle. \tag{4.11}$$

Comparing these two equations, we finally get

$$\left| \langle 0 | \mathcal{O}_i(0) | n \rangle \right| = U_i X_i V^{1/2} \left(\frac{\cos^2 \delta(p_n)}{|\delta'(p_n) + \phi'(q_n)|} \frac{p_n^2}{2\pi} \right)^{1/2}. \tag{4.12}$$

4.2. Three-point function

Next, let us consider the current matrix elements in a finite volume $F_i = F_i(p, |\mathbf{Q}|)$, $i = 1, 2, 3$, which appear on the r.h.s. of Eq. (3.5). The derivation which is given below is essentially similar to Eqs. (65)–(70) of Ref. [40]. We start from the calculation of the three-point function, summing up the bubble diagrams in the non-relativistic effective theory. There are two types of diagrams, which are shown in Fig. 3 to which one has to add the diagrams obtained by adding any number of pion loops to the initial states interaction (see Fig. 4). The self-energy insertions in the outgoing nucleon line can be safely ignored since the nucleon is a stable particle (see discussion below) and hence such diagrams lead to the exponentially suppressed contributions in a finite volume. As a result, the matrix element is written as a sum of two contributions

$$\begin{aligned} \langle 0 | \mathcal{O}_i(x_0) J^a(0) | Q, \varepsilon \rangle = U_i X_i \int_{-\infty}^{\infty} \frac{dP_0}{2\pi} e^{i P_0 x_0} \frac{p \cot \delta(p)}{8\pi \sqrt{s}} T(P_0) \\ \times \left(-i J(P_0) \bar{F}_i^{(A)}\left(p, |\mathbf{Q}|\right) + \hat{F}_i^{(B)}\left(p, |\mathbf{Q}|\right) \right), \end{aligned} \tag{4.13}$$

[4] The normalization of the one-particle states here differs from the one used in Ref. [40]. Here, we use the normalization $\langle p | q \rangle = 2 p_0 V \delta_{pq}$.

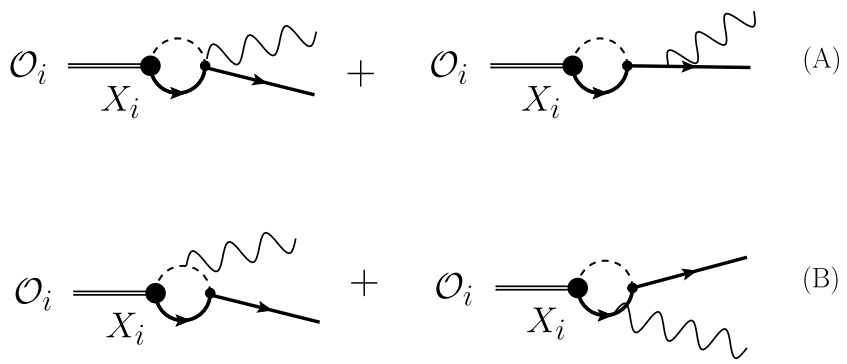

Fig. 3. Typical diagrams contributing to the $\Delta N\gamma^*$ transition form factor: (A) point vertex and emission of the photon from the external nucleon line; (B) emission of the photon from the internal lines. As in Fig. 2, the quantity X_i stands for the coupling of the operator $\mathcal{O}_i$ to the pion–nucleon pair in the intermediate state.

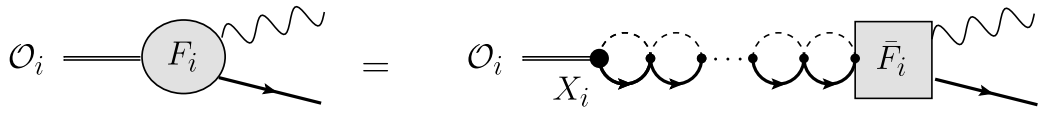

Fig. 4. Initial-state pion–nucleon interactions in the $\Delta N\gamma^*$ transition form factor. The quantity $\bar{F}_i$ denotes the sum of all irreducible diagrams.

where $F_i^{(A)}(p, |\mathbf{Q}|)$ does not depend on L (up to the exponentially suppressed contributions) and the indices a, ε have been suppressed for brevity.

The diagrams of the type (B) can be potentially dangerous. Indeed in the case of the elastic form factor, such diagrams lead to the so-called finite fixed points, see Ref. [40]. However, the fact that one of the external particles (the nucleon) is stable simplifies matters considerably. As shown in Section 4.2.2 (see Eq. (4.39)), in that case the quantity $\hat{F}_i^{(B)}(p, |\mathbf{Q}|))$ can be written as a product of two factors:

$$\hat{F}_i^{(B)}\big(p, |\mathbf{Q}|\big) = -iJ(P_0)\bar{F}_i^{(B)}\big(p, |\mathbf{Q}|\big), \tag{4.14}$$

where $\bar{F}_i^{(B)}(p, |\mathbf{Q}|)$, again, does not depend on L up to the exponentially suppressed contributions. Physically, this corresponds to the Taylor expansion of the pion propagator attached to the nucleon in diagram Fig. 5: this propagator shrinks to a point (a similar discussion holds when the photon is attached to the nucleon line) and the contributions of diagrams (B) to the matrix element are equivalent to the one of diagrams (A).

Consequently, we can rewrite Eq. (4.13)

$$\begin{aligned}&\langle 0|\mathcal{O}_i(x_0)J^a(0)|Q,\varepsilon\rangle\\ &\quad= U_i X_i \int\limits_{-\infty}^{\infty} \frac{dP_0}{2\pi} e^{iP_0x_0}\big(-iJ(P_0)\big)\frac{p\cot\delta(p)}{8\pi\sqrt{s}}T(P_0)\bar{F}_i\big(p, |\mathbf{Q}|\big),\end{aligned} \tag{4.15}$$

where $\bar{F}_i(p, |\mathbf{Q}|) = \bar{F}_i^{(A)}(p, |\mathbf{Q}|) + \bar{F}_i^{(B)}(p, |\mathbf{Q}|)$ denotes the full irreducible amplitude for the $\pi N \to \gamma^* N$ transition.

Performing now the Cauchy integral over P_0 and comparing to the spectral representation of the three-point function, we get

$$\langle 0|\mathcal{O}_i(0)|n\rangle\frac{1}{4w_{1n}w_{2n}}F_i\big(p_n, |\mathbf{Q}|\big) = X_iU_i\frac{\cos^2\delta(p_n)}{\delta'(p_n)+\phi'(q_n)}\frac{p_n^2}{8\pi w_{1n}w_{2n}}\bar{F}_i\big(p_n, |\mathbf{Q}|\big). \tag{4.16}$$

From Eqs. (4.12) and Eq. (4.16) one obtains

$$\left|\bar{F}_i\left(p_n, |\mathbf{Q}|\right)\right| = V^{1/2}\left(\frac{\cos^2\delta(p_n)}{|\delta'(p_n)+\phi'(q_n)|}\frac{p_n^2}{2\pi}\right)^{-1/2}\left|F_i\left(p_n, |\mathbf{Q}|\right)\right|. \tag{4.17}$$

Before we proceed further, an important remark is in order. As already discussed in Section 2, the form factor can be defined either on the real energy axis, or at the resonance pole (although, strictly speaking, only the latter definition is a rigorous one, the former is process-dependent). Below we shall provide the formulae which enable one to "translate" lattice data into one of these definitions.

4.2.1. Real energy axis

On the *real* energy axis, the infinite-volume matrix element, corresponding to the scattering process $\pi N \to \gamma^* N$ at low energies, is given by a geometric series of the pion–nucleon bubbles in the final state. This series sums up into the following expression:

$$\mathcal{A}_i\left(p, |\mathbf{Q}|\right) = \frac{p\cot\delta(p)}{p\cot\delta(p) - ip}\bar{F}_i\left(p, |\mathbf{Q}|\right) = e^{i\delta(p)}\cos\delta(p)\bar{F}_i\left(p, |\mathbf{Q}|\right). \tag{4.18}$$

Here, we have assumed that the quantity $\bar{F}_i(p, |\mathbf{Q}|)$ has a smooth infinite-volume limit (see the proof below). The amplitudes $\mathcal{A}_i$ are proportional to the linear combinations of the so-called transverse magnetic (M), transverse electric (E) and scalar (S) multipoles. The latter appear in the partial wave decomposition of the $\pi N \to \gamma^* N$ scattering amplitude (see Appendix A for the details) and can be extracted from the analysis of the experimental data. The multipoles contain information on the resonance states.[5]

Note that Eq. (4.18) is nothing but Watson's theorem, which indeed holds near the Δ-resonance in the elastic region. At a first glance, $\mathcal{A}_i(p, |\mathbf{Q}|)$ vanishes when $\delta = 90°$. In order to show that this is not the case, we rewrite Eq. (4.18) as follows:

$$\mathcal{A}_i\left(p, |\mathbf{Q}|\right) = \frac{e^{i\delta(p)}}{p^3}\sin\delta(p)p^3\cot\delta(p)\bar{F}_i\left(p, |\mathbf{Q}|\right), \tag{4.19}$$

Assuming that the effective-range expansion holds in the resonance region, one may write

$$p^3\cot\delta(p) \doteq h\left(p^2\right) = -\frac{1}{a} + \frac{1}{2}rp^2 + \cdots, \tag{4.20}$$

where a is the P-wave scattering volume and r is the effective range. The function $h(p^2)$ should have a zero at $p^2 = p_A^2$, where the scattering phase passes through 90°. It is easy to get convinced that the quantity $\bar{F}_i(p, |\mathbf{Q}|)$ should have a pole exactly at the same value of p^2. This pole corresponds to the exchange of the bare Δ in the s-channel (since our effective non-relativistic Lagrangian does not include the explicit Δ, the pole will manifest itself in the divergence on the perturbative series at $p^2 = p_A^2$). Consequently, not the quantity $\bar{F}_i(p, |\mathbf{Q}|)$ alone, but the product $p^3\cot\delta(p)\bar{F}_i(p, |\mathbf{Q}|)$ is a low-energy polynomial that can be safely expanded in the resonance region and that, in general, does not vanish at $p^2 = p_A^2$. It follows from this that the multipoles $\mathcal{A}_i$, defined by Eq. (4.19), take finite values at the resonance.

Finally, combining the above equations, we arrive at an analogue of the Lüscher–Lellouch equation for the photoproduction amplitude in the elastic region

[5] We would like to mention here that in Ref. [51] the calculation of the deuteron photodisintegration amplitude in a finite volume was addressed by using a slightly different technique.

$$\mathcal{A}_i\big(p_n, |\mathbf{Q}|\big) = e^{i\delta(p_n)}\, V^{1/2}\left(\frac{1}{|\delta'(p_n)+\phi'(q_n)|}\,\frac{p_n^2}{2\pi}\right)^{-1/2}\big|F_i\big(p_n, |\mathbf{Q}|\big)\big|. \tag{4.21}$$

Eq. (4.21) comprises one of the main results of the present article. It allows to extract the multipole amplitudes from lattice data.

In order to obtain the $\Delta N\gamma^*$ matrix elements F_i^A, defined on the real axis, one parameterizes the imaginary parts of the multipoles through the matrix element of the electromagnetic current between N and Δ states (see, e.g., Ref. [43]). Then, in the narrow width approximation, for the amplitudes $\mathcal{A}_i(p, |\mathbf{Q}|)$ we get:

$$\big|\mathrm{Im}\,\mathcal{A}_i\big(p_A, |\mathbf{Q}|\big)\big| = \sqrt{\frac{8\pi}{p_A\Gamma}}\big|F_i^A\big(p_A, |\mathbf{Q}|\big)\big|, \tag{4.22}$$

where all quantities are *real* and taken at the Breit–Wigner pole $p = p_A$, the Γ is the total width of the Δ-resonance.

4.2.2. Complex energy plane

Next, we consider the extraction of the form factor at the resonance pole. This implies the analytic continuation of the above result into the complex p-plane. In order to do this, let us first consider the two-point function in the infinite volume

$$\langle 0|O_i(x)\bar{O}_i(y)|0\rangle = \int \frac{d^4P}{(2\pi)^4} e^{iP(x-y)} D_i\big(P^2\big), \tag{4.23}$$

where, in the CM system $P_\mu = (P_0, \mathbf{0})$ the quantity $D_i(P^2)$ takes the form (cf. Eq. (4.5))

$$D_i\big(P^2\big) = U_i X_i\big(-iJ_\infty(P_0) - J_\infty^2(P_0)T_\infty(P_0)\big)X_i\bar{U}_i. \tag{4.24}$$

Here, the quantities $J_\infty(P_0)$ and $T_\infty(P_0)$ denote the infinite-volume counterparts of the quantities defined by Eqs. (4.6) and (4.7). In the Minkowski space, with $P_0 = i\sqrt{s}$, these quantities are given by

$$J_\infty(P_0) = -\frac{p}{8\pi\sqrt{s}}, \qquad T_\infty(P_0) = \frac{8\pi\sqrt{s}}{p\cot\delta(p) - ip}. \tag{4.25}$$

These expressions are valid on the first Riemann sheet. On the second sheet, the relative momentum p changes sign.

Suppose now that the scattering amplitude $T_\infty(P_0)$ has a pole at $s = s_R$ on the second Riemann sheet. Writing down the effective-range expansion in a form of Eq. (4.20), one first finds the pole position in the complex plane from the equation

$$-\frac{1}{a} + \frac{1}{2}rp_R^2 + \cdots = -ip_R^3. \tag{4.26}$$

Further, in the vicinity of the pole $p = p_R$ we get

$$p^2\big(p\cot\delta(p) + ip\big) = (s - s_R)\big(2p_R h'\big(p_R^2\big) + 3ip_R^2\big)\frac{w_{1R}w_{2R}}{2p_R s_R} + O\big((s-s_R)^2\big) \tag{4.27}$$

where $w_{1R} = \sqrt{m_N^2 + p_R^2}$, $w_{2R} = \sqrt{M_\pi^2 + p_R^2}$, $s_R = E_R^2 = (w_{1R} + w_{2R})^2$ and the derivative of h is taken with respect to the variable p^2. Using this expansion, one may obtain the value of the wave function renormalization constant at the pole:

$$D_i(s) \to U_i X_i \frac{Z_R}{s_R - s} X_i \bar{U}_i + \text{regular terms at } s \to s_R,$$
$$Z_R = \left(\frac{p_R}{8\pi E_R}\right)^2 \left(\frac{16\pi p_R^3 E_R^3}{w_{1R} w_{2R}(2p_R h'(p_R^2) + 3ip_R^2)}\right). \tag{4.28}$$

The three-point function in the infinite volume is given by

$$\langle 0|O_i(x)J^a(0)|Q,\varepsilon\rangle = U_i X_i \int \frac{d^4P}{(2\pi)^4} e^{iPx}\big(-iJ_\infty(P_0)\big)\frac{p\cot\delta(p)}{8\pi\sqrt{s}} T_\infty(P_0)\bar{F}_i\big(p,|\mathbf{Q}|\big), \tag{4.29}$$

where $\bar{F}_i(p,|\mathbf{Q}|)$ is the same as in Eq. (4.15).

Next, we assume that the two-particle irreducible part $\bar{F}_i(p_n,|\mathbf{Q}|)$ can be analytically continued into the complex plane. Separating the pole contribution in the three-point function, we get our final expression for the resonance matrix element F_i^R, evaluated at the pole

$$F_i^R\big(p_R,|\mathbf{Q}|\big) = Z_R^{1/2}\bar{F}_i\big(p_R,|\mathbf{Q}|\big). \tag{4.30}$$

As a test of our final formula, let us consider the case when the resonance is infinitely narrow. Then, the pole tends to the real axis, and $E_R \to E_n$, $p_R \to p_n$. Still, we assume that the (real) energy E_R is above the two-particle threshold.

First, we can express the amplitudes $\mathcal{A}_i$ through F_i^R:

$$\mathcal{A}_i\big(p_R,|\mathbf{Q}|\big) = Z_R^{-1/2} F_i^R\big(p_R,|\mathbf{Q}|\big). \tag{4.31}$$

Further, since $h(p^2) = p^3\cot\delta(p)$, at the resonance we have

$$2p_R h'\big(p_R^2\big) + 3ip_R^2 = -\frac{p_R^3\delta'(p_R)}{\sin^2\delta(p_R)}. \tag{4.32}$$

Moreover, in the vicinity of an infinitely narrow resonance, the derivative of the phase shift behaves as

$$\delta'(p_R) = \frac{2}{\Gamma}\frac{p_R E_R}{w_{1R} w_{2R}}, \tag{4.33}$$

where Γ is the Breit–Wigner width of the resonance. The renormalization constant Z_R becomes

$$Z_R = -\frac{p_R\Gamma}{8\pi}, \tag{4.34}$$

and we finally obtain

$$\big|\operatorname{Im}\mathcal{A}_i\big(p_R,|\mathbf{Q}|\big)\big| = \sqrt{\frac{8\pi}{p_R\Gamma}}\big|F_i^R\big(p_R,|\mathbf{Q}|\big)\big|, \tag{4.35}$$

where $p_R \to p_A$. This formula coincides exactly with Eq. (4.22).

Further, in the limit considered, the derivative of the phase shift explodes (see Eq. (4.33)) whereas the quantity $\phi'(q_n)$ stays finite. Consequently, one may neglect $\phi'(q_n)$ in all formulae. Expressing the quantity $\bar{F}_i(p_R,|\mathbf{Q}|)$ through $F_i(p_R,|\mathbf{Q}|)$ by using Eq. (4.17) and substituting in Eq. (4.30), we arrive at a fairly simple result in this limit:

$$F_i^R\big(p_n,|\mathbf{Q}|\big) = V^{1/2}\left(\frac{E_n}{2w_{1n}w_{2n}}\right)^{1/2} F_i\big(p_n,|\mathbf{Q}|\big). \tag{4.36}$$

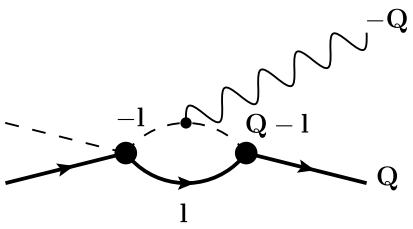

Fig. 5. A potentially dangerous diagram which involves the irreducible vertex $\bar{F}_i$. A diagram where the photon is attached to the nucleon line, can be treated similarly. The case when the photon is attached to a local $\pi N \to \gamma^* N$ vertex is trivial, because, obviously, the corresponding diagram is a low-energy polynomial.

Note that the factor in front of F_i on the r.h.s. of the above equation exactly accounts for the difference in the normalization of the one- and two-particle states in a finite volume (we remind the reader that the energy E_R lies above threshold, so that the resonance still decays into the two-particle state, albeit with an infinitesimally small rate).

4.3. Analytic continuation of the loop diagram

Finally, we want to demonstrate that the analytic continuation of the quantity $\bar{F}_i(p_n, |\mathbf{Q}|)$ into the complex plane is possible. In case of the elastic form factor, this procedure has led to serious difficulties due the existence of the so-called finite fixed points [40]. However, such difficulties do not arise in case of the transition form factors, as can be easily seen by considering the potentially dangerous triangle diagram where the photon is attached to the pion line (see Fig. 5). For simplicity, we neglect all numerators, which are low-energy polynomials. In the rest-frame of the Δ-resonance, the diagram shown in Fig. 5 is equal to

$$I = \frac{1}{V}\sum_{\mathbf{l}} \frac{1}{8w_1(\mathbf{l})w_2(-\mathbf{l})w_2(\mathbf{Q}-\mathbf{l})} \frac{1}{(w_1(\mathbf{l})+w_2(-\mathbf{l})-E_n)(w_1(\mathbf{l})+w_2(\mathbf{Q}-\mathbf{l})-Q^0)}. \tag{4.37}$$

This diagram can be simplified by using the following algebraic identity (see Ref. [39])

$$\frac{1}{4w_1(\mathbf{l})w_2(-\mathbf{l})} \frac{1}{(w_1(\mathbf{l})+w_2(-\mathbf{l})-E_n)} = \frac{1}{2E_n(\mathbf{l}^2-p_n^2)} + \text{non-singular terms}. \tag{4.38}$$

Since the second denominator in Eq. (4.37) is non-singular, up to the exponentially suppressed terms we get

$$I = \frac{1}{V}\sum_{\mathbf{l}} \frac{1}{2E_n(\mathbf{l}^2-p_n^2)} \frac{1}{2}\int_{-1}^{1} dy \frac{1}{2\hat{w}_2(\hat{w}_1+\hat{w}_2-Q^0)}, \tag{4.39}$$

where

$$\hat{w}_1 = \sqrt{m_N^2+p_n^2}, \qquad \hat{w}_2 = \sqrt{M_\pi^2+p_n^2+\mathbf{Q}^2-2|\mathbf{Q}|p_n y}. \tag{4.40}$$

Since the first factor on the r.h.s. of Eq. (4.39) can be replaced by $p_n \cot\delta(p_n)$ from the Lüscher equation, and the remaining integral over y is a low-energy polynomial, we see that the quantity $p^2 I$ is a low-energy polynomial in p^2 as well. No finite fixed points arise and the analytic continuation can be performed without any problem. Moreover, there exist only exponentially suppressed corrections to the infinite-volume limit. Finally, it is now easy to check that the

quantity $\hat{F}_i^{(B)}(p,|\mathbf{Q}|)$ in Eq. (4.13) can be decomposed as in Eq. (4.14), with the irreducible vertex $\bar{F}_i^{(B)}(p,|\mathbf{Q}|)$ containing only exponentially suppressed finite-volume corrections. The same method can be used for the calculation of the three-point function in the infinite volume, see Eq. (4.29). The sum over the momentum $\mathbf{l}$ in Eq. (4.39) is replaced by the integral and gives a pion–nucleon loop, whereas the remainder is again identified with the irreducible vertex $\bar{F}_i^{(B)}(p,|\mathbf{Q}|)$.

5. A prescription for the measurement of the transition form factors

This section contains a short summary of all our findings. We give a prescription for calculating the $\Delta N\gamma^*$ transition form factors on the lattice, in the rest-frame of the Δ-resonance:

1. The matrix elements $F_i = F_i(p,|\mathbf{Q}|)$ in the right-hand side of Eq. (3.5) are functions of the kinematic variables p and $|\mathbf{Q}|$. Measure these matrix elements at different values of the variable p in the resonance region, keeping the other variable fixed, as explained in Section 3. The scattering phase should be measured at the same values of p.
2. The multipoles for the pion photoproduction are given by
$$\mathcal{A}_i\big(p_n,|\mathbf{Q}|\big) = e^{i\delta(p_n)}\,V^{1/2}\left(\frac{p_n^2}{2\pi|\delta'(p_n)+\phi'(q_n)|}\right)^{-1/2}\big|F_i\big(p_n,|\mathbf{Q}|\big)\big|. \tag{5.1}$$
3. The resonance matrix elements, defined at real energies, are proportional to the imaginary part of the multipoles at $p = p_A$, where the phase shift passes through 90°. In the narrow width approximation one has
$$\big|\operatorname{Im}\mathcal{A}_i\big(p_A,|\mathbf{Q}|\big)\big| = \sqrt{\frac{8\pi}{p_A\Gamma}}\,\big|F_i^A\big(p_A,|\mathbf{Q}|\big)\big|. \tag{5.2}$$
4. In order to extract the matrix element at the resonance pole, we first multiply each F_i by the pertinent Lüscher–Lellouch factor
$$\bar{F}_i\big(p_n,|\mathbf{Q}|\big) = V^{1/2}\left(\frac{\cos^2\delta(p_n)}{|\delta'(p_n)+\phi'(q_n)|}\,\frac{p_n^2}{2\pi}\right)^{-1/2}F_i\big(p_n,|\mathbf{Q}|\big). \tag{5.3}$$
5. Further, we fit the functions $p^3\cot\delta(p)\bar{F}_i(p,|\mathbf{Q}|)$ by the effective-range formula
$$p^3\cot\delta(p)\bar{F}_i\big(p,|\mathbf{Q}|\big) = A_i\big(|\mathbf{Q}|\big) + p^2B_i\big(|\mathbf{Q}|\big) + \cdots. \tag{5.4}$$
6. Finally, we evaluate the resonance matrix elements by substitution
$$F_i^R\big(p_R,|\mathbf{Q}|\big) = ip_R^{-3}Z_R^{1/2}\big(A_i\big(|\mathbf{Q}|\big) + p_R^2B_i\big(|\mathbf{Q}|\big) + \cdots\big). \tag{5.5}$$
The quantities p_R and Z_R should be evaluated separately from the measured phase shifts. Note that the form factors are related to the resonance matrix elements via the formulae given in Eq. (3.6). The kinematic factors in front of the form factors are low-energy polynomials. We emphasize again that, from the two definitions of the resonance matrix elements, given above, only the one which implies the analytic continuation to the resonance pole, yields the result which is process-independent.

6. Conclusions

(i) In this paper, we have formulated an explicit prescription for the measurement of the $\Delta N\gamma^*$ transition form factors on the lattice. The Δ is considered as a resonance, not as a stable particle. The spins of all particles are included, and three different scalar form factors are projected out.

(ii) The framework is based on the use of the non-relativistic effective field theory in a finite volume. This is in accordance with the assumption of validity of the effective range expansion in the vicinity of a resonance that is used for performing the analytic continuation into the complex plane. If this assumption proves to be very restrictive, our approach can be easily adapted for the use of the alternative techniques (e.g., expanding the amplitude in the vicinity of some point near the resonance energy, rather than expanding around threshold).

(iii) The extraction of the elastic resonance form factors from data is a rather subtle procedure due to the presence of the so-called finite fixed points. In case of the transition form factors, considered in the present paper, the method is straightforward. The complexity of the extraction is similar to the one of determining the energy and width of the Δ-resonance. For this reason, we believe that the lattice study of the transition form factors may become feasible in a foreseeable future.

(iv) The extraction of the form factors have been carried out in the rest-frame of the Δ-resonance. There are no serious obstacles to carrying out the same procedure in the moving frames as well, except the mixing between S- and P-waves which takes place, if the Δ is not at the rest.

Acknowledgements

The authors thank J. Gegelia, Ch. Lang, H. Meyer, S. Prelovsek, A. Sarantsev, S. Sharpe and G. Schierholz for interesting discussions. This work is partly supported by the EU Integrated Infrastructure Initiative HadronPhysics3 Project under Grant Agreement no. 283286. We also acknowledge the support by the DFG (CRC 16, "Subnuclear Structure of Matter"), by the Shota Rustaveli National Science Foundation (Project DI/13/02) and by the Bonn–Cologne Graduate School of Physics and Astronomy. This research is supported in part by Volkswagenstiftung under contract no. 86260.

Appendix A. Photoproduction amplitudes

In this appendix, we shall establish the connection between our photoproduction amplitude, defined in non-relativistic effective field theory with the relativistic amplitude. Note that in the present paper we deal with the P-wave in the $\gamma^* p \to \pi^0 p$ channel with the total isospin $I = 3/2$ and total spin $J = 3/2$. Below, we give the expressions, using the relativistic normalization of the Dirac spinors [49].

The relativistic photoproduction amplitude can be written in the rest frame of the pion–nucleon system as

$$T = 8\pi E \chi^\dagger(2) \mathcal{F} \chi(1), \tag{A.1}$$

where E is the total energy of the πN system. The Pauli spinors $\chi(1)$, $\chi(2)$ carry the information on the spin states of the nucleons.

The matrix $\mathcal{F}$ has a decomposition (see, e.g., [44])

$$\begin{aligned}\mathcal{F} = {} & i\tilde{\boldsymbol{\sigma}}\cdot\boldsymbol{\epsilon}\,F_1 + (\boldsymbol{\sigma}\cdot\hat{\boldsymbol{q}})\big(\boldsymbol{\epsilon}\cdot(\boldsymbol{\sigma}\times\hat{\boldsymbol{k}})\big)F_2 + i(\tilde{\boldsymbol{q}}\cdot\boldsymbol{\epsilon})(\boldsymbol{\sigma}\cdot\hat{\boldsymbol{k}})F_3 + i(\tilde{\boldsymbol{q}}\cdot\boldsymbol{\epsilon})(\boldsymbol{\sigma}\cdot\hat{\boldsymbol{q}})F_4 \\ & + i(\hat{\boldsymbol{k}}\cdot\boldsymbol{\epsilon})(\boldsymbol{\sigma}\cdot\hat{\boldsymbol{k}})F_5 + i(\hat{\boldsymbol{k}}\cdot\boldsymbol{\epsilon})(\boldsymbol{\sigma}\cdot\hat{\boldsymbol{q}})F_6 - \epsilon_0\big[i(\boldsymbol{\sigma}\cdot\hat{\boldsymbol{q}})F_7 + i(\boldsymbol{\sigma}\cdot\hat{\boldsymbol{k}})F_8\big],\end{aligned} \tag{A.2}$$

where $\epsilon^\mu = (\epsilon_0, \boldsymbol{\epsilon})$ is the photon polarization vector, $\hat{\boldsymbol{k}} = \boldsymbol{k}/|\boldsymbol{k}|$ and $\hat{\boldsymbol{q}} = \boldsymbol{q}/|\boldsymbol{q}|$ are the unit vectors for the photon and pion momenta respectively, and $\tilde{\boldsymbol{a}} = \boldsymbol{a} - (\boldsymbol{a}\cdot\hat{\boldsymbol{k}})\hat{\boldsymbol{k}}$ is a vector with purely transverse components. The eight amplitudes $F_1, ..., F_8$ are functions of three independent variables, e.g., the total energy E, the pion angle θ, and the four-momentum squared of the virtual photon, $Q^2 = \boldsymbol{k}^2 - \omega^2 > 0$.

Current conservation additionally implies that

$$|\boldsymbol{k}|F_5 = \omega F_8, \qquad |\boldsymbol{k}|F_6 = \omega F_7. \tag{A.3}$$

Further, the six independent amplitudes $F_1, ..., F_6$ have a multipole decomposition

$$\begin{aligned}F_1 &= \sum_{l\geq 0}\big\{(lM_{l+} + E_{l+})P'_{l+1} + \big[(l+1)M_{l-} + E_{l-}\big]P'_{l-1}\big\}, \\ F_2 &= \sum_{l\geq 1}\big[(l+1)M_{l+} + lM_{l-}\big]P'_l, \\ F_3 &= \sum_{l\geq 1}\big[(E_{l+} - M_{l+})P''_{l+1} + ((E_{l-} + M_{l-})P''_{l-1}\big], \\ F_4 &= \sum_{l\geq 2}(M_{l+} - E_{l+} - M_{l-} - E_{l-})P''_l, \\ F_5 &= \sum_{l\geq 0}\big[(l+1)L_{1+}P'_{l+1} - lL_{l-}P'_{l-1}\big], \\ F_6 &= \sum_{l\geq 1}\big[lL_{1-} - (l+1)L_{l+}\big]P'_l,\end{aligned} \tag{A.4}$$

where l is a pion angular momentum and the sign $\pm$ refers to the total spin $J = l \pm 1/2$. The P'_l are the derivatives of the Legendre polynomials $P_l = P_l(\cos\theta)$. Note that in the literature the longitudinal transitions are often described by $S_{l\pm}$ multipoles, related to the $L_{l\pm}$ by

$$S_{l\pm} = |\boldsymbol{k}|L_{l\pm}/\omega. \tag{A.5}$$

In case of scattering in the channel with the quantum numbers of the Δ-resonance, we retain only $\ell\pm = 1+$ partial wave and choose the momentum $\hat{\boldsymbol{k}}$ along the third axis. The pertinent scattering amplitudes then take the form

$$\begin{aligned}\tilde{T}_{1/2} &= \sqrt{4\pi}\left[\sqrt{\frac{1}{3}}\chi^\dagger_{-1/2}Y_{11}(\hat{\boldsymbol{q}}) + \sqrt{\frac{2}{3}}\chi^\dagger_{1/2}Y_{10}(\hat{\boldsymbol{q}})\right]\chi_{1/2}\tilde{\mathcal{A}}_{1/2}, \\ T_{1/2} &= \sqrt{4\pi}\left[\sqrt{\frac{1}{3}}\chi^\dagger_{-1/2}Y_{11}(\hat{\boldsymbol{q}}) + \sqrt{\frac{2}{3}}\chi^\dagger_{1/2}Y_{10}(\hat{\boldsymbol{q}})\right]\chi_{-1/2}\mathcal{A}_{1/2}, \\ T_{3/2} &= \sqrt{4\pi}\big[\chi^\dagger_{1/2}Y_{11}(\hat{\boldsymbol{q}})\big]\chi_{1/2}\mathcal{A}_{3/2}.\end{aligned} \tag{A.6}$$

Further, in order to relate the amplitudes $\mathcal{A}_i$ to the multipoles M, E, S, we make the following choice of the polarization vectors

$$
\begin{aligned}
&i=1: \quad \epsilon_0=\frac{|\boldsymbol{k}|}{Q}, \quad \boldsymbol{\epsilon}=\frac{1}{Q}(0,0,\omega),\\
&i=2: \quad \epsilon_0=0, \quad \boldsymbol{\epsilon}=\frac{1}{\sqrt{2}}(1,i,0),\\
&i=3: \quad \epsilon_0=0, \quad \boldsymbol{\epsilon}=\frac{1}{\sqrt{2}}(1,i,0).
\end{aligned}
\tag{A.7}
$$

Below, we shall demonstrate the procedure explicitly for the choice $i=1$. Retaining only the $\ell\pm=1+$ partial wave in Eq. (A.4) and substituting the explicit polarization vectors from Eq. (A.7) into Eq. (A.2), one obtains:

$$
\mathcal{F}=\frac{Q}{|\boldsymbol{k}|}\big[-6i(\boldsymbol{\sigma}\cdot\hat{\boldsymbol{k}})\cos\theta+2i(\boldsymbol{\sigma}\cdot\hat{\boldsymbol{q}})\big]S_{1+} \tag{A.8}
$$

The expression $\chi^\dagger(2)\,(\boldsymbol{\sigma}\cdot\hat{\boldsymbol{k}})\cos\theta\,\chi(1)$ can be brought into the form

$$
\begin{aligned}
\chi^\dagger(2)(\boldsymbol{\sigma}\cdot\hat{\boldsymbol{k}})\cos\theta\,\chi(1)=\frac{\sqrt{2}}{3}\sqrt{4\pi}\left[\sqrt{\frac{1}{3}}\chi^\dagger_{-1/2}Y_{11}(\hat{\boldsymbol{q}})+\sqrt{\frac{2}{3}}\chi^\dagger_{1/2}Y_{10}(\hat{\boldsymbol{q}})\right]\chi(1)\\
-\frac{1}{3}\sqrt{4\pi}\left[\sqrt{\frac{2}{3}}\chi^\dagger_{-1/2}Y_{11}(\hat{\boldsymbol{q}})-\sqrt{\frac{1}{3}}\chi^\dagger_{1/2}Y_{10}(\hat{\boldsymbol{q}})\right]\chi(1).
\end{aligned}
\tag{A.9}
$$

On the other hand, since

$$
\chi^\dagger(2)(\boldsymbol{\sigma}\cdot\hat{\boldsymbol{q}})\chi(1)=\sqrt{4\pi}\left[\sqrt{\frac{2}{3}}\chi^\dagger_{1/2}Y_{10}(\hat{\boldsymbol{q}})-\sqrt{\frac{1}{3}}\chi^\dagger_{-1/2}Y_{11}(\hat{\boldsymbol{q}})\right]\chi(1), \tag{A.10}
$$

the quantity $\chi^\dagger(2)\,(\boldsymbol{\sigma}\cdot\hat{\boldsymbol{q}})\chi(1)$ gives a $J=1/2$ contribution only. Consequently, the $J=3/2$ partial wave contribution to the relativistic amplitude of Eq. (A.1) is

$$
\tilde{T}_{1/2}=\left(-16\pi iE\sqrt{2}\frac{Q}{|\boldsymbol{k}|}S_{1+}\right)\sqrt{4\pi}\left[\sqrt{\frac{1}{3}}\chi^\dagger_{-1/2}Y_{11}(\hat{\boldsymbol{q}})+\sqrt{\frac{2}{3}}\chi^\dagger_{1/2}Y_{10}(\hat{\boldsymbol{q}})\right]\chi_{1/2}. \tag{A.11}
$$

Comparing this formula with Eq. (A.6), we finally obtain

$$
\tilde{\mathcal{A}}_{1/2}=-16\pi iE\sqrt{2}\frac{Q}{|\boldsymbol{k}|}S_{1+}. \tag{A.12}
$$

The two other cases in Eq. (A.7) can be considered along the same lines. We get

$$
\begin{aligned}
\mathcal{A}_{1/2}&=-\frac{1}{2}(3E_{1+}+M_{1+})(-16\pi iE),\\
\mathcal{A}_{3/2}&=\frac{\sqrt{3}}{2}(E_{1+}-M_{1+})(-16\pi iE).
\end{aligned}
\tag{A.13}
$$

References

[1] C. Alexandrou, G. Koutsou, J.W. Negele, Y. Proestos, A. Tsapalis, Phys. Rev. D 83 (2011) 014501, arXiv:1011.3233 [hep-lat].

[2] C. Alexandrou, AIP Conf. Proc. 1432 (2012) 62, arXiv:1108.4112 [hep-lat].

[3] C. Alexandrou, G. Koutsou, H. Neff, J.W. Negele, W. Schroers, A. Tsapalis, Phys. Rev. D 77 (2008) 085012, arXiv:0710.4621 [hep-lat].

[4] C. Alexandrou, T. Korzec, G. Koutsou, T. Leontiou, C. Lorce, J.W. Negele, V. Pascalutsa, A. Tsapalis, et al., Phys. Rev. D 79 (2009) 014507, arXiv:0810.3976 [hep-lat].

[5] C. Alexandrou, E.B. Gregory, T. Korzec, G. Koutsou, J.W. Negele, T. Sato, A. Tsapalis, arXiv:1304.4614 [hep-lat].
[6] C. Alexandrou, J.W. Negele, M. Petschlies, A. Strelchenko, A. Tsapalis, arXiv:1305.6081 [hep-lat].
[7] M. Lüscher, Nucl. Phys. B 354 (1991) 531.
[8] S. Aoki, et al., CS Collaboration, Phys. Rev. D 84 (2011) 094505, arXiv:1106.5365 [hep-lat].
[9] M. Gockeler, et al., QCDSF Collaboration, PoS LATTICE 2008 (2008) 136, arXiv:0810.5337 [hep-lat].
[10] D. Mohler, S. Prelovsek, R.M. Woloshyn, Phys. Rev. D 87 (3) (2013) 034501, arXiv:1208.4059 [hep-lat]; S. Prelovsek, L. Leskovec, C.B. Lang, D. Mohler, arXiv:1307.0736 [hep-lat].
[11] K. Rummukainen, S.A. Gottlieb, Nucl. Phys. B 450 (1995) 397, arXiv:hep-lat/9503028.
[12] Z. Fu, Phys. Rev. D 85 (2012) 014506, arXiv:1110.0319 [hep-lat].
[13] V. Bernard, M. Lage, U.-G. Meißner, A. Rusetsky, J. High Energy Phys. 0808 (2008) 024, arXiv:0806.4495 [hep-lat].
[14] T. Luu, M.J. Savage, Phys. Rev. D 83 (2011) 114508, arXiv:1101.3347 [hep-lat].
[15] L. Leskovec, S. Prelovsek, Phys. Rev. D 85 (2012) 114507, arXiv:1202.2145 [hep-lat].
[16] M. Göckeler, R. Horsley, M. Lage, U.-G. Meißner, P.E.L. Rakow, A. Rusetsky, G. Schierholz, J.M. Zanotti, Phys. Rev. D 86 (2012) 094513, arXiv:1206.4141 [hep-lat].
[17] N. Li, C. Liu, Phys. Rev. D 87 (2013) 014502, arXiv:1209.2201 [hep-lat].
[18] R.A. Briceno, Z. Davoudi, T.C. Luu, Phys. Rev. D 88 (2013) 034502, arXiv:1305.4903 [hep-lat].
[19] M. Döring, U.-G. Meißner, E. Oset, A. Rusetsky, Eur. Phys. J. A 47 (2011) 139, arXiv:1107.3988 [hep-lat].
[20] M. Döring, U.G. Meißner, E. Oset, A. Rusetsky, Eur. Phys. J. A 48 (2012) 114, arXiv:1205.4838 [hep-lat].
[21] A.M. Torres, L.R. Dai, C. Koren, D. Jido, E. Oset, Phys. Rev. D 85 (2012) 014027, arXiv:1109.0396 [hep-lat]; M. Döring, U.-G. Meißner, J. High Energy Phys. 1201 (2012) 009, arXiv:1111.0616 [hep-lat]; M. Döring, M. Mai, U.-G. Meißner, Phys. Lett. B 722 (2013) 185, arXiv:1302.4065 [hep-lat].
[22] M. Lage, U.-G. Meißner, A. Rusetsky, Phys. Lett. B 681 (2009) 439, arXiv:0905.0069 [hep-lat].
[23] V. Bernard, M. Lage, U.-G. Meißner, A. Rusetsky, J. High Energy Phys. 1101 (2011) 019, arXiv:1010.6018 [hep-lat].
[24] C. Liu, X. Feng, S. He, J. High Energy Phys. 0507 (2005) 011, arXiv:hep-lat/0504019; C. Liu, X. Feng, S. He, Int. J. Mod. Phys. A 21 (2006) 847, arXiv:hep-lat/0508022.
[25] M.T. Hansen, S.R. Sharpe, Phys. Rev. D 86 (2012) 016007, arXiv:1204.0826 [hep-lat].
[26] R.A. Briceno, Z. Davoudi, arXiv:1204.1110 [hep-lat].
[27] N. Li, C. Liu, Phys. Rev. D 87 (2013) 014502, arXiv:1209.2201 [hep-lat].
[28] P. Guo, J. Dudek, R. Edwards, A.P. Szczepaniak, Phys. Rev. D 88 (2013) 014501, arXiv:1211.0929 [hep-lat].
[29] P. Guo, Phys. Rev. D 88 (2013) 014507, arXiv:1304.7812 [hep-lat].
[30] P.F. Bedaque, Phys. Lett. B 593 (2004) 82, arXiv:nucl-th/0402051.
[31] C.T. Sachrajda, G. Villadoro, Phys. Lett. B 609 (2005) 73, arXiv:hep-lat/0411033.
[32] G.M. de Divitiis, R. Petronzio, N. Tantalo, Phys. Lett. B 595 (2004) 408, arXiv:hep-lat/0405002; G.M. de Divitiis, N. Tantalo, arXiv:hep-lat/0409154.
[33] P.F. Bedaque, J.-W. Chen, Phys. Lett. B 616 (2005) 208, arXiv:hep-lat/0412023.
[34] D. Agadjanov, U.-G. Meißner, A. Rusetsky, arXiv:1310.7183 [hep-lat].
[35] K. Polejaeva, A. Rusetsky, Eur. Phys. J. A 48 (2012) 67, arXiv:1203.1241 [hep-lat].
[36] P. Guo, arXiv:1303.3349 [hep-lat].
[37] R.A. Briceno, Z. Davoudi, Phys. Rev. D 87 (2013) 094507, arXiv:1212.3398 [hep-lat].
[38] M. Hansen, S. Sharpe, talk at the LATTICE 2013 Symposium.
[39] D. Hoja, U.-G. Meißner, A. Rusetsky, J. High Energy Phys. 1004 (2010) 050, arXiv:1001.1641 [hep-lat].
[40] V. Bernard, D. Hoja, U.-G. Meißner, A. Rusetsky, J. High Energy Phys. 1209 (2012) 023, arXiv:1205.4642 [hep-lat].
[41] S. Mandelstam, Proc. R. Soc. Lond. A 233 (1955) 248.
[42] K. Huang, H.A. Weldon, Phys. Rev. D 11 (1975) 257.
[43] I.G. Aznauryan, V.D. Burkert, T.-S.H. Lee, arXiv:0810.0997 [nucl-th].
[44] D. Drechsel, O. Hanstein, S.S. Kamalov, L. Tiator, Nucl. Phys. A 645 (1999) 145, arXiv:nucl-th/9807001.
[45] R.L. Workman, L. Tiator, A. Sarantsev, Phys. Rev. C 87 (6) (2013) 068201, arXiv:1304.4029 [nucl-th].
[46] J. Gegelia, S. Scherer, Eur. Phys. J. A 44 (2010) 425, arXiv:0910.4280 [hep-ph]; T. Bauer, J. Gegelia, S. Scherer, Phys. Lett. B 715 (2012) 234, arXiv:1208.2598 [hep-ph].
[47] H.F. Jones, M.D. Scadron, Ann. Phys. 81 (1973) 1.
[48] V. Pascalutsa, M. Vanderhaeghen, S.N. Yang, Phys. Rep. 437 (2007) 125, arXiv:hep-ph/0609004.
[49] C. Itzykson, J.B. Zuber, International Series in Pure and Applied Physics, McGraw–Hill, New York, USA, 1980.
[50] M. Göckeler, et al., QCDSF and UKQCD Collaborations, PoS LATTICE 2008 (2008) 138.
[51] H.B. Meyer, arXiv:1202.6675 [hep-lat].

CHAPTER 3

Rare $B \to K^* l^+ l^-$ decay

3.1 Summary

At present, there are several rare B meson decay modes that are very promising in the search for physics beyond the Standard Model. The $B \to K^* l^+ l^-$ is, in particular, regarded as one of the most important processes, since the polarization of the $K^*(892)$ resonance results in many observables. Recently, the LCHb and Belle collaborations have seen an interesting pattern of deviations from the SM predictions in this mode.

The form factors of the corresponding hadronic matrix elements, which enter the analysis of the experimental data, are one of the sources of the theoretical uncertainties. They have been recently determined on the lattice. Although this is the first unquenched lattice calculation, the K^* was stable due to the large value of the pion mass.

The present work considers a scenario when the K^* eventually decays into πK, and the finite volume formalism for the analysis of the lattice data has to be applied. The results can be summarized as follows:

- The two-channel analogue of the Lellouch-Lüscher formula is re-derived in the non-relativistic EFT. This allows one the determine the approximate value of the decay amplitude in the low-recoil region.
- The procedure to determine the $B \to K^*$ form factors at the complex pole position is worked out.
- The presence of the ηK threshold is taken into account. One could expect that the effect of this threshold might be seen in the lattice data.
- The infinitely-narrow width approximation of the results in the two-channel problem is studied. It is shown that, even though taking this limit is more involved in the multi-channel case, the final expressions have a simple form.

Available online at www.sciencedirect.com

ScienceDirect

Nuclear Physics B 910 (2016) 387–409

NUCLEAR PHYSICS B

www.elsevier.com/locate/nuclphysb

The $B \to K^*$ form factors on the lattice

Andria Agadjanov [a,*], Véronique Bernard [b], Ulf-G. Meißner [a,c], Akaki Rusetsky [a]

[a] *Helmholtz-Institut für Strahlen- und Kernphysik (Theorie) and Bethe Center for Theoretical Physics, Universität Bonn, D-53115 Bonn, Germany*

[b] *Institut de Physique Nucléaire, UMR 8608, CNRS, Univ. Paris-Sud, Université Paris-Saclay, F-91406 Orsay Cedex, France*

[c] *Institute for Advanced Simulation (IAS-4), Institut für Kernphysik (IKP-3) and Jülich Center for Hadron Physics, Forschungszentrum Jülich, D-52425 Jülich, Germany*

Received 25 May 2016; accepted 5 July 2016

Available online 11 July 2016

Editor: Hong-Jian He

Abstract

The extraction of the $B \to K^*$ transition form factors from lattice data is studied, applying non-relativistic effective field theory in a finite volume. The possible mixing of πK and ηK states is taken into account. The two-channel analogue of the Lellouch–Lüscher formula is reproduced. Due to the resonance nature of the K^*, an equation is derived, which allows to determine the form factors at the pole position in a process-independent manner. The infinitely-narrow width approximation of the results is discussed.

1. Introduction

Rare B decay modes provide one of the best opportunities in the search for physics beyond the Standard Model (BSM). Among them, $B \to K^* l^+ l^-$ is regarded as one of the most important channels, as the polarization of the K^* allows a precise angular reconstruction resulting in many observables which can be tested in the Standard Model (SM) and its extensions [1–6]. In 2013,

* Corresponding author.
E-mail address: aagadjanov@hiskp.uni-bonn.de (A. Agadjanov).

http://dx.doi.org/10.1016/j.nuclphysb.2016.07.005

LHCb [7] published the first analysis of a set of optimized observables, presenting an interesting pattern of deviations, confirmed by later measurements with a larger statistics [8], as well as by a recent analysis from the Belle Collaboration [9]. A first interpretation of this pattern of deviation was proposed [10], where the Wilson coefficient C_9 of the pertinent semileptonic operator (and, possibly, other coefficients as well), received contribution from the BSM physics. Further experimental results have indicated deviations concerning the branching ratios of $B \to K^* \mu^+ \mu^-$, but also $B_s \to \phi \mu^+ \mu^-$ and $B \to K \mu^+ \mu^-$, with the possibility of a violation of lepton flavor universality between electron and muon modes [11–13]. These results triggered lots of activities on the theoretical side and, in particular, their consequences on global fits are being studied [14–16]. In these global fits, a special attention has to be paid to the theoretical uncertainties arising from the *form factors* of the corresponding hadronic matrix elements, which affect the branching ratios involved in the fit. In the low recoil region, which will be our main focus here, these form factors are mostly known from light cone sum rules, which suffer from relatively large uncertainties [17, 18]. It would thus be particularly interesting to have information on these quantities from lattice QCD simulations. Also, the method used to calculate these form factors could be applied to other interesting processes as, for example, $B \to K^* \gamma$.

Recently, the first unquenched lattice QCD calculations of the $B \to K^*$ form factors have appeared [19–21] (see also Refs. [22–28] for quenched results). Although this work represents a major progress in the field, the simulations have been performed at such quark mass values that the $K^*(892)$ resonance has been treated as a stable particle. Correspondingly, the standard methods of the lattice QCD could be used for the analysis of the data. However, they are not applicable anymore, when the K^* eventually decays into πK.

The following question has to be addressed: how to compute the matrix elements involving two strongly interacting particles in the in- or out-state? Briefly, the answer is given by the so-called Lellouch–Lüscher method [29]. It is a generalization of the Lüscher finite-volume approach [30], which provides a method to extract the elastic phase shifts and the resonance parameters (the mass and width) from the two-particle discrete energy levels spectrum, measured on the lattice.

At the next step, it should be understood, how to *define* the matrix elements involving resonances such as K^*, ρ, or Δ. As it has been argued in Refs. [31,32], the only plausible field-theoretical definition necessitates an analytic continuation of the matrix element to the resonance pole position in the complex plane. Therefore, strictly speaking, the corresponding form factor can only be defined at the resonance pole. The other well known definition of the form factor is based on the Breit–Wigner parameterization of the resonant amplitude (see, e.g., Refs. [33,34]). However, this definition yields a model- and process-dependent result, since the background is unknown. If the width of the resonance is not very small (it is roughly 50 MeV in the case of the $K^*(892)$), using different definitions might have an effect on the extracted observables.

There is an additional effect, which is due to the presence of the ηK threshold. For physical quark masses, it is approximately 150 MeV above the K^* mass, and this value will be reduced when the light quark masses, used in the simulations, are higher. One could expect that the effect of this threshold might be seen in the data. The recent lattice calculation by the Hadron Spectrum Collaboration, however, indicates that the coupling between the ηK and πK channels remains small even at the pion mass as large as roughly 400 MeV [35,36]. Nevertheless, the two-channel problem has to be addressed. Although of academic interest in the present context, a similar theoretical framework could be useful, e.g., for the lattice extraction of the electromagnetic form factors of the $\Lambda(1405)$ resonance (see Refs. [37,38] for the recent lattice results).

Recently, the Lellouch–Lüscher method has been generalized to include multiple strongly-coupled decay channels [39–42]. In particular, the authors of Ref. [41] provide general formulas for spinless particles, which are also valid for the $B \to \pi K(\eta K)$ transition. On the contrary, the extraction of the form factors at the resonance pole in the multi-channel case has not been studied yet. It has been done only in the one-channel problem [31]. In the present work, we fill this gap by considering the πK–ηK coupled-channel system.

In order to establish a relation between the finite volume quantities, measured on the lattice, and infinite volume observables, a systematic theoretical framework is needed. We apply the so-called non-relativistic effective field theory in a finite volume in its covariant formulation [43,44]. We find this approach algebraically simpler than the one based on the Bethe–Salpeter equation (see, e.g., Refs. [45,46]). In the end, both methods have the same range of applicability and one arrives at the same results.

The paper is organized as follows: In section 2, we introduce form factors governing the $B \to K^*$ transition. We also consider the proper kinematics, which should be used in lattice measurements of matrix elements. Further, in section 3, we set up the non-relativistic effective field theory in a finite volume. The two-channel analogue of the Lellouch–Lüscher formula is re-derived. In section 4, we obtain the equation for the extraction of the form factors at the resonance pole in the two-channel case. Additionally, in view of different opinions expressed in the literature (see, e.g., Refs. [47,48]), we address the issue of defining the photon virtuality at the resonance pole. In section 5, we consider the infinitely small width approximation for our results. Section 6 contains our conclusions.

2. Matrix elements on the lattice

2.1. Formalism

The effective theory of the $b \to s$ decays is based on the weak Hamiltonian [49–54]

$$\mathcal{H}_{\text{eff}} = -\frac{4G_F}{\sqrt{2}} V_{ts}^* V_{tb} \sum_i C_i W_i \,, \tag{1}$$

where G_F denotes the Fermi constant, V_{ts}, V_{tb} are elements of the CKM matrix and the C_i are Wilson coefficients. In the SM, one has 10 effective local operators W_i. Such a description is applicable at energies much below the masses of the weak gauge bosons.

The seven $B \to K^*$ form factors are contained in the matrix elements of the W_7, W_9 and W_{10} operators:

$$\begin{aligned} W_7 &= \frac{m_b e}{16\pi^2} \bar{s}\sigma^{\mu\nu} P_R b \, F_{\mu\nu}, \quad W_9 = \frac{e^2}{16\pi^2} \bar{s}\gamma^\mu P_L b \, \bar{\ell}\gamma_\mu \ell, \\ W_{10} &= \frac{e^2}{16\pi^2} \bar{s}\gamma^\mu P_L b \, \bar{\ell}\gamma_\mu \gamma^5 \ell, \end{aligned} \tag{2}$$

where $F_{\mu\nu}$ is the electromagnetic field strength tensor, and

$$P_{L/R} = \tfrac{1}{2}(1 \mp \gamma^5), \quad \sigma^{\mu\nu} = \tfrac{i}{2}[\gamma^\mu, \gamma^\nu]. \tag{3}$$

They are defined, in Minkowski space, through the following expressions (see, e.g., Ref. [20]):

$$\langle V(k,\lambda)|\bar{s}\gamma^\mu b|B(p)\rangle = \frac{2iV(q^2)}{m_B + m_V} \epsilon^{\mu\nu\rho\sigma} \epsilon_\nu^* k_\rho p_\sigma \,, \tag{4}$$

$$\begin{aligned}
&\langle V(k,\lambda)|\bar{s}\gamma^\mu\gamma^5 b|B(p)\rangle \\
&\quad = 2m_V A_0(q^2)\frac{\epsilon^*\cdot q}{q^2}q^\mu + (m_B+m_V)A_1(q^2)\left(\epsilon^{*\mu} - \frac{\epsilon^*\cdot q}{q^2}q^\mu\right) \\
&\qquad - A_2(q^2)\frac{\epsilon^*\cdot q}{m_B+m_V}\left[(p+k)^\mu - \frac{m_B^2-m_V^2}{q^2}q^\mu\right], \qquad (5)\\
&q_\nu\langle V(k,\lambda)|\bar{s}\sigma^{\mu\nu} b|B(p)\rangle = 2T_1(q^2)\epsilon^{\mu\rho\tau\sigma}\epsilon^*_\rho p_\tau k_\sigma, \qquad (6)\\
&q_\nu\langle V(k,\lambda)|\bar{s}\sigma^{\mu\nu}\gamma^5 b|B(p)\rangle = iT_2(q^2)[(\epsilon^*\cdot q)(p+k)^\mu - \epsilon^{*\mu}(m_B^2-m_V^2)] \\
&\qquad\qquad + iT_3(q^2)(\epsilon^*\cdot q)\left[\frac{q^2}{m_B^2-m_V^2}(p+k)^\mu - q^\mu\right], \qquad (7)
\end{aligned}$$

where $q = p - k$ is a momentum transfer to the lepton pair, and $\epsilon(k,\lambda)$ denotes a polarization vector of the vector meson (K^*) with momentum k and spin polarization $\lambda = 1, 2, 3$ (see, e.g., Ref. [20]). Here, it is assumed that the K^* is a stable particle with mass m_V and appropriate quantum numbers.

There are also contributions of non-local operators to the full decay amplitude. However, the method described below does not yet allow to deal with them. Thus, we will consider the decay process in the low recoil region and assume that these contributions are small, so that the amplitude, extracted from lattice data, coincides approximately with the full one. In fact, there are some arguments that this is true in this kinematic region at least for most of the operators involved, see Refs. [55–59].

2.2. Finite volume

Since lattice simulations are performed in a finite spatial volume, the continuous rotational symmetry is broken down to the cubic one. Consequently, some particular irreducible representations (irreps) of the cubic group, or its subgroups in the moving frames, should be chosen. Taking into account the fact that, at energies below multi-particle thresholds the neglect of D- and higher partial waves seems to be justified, in order to clearly extract the P-wave scattering phase shift through the Lüscher equation, it is preferable to choose irreps, in which no mixing between S- and P-waves occurs. For that purpose, we consider the process in the K^* rest frame:

$$\mathbf{k} = 0, \quad \mathbf{p} = \mathbf{q} = \frac{2\pi}{L}\mathbf{d}, \quad \mathbf{d}\in\mathbb{Z}^3, \qquad (8)$$

where L denotes the side length of the volume, $V = L^3$. When the K^* is not at rest, only some of the form factors can be extracted without mixing. We provide the details in Appendix A. In the following, we write down the expressions for the current matrix elements, when the $\mathbf{d}$ vector is chosen along the third axis $\mathbf{d} = (0, 0, n)$. The two other cases, $\mathbf{d} = (n, n, 0)$ and $\mathbf{d} = (n, n, n)$ can be treated along the same lines.

The polarization vector of the free massive spin-1 particle with momentum $\mathbf{k}$ takes the form:

$$\epsilon^\mu(k,\lambda) = \left(\frac{\mathbf{k}\cdot\boldsymbol{\epsilon}^{(\lambda)}}{m_V}, \boldsymbol{\epsilon}^{(\lambda)} + \frac{\mathbf{k}\cdot\boldsymbol{\epsilon}^{(\lambda)}}{m_V(k_0+m_V)}\mathbf{k}\right), \qquad (9)$$

where the arbitrary vectors $\boldsymbol{\epsilon}^{(\lambda)}$ form an orthonormal basis. In particular, one can choose them as

$$\boldsymbol{\epsilon}^{(+)} = \frac{1}{\sqrt{2}}(1,i,0), \quad \boldsymbol{\epsilon}^{(-)} = \frac{1}{\sqrt{2}}(1,-i,0), \quad \boldsymbol{\epsilon}^{(0)} = (0,0,1). \qquad (10)$$

Obviously, the polarization vectors $\epsilon^\mu(k,\lambda)$ satisfy the gauge invariance condition

$$k_\mu \cdot \epsilon^\mu(k,\lambda) = 0, \quad \lambda = +,-,0. \tag{11}$$

Further, the Eqs. (4)–(7) first have to be rewritten in the Euclidean space. This can be done by applying the prescription

$$a_\mu^E = (\mathbf{a}, ia_0), \quad \gamma_\mu^E = (-i\boldsymbol{\gamma}, \gamma_0), \quad \gamma_5^E = \gamma^5, \qquad \mu = 1,2,3,4, \tag{12}$$

where a^μ is an arbitrary four-momentum in Minkowski space. The superscript E will be suppressed from now on.

With this in mind, we pick up the following current matrix elements

$$\begin{aligned}
\langle V(+)|J^{(+)}|B(p)\rangle &= -\frac{2im_V|\mathbf{q}|V(q^2)}{m_B+m_V},\\
\langle V(0)|i(E_B-m_V)J_A + |\mathbf{q}|J_A^{(0)}|B(p)\rangle &= -2im_V|\mathbf{q}|A_0(q^2),\\
\langle V(+)|J_A^{(+)}|B(p)\rangle &= -i(m_B+m_V)A_1(q^2),\\
\langle V(0)|i(E_B-m_V)J_A^{(0)} - |\mathbf{q}|J_A|B(p)\rangle &= 8m_Bm_VA_{12}(q^2),\\
\langle V(+)|i(E_B-m_V)I^{(+)} + |\mathbf{q}|I_0^{(+)}|B(p)\rangle &= 2im_V|\mathbf{q}|T_1(q^2),\\
\langle V(+)|i(E_B-m_V)I_A^{(+)} + |\mathbf{q}|I_{0A}^{(+)}|B(p)\rangle &= -i(m_B^2-m_V^2)T_2(q^2),\\
\langle V(0)|I_A^{(0)}|B(p)\rangle &= -\frac{4m_Bm_V}{m_B+m_V}T_{23}(q^2),
\end{aligned} \tag{13}$$

where $E_B = \sqrt{m_B^2+\mathbf{q}^2}$ is energy of the B meson, and $\langle V(+)|$ is a state vector with a positive circular polarization,

$$\langle V(+)| = \frac{\langle V(1)| - i\langle V(2)|}{\sqrt{2}}\,. \tag{14}$$

Here, the current operators are given by

$$\begin{aligned}
J^{(\pm)} &= \frac{1}{\sqrt{2}}\bar{s}(\gamma_1 \pm i\gamma_2)b, \quad J_A^{(\pm)} = \frac{1}{\sqrt{2}}\bar{s}(\gamma_1 \pm i\gamma_2)\gamma_5 b,\\
J_A^{(0)} &= \bar{s}\gamma_3\gamma_5 b, \quad J_A = \bar{s}\gamma_4\gamma_5 b, \quad I_A^{(0)} = \bar{s}\sigma_{34}\gamma_5 b,\\
I_0^{(\pm)} &= \frac{1}{\sqrt{2}}\bar{s}(\sigma_{13} \pm i\sigma_{23})b, \quad I_{0A}^{(\pm)} = \frac{1}{\sqrt{2}}\bar{s}(\sigma_{13} \pm i\sigma_{23})\gamma_5 b,\\
I^{(\pm)} &= \frac{1}{\sqrt{2}}\bar{s}(\sigma_{14} \pm i\sigma_{24})b, \quad I_A^{(\pm)} = \frac{1}{\sqrt{2}}\bar{s}(\sigma_{14} \pm i\sigma_{24})\gamma_5 b,
\end{aligned} \tag{15}$$

and the quantities $A_{12}(q^2)$, $T_{23}(q^2)$ are related to the form factors through

$$A_{12}(q^2) = \frac{(m_B+m_V)^2(m_B^2-m_V^2-q^2)A_1(q^2) - \lambda A_2(q^2)}{16m_Bm_V^2(m_B+m_V)}, \tag{16}$$

$$T_{23}(q^2) = \frac{m_B+m_V}{8m_Bm_V^2}\left[\left(m_B^2+3m_V^2-q^2\right)T_2(q^2) - \frac{\lambda T_3(q^2)}{m_B^2-m_V^2}\right], \tag{17}$$

where $\lambda \equiv \lambda(m_B^2, m_V^2, q^2) = [(m_B+m_V)^2-q^2][(m_B-m_V)^2-q^2]$ denotes the Källén triangle function. In the following, we denote the matrix elements Eq. (13) shortly as F^M, $M = 1,\ldots,7$.

Table 1
Extraction of matrix elements in the irreps without partial-wave mixing.

Little group	Irrep	Form factor
C_{4v}	$\mathbb{E}$	V, A_1, T_1, T_2
	$\mathbb{A}_1$	A_0, A_{12}, T_{23}

When the K^* is taken at rest, it is necessary to consider lattice simulations in asymmetric boxes (see below). These boxes, which are of the type $L \times L \times L'$, have the same symmetry properties as the symmetric ones boosted in the $\mathbf{d} = (0, 0, n)$ direction. In Table 1, the irreps of the corresponding little group, where the matrix elements Eq. (13) should be measured, are listed.

The states $\langle V(\pm)|$, $\langle V(0)|$ are created by acting with the following local field operators, transforming according to these irreps, on the vacuum state $\langle 0|$:

$$\mathcal{O}^{(\pm)}_{\mathbb{E}}(\mathbf{0}, t) = \frac{1}{\sqrt{2}} \sum_{\mathbf{x}} \big(O_1(\mathbf{x}, t) \mp i\, O_2(\mathbf{x}, t)\big), \quad \mathcal{O}^{(0)}_{\mathbb{A}_1}(\mathbf{0}, t) = \sum_{\mathbf{x}} O_3(\mathbf{x}, t), \tag{18}$$

where $O_i(x)$ are spatial components of the vector field potential (see, e.g., Ref. [60]). Such operators are constructed out of the local quark bilinears. In practice, it is important to add also meson–meson-type non-local operators in lattice simulations. These can be constructed along the lines described in Ref. [60].

Until now, the K^* has been assumed to be a stable vector meson. When the K^* becomes a resonance in lattice simulations, the matrix elements of Eq. (13) can still be measured. However, one gets the matrix elements of the current between a one-meson state $|B(p)\rangle$ and a certain eigenstate of the finite-volume Hamiltonian. The mass m_V is now replaced by the discrete energy E_n of the n-th eigenstate ($n = 0, 1, \ldots$). The dependence of the energy E_n on the volume is not suppressed exponentially (unlike the case of a stable K^*) [30]. A similar statement holds for the quantities F^M.

The matrix elements F^M are functions of the total center-of mass (CM) energy E_n and 3-momentum $|\mathbf{q}|$ of the B meson: $F^M = F^M(E_n, |\mathbf{q}|)$. As it has been previously discussed in case of the $\Delta N\gamma^*$ transition in Ref. [31], in order to determine the form factors at the K^* resonance pole, the quantities F^M should be measured at different values of the energy E_n (for a given value of n), while keeping $|\mathbf{q}|$ fixed. Again, this could be achieved by applying asymmetric volumes with asymmetry along the third axes $L \times L \times L'$ or (partial) twisting in the b-quark (see Ref. [31] for more details).

Below, we study in detail the extraction of the form factors on the real energy axis as well as at the complex resonance pole. We emphasize once more, that only the definition, which implies the analytic continuation, leads to the process-independent values of the resonance form factors.

3. Lellouch–Lüscher formula

3.1. Infinite volume

In this section, the analogue of the Lellouch–Lüscher formula in the two-channel case is reproduced. For that purpose, we apply the non-relativistic effective field theory in a finite volume along the lines of Refs. [32,31]. We generalize the formulas given there appropriately so that they

can suit our needs. In the following, the K^* is taken at rest, so that there is no S- and P-wave mixing.

Further, we specify the matrix elements of the scattering amplitude. The actual physics can not, of course, depend on the chosen parameterization. In the literature, there exists a parameterization of the S-matrix due to Stapp et al. [61]. In this work, we rather follow the one from Refs. [39,62] and write the T-matrix in terms of three real parameters: the so-called eigenphases $\delta_1(p_1)$, $\delta_2(p_2)$ and mixing parameter $\varepsilon(E)$

$$T = 8\pi\sqrt{s}\begin{pmatrix} \frac{1}{p_1}(c_\varepsilon^2 e^{i\delta_1}\sin\delta_1 + s_\varepsilon^2 e^{i\delta_2}\sin\delta_2) & \frac{1}{\sqrt{p_1 p_2}}c_\varepsilon s_\varepsilon(e^{i\delta_1}\sin\delta_1 - e^{i\delta_2}\sin\delta_2) \\ \frac{1}{\sqrt{p_1 p_2}}c_\varepsilon s_\varepsilon(e^{i\delta_1}\sin\delta_1 - e^{i\delta_2}\sin\delta_2) & \frac{1}{p_2}(c_\varepsilon^2 e^{i\delta_2}\sin\delta_2 + s_\varepsilon^2 e^{i\delta_1}\sin\delta_1) \end{pmatrix}, \tag{19}$$

where $s_\varepsilon \equiv \sin\varepsilon(E)$, $c_\varepsilon \equiv \cos\varepsilon(E)$. Here, p_1 and p_2 denote the relative 3-momenta in the πK and ηK channels, respectively. They are related to the total energy E through the equations

$$|p_1| = \frac{\lambda(m_\pi^2, m_K^2, s)}{2\sqrt{s}}, \quad |p_2| = \frac{\lambda(m_\eta^2, m_K^2, s)}{2\sqrt{s}}, \tag{20}$$

where $s = E^2$. We note that the eigenphases δ_1, δ_2 have the meaning of phase shifts in the corresponding channels πK and ηK, respectively, only in the decoupling limit $\varepsilon \to 0$. Otherwise, their behavior with energy is non-trivial (see, e.g., Refs. [63,64]). Firstly, thanks to the no-crossing theorem [65], the curves of the functions $\delta_1(E)$, $\delta_2(E)$ cannot intersect. Secondly, assuming the Breit–Wigner approximation, it can be shown that only one of these curves crosses $\pi/2$ in the vicinity of the resonance energy (see below). Lattice data should not be in contradiction with these properties.

On the other hand, the T-matrix obeys Lippmann–Schwinger equation (see Ref. [32]):

$$T = V + VGT, \tag{21}$$

where the angular momentum index l has been suppressed. Here, V denotes a potential and $G(s)$ is a loop function matrix given by

$$G = \begin{pmatrix} \frac{ip_1}{8\pi\sqrt{s}} & 0 \\ 0 & \frac{ip_2}{8\pi\sqrt{s}} \end{pmatrix}. \tag{22}$$

In Eq. (21), all quantities have been taken on the energy shell $p_1 = p_1'$, $p_2 = p_2'$, where p_1, p_2 and p_1', p_2' are respective relative momenta in the initial and final two-particle states.

The parameterization of the potential V in terms of parameters $\delta_1(p_1)$, $\delta_2(p_2)$ and $\varepsilon(E)$ is obtained readily from Eqs. (19) and (21):

$$V = 8\pi\sqrt{s}\begin{pmatrix} \frac{1}{p_1}(t_1 + s_\varepsilon^2 t) & -\frac{1}{\sqrt{p_1 p_2}}c_\varepsilon s_\varepsilon t \\ -\frac{1}{\sqrt{p_1 p_2}}c_\varepsilon s_\varepsilon t & \frac{1}{p_2}(t_2 - s_\varepsilon^2 t) \end{pmatrix}, \tag{23}$$

where $t_i \equiv \tan\delta_i(p_i)$ and $t = t_2 - t_1$. Clearly, the potential matrix V is real and symmetric.

3.2. Finite volume

3.2.1. Two-point function

We return to the derivation of the two-channel Lellouch–Lüscher formula. Our goal is to calculate the two- and three-point correlation functions relevant to the $B \to K^*$ form factors. Let

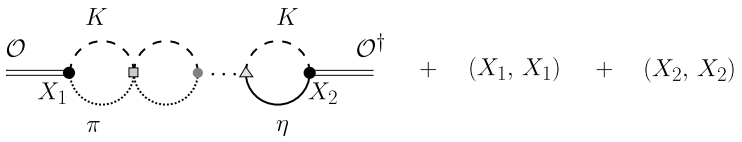

Fig. 1. Two-point function $D(x_0 - y_0)$ in the non-relativistic effective field theory in a finite volume. The grey circle, square, and triangle depict different couplings in the πK–ηK system. The quantities X_1, X_2 are couplings of the operator $\mathcal{O}$ to the respective channels. Similar diagrams are obtained by replacements $X_1 \to X_2$ and $X_2 \to X_1$.

$O(x)$ be a local operator with quantum numbers of the K^* that transforms according to the given irrep, as provided explicitly in Eq. (18). According to the methodology of the lattice calculations, one is interested in the Euclidean two-point function of the form

$$D(x_0 - y_0) = \langle 0|\mathcal{O}(x_0)\mathcal{O}^\dagger(y_0)|0\rangle, \tag{24}$$

where $\mathcal{O}(t)$ is given by the Fourier transformation of the $O(x)$ in the rest frame:

$$\mathcal{O}(t) = \sum_{\mathbf{x}} O(\mathbf{x}, t). \tag{25}$$

Note that we always work in the limit of zero lattice spacing, in which the right-hand side of Eq. (25) contains an integral over the finite volume instead of a sum over the lattice sites.

It is clear from the spectral representation[1] of the function $D(x_0 - y_0)$,

$$D(x_0 - y_0) = \sum_n e^{-E_n(x_0 - y_0)} |\langle 0|\mathcal{O}(0)|E_n\rangle|^2, \tag{26}$$

that energy levels E_n can be extracted by studying the decay pattern of $D(x_0 - y_0)$ in the formal limit $x_0 \to +\infty$, $y_0 \to -\infty$.

The diagrammatic representation of the two-point function Eq. (24) within the non-relativistic effective field theory below the inelastic threshold is shown in Fig. 1. The quantities X_α, $\alpha = 1, 2$, denote the couplings of the operator $\mathcal{O}$ to respective channels. Since the corresponding Lagrangian contains terms with arbitrary number of spatial derivatives, one has $X_\alpha = A_\alpha + B_\alpha \mathbf{p}_\alpha^2 + \cdots$, where $A_\alpha, B_\alpha, \ldots$ contain only short-range physics. Here, $\mathbf{p}_\alpha^2$, $\alpha = 1, 2$, are *external* relative 3-momenta squared in the corresponding channels. Although the expansion for X_α is written in the CM frame, it can be brought to the covariant form in an arbitrary moving frame (see Ref. [44]). It is important to note that quantities X_α will drop out in the final result.

After summing up all two-particle reducible diagrams, the two-point function reads

$$D(x_0 - y_0) = \mathcal{V} \int_{-\infty}^{+\infty} \frac{dP_0}{2\pi} e^{iP_0(x_0 - y_0)} X^T [G_L(P_0) + G_L(P_0) T_L(P_0) G_L(P_0)] X, \tag{27}$$

where $X^T = (X_1, X_2)$, $\mathcal{V}$ is the lattice volume, and G_L denotes a finite-volume counterpart of the loop function matrix Eq. (22):

$$G_L = \begin{pmatrix} -\frac{p_1}{8\pi\sqrt{s}} \cot\phi(p_1) & 0 \\ 0 & -\frac{p_2}{8\pi\sqrt{s}} \cot\phi(p_2) \end{pmatrix}, \quad s = -P_0^2. \tag{28}$$

[1] In this work, we use a different form from Ref. [31] normalization of the eigenstates of the total Hamiltonian. While the single B-meson state in a finite volume is still normalized, according to $\langle B(p)|B(p)\rangle = 2E_B$, the normalization of the two-particle states E_n is given by $\langle E_n|E_n\rangle = 1$.

Here, $\phi(p_\alpha)$ are the volume-dependent functions that are related to the Lüscher zeta-function. They are given by the following expressions in the irreps of interest $\mathbb{E}$ and $\mathbb{A}_1$ (see, e.g., Ref. [60]):

$$\cot\phi^{\mathbb{E}}(p_\alpha) = -\frac{1}{\pi^{3/2}\eta_\alpha}\left\{\hat{Z}_{00}(1;\eta_\alpha^2) - \frac{1}{\sqrt{5}\eta_\alpha^2}\hat{Z}_{20}(1;\eta_\alpha^2)\right\}, \tag{29}$$

$$\cot\phi^{\mathbb{A}_1}(p_\alpha) = -\frac{1}{\pi^{3/2}\eta_\alpha}\left\{\hat{Z}_{00}(1;\eta_\alpha^2) + \frac{2}{\sqrt{5}\eta_\alpha^2}\hat{Z}_{20}(1;\eta_\alpha^2)\right\}, \tag{30}$$

where $\eta_\alpha = p_\alpha L/2\pi$. The Lüscher zeta-function $\hat{Z}_{lm}(1;\eta^2)$ for generic asymmetric volumes $L\times L\times L'$ with $L' = xL$ reads

$$\hat{Z}_{lm}(1;\eta^2) = \frac{1}{x}\sum_{\mathbf{n}\in\mathbb{Z}^3}\frac{\mathcal{Y}_{lm}(\mathbf{r})}{\mathbf{r}^2-\eta^2}, \qquad r_{1,2} = n_{1,2}, \quad r_3 = \frac{1}{x}n_3, \qquad \hat{Z}_{20}(1;\eta^2)\neq 0. \tag{31}$$

Further, the T_L-matrix is a scattering amplitude in a finite volume that is defined formally also through a Lippmann–Schwinger equation with the same potential V:

$$T_L = V + VG_LT_L. \tag{32}$$

Substituting the potential V, Eq. (23), into this equation, we obtain:

$$T_L = \frac{8\pi\sqrt{s}}{f(E)}\begin{pmatrix} \frac{1}{p_1}[t_1\tau_1(t_2+\tau_2)+s_\varepsilon^2\tau_1\tau_2 t] & -\frac{1}{\sqrt{p_1p_2}}c_\varepsilon s_\varepsilon\tau_1\tau_2 t \\ -\frac{1}{\sqrt{p_1p_2}}c_\varepsilon s_\varepsilon\tau_1\tau_2 t & \frac{1}{p_2}[t_2\tau_2(t_1+\tau_1)-s_\varepsilon^2\tau_1\tau_2 t]\end{pmatrix}, \tag{33}$$

where $\tau_\alpha \equiv \tan\phi(p_\alpha)$ and

$$f(E) \equiv (t_1+\tau_1)(t_2+\tau_2) + s_\varepsilon^2(t_2-t_1)(\tau_2-\tau_1). \tag{34}$$

The two-channel Lüscher equation [39,66,67], which allows to determine the infinite-volume T-matrix elements [39,68,69], follows directly from Eq. (34)

$$(t_1+\tau_1)(t_2+\tau_2) + s_\varepsilon^2(t_2-t_1)(\tau_2-\tau_1)\big|_{E=E_n} = 0, \tag{35}$$

where all quantities are taken at the energies $E = E_n$ of the simple poles of the T_L-matrix, or equivalently, the eigenvalues of the corresponding strong Hamiltonian in a finite volume.

The integral Eq. (27) is evaluated by applying Cauchy's theorem. It can be shown explicitly that only the poles of the $T_L(P_0)$-matrix contribute to the integral, while free poles cancel in the integrand [32,41]. The residues of the $T_L(P_0)$ factorize in the n-th pole $P_0 = iE_n$:

$$T_L^{\alpha\beta} = \frac{f_\alpha f_\beta}{E_n + iP_0} + \cdots. \tag{36}$$

Here, the quantities f_1, f_2 can be brought to the following form by applying the Lüscher equation:

$$f_1^2 = \frac{8\pi\sqrt{s}}{p_1}\frac{\tau_1^2(t_2+\tau_2-s_\varepsilon^2 t)}{f'(E)}\bigg|_{E=E_n}, \qquad f_2^2 = \frac{8\pi\sqrt{s}}{p_2}\frac{\tau_2^2(t_1+\tau_1+s_\varepsilon^2 t)}{f'(E)}\bigg|_{E=E_n}, \tag{37}$$

where $f'(E) \equiv df(E)/dE$. Performing the integration over P_0, we get

$$D(x_0-y_0) = \frac{\mathcal{V}}{64\pi^2E_n^2}\sum_n e^{-E_n(x_0-y_0)}\left[\sum_{\alpha=1}^{2}X_\alpha p_\alpha(E_n)\tau_\alpha^{-1}(E_n)f_\alpha(E_n)\right]^2. \tag{38}$$

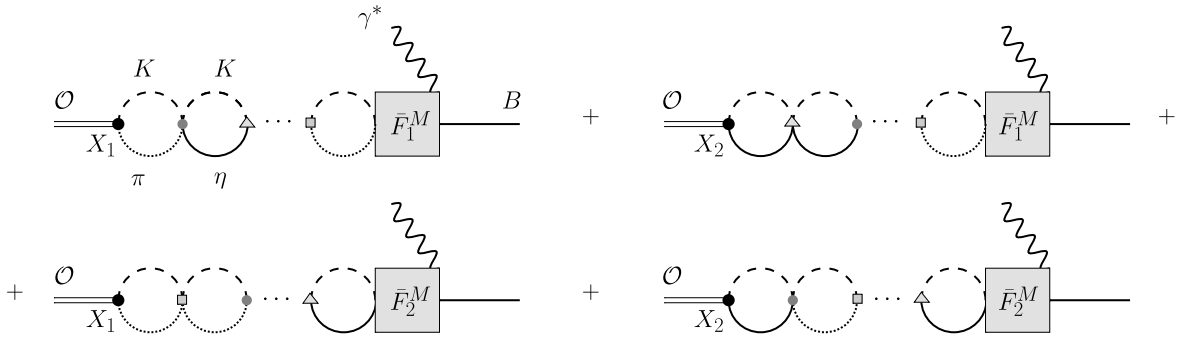

Fig. 2. Diagrams contributing to the $B \to K^*$ transition in a finite volume (see Fig. 1 for notations). The quantities $\bar{F}_\alpha^M(E, |\mathbf{q}|)$, $\alpha = 1, 2$, are volume-independent up to exponentially suppressed contributions.

Comparing this equation with the spectral representation Eq. (26), we finally obtain

$$|\langle 0|\mathcal{O}(0)|E_n\rangle| = \frac{\mathcal{V}^{1/2}}{8\pi E_n}\left|\sum_{\alpha=1}^{2} X_\alpha p_\alpha(E_n)\tau_\alpha^{-1}(E_n) f_\alpha(E_n)\right|. \tag{39}$$

3.2.2. Three-point function

We proceed to evaluate the current matrix elements $F^M(E, |\mathbf{q}|)$ in a finite volume. To this end, we start from the quantity

$$\Gamma^M(x_0, p) = \langle 0|\mathcal{O}(x_0) J^M(0)|B(p)\rangle, \quad M = 1, \dots 7. \tag{40}$$

Here, the $J^M(0)$ denote the operators in the matrix elements of Eq. (13). Inserting a complete set of states, we get the spectral representation of $\Gamma^M(x_0, p)$

$$\Gamma^M(x_0, p) = \sum_n e^{-E_n x_0}\langle 0|\mathcal{O}(0)|E_n\rangle F^M(E_n, |\mathbf{q}|). \tag{41}$$

Diagrammatically, the $B \to K^*$ transition matrix elements are shown in Fig. 2. The quantities $\bar{F}_\alpha^M(E, |\mathbf{q}|)$, $\alpha = 1, 2$, denote the sum of all two-particle irreducible diagrams in the respective channels. They do not depend on the volume up to exponentially suppressed contributions. The volume dependence arises due to the final-state meson interaction. We note that the diagrams, in which the photon is attached to one of the internal lines or the B meson external line do not contribute to the matrix elements of *flavor changing neutral currents*. As a result, summing up the bubble diagrams we obtain

$$\Gamma^M(x_0, p) = \mathcal{V}^{-1/2}\int_{-\infty}^{+\infty}\frac{dP_0}{2\pi} e^{iP_0 x_0} X^T[G_L(P_0) + G_L(P_0)T_L(P_0)G_L(P_0)]\bar{F}^M(P_0, |\mathbf{q}|), \tag{42}$$

where $\bar{F}^M(P_0, |\mathbf{q}|)$ denotes a two-component vector with elements $\bar{F}_\alpha^M(P_0, |\mathbf{q}|)$. Similarly to the case of the two-point function, only the poles of the $T_L(P_0)$-matrix contribute to the integral. Integrating over P_0, one gets

$$\Gamma^M(x_0, p) = \frac{\mathcal{V}^{-1/2}}{64\pi^2 E_n^2}\sum_n e^{-E_n x_0}\sum_{\alpha,\beta=1}^{2}[X_\alpha p_\alpha(E_n)\tau_\alpha^{-1}(E_n) f_\alpha(E_n)]$$
$$\times [p_\beta(E_n)\tau_\beta^{-1}(E_n) f_\beta(E_n)\bar{F}_\beta^M(E_n, |\mathbf{q}|)]. \tag{43}$$

Comparing this formula with Eq. (41) and using Eq. (39), we arrive at the final result:

$$|F^M(E_n, |\mathbf{q}|)| = \frac{\mathcal{V}^{-1}}{8\pi E} \left| p_1 \tau_1^{-1} f_1 \bar{F}_1^M + p_2 \tau_2^{-1} f_2 \bar{F}_2^M \right| \Big|_{E=E_n} . \tag{44}$$

The last step that needs to be done is to relate the above defined quantities $\bar{F}_1^M$, $\bar{F}_2^M$ to the (infinite-volume) decay amplitudes $\mathcal{A}_1^M(B \to \pi K l^+ l^-)$ and $\mathcal{A}_2^M(B \to \eta K l^+ l^-)$ through the two-channel Watson theorem. After summing up the two-particle reducible diagrams in the infinite volume, one gets

$$\mathcal{A}^M = (1 - VG)^{-1} \bar{F}^M, \tag{45}$$

or

$$\mathcal{A}^M = T V^{-1} \bar{F}^M, \tag{46}$$

where the Lippmann–Schwinger equation has been used. We obtain:

$$\mathcal{A}_1^M = \frac{1}{\sqrt{p_1}} (u_1^M c_\varepsilon e^{i\delta_1} - u_2^M s_\varepsilon e^{i\delta_2}), \quad \mathcal{A}_2^M = \frac{1}{\sqrt{p_2}} (u_2^M c_\varepsilon e^{i\delta_2} + u_1^M s_\varepsilon e^{i\delta_1}), \tag{47}$$

where

$$u_1^M = (\sqrt{p_1} c_\varepsilon \bar{F}_1^M + \sqrt{p_2} s_\varepsilon \bar{F}_2^M) \cos\delta_1, \quad u_2^M = (\sqrt{p_2} c_\varepsilon \bar{F}_2^M - \sqrt{p_1} s_\varepsilon \bar{F}_1^M) \cos\delta_2. \tag{48}$$

We have arrived at the two-channel analog of the Lellouch–Lüscher formula for the $B \to K^*$ transition. Note that, writing Eq. (44) in terms of the amplitudes u_1^M, u_2^M, one obtains the expressions similar to ones given in Ref. [39]. Later, we will consider the limit of this result, when the K^* resonance is infinitely narrow.

Hence, in the two-channel case, two quantities $\bar{F}_1^M$, $\bar{F}_2^M$ and their relative sign have to be determined from one equation, whereas in the one-channel case, only one quantity for one equation was involved. Consequently, one needs at least three different measurements at the same energy. This involves the extraction of the excited energy levels (see Ref. [39]). An alternative would be to measure the same energy level in asymmetric volumes of type $yL \times yL \times L'$ for different values of parameter y and L' fixed. Also, as long as one does not insist on keeping the variable $|\mathbf{q}|$ fixed and is ready to perform a two-variable fit for the quantities $\bar{F}_\alpha^M$, (partial) twisting in the s-quark or boosts can be applied. Then, the spectrum becomes dependent on the value of the twisting angle and/or the boost momentum. Although this option appears to be promising [69], the (potentially large) S- and P-wave mixing is inevitable in this case.

4. Form factors at the K^* resonance pole

The current matrix elements involving resonances have the proper field-theoretical meaning only if they are analytically continued to the resonance pole position. The advantage of such a definition is that it is process-independent. On the other hand, the definition based on the Breit–Wigner parameterization is, generally, not free of process- and model-dependent ambiguities, since the non-resonant background is unknown.

4.1. Effective-range expansion

The first step towards the pole extraction of the $B \to K^*$ form factors consists in the determination of the K^* resonance position. As is well known, the resonances are associated with

complex poles of the scattering amplitude T on unphysical Riemann sheets in the energy plane (s plane). The T-matrix itself is analytic on the whole plane except for cuts and poles. Here we will assume that all distant singularities from the pole do not affect the determination of its position. Thus, from the analytic structure of the functions $p_1(E)$, $p_2(E)$, Eq. (20), the only relevant singularities for our purpose are two cuts, which run from branch points at the threshold energies $E_1 = m_K + m_\pi$ and $E_2 = m_K + m_\eta$, respectively, along the positive axis to infinity. The imaginary parts of the $p_\alpha(s)$, $\alpha = 1, 2$, change the sign, when one goes from one sheet to another through these cuts. The four Riemann sheets are classified according to the signs of $\mathrm{Im}p_1$ and $\mathrm{Im}p_2$ (see, e.g., Ref. [70]). For example, on the sheet II one has $\mathrm{Im}p_1 < 0$ and $\mathrm{Im}p_2 > 0$, etc.

Further, it is convenient to formulate the problem in the K-matrix formalism. The $l = 1$ partial-wave amplitude T is defined in terms of K-matrix as follows:

$$T = (8\pi\sqrt{s})(K^{-1} - iP)^{-1}, \tag{49}$$

where $P = \mathrm{diag}(p_1, p_2)$ is a diagonal matrix. A comparison of this equation with Eq. (21) leads to the conclusion that the K-matrix is proportional to the potential V:

$$K = (8\pi\sqrt{s})^{-1}V. \tag{50}$$

The poles of the scattering amplitude T appear as the complex solutions of the secular equation, which we write as

$$\det(PK^{-1}P - iP^3) = 0. \tag{51}$$

The explicit form of this equation is different on each Riemann sheet. For instance, if one is interested in the solutions on the sheets II and III, then the matrix P must be chosen as $P_{II} = \mathrm{diag}(-p_1, p_2)$ and $P_{III} = \mathrm{diag}(-p_1, -p_2)$, respectively. The change of sign of momenta p_1 and/or p_2 is equivalent to the transition from one sheet to another.

The analytic properties of the K-matrix ensure that the $PK^{-1}P$ function obeys a polynomial expansion of the form (see Refs. [70,71])

$$PK^{-1}P = A + B(E - E_0) + \cdots, \tag{52}$$

where E_0 is an arbitrary point on the real axis, around which the Taylor expansion is made. The formula Eq. (52) is a multi-channel generalization of the well-known effective-range approximation [72]. Its additional advantage is the freedom to choose the value of the energy E_0: one does not need to start the expansion at threshold energies, as it is usually done. Consequently, the convergence of the series in Eq. (52) could be substantially improved. Also, the analytic continuation to the resonance pole position will not be spoiled by the presence of the distant singularities. This expansion, in particular, might be useful in case of the ρ resonance, when lattice simulations are performed at nearly physical quark masses.

In principle, one could also expand the K-matrix, see, e.g., Refs. [70,73]. However, such an expansion contains pole terms, which makes the fitting to data more complicated, although not impossible. In fact both parameterizations of the K-matrix have been recently used in the lattice study of the resonances in the coupled πK–ηK system [35,36].

The procedure to determine the resonance pole position consists in the following steps:

a) The K-matrix is numerically extracted on the lattice, by applying the Lüscher approach;
b) The parameters A, B, ... are fitted to lattice data;
c) Eq. (51) is solved on each unphysical Riemann sheet. The complex solution, which is numerically closest to the πK, ηK thresholds is identified with the K^* resonance pole.

Next, we assume that the K^* resonance is located on the sheet II. Other cases can be studied along the same lines.

4.2. Pole extraction of the form factors

We proceed with the evaluation of two- and three-point functions in the infinite volume. Afterwards, the result will be analytically continued to the resonance pole. The two-point function in Minkowski space is given by

$$i\,\langle 0|T[O(x)O^\dagger(y)]|0\rangle = \int \frac{d^4P}{(2\pi)^4}\, e^{-iP(x-y)} D(P^2), \tag{53}$$

where the function $D(P^2)$ reads

$$D(P^2) = X^T [G_{II}(s) + G_{II}(s) T_{II}(s) G_{II}(s)] X. \tag{54}$$

Here, $P^2 = s$ and the loop function $G_{II}(s)$ is chosen as

$$G_{II}(s) = \begin{pmatrix} -\frac{ip_1}{8\pi\sqrt{s}} & 0 \\ 0 & \frac{ip_2}{8\pi\sqrt{s}} \end{pmatrix}. \tag{55}$$

The form of the G_{II} guaranties that the scattering amplitude T, which is obtained from the Lippmann–Schwinger equation,

$$T_{II} = (V^{-1} - G_{II})^{-1}, \tag{56}$$

has poles on the sheet II. The simplest way to determine the T_{II}-matrix is to make the replacements $\tau_1 \to -i$, $\tau_2 \to +i$ in Eqs. (33), (34). We get

$$T_{II} = \frac{8\pi\sqrt{s}}{h(E)} \begin{pmatrix} \frac{1}{p_1}[t_1(1-it_2) + s_\varepsilon^2 t] & -\frac{1}{\sqrt{p_1 p_2}} c_\varepsilon s_\varepsilon t \\ -\frac{1}{\sqrt{p_1 p_2}} c_\varepsilon s_\varepsilon t & \frac{1}{p_2}[t_2(1+it_1) - s_\varepsilon^2 t] \end{pmatrix}, \tag{57}$$

where the quantity $h(E)$ is given by

$$h(E) \equiv (t_1 - i)(t_2 + i) + 2is_\varepsilon^2 (t_2 - t_1). \tag{58}$$

The resonance pole position $E = E_R \equiv \sqrt{s_R}$ is obtained from the equation

$$h(E_R) = 0. \tag{59}$$

Inverting the integral Eq. (53) and performing the integration over all variables, we get

$$D(P^2) = \frac{Z_R}{s_R - P^2}, \tag{60}$$

where Z_R is the (complex) wave-function renormalization constant of the resonance. From Eq. (60) it follows that

$$Z_R = \lim_{P^2 \to s_R} (s_R - P^2)\, D(P^2). \tag{61}$$

On the other hand, the $T(s)$-matrix on the second Riemann sheet has a pole at $P^2 = s_R$. In the vicinity of the pole, one has

$$T_{II}^{\alpha\beta}(s) = \frac{h_\alpha h_\beta}{s_R - P^2} + \cdots. \tag{62}$$

Here, the quantities h_1, h_2 are given by

$$h_1^2 = -\frac{8\pi\sqrt{s}}{p_1}\frac{2E(t_2+i-s_\varepsilon^2 t)}{h'(E)}\bigg|_{E=E_R}, \quad h_2^2 = -\frac{8\pi\sqrt{s}}{p_2}\frac{2E(t_1-i+s_\varepsilon^2 t)}{h'(E)}\bigg|_{E=E_R}, \tag{63}$$

where $h'(E) \equiv dh(E)/dE$. Consequently, we obtain the renormalization constant Z_R:

$$Z_R = -\frac{1}{64\pi^2 E_R^2}\left[\sum_{\alpha=1}^{2}(-1)^\alpha X_\alpha p_\alpha(E_R) h_\alpha(E_R)\right]^2. \tag{64}$$

The calculation of the three-point function in the infinite volume proceeds in a similar manner. One gets

$$i\,\langle 0|T[O(x)J^M(0)]|B(p)\rangle = \int \frac{d^4P}{(2\pi)^4}\, e^{-iPx}\Gamma^M(P,p), \tag{65}$$

where the quantity $\Gamma^M(P,p)$ in the frame $P^\mu = (P_0, \mathbf{0})$, $p^\mu = (\sqrt{m_B^2+\mathbf{q}^2}, \mathbf{q})$ reads

$$\Gamma^M(P,p) = X^T[G_{II}(s) + G_{II}(s)T_{II}(s)G_{II}(s)]\bar{F}^M(P_0,|\mathbf{q}|). \tag{66}$$

Further, recall that the irreducible amplitudes $\bar{F}_\alpha^M(P_0,|\mathbf{q}|)$, $\alpha = 1,2$, are analytic functions in the complex energy plane. Then, following Refs. [74,75], in which the case of matrix elements between the bound states has been first studied, we *define* the current matrix elements at the resonance pole as

$$F_R^M = \lim_{P^2\to s_R} Z_R^{-1/2}(s_R - P^2)\,\Gamma(P,p). \tag{67}$$

Using Eqs. (62), (66), (67), we arrive at the final result:

$$F_R^M(E_R,|\mathbf{q}|) = -\frac{i}{8\pi E}\left(p_1 h_1 \bar{F}_1^M - p_2 h_2 \bar{F}_2^M\right)\bigg|_{E=E_R}. \tag{68}$$

Note that one still has an overall sign ambiguity in this formula. The corresponding form factors can be read off from Eq. (13), in which the kinematic factors are low-energy polynomials.

In order to reproduce the one-channel result of Ref. [31], the mixing between the channels should be neglected. Then, $h(E)$ takes the form

$$h(E) = (t_1 - i)(t_2 + i). \tag{69}$$

So, one has at the pole position either $t_1(E_R) = +i$ or $t_2(E_R) = -i$. Consider, for instance, the first alternative $t_1(E_R) - i = 0$. The derivative $h'(E)$ at $E = E_R$ reads

$$h'(E_R) = (t_2(E_R) + i)t_1'(E_R), \tag{70}$$

so that the quantities h_1, h_2 are given by

$$h_1^2 = -\frac{16\pi E^2}{p_1 t_1'(E)}\bigg|_{E=E_R}, \quad h_2^2 = 0. \tag{71}$$

Consequently, from Eq. (68) we obtain

$$F_R^M(E_R,|\mathbf{q}|) = \sqrt{\frac{p_1}{4\pi\, t_1'(E)}}\,\bar{F}_1^M(E,|\mathbf{q}|)\bigg|_{E=E_R}. \tag{72}$$

A similar formula holds for the $K\eta$ channel.

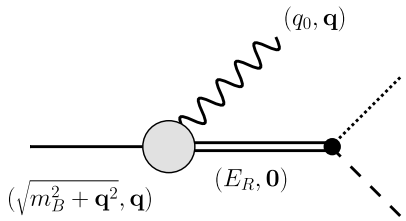

Fig. 3. The factorization of the amplitudes at the resonance pole (see Fig. 2 for notations). The photon virtuality, given by Eq. (73), is complex.

4.3. Photon virtuality

The analytic continuation to the resonance pole yields the quantity $F_R^M(E_R, |\mathbf{q}|)$. Below, we would like to briefly discuss a few conceptual issues, related to the interpretation of this quantity. Namely, we wish to know:

- What is the photon virtuality q^2 for the resonance form factor, extracted at the pole?
- How should one compare with the experimental results?

In the literature, different statements have been made on this issue so far. We think that a clarification is needed at this point.

According to the procedure, which is proposed in the present paper (see also Ref. [31]), the finite-volume matrix element is measured at different two-particle energies $E_n(L)$ and a fixed value of $|\mathbf{q}|$. After that, an analytic continuation is performed to the complex resonance pole, keeping $|\mathbf{q}|$ fixed. Further, the photon virtuality becomes complex at the pole

$$q^2 = \left(E_R - \sqrt{m_B^2 + \mathbf{q}^2}\right)^2 - \mathbf{q}^2 \,. \tag{73}$$

On the other hand, in Refs. [47,48], where the $\rho \to \pi\gamma^*$ transition form factor is considered, the authors simultaneously parameterize the energy- and q^2-dependence of the measured matrix element by some phenomenological fit function and perform the analytic continuation to the complex value of energy at a fixed q^2. The quantity q^2 is taken real at the pole.

Having two different procedures for the determination of the matrix element at the pole, it seems that the result is not unique. In order to show that the form factor can be uniquely defined, we note that the residue of the full amplitude at the pole should factorize in the product of the resonance form factor and the vertex, describing the transition of a resonance into the final state, see Fig. 3. The background becomes irrelevant, which leads to the determination of the form factor at the pole in a process-independent manner. From this figure it is clear that the photon virtuality, defined through the use of the 4-momentum conservation, coincides with the one given in Eq. (73) and thus must be complex. One could of course consider the electroproduction amplitude at a different (even at a real) photon virtuality as well. However, in this case, the background does not vanish completely, so the continuation to the pole does not make sense, since the result is process-dependent anyway. It should be stressed that this argument equally holds both in the analysis of the data from the electroproduction experiments as well as for the results of lattice QCD simulations.

Another argument addresses the analytic properties of the amplitudes which are extrapolated into the complex plane. We have shown that the irreducible amplitudes are low-energy polynomials in the vicinity of a resonance in the CM energy E, if the photon 3-momentum $|\mathbf{q}|$ is

fixed (see Ref. [31]). This fact implies that the analytic continuation to the complex energies is robust. To the best of our knowledge, no such statement exists in case of the function of two independent variables E, q^2 that might render the analytic continuation unstable. It remains to be seen, whether the information about the analytic properties of the form factors in the variable q^2 can be reasonably included. This could greatly constrain the fit and would be very useful in the analysis of the presently available data, which correspond to different values of q^2 (see, e.g., Refs. [47,48]).

5. Infinitely narrow width

In this section, for illustrative purposes, we consider the case of a resonance with an infinitely narrow width having in mind the hypothetical case of a K^* pole located above the ηK threshold with a very small width. The arguments follow the path of Ref. [31], where the same problem has been considered in case of the elastic scattering (see also Ref. [42]). It has been shown there that, in the limit of the infinitely narrow width, the matrix element, measured on the lattice, coincides with the infinite-volume resonance form factor up to a constant, which takes into account the difference between the normalization of the one- and two-particle states in a finite volume. However, the multi-channel case is more subtle, since different two-particle states occur, and the relation between the infinite- and finite-volume matrix elements becomes obscure. Still, as we will see, the final result has exactly the same form as in the one-channel problem.[2]

We start with the two-body potential from Eq. (23), which can be written in the following form

$$V = 8\pi\sqrt{s}\,P^{-1/2}\,O\,\tilde{V}\,O^T\,P^{-1/2}\,, \tag{74}$$

where

$$P = \mathrm{diag}\,(p_1, p_2)\,, \qquad \tilde{V} = \mathrm{diag}\,(t_1, t_2)\,, \qquad O = \begin{pmatrix} c_\varepsilon & -s_\varepsilon \\ s_\varepsilon & c_\varepsilon \end{pmatrix}. \tag{75}$$

Suppose that the resonance behavior near the (real) energy $E = E_0$ emerges in the quantity $t_1 = \tan\delta_1$, whereas the quantity t_2 stays regular in this energy interval. Then, in the vicinity of $E = E_0$, one can write

$$\delta_1(E) = \delta_R(E) + \phi(E)\,, \qquad \tan\delta_R(E) = \frac{\Gamma_0/2}{E_0 - E}\,, \tag{76}$$

and assume that a (small) background phase $\phi(E)$ stays regular. Further, one may straightforwardly ensure that

$$\cot\delta_1(E) = \frac{E_{BW} - E}{\Gamma/2} + \cdots\,, \tag{77}$$

where

$$E_{BW} = E_0 - \frac{\Gamma_0}{2}\tan\phi(E_{BW})\,, \qquad \frac{\Gamma}{2} = \frac{\Gamma_0}{2}\left(1 + \tan^2\phi(E_{BW})\right). \tag{78}$$

This shows that, in the vicinity of a narrow resonance, one can always get rid of the background phase by a redefinition of the resonance parameters. We note that the second background phase

[2] Inadvertently, in Ref. [31], the factor $\mathcal{V}^{-1/2}$ was missing on the right-hand side of the counterpart of Eq. (42).

still remains. The quantities E_{BW} and Γ are the Breit–Wigner mass and width of the (narrow) resonance.

In the vicinity of a narrow resonance, the scattering amplitude Eq. (19), which can be represented on the first Riemann sheet as

$$T = 8\pi\sqrt{s}\,P^{-1/2}\,O\tilde{T}\,O^T\,P^{-1/2}, \quad \tilde{T} = \mathrm{diag}\,(e^{i\delta_1}\sin\delta_1, e^{i\delta_2}\sin\delta_2), \tag{79}$$

becomes

$$T_{\alpha\beta} = \frac{b_\alpha b_\beta}{s_{BW} - s - i\sqrt{s_{BW}}\,\Gamma} + \text{regular terms at } E \to E_{BW}\,, \tag{80}$$

where $s_{BW} = E_{BW}^2$. Here, the quantities b_1, b_2 are given by

$$b_1 = \sqrt{\frac{8\pi s_{BW}\Gamma}{p_1}}\,c_\varepsilon\,, \quad b_2 = \sqrt{\frac{8\pi s_{BW}\Gamma}{p_2}}\,s_\varepsilon\,, \tag{81}$$

and the regular terms emerge from the contribution of t_2.

In order to find a complex pole on the second Riemann sheet, one has to solve the secular equation, Eq. (59), $h(E_R) = 0$. Recalling that t_1, t_2 are single-valued functions and using the explicit representation of t_1 from Eq. (77), at $E = E_R$ we get

$$t_1(E_R) = \frac{\Gamma/2}{E_{BW} - E_R} = \left.\frac{i(t_2+i) - 2is_\varepsilon^2 t_2}{t_2 + i - 2is_\varepsilon^2}\right|_{E=E_R}. \tag{82}$$

5.1. Real axis

On the real energy axis, one can introduce the infinite-volume quantities ("form factors"), which parameterize the imaginary parts of the decays amplitudes $\mathcal{A}_1^M$, $\mathcal{A}_2^M$ in the vicinity of the Breit–Wigner resonance. We denote these volume-independent matrix elements as $F_A^M(E, |\mathbf{q}|)$. In analogy to the one-channel case (see, e.g. Refs. [33,34,42]), we consider the resonance exchange mechanism at tree level, as shown in Fig. 4. Consequently, the amplitudes $\mathcal{A}_1^M$, $\mathcal{A}_2^M$ near $E = E_{BW}$ read

$$\mathcal{A}_\alpha^M(E, |\mathbf{q}|) = \frac{b_\alpha F_A^M(E_{BW}, |\mathbf{q}|)}{E_{BW}^2 - E^2 - iE_{BW}\Gamma} + \cdots, \quad \alpha = 1, 2, \tag{83}$$

where the ellipses stand for the terms emerging from the regular contributions in Eq. (80). Setting further $E = E_{BW}$, we get the imaginary parts of the $\mathcal{A}_\alpha^M$

$$\begin{aligned}
\mathrm{Im}\mathcal{A}_1^M(E_{BW}, |\mathbf{q}|) &= \sqrt{\frac{8\pi}{p_1\Gamma}}\,F_A^M(E_{BW}, |\mathbf{q}|)c_\varepsilon + O(1)\,,\\
\mathrm{Im}\mathcal{A}_2^M(E_{BW}, |\mathbf{q}|) &= \sqrt{\frac{8\pi}{p_2\Gamma}}\,F_A^M(E_{BW}, |\mathbf{q}|)s_\varepsilon + O(1)\,.
\end{aligned} \tag{84}$$

Note that the leading terms in this expression are of order $\Gamma^{-1/2}$, and the sub-leading $O(1)$ terms emerge from the regular contributions.

Further, comparing Eqs. (47) and (84), we see that the following condition has to be satisfied at the Breit–Wigner pole $E = E_{BW}$:

$$u_2^M(E_{BW}, |\mathbf{q}|) = O(1), \tag{85}$$

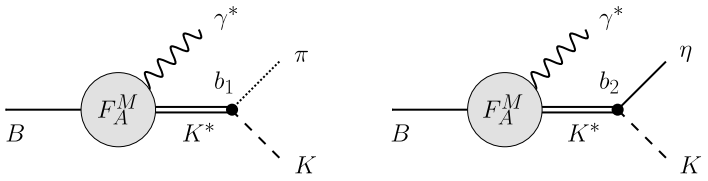

Fig. 4. Decay amplitudes $\mathcal{A}_\alpha^M$, $\alpha = 1, 2$, in the vicinity of the infinitely narrow K^*. The quantities b_α, $\alpha = 1, 2$, denote the couplings of the K^* to the respective channels at $E = E_{BW}$.

while for the amplitudes $u_1^M(E_{BW}, |\mathbf{q}|)$ one has

$$u_1^M(E_{BW}, |\mathbf{q}|) = \sqrt{p_1} c_\varepsilon \, \mathrm{Im}\mathcal{A}_1^M(E, |\mathbf{q}|)\big|_{E_n \to E_{BW}} + \sqrt{p_2} s_\varepsilon \, \mathrm{Im}\mathcal{A}_2^M(E, |\mathbf{q}|)\big|_{E_n \to E_{BW}}, \quad (86)$$

or

$$u_1^M(E_{BW}, |\mathbf{q}|) = \sqrt{\frac{8\pi}{\Gamma}} F_A^M(E_{BW}, |\mathbf{q}|) + O(1) = O(\Gamma^{-1/2}). \quad (87)$$

Consequently, in the limit $\Gamma \to 0$, the leading contribution to the $\mathcal{A}_\alpha^M$ comes from u_1^M.

However, the amplitudes u_α^M, $\alpha = 1, 2$ are not low-energy polynomials in the vicinity of $E = E_{BW}$. In order to establish quantities, which have such a property, we first note that in case of a very narrow resonance, the function $\cot\delta_1(E)$ is a polynomial in E (see Eq. (77)). It can be further assumed that the mixing parameter $s_\epsilon(E)$ and $\cot\delta_2(E)$ are also low-energy polynomials in the vicinity of the resonance. Furthermore, even if the radius of convergence of the modified effective range expansion, Eq. (52), is assumed to be much larger than the width Γ, it is still limited from above by the distance to the nearest threshold. Since the limit $\Gamma \to 0$ is considered here, it is natural to assume that the mixing parameter $s_\epsilon(E)$ and $\cot\delta_2(E)$ are also low-energy polynomials in the vicinity of the resonance. It is then straightforward to check that the functions

$$\tilde{u}_\alpha^M = \frac{u_\alpha^M}{\sin\delta_\alpha} \quad (88)$$

are low-energy polynomials. Indeed, the irreducible amplitudes $\bar{F}_\alpha^M$, $\alpha = 1, 2$, diverge at $E = E_{BW}$, due to the propagation of the bare K^* in the s-channel (see Ref. [31]). According to Eqs. (48) and (88), this divergence is exactly canceled in the amplitudes $\tilde{u}_\alpha^M$, $\alpha = 1, 2$. Consequently, they can be safely expanded in the vicinity of the narrow resonance. This property, in particular, is important, if one considers an analytic continuation into the complex plane.

Rewriting the two-channel Lellouch–Lüscher formula in terms of $\tilde{u}_\alpha^M$, we get

$$\left|F^M(E_n, |\mathbf{q}|)\right| = \frac{\mathcal{V}^{-1}}{\sqrt{8\pi E}} \left(a_1 \tilde{u}_1^M + a_2 \tilde{u}_2^M\right)\Big|_{E=E_n}, \quad (89)$$

where the quantities a_1, a_2 are given by

$$a_1^2 = t_1^2 \frac{t_2 + \tau_2 - s_\varepsilon^2(\tau_2 - \tau_1)}{f'(E)}\Big|_{E=E_n},$$
$$a_2^2 = t_2^2 \frac{t_1 + \tau_1 + s_\varepsilon^2(\tau_2 - \tau_1)}{f'(E)}\Big|_{E=E_n}. \quad (90)$$

Evaluating the quantities a_1, a_2 in the limit of the infinitely narrow width is somewhat less trivial than in the one-channel case. In order to proceed further here, let us first recall the line

of reasoning used in the one-channel case. In this case, the Lüscher equation has a simple form

$$\delta_1 + \varphi_1 = n\pi\,, \qquad n \in \mathbb{Z}\,, \qquad \tan\varphi_1 = \tau_1\,. \tag{91}$$

For sufficiently small Γ, this equation will have a solution at $E_n = E_{BW} + O(\Gamma)$. At this energy, the quantities t_1, τ_1 are of order $O(1)$. However, the *derivatives* of t_1 and τ_1 behave differently at $E_n \to E_{BW}$. One has $t_1' = \delta_1'/\cos^2\delta_1$ and $\tau_1' = \varphi_1'/\cos^2\varphi_1$, where $\cos^2\delta_1 = \cos^2\varphi_1$, due to the Lüscher equation. According to Eq. (77), the derivative of the phase shift δ_1 diverges as Γ^{-1} whereas φ_1' stays finite as $E_n \to E_{BW}$, since it is a kinematical function that does not contain any small scales of order Γ. Consequently, as $E_n \to E_{BW}$ and $\Gamma \to 0$, one may neglect τ_1' as compared to t_1'.

A similar argument can be carried out in the two-channel case, rewriting the Lüscher equation in the form

$$\delta_1 + \varphi_1 = n\pi\,, \qquad \tan\varphi_1 = \frac{\tau_1(t_2+\tau_2) + s_\varepsilon^2 t_2(\tau_2-\tau_1)}{t_2+\tau_2 - s_\varepsilon^2(\tau_2-\tau_1)}\,. \tag{92}$$

The function φ_1 is not purely kinematical as it contains t_2. However, it still does not contain small scales of order Γ. Consequently, the derivatives of φ_1 are finite and the quantities τ_1', τ_2' are of order $O(1)$, while $t_1' = O(\Gamma^{-1})$.

Next, retaining only the most divergent terms in $f'(E_n)$ at $E_n \to E_{BW}$, one gets

$$f'(E_n \to E_{BW}) = t_1'\big(t_2+\tau_2 - s_\varepsilon^2(\tau_2-\tau_1)\big)\big|_{E_n\to E_{BW}} + \cdots\,. \tag{93}$$

Consequently, the quantities a_1^2, a_2^2 take the values

$$\begin{aligned} a_1^2 &= \frac{t_1^2}{t_1'}\bigg|_{E_n\to E_{BW}} = \frac{\Gamma}{2} + O(\Gamma^2), \\ a_2^2 &= \frac{t_2^2}{t_1'}\,\frac{t_1+\tau_1+s_\varepsilon^2(\tau_2-\tau_1)}{t_2+\tau_2-s_\varepsilon^2(\tau_2-\tau_1)}\bigg|_{E_n\to E_{BW}} = O(\Gamma). \end{aligned} \tag{94}$$

Hence, it follows that the leading contribution to the matrix element $F^M(E_n, |\mathbf{q}|)$ in the limit $\Gamma \to 0$ comes only from the term, proportional to $\tilde{u}_1^M$, whereas the second term is sub-leading. As a result, we obtain

$$\big|F^M(E_n,|\mathbf{q}|)\big| = \frac{\mathcal{V}^{-1}}{\sqrt{2E_n}}\,\big|F_A^M(E_n,|\mathbf{q}|)\big| + O(\Gamma^{1/2}), \quad E_n = E_{BW} + O(\Gamma). \tag{95}$$

As seen, the Lellouch–Lüscher formula has a fairly simple form in the vicinity of the Breit–Wigner resonance: the infinite-volume quantities $F_A^M(E_{BW}, |\mathbf{q}|)$ are equal to the current matrix elements $F^M(E_{BW}, |\mathbf{q}|)$, measured on the lattice, up to a normalization factor (note that, in Ref. [31], a different normalization of the states has been used). The form factors can be found from Eq. (13).

5.2. Complex plane

The values of the form factors at the resonance pole in the infinitely narrow width limit can be determined along the same lines, as discussed above. We again express the final result Eq. (68)

through the amplitudes $\tilde{u}_1^M$, $\tilde{u}_2^M$ to get

$$F_R^M(E_R, |\mathbf{q}|) = \frac{1}{\sqrt{4\pi}} \left(r_1 \tilde{u}_1^M + r_2 \tilde{u}_2^M\right)\Big|_{E=E_R}. \tag{96}$$

Here, the quantities r_1, r_2 read

$$\begin{aligned} r_1^2 &= t_1^2 \frac{t_2 + i - 2is_\varepsilon^2}{h'(E)}\Big|_{E=E_R}, \\ r_2^2 &= t_2^2 \frac{t_1 - i + 2is_\varepsilon^2}{h'(E)}\Big|_{E=E_R}. \end{aligned} \tag{97}$$

Since the functions $\tilde{u}_\alpha^M$ are low-energy polynomials in the vicinity of the Breit–Wigner pole, one can analytically continue them from the real axis to the pole. Consequently, in the limit $\Gamma \to 0$, their values at the pole and at the real axis are equal, up to the terms of order $O(\Gamma)$. We note that this procedure cannot be applied to the u_α^M. Calculating the quantities r_1, r_2 at $E_R \to E_{BW}$, we get

$$\begin{aligned} r_1^2 &= \frac{t_1^2}{t_1'}\Big|_{E_R \to E_{BW}} = \frac{\Gamma}{2} + O(\Gamma^2), \\ r_2^2 &= \frac{t_1^2}{t_1'} \frac{t_2 + i - 2is_\varepsilon^2}{t_1 - i + 2is_\varepsilon^2}\Big|_{E_R \to E_{BW}} = O(\Gamma). \end{aligned} \tag{98}$$

As on the real axis, the leading contribution to the F_R^M is dominated by the $\tilde{u}_1^M$ term in Eq. (96). The final expression takes the form

$$F_R^M(E_R, |\mathbf{q}|)\big|_{\Gamma \to 0} = F_A^M(E_{BW}, |\mathbf{q}|) + O(\Gamma^{1/2}). \tag{99}$$

As expected, for infinitely narrow resonance, the form factors $F_A^M(E, |\mathbf{q}|)$ and $F_R^M(E, |\mathbf{q}|)$, defined on the real energy axis and complex plane, respectively, coincide.

6. Conclusions

In this work, we have studied the extraction of the $B \to K^*$ transition form factors on the lattice. We have taken into account, in particular, the possible admixture of the ηK to πK final states. To this end, we have applied the non-relativistic effective field theory in a finite volume and reproduced the two-channel analogue of the Lellouch–Lüscher formula, which allows to extract the $B \to K^* l^+ l^-$ decay amplitude in the low-recoil region.

Since the K^* is a resonance, the corresponding current matrix elements are properly defined and free of process-dependent ambiguities only if the analytic continuation in the complex energy plane to the resonance pole position is performed. Consequently, we have set up a framework for the determination of the form factors at the K^* pole. This is a generalization of the one-channel formula, which has been derived in Ref. [31]. In addition, we have discussed in detail the consistent determination of the photon virtuality at the resonance pole.

Finally, we have considered the limit of an infinitely small width in our results. The equations in the multi-channel case are more involved and this limit cannot be performed in a straightforward manner. Nevertheless, we have demonstrated that, even in the multi-channel case, the current matrix element measured on the lattice is equal to the one in the infinite volume, up to a normalization factor that does not depend on the dynamics. This result represents a useful check of our framework.

Acknowledgements

We thank R. Briceño and M. Mai for useful discussions. We acknowledge the support by the DFG (CRC 16, "Subnuclear Structure of Matter" and CRC 110 "Symmetries and the Emergence of Structure in QCD") and by the Bonn-Cologne Graduate School of Physics and Astronomy. This research is supported in part by Volkswagenstiftung under contract no. 86260, and by the Chinese Academy of Sciences (CAS) President's International Fellowship Initiative (PIFI) (Grant No. 2015VMA076).

Appendix A. The $B \to K^*$ form factors in rest frame of the B meson

Since the πK–ηK system is in the P-wave, it is preferable to extract the finite-volume energy spectrum in the reference frame, in which the K^* has non-zero 3-momentum. Consequently, as an alternative to the case considered in the main text, we also consider the following kinematics:

$$\mathbf{p} = 0, \quad \mathbf{k} = -\mathbf{q} = \frac{2\pi}{L}\mathbf{d}, \quad \mathbf{d} = (0,0,n)\ . \tag{A.1}$$

The current matrix elements of Eq. (13) in this moving frame take the form

$$\begin{aligned}
\langle V(k,+)|J^{(+)}|B\rangle &= -\frac{2im_B|\mathbf{q}|V(q^2)}{m_B+m_V},\\
\langle V(k,0)|i(m_B-E_V)J_A + |\mathbf{q}|J_A^{(0)}|B\rangle &= -2im_B|\mathbf{q}|A_0(q^2),\\
\langle V(k,+)|J_A^{(+)}|B\rangle &= -i(m_B+m_V)A_1(q^2),\\
\langle V(k,0)|i(m_B-E_V)J_A^{(0)} - |\mathbf{q}|J_A|B\rangle &= 8m_Bm_VA_{12}(q^2),\\
\langle V(k,+)|i(m_B-E_V)I^{(+)} + |\mathbf{q}|I_0^{(+)}|B\rangle &= 2im_B|\mathbf{q}|T_1(q^2),\\
\langle V(k,+)|i(m_B-E_V)I_A^{(+)} + |\mathbf{q}|I_{0A}^{(+)}|B\rangle &= -i(m_B^2-m_V^2)T_2(q^2),\\
\langle V(k,0)|I_A^{(0)}|B\rangle &= -\frac{4m_Bm_V}{m_B+m_V}T_{23}(q^2),
\end{aligned} \tag{A.2}$$

where $E_V = \sqrt{m_V^2+\mathbf{q}^2}$ is energy of the K^* meson, which is treated as a stable particle. As seen from Eq. (A.1) (see, e.g., also Ref. [60]), the matrix elements should be measured in the irreps $\mathbb{E}$ and $\mathbb{A}_1$ of the little group C_{4v}. However, because K^* is not at rest now, the S- and P-waves mix in the irrep $\mathbb{A}_1$. Consequently, only the form factors V, A_1, T_1, and T_2 could be extracted by applying formulas that are similar to the ones given in the previous sections. For other form factors A_0, A_{12}, T_{23} one should either assume that the mixing is small, or use more general equations, derived in Ref. [41], which include it.

Further, one applies the following operators to create the states $\langle V(k,\pm)|$, $\langle V(k,0)|$ from the vacuum:

$$\mathcal{O}_{\mathbb{E}}^{(\pm)}(\mathbf{k},t) = \frac{1}{\sqrt{2}}\sum_{\mathbf{x}} e^{i\mathbf{kx}}\big(O_1(\mathbf{x},t) \mp i\,O_2(\mathbf{x},t)\big), \quad \mathcal{O}_{\mathbb{A}_1}^{(0)}(\mathbf{k},t) = \sum_{\mathbf{x}} e^{i\mathbf{kx}}O_3(\mathbf{x},t). \tag{A.3}$$

When the K^* becomes unstable, the mass m_V should be replaced by the CM energy value E_n^* of the two-particle state in a finite volume. Then, the matrix elements Eq. (A.2) are functions of E_n^* and $|\mathbf{q}|$. Analogously, in order to keep $|\mathbf{q}|$ fixed at different values of energy E_n^*, one could resort to asymmetric volumes of type $L \times L \times L'$ or twist the s-quark.

References

[1] A. Ali, P. Ball, L.T. Handoko, G. Hiller, Phys. Rev. D 61 (2000) 074024, arXiv:hep-ph/9910221.
[2] C. Bobeth, G. Hiller, D. van Dyk, Phys. Rev. D 87 (2013) 034016, arXiv:1212.2321 [hep-ph].
[3] D. Melikhov, N. Nikitin, S. Simula, Phys. Lett. B 442 (1998) 381, arXiv:hep-ph/9807464.
[4] F. Kruger, J. Matias, Phys. Rev. D 71 (2005) 094009, arXiv:hep-ph/0502060.
[5] W. Altmannshofer, P. Ball, A. Bharucha, A.J. Buras, D.M. Straub, M. Wick, J. High Energy Phys. 0901 (2009) 019, arXiv:0811.1214 [hep-ph].
[6] J. Matias, F. Mescia, M. Ramon, J. Virto, J. High Energy Phys. 1204 (2012) 104, arXiv:1202.4266 [hep-ph].
[7] R. Aaij, et al., LHCb Collaboration, Phys. Rev. Lett. 111 (2013) 191801, arXiv:1308.1707 [hep-ex].
[8] R. Aaij, et al., LHCb Collaboration, J. High Energy Phys. 1602 (2016) 104, arXiv:1512.04442 [hep-ex].
[9] A. Abdesselam, et al., Belle Collaboration, arXiv:1604.04042 [hep-ex].
[10] S. Descotes-Genon, J. Matias, J. Virto, Phys. Rev. D 88 (2013) 074002, arXiv:1307.5683 [hep-ph].
[11] R. Aaij, et al., LHCb Collaboration, J. High Energy Phys. 1406 (2014) 133, arXiv:1403.8044 [hep-ex].
[12] R. Aaij, et al., LHCb Collaboration, Phys. Rev. Lett. 113 (2014) 151601, arXiv:1406.6482 [hep-ex].
[13] R. Aaij, et al., LHCb Collaboration, J. High Energy Phys. 1504 (2015) 064, arXiv:1501.03038 [hep-ex].
[14] W. Altmannshofer, D.M. Straub, Eur. Phys. J. C 75 (8) (2015) 382, arXiv:1411.3161 [hep-ph].
[15] T. Hurth, F. Mahmoudi, S. Neshatpour, arXiv:1603.00865 [hep-ph].
[16] S. Descotes-Genon, L. Hofer, J. Matias, J. Virto, arXiv:1510.04239 [hep-ph].
[17] P. Ball, R. Zwicky, Phys. Rev. D 71 (2005) 014029, arXiv:hep-ph/0412079.
[18] A. Bharucha, D.M. Straub, R. Zwicky, arXiv:1503.05534 [hep-ph].
[19] Z. Liu, S. Meinel, A. Hart, R.R. Horgan, E.H. Müller, M. Wingate, arXiv:1101.2726 [hep-ph].
[20] R.R. Horgan, Z. Liu, S. Meinel, M. Wingate, Phys. Rev. D 89 (9) (2014) 094501, arXiv:1310.3722 [hep-lat].
[21] R.R. Horgan, Z. Liu, S. Meinel, M. Wingate, PoS LATTICE 2014 (2015) 372, arXiv:1501.00367 [hep-lat].
[22] UKQCD Collaboration, K.C. Bowler, et al., Phys. Rev. Lett. 72 (1994) 1398, arXiv:hep-lat/9311004.
[23] C.W. Bernard, P. Hsieh, A. Soni, Phys. Rev. Lett. 72 (1994) 1402, arXiv:hep-lat/9311010.
[24] UKQCD Collaboration, D.R. Burford, et al., Nucl. Phys. B 447 (1995) 425, arXiv:hep-lat/9503002.
[25] A. Abada, et al., Phys. Lett. B 365 (1996) 275, arXiv:hep-lat/9503020.
[26] D. Bećirević, V. Lubicz, F. Mescia, Nucl. Phys. B 769 (2007) 31, arXiv:hep-ph/0611295.
[27] SPQcdR Collaboration, A. Abada, et al., Nucl. Phys. B, Proc. Suppl. 119 (2003) 625, arXiv:hep-lat/0209116.
[28] UKQCD Collaboration, K.C. Bowler, J.F. Gill, C.M. Maynard, J.M. Flynn, J. High Energy Phys. 05 (2004) 035, arXiv:hep-lat/0402023.
[29] L. Lellouch, M. Lüscher, Commun. Math. Phys. 219 (2001) 31, arXiv:hep-lat/0003023.
[30] M. Lüscher, Nucl. Phys. B 354 (1991) 531.
[31] A. Agadjanov, V. Bernard, U.-G. Meißner, A. Rusetsky, Nucl. Phys. B 886 (2014) 1199, arXiv:1405.3476 [hep-lat].
[32] V. Bernard, D. Hoja, U.-G. Meißner, A. Rusetsky, J. High Energy Phys. 1209 (2012) 023, arXiv:1205.4642 [hep-lat].
[33] I.G. Aznauryan, V.D. Burkert, T.-S.H. Lee, arXiv:0810.0997 [nucl-th].
[34] D. Drechsel, O. Hanstein, S.S. Kamalov, L. Tiator, Nucl. Phys. A 645 (1999) 145, arXiv:nucl-th/9807001.
[35] J.J. Dudek, et al., Hadron Spectrum Collaboration, Phys. Rev. Lett. 113 (18) (2014) 182001, arXiv:1406.4158 [hep-ph].
[36] D.J. Wilson, J.J. Dudek, R.G. Edwards, C.E. Thomas, Phys. Rev. D 91 (5) (2015) 054008, arXiv:1411.2004 [hep-ph].
[37] B.J. Menadue, W. Kamleh, D.B. Leinweber, M. Selim Mahbub, B.J. Owen, PoS LATTICE 2013 (2014) 280, arXiv:1311.5026 [hep-lat].
[38] J.M.M. Hall, W. Kamleh, D.B. Leinweber, B.J. Menadue, B.J. Owen, A.W. Thomas, R.D. Young, Phys. Rev. Lett. 114 (13) (2015) 132002, arXiv:1411.3402 [hep-lat].
[39] M.T. Hansen, S.R. Sharpe, Phys. Rev. D 86 (2012) 016007, arXiv:1204.0826 [hep-lat].
[40] R.A. Briceño, Z. Davoudi, Phys. Rev. D 88 (9) (2013) 094507, arXiv:1204.1110 [hep-lat].
[41] R.A. Briceño, M.T. Hansen, A. Walker-Loud, Phys. Rev. D 91 (3) (2015) 034501, arXiv:1406.5965 [hep-lat].
[42] R.A. Briceño, M.T. Hansen, Phys. Rev. D 92 (7) (2015) 074509, arXiv:1502.04314 [hep-lat].
[43] G. Colangelo, J. Gasser, B. Kubis, A. Rusetsky, Phys. Lett. B 638 (2006) 187, arXiv:hep-ph/0604084.
[44] J. Gasser, B. Kubis, A. Rusetsky, Nucl. Phys. B 850 (2011) 96, arXiv:1103.4273 [hep-ph].
[45] C.H. Kim, C.T. Sachrajda, S.R. Sharpe, Nucl. Phys. B 727 (2005) 218, arXiv:hep-lat/0507006.
[46] N.H. Christ, C.H. Kim, T. Yamazaki, Phys. Rev. D 72 (2005) 114506, arXiv:hep-lat/0507009.
[47] R.A. Briceño, J.J. Dudek, R.G. Edwards, C.J. Shultz, C.E. Thomas, D.J. Wilson, Phys. Rev. Lett. 115 (2015) 242001, arXiv:1507.06622 [hep-ph].

[48] R.A. Briceño, J.J. Dudek, R.G. Edwards, C.J. Shultz, C.E. Thomas, D.J. Wilson, Phys. Rev. D 93 (2016) 114508, arXiv:1604.03530 [hep-ph].
[49] B. Grinstein, R.P. Springer, M.B. Wise, Phys. Lett. B 202 (1988) 138.
[50] B. Grinstein, R.P. Springer, M.B. Wise, Nucl. Phys. B 339 (1990) 269.
[51] A.J. Buras, M. Misiak, M. Munz, S. Pokorski, Nucl. Phys. B 424 (1994) 374, arXiv:hep-ph/9311345.
[52] M. Ciuchini, E. Franco, G. Martinelli, L. Reina, L. Silvestrini, Phys. Lett. B 316 (1993) 127, arXiv:hep-ph/9307364.
[53] M. Ciuchini, E. Franco, L. Reina, L. Silvestrini, Nucl. Phys. B 421 (1994) 41, arXiv:hep-ph/9311357.
[54] M. Ciuchini, E. Franco, G. Martinelli, L. Reina, L. Silvestrini, Phys. Lett. B 334 (1994) 137, arXiv:hep-ph/9406239.
[55] A. Khodjamirian, R. Ruckl, G. Stoll, D. Wyler, Phys. Lett. B 402 (1997) 167, arXiv:hep-ph/9702318.
[56] A. Khodjamirian, T. Mannel, A.A. Pivovarov, Y.-M. Wang, J. High Energy Phys. 1009 (2010) 089, arXiv:1006.4945 [hep-ph].
[57] B. Grinstein, D. Pirjol, Phys. Rev. D 70 (2004) 114005, arXiv:hep-ph/0404250.
[58] M. Beylich, G. Buchalla, T. Feldmann, Eur. Phys. J. C 71 (2011) 1635, arXiv:1101.5118.
[59] J. Lyon, R. Zwicky, arXiv:1406.0566 [hep-ph].
[60] M. Göckeler, R. Horsley, M. Lage, U.-G. Meißner, P.E.L. Rakow, A. Rusetsky, G. Schierholz, J.M. Zanotti, Phys. Rev. D 86 (2012) 094513, arXiv:1206.4141 [hep-lat].
[61] H.P. Stapp, T.J. Ypsilantis, N. Metropolis, Phys. Rev. 105 (1957) 302.
[62] J.M. Blatt, L.C. Biedenharn, Phys. Rev. 86 (1952) 399.
[63] R.H. Dalitz, R.G. Moorhouse, Proc. R. Soc. Lond. 318 (1970) 279.
[64] R.L. Workman, R.A. Arndt, W.J. Briscoe, M.W. Paris, I.I. Strakovsky, Phys. Rev. C 86 (2012) 035202, arXiv:1204.2277 [hep-ph].
[65] E.P. Wigner, J. von Neumann, Z. Phys. 30 (1929) 467.
[66] S. He, X. Feng, C. Liu, J. High Energy Phys. 0507 (2005) 011, arXiv:hep-lat/0504019.
[67] C. Liu, X. Feng, S. He, Int. J. Mod. Phys. A 21 (2006) 847, arXiv:hep-lat/0508022.
[68] V. Bernard, M. Lage, U.-G. Meißner, A. Rusetsky, J. High Energy Phys. 1101 (2011) 019, arXiv:1010.6018 [hep-lat].
[69] M. Döring, U.-G. Meißner, E. Oset, A. Rusetsky, Eur. Phys. J. A 47 (2011) 139, arXiv:1107.3988 [hep-lat].
[70] A.M. Badalian, L.P. Kok, M.I. Polikarpov, Y.A. Simonov, Phys. Rep. 82 (1982) 31.
[71] M.H. Ross, G.L. Shaw, Ann. Phys. 13 (1961) 147.
[72] H.A. Bethe, Phys. Rev. 76 (1949) 38.
[73] B. Hyams, et al., Nucl. Phys. B 64 (1973) 134.
[74] S. Mandelstam, Proc. R. Soc. Lond. A 233 (1955) 248.
[75] K. Huang, H.A. Weldon, Phys. Rev. D 11 (1975) 257.

CHAPTER 4

Low-energy nucleon Compton scattering

4.1 Summary

The main objective of the work is to test the Reggeon dominance hypothesis by means of lattice simulations. The existence of the so-called fixed pole in the nucleon Compton scattering amplitude is still an open question. For that purpose, one has to determine the relevant subtraction function in forward doubly virtual Compton scattering. A comparison of the result with its recent phenomenological determination, based on the aforementioned hypothesis, will shed more light on the issue. Also, one might obtain a better constraint on the two-photon exchange contribution to the Lamb shift in muonic hydrogen.

The external field method provides a feasible approach to investigate the low-energy Compton scattering on the lattice. The obtained results can be summarized as follows:

- An appropriate external magnetic field configuration is found, which is suitable for the extraction of the subtraction function at nonzero photon virtuality.
- The energy shift of a nucleon in a static periodic magnetic field is calculated in the non-relativistic EFT. It is shown that the second-order correction in the external field strength is proportional to the value of the subtraction function.
- The practical applicability of the result is discussed. The upper bound on the magnetic field strength and the lower bound on the value of the photon virtuality are estimated.

PHYSICAL REVIEW D **95,** 031502(R) (2017)

Nucleon in a periodic magnetic field

Andria Agadjanov,[1] Ulf-G. Meißner,[1,2] and Akaki Rusetsky[1]

[1]*Helmholtz-Institut für Strahlen- und Kernphysik (Theorie) and Bethe Center for Theoretical Physics, Universität Bonn, D-53115 Bonn, Germany*

[2]*Institute for Advanced Simulation (IAS-4), Institut für Kernphysik (IKP-3) and Jülich Center for Hadron Physics, Forschungszentrum Jülich, D-52425 Jülich, Germany*

(Received 25 October 2016; published 27 February 2017)

The energy shift of a nucleon in a static periodic magnetic field is evaluated at second order in the external field strength in perturbation theory. It is shown that the measurement of this energy shift on the lattice allows one to determine the unknown subtraction function in the forward doubly virtual Compton scattering amplitude. The limits of applicability of the obtained formula for the energy shift are discussed.

DOI: 10.1103/PhysRevD.95.031502

I. INTRODUCTION

The doubly virtual Compton scattering process has several important phenomenological implications at low energies. The analysis of the proton-neutron mass difference[1] [3–6] relies on the knowledge of the relevant spin-independent invariant amplitudes T_1 and T_2. The same amplitudes appear in the study of the Lamb shift in the muonic hydrogen (see, e.g., Refs. [7–9]).

The experimental data on the structure functions completely determine the amplitude T_2. However, they do not fix the subtraction function S_1 in the dispersion relation for the amplitude T_1. This function depends on the photon virtuality q^2. The low-energy theorem establishes a relation between the value of the $S_1(q^2)$ at $q^2 = 0$ and the magnetic polarizability of the nucleon. Further, the asymptotic behavior of this function for large spacelike q^2 is fixed by the operator product expansion in QCD [6,10,11]. The behavior of the function at intermediate values of q^2 is, however, completely arbitrary. Earlier calculations of the forward Compton scattering amplitude within chiral effective field theories at low photon virtualities have been carried out in Refs. [12–15]. The latest calculations of the quantity S_1 are contained in Refs. [7,9,16–19]. The convergence of the chiral expansion is, however, questionable even at very low q^2. Further, several authors have used phenomenological parametrizations of the function S_1 in their calculations [5,6,8]. Unfortunately, this introduces a systematic uncertainty in the calculated observables that is very hard to control.

An interesting possibility to determine the subtraction function S_1 was discussed in Refs. [3,4]. If the forward scattering amplitude does not contain any so-called fixed pole (this issue is related to the so-called Reggeon dominance hypothesis), then $S_1(q^2)$ for all $q^2 < 0$ is uniquely determined by the dispersion integral over the electroproduction cross sections in the physical region. Therefore, if one could calculate the function $S_1(q^2)$ directly and compare with the result obtained by using the Reggeon dominance hypothesis, in principle one would be able to answer a question, whether a fixed pole is present in the forward Compton amplitude or not (for the recent phenomenological evaluation of S_1, see Refs. [4,20,21]). For instance, note that the universality hypothesis, stated in Ref. [22], does not exclude the presence of a fixed pole in T_1. Further, a calculation of $S_1(q^2)$ would allow one to evaluate the proton-neutron electromagnetic mass shift and the two-photon exchange contribution to the muonic hydrogen Lamb shift in a manner devoid of any model dependence. Hence, there is strong interest in a direct calculation of the function $S_1(q^2)$.

At present, lattice QCD is the only first-principle approach capable of handling the above problem. There are two ways to determine S_1. In the first method, one directly calculates the four-point function that describes Compton scattering. This is a straightforward but computationally very demanding task. Until now, this approach has been used in the computation of light-by-light scattering [23], and also in the study of the long-distance effects in rare kaon decays [24,25]. An alternative method is based on the observation that the Compton scattering amplitude can be inferred from the behavior of the nucleon two-point function in the presence of a weak external electromagnetic field. In recent years, the external field method has become a powerful tool to study the electromagnetic properties of the nucleon and light nuclei. In particular, it has been used for the case of a constant and uniform magnetic field [26–28]. Such a field configuration allows one to determine the magnetic moments and magnetic polarizabilities through the extracted energy shift induced by the magnetic field. By applying nonuniform and time-dependent fields, one can determine spin polarizabilities as well (see, e.g., Refs. [29,30]). Hence, the external field approach for the calculation of S_1 should be feasible in practice.

[1]Note that, recently, a substantial progress has been achieved in the direct evaluation of this difference on the lattice [1,2]. A comparison of different approaches provides constaints on the behavior of the Compton amplitudes.

In this paper, we demonstrate that measuring the energy shift of a single nucleon state in a *static periodic* magnetic field on the lattice enables one to determine the function $S_1(q^2)$ at nonzero values of q^2. Unlike a constant magnetic field, which generates the harmonic oscillator potential and Landau levels, in the present case the spectrum and the eigenstates of the Hamiltonian can not be obtained analytically. Nevertheless, the energy is still conserved in the static magnetic field and, as long as the potential remains "small," perturbation theory can be applied to the free energy spectrum (there is a similar approach in solid-state physics, which is called the nearly free electron model, and more generally, the empty lattice approximation [31]). We show that, at second order in the magnetic field strength, the energy shift of the one-nucleon ground state is proportional to the quantity $S_1(q^2)$. The limits of applicability of this perturbative expression are also discussed.

II. COMPTON SCATTERING

Let us start with the basic definitions. The Compton scattering amplitude is given by

$$T^{\mu\nu}(p',s';p,s;q)=\frac{i}{2}\int d^4x e^{iq\cdot x}\langle p',s'|Tj^\mu(x)j^\nu(0)|p,s\rangle. \tag{1}$$

Here, $j^\mu(x)$ denotes the electromagnetic current, q is the four-momentum of the final photon, $p(p')$ and $s(s')$ are the four-momenta and spins of the initial (final) nucleon, respectively. Considering forward scattering $p'=p$ and performing the spin-averaging in Eq. (1), one arrives at

$$T^{\mu\nu}(p,q)=\frac{1}{2}\sum_s T^{\mu\nu}(p,s;p,s;q). \tag{2}$$

The tensor $T^{\mu\nu}(p,q)$ is related to the invariant amplitudes T_1, T_2 through the expression (see, e.g., Refs. [4,32,33]):

$$T^{\mu\nu}(p,q)=T_1(\nu,q^2)K_1^{\mu\nu}+T_2(\nu,q^2)K_2^{\mu\nu}, \tag{3}$$

where the kinematic structures $K_1^{\mu\nu}$, $K_2^{\mu\nu}$ read

$$K_1^{\mu\nu}=q^\mu q^\nu-g^{\mu\nu}q^2,$$
$$K_2^{\mu\nu}=\frac{1}{m^2}\{(p^\mu q^\nu+p^\nu q^\mu)p\cdot q-g^{\mu\nu}(p\cdot q)^2-p^\mu p^\nu q^2\}. \tag{4}$$

Here, m is the nucleon mass and $\nu\equiv p\cdot q/m$. The subtraction function S_1 is defined as

$$S_1(q^2)=T_1(0,q^2). \tag{5}$$

The quantity $S_1(q^2)$ can be split into the elastic and inelastic parts (see, e.g., Ref. [4]). The elastic part is singular at $q^2\to 0$, whereas the inelastic part is regular and is related to the nucleon magnetic polarizability at $q^2=0$. Note that the quantity $S_1(q^2)$ is real, because in this kinematical region there are no multi-particle singularities. Indeed, introducing the Mandelstam variable $s=(p+q)^2=m^2+2m\nu+q^2$, it is immediately seen that, for $\nu=0$ and $q^2<0$, we have $s<m^2$, meaning that one is below the inelastic threshold.

It is well known that the Compton tensor given in Eq. (1) can be obtained by expanding the two-point function of a nucleon in an external electromagnetic field to second order. Introducing the notation $A_\mu(x)$ for the external potential, it is actually seen that the nucleon propagator can be expanded as follows:

$$\langle 0|T\Psi(x)\overline{\Psi}(y)|0\rangle_A=\langle 0|T\Psi(x)\overline{\Psi}(y)|0\rangle_0+\frac{i}{1!}\int d^4z A_\mu(z)\langle 0|T\Psi(x)\overline{\Psi}(y)j^\mu(z)|0\rangle_0$$
$$+\frac{i^2}{2!}\int d^4z d^4v A_\mu(z)A_\nu(v)\langle 0|T\Psi(x)\overline{\Psi}(y)j^\mu(z)j^\nu(v)|0\rangle_0+\cdots. \tag{6}$$

Here, $\Psi(x)$ denotes the (composite) nucleon field operator in QCD and the subscript "0" refers to the quantities evaluated in QCD without any external field. Note that Eq. (6) is written down for connected matrix elements (the subscript "conn" is omitted everywhere for brevity). Further, performing the Fourier transform in Eq. (6), amputating the external nucleon legs, and putting external nucleons on the mass shell, we see that the nucleon electromagnetic vertex $\langle p',s'|j^\mu(0)|p,s\rangle$ emerges at order A. At order A^2, as already mentioned, the scattering amplitude given in Eq. (1) is obtained from the matrix element $\langle 0|T\Psi(x)\overline{\Psi}(y)j^\mu(z)j^\nu(v)|0\rangle_0$, and so on.

On the other hand, since one is below the inelastic threshold, one may describe the nucleon two-point function within the nonrelativistic effective field theory as well, matching the couplings of the effective Lagrangian to the pertinent expressions in QCD. The advantage of this approach will become apparent, when the energy spectrum of a system in a finite box will be considered, as in the nonrelativistic effective theory, the energy levels are obtained by merely solving the Schrödinger equation.

In the present work we consider the matching and the subsequent calculation of the energy shift in a very condensed manner. A detailed treatment of these issues, as well as a thorough study of the finite-volume spectrum of the Hamiltonian with periodic potentials wil be the subject of a separate publication [34]. In brief, the procedure looks as follows. At the first stage, the matching of the relativistic and nonrelativistic theories is carried out in the infinite volume. The matching ensures that the on-shell coefficients in the expansion of the two-point function up to and including $O(A^2)$ are reproduced in the nonrelativistic theory. At the next step, one uses the nonrelativistic Hamiltonian, whose couplings are fixed through the matching, to calculate the energy levels in a finite volume. Note that this procedure is self-consistent, since the couplings of the effective Hamiltonian encode solely the short-range physics that does not get altered by placing the system in a large box.

Above, we have already written down the expansion of the nucleon two-point function in the external field in QCD. Now, we want to do the same in the effective theory. The corresponding Lagrangian, which describes the gauge-invariant interaction of the nucleon with an external electromagnetic field, has the following general form:

$$\mathcal{L}_{\rm eff} = \mathcal{L}_0 + \mathcal{L}_1 + \mathcal{L}_2 + \cdots. \tag{7}$$

Here, $\mathcal{L}_0$ is the free nucleon Lagrangian (we remind the reader that we are below the inelastic cuts),

$$\mathcal{L}_0 = \psi^\dagger 2W(i\partial_t - W)\psi, \qquad W = \sqrt{m^2 - \nabla^2}. \tag{8}$$

In the above expression, $\psi(x)$ is a two-component field that describes the nonrelativistic nucleon. It is seen that the relativistic dispersion relation for the energy of the free nucleon with the three-momentum p, $w(p) = \sqrt{m^2 + p^2}$, is satisfied. Also, the factor $2W$ ensures that the one-particle states have the relativistic normalization (see, e.g., Refs. [35,36]).

Further, $\mathcal{L}_1$ is linear in the external field A_μ, $\mathcal{L}_2$ is quadratic in A_μ, and so on. Note that $\mathcal{L}_1$ and $\mathcal{L}_2$ should contain an infinite set of operators with an arbitrary number of space derivatives, which act on the fermion and external fields. This differs from the situation for vanishing q^2 (the pertinent Lagrangian is given, e.g., in Ref. [29]). However, as we shall see, the infinite number of terms will effectively sum up in a single function.

Applying the equation of motion to eliminate the time derivatives, and performing partial integration, $\mathcal{L}_1$ and $\mathcal{L}_2$ can be brought into the form

$$\begin{aligned}
\mathcal{L}_1 &= \sum_{m,n=0} A_\mu(x)[\partial_{i_1}\ldots\partial_{i_n}\psi^\dagger_{s'}(x)]\Gamma^{i_1\ldots i_n,j_1\ldots j_m,\mu}_{s's}[\partial_{j_1}\ldots\partial_{j_m}\psi_s(x)],\\
\mathcal{L}_2 &= \sum_{l,m,n=0} A_\nu(x)[\partial_{\mu_1}\ldots\partial_{\mu_l}A_\mu(x)][\partial_{i_1}\ldots\partial_{i_n}\psi^\dagger_{s'}(x)]\Pi^{i_1\ldots i_n,j_1\ldots j_m,\mu_1\ldots\mu_l,\mu\nu}_{s's}[\partial_{j_1}\ldots\partial_{j_m}\psi_s(x)],
\end{aligned} \tag{9}$$

where $\Gamma^{i_1\ldots i_n,j_1\ldots j_m,\mu}_{s's}$ and $\Pi^{i_1\ldots i_n,j_1\ldots j_m,\mu_1\ldots\mu_l,\mu\nu}_{s's}$ denote low-energy constants. The Latin indices run from 1 to 3 (only space derivatives), whereas the Greek indices run from 0 to 3. The derivatives in the square brackets act only on the function within the brackets. Also, as a convention, the values m, $n = 0$ correspond to no derivatives in Eq. (9).

The comparison of the two-point functions at $O(A)$, calculated in the different theories, leads to the matching condition

$$\sum_{m,n=0} (-ip')_{i_1}\ldots(-ip')_{i_n}(ip)_{j_1}\ldots(ip)_{j_m}\Gamma^{i_1\ldots i_n,j_1\ldots j_m,\mu}_{s's} = \langle p',s'|j^\mu(0)|p,s\rangle. \tag{10}$$

The expression of the second derivative of the two-point function with respect to the external field in the effective theory consists of two parts: the contribution from $\mathcal{L}_2$ and the nucleon pole term, denoted by $U^{\mu\nu}(p',s';p,s;q)$, which is obtained by the insertion of two vertices $\mathcal{L}_1$. The latter can be expressed through the nucleon vertex (an explicit expression is given below). The matching condition at $O(A^2)$ takes the form

$$\sum_{l,m,n=0} (-ip')_{i_1}\ldots(-ip')_{i_n}(ip)_{j_1}\ldots(ip)_{j_m}(iq)_{\mu_1}\ldots(iq)_{\mu_l}\Pi^{i_1\ldots i_n,j_1\ldots j_m,\mu_1\ldots\mu_l,\mu\nu}_{s's} = T^{\mu\nu}(p',s';p,s;q) - U^{\mu\nu}(p',s';p,s;q). \tag{11}$$

As can be seen, the low-energy constants of the effective field theory are uniquely fixed by the Taylor expansion of the nucleon vertex and the Compton scattering amplitude in the external three-momenta.

III. ENERGY SHIFT

Up to now, we have considered the problem in a generic external field. We next limit ourselves to a static periodic magnetic field of the form

$$\mathbf{B} = (0, 0, B_3), \qquad B_3 = -B\cos(\omega x_2), \tag{12}$$

where B denotes the strength of the field and the real parameter ω takes nonzero values. The components of the gauge field $A^\mu(x)$ read

$$A_1 = \frac{B}{\omega}\sin(\omega x_2), \qquad A_0 = A_2 = A_3 = 0. \tag{13}$$

The parameter ω allows one to scan the virtuality of the photon.

Since lattice simulations are performed in a finite spatial volume, the magnetic flux is quantized [37]. Consequently, the parameter ω can take only particular values (see, e.g., Refs. [38,39]),

$$\omega = \frac{2\pi N}{L}, \qquad N \in \mathbb{Z}\backslash\{0\}, \tag{14}$$

whereas the field strength B is not quantized. Here, L denotes the spatial size of the lattice. The quantization condition Eq. (14) also guaranties the proper implementation of the magnetic field on a torus [38]. We note that, for $\omega \neq 0$, there exists an alternative procedure that implies the quantization of the field strength B instead of ω [38]. In the present paper, however, we do not consider this option.

The quantum-mechanical Hamiltonian, which acts on the single-nucleon wave function as a differential operator, can be straightforwardly derived from the effective Lagrangian, Eq. (7). It is convenient to first rescale the nucleon field,

$$\psi(x,t) \to \frac{1}{\sqrt{2W(\nabla)}}\psi(x,t). \tag{15}$$

The terms in the Hamiltonian can be again ordered, according to the powers of A_μ:

$$H = H_0 + H_1 + H_2 + O(A^3). \tag{16}$$

For instance, the free Hamiltonian reads $H_0 = W(\boldsymbol{\nabla})\delta_{s's}$, and so on. To the best of our knowledge, an analytic solution of the Schrödinger equation in the periodic magnetic field is not available in the literature. For this reason, we resort to perturbation theory. The solutions must obey periodic boundary conditions. Denoting the Hilbert-state vector in the nonrelativistic theory, corresponding to the unperturbed solution, by $|\mathbf{k}_n, s\rangle\!\rangle$, one has

$$\langle\!\langle \mathbf{x}|\mathbf{k}_n, s\rangle\!\rangle = \frac{1}{L^{3/2}}e^{i\,\mathbf{k}_n\,\mathbf{x}}\chi_s, \tag{17}$$

where χ_s denotes a Pauli spinor and

$$w(\mathbf{k}_n) = \sqrt{m^2 + \mathbf{k}_n^2}, \qquad \mathbf{k}_n = \frac{2\pi\mathbf{n}}{L}, \qquad \mathbf{n} \in \mathbb{Z}^3. \tag{18}$$

These vectors are normalized, according to $\langle\!\langle \mathbf{k}_m, s'|\mathbf{k}_n, s\rangle\!\rangle = \delta_{\mathbf{mn}}\delta_{s's}$.

Next, we evaluate the energy shift of the nucleon ground state up to order A^2. Since the unperturbed solution is twofold degenerate due to the nucleon spin, one should use perturbation theory for the degenerate states. First, one may check that the first-order energy shift vanishes identically for $\omega \neq 0$, since, in this case, $\langle\!\langle \mathbf{0}, s|H_1|\mathbf{0}, s'\rangle\!\rangle = 0$ due to three-momentum conservation. Further, in order to determine the spin-averaged shift δE at second order, the calculation of the diagonal matrix elements suffices,

$$\delta E = \frac{1}{2}\sum_s(\delta E_s' + \delta E_s''), \tag{19}$$

where the first contribution (the nucleon pole term) emerges from the second iteration of H_1 and the second term is the matrix element of H_2. The explicit expressions are

$$\delta E_s' = \sum_{\mathbf{k}_n \neq \mathbf{0}}\sum_\sigma \frac{\langle\!\langle\, \mathbf{0}, s|H_1|\,\mathbf{k}_n, \sigma\rangle\!\rangle\langle\!\langle\,\mathbf{k}_n, \sigma|H_1|\,\mathbf{0}, s\rangle\!\rangle}{w(\mathbf{0}) - w(\mathbf{k}_n)},$$
$$\delta E_s'' = \langle\!\langle \mathbf{0}, s|H_2|\mathbf{0}, s\rangle\!\rangle. \tag{20}$$

The calculation of these corrections is straightforward, and we obtain

$$\delta E_s' = \frac{B^2}{8m\omega^2}[F(\boldsymbol{\omega}) + F(-\boldsymbol{\omega})],$$
$$\delta E_s'' = -\frac{B^2}{4m\omega^2}[T^{11}(0,s;0,s;\hat{q}) - U^{11}(0,s;0,s;\hat{q})], \tag{21}$$

where $\boldsymbol{\omega} = (0, \omega, 0)$, $\hat{q} = (0, \boldsymbol{\omega})$ and

$$F(\boldsymbol{\omega}) = \sum_\sigma \frac{\langle\,\mathbf{0}, s|j^1(0)|\boldsymbol{\omega}, \sigma\rangle\langle\boldsymbol{\omega}, \sigma|j^1(0)|\,\mathbf{0}, s\rangle}{2w(\boldsymbol{\omega})(w(\mathbf{0}) - w(\boldsymbol{\omega}))}. \tag{22}$$

The crucial step in getting these formulas has been to apply the matching conditions Eqs. (10) and (11). Note also that here, having used the matching condition, we switched back to the relativistic normalization of the state vectors.

It remains to calculate the quantity $U^{11}(0,s;0,s;\hat{q})$. Inserting a complete set of the one-nucleon states into the pertinent matrix element and using the matching condition Eq. (10) once more, we obtain

$$U^{11}(0,s;0,s;\hat{q}) = -\frac{1}{2}[F(\boldsymbol{\omega}) + F(-\boldsymbol{\omega})]. \tag{23}$$

Finally, adding everything together, we get a remarkably simple formula for the spin-averaged energy shift

$$\delta E = \frac{B^2}{4m} T_1(0,-\omega^2) + O(B^3) = \frac{B^2}{4m} S_1(-\omega^2) + O(B^3), \quad (24)$$

where the expression for the spin-averaged tensor Eq. (3) has been explicitly used. This is the main result of the present work. Note that the quantity S_1 here is the full one and not the inelastic part only.

IV. DISCUSSION AND CONCLUSIONS

The applicability of the formula Eq. (24) is limited for several reasons. First, the strength of the magnetic field has to be chosen sufficiently small, so that perturbation theory provides a meaningful result. A necessary condition for this is that the structure of the perturbed and the unperturbed spectrum remains the same.

An estimate for the upper bound on the magnitude of B can be obtained as follows. It can be straightforwardly checked that using the periodic external field, Eq. (13), in the Schrödinger equation leads to a periodic potential with magnitude $V_0 = e^2B^2/(2m\omega^2)$ and period $d = \omega^{-1}$. Considering a single period as a potential well, perturbation theory is applicable, if the well is shallow enough, so that no bound states are formed (in the periodic potential, the band structure arises instead of the isolated energy levels). Using, for simplicity, the known formula for the square well gives the condition $eB < 2\omega^2$. Of course, this should only be considered as a crude order-of-magnitude estimate of the critical value of B. Note also that, from the point of view of phenomenological applications, the region of the small ω^2 (smaller than a few GeV^2) is the most relevant one.

As seen from Eq. (24), the perturbative result is valid up to terms of order B^3. Albeit, in principle, it is possible to give some crude estimate of the neglected terms by using ChPT, it is important to note that the validity of the formula can be checked *a posteriori* on the lattice—by ensuring that the energy shift grows quadratically with B.

On the other hand, the value of B should be large enough so that the energy shift δE is measurable. Moreover, the accuracy of the extraction should be sufficient to allow for a disentanglement of the inelastic and elastic contributions. The latter is given by [4]

$$S_1^{\rm el}(q^2) = -\frac{4m^2}{q^2(4m^2-q^2)}\{G_E^2(q^2) - G_M^2(q^2)\}, \quad (25)$$

where G_E, G_M denote the electric and magnetic form factors, respectively. Further, the inelastic contribution at $q^2 = 0$ is related to the magnetic polarizability by [4]

$$S_1^{\rm inel}(0) = -\frac{\kappa^2}{4m^2} - \frac{m}{\alpha}\beta_M, \quad (26)$$

where κ denotes the anomalous magnetic moment of a nucleon and α is the fine-structure constant. Experimental values for the proton and neutron polarizabilities are $\beta_M^p = (3.15 \pm 0.50) \times 10^{-4}$ fm^3 [40] and $\beta_M^n = (3.65 \pm 1.50) \times 10^{-4}$ fm^3 [41], respectively. As already mentioned, little is known about the q^2 dependence of $S_1(q^2)$. For a crude estimate, however, we assume that [4]

$$S_1^{\rm inel}(q^2) = \frac{S_1^{\rm inel}(0)}{(1 - q^2/0.71\ \text{GeV}^2)^2}. \quad (27)$$

Using now Eq. (24), it is immediately seen that the inelastic shift $\delta E^{\rm inel}$ obeys the following relation:

$$eB = \left(\frac{16\pi\alpha m \delta E^{\rm inel}}{S_1^{\rm inel}(q^2)}\right)^{1/2} = c \times |\delta E^{\rm inel}|^{1/2}. \quad (28)$$

Taking now $-q^2 = \omega_{\rm max}^2 = 2$ GeV^2 as the upper bound of the interval, we get a crude estimate of the coefficient $c = 0.90$ GeV$^{3/2}$ for the proton and $c = 0.83$ GeV$^{3/2}$ for the neutron. Note that, using a rather generous estimate $|\delta E^{\rm inel}| = 0.05m$, the bound Eq. (28) at $-q^2 = \omega^2$ is comfortably consistent with the upper bound $eB < 2\omega^2$, except very small values of ω^2.

The total energy shift $\delta E = \delta E^{\rm el} + \delta E^{\rm inel}$ can be much larger than the inelastic shift alone, especially as ω^2 is small. As seen from Eq. (25), the elastic contribution is singular as $\omega^2 \to 0$, whereas the inelastic contribution is regular. As an order-of-magnitude estimate, one may ask, at what value of ω^2 the magnitude of the inelastic contribution amounts to a 10% of the singular piece of the elastic contribution, which behaves like $1/\omega^2$. The estimate gives $\omega_{\rm min}^2 = 0.11$ GeV^2 for the proton and $\omega_{\rm min}^2 = 0.05$ GeV^2 for the neutron. Of course, setting a lower bound on the ω^2-interval critically depends on our ability to extract the proton and neutron form factors on the lattice with high accuracy. Note also that, even for the lowest value of $\omega_{\rm min}^2$, the quantity $M_\pi L$ is of order 4—in other words, the calculations can be performed at the volumes which are feasible at present (here, M_π is the pion mass).

Another interesting issue is the study of the limit $\omega \to 0$. In the present framework, this limit is singular and is intertwined with the limit $L \to \infty$. Indeed, recall that the values of ω are quantized: $\omega = 2\pi N/L$. For nonzero values of N, the limit $\omega \to 0$ thus implies $L \to \infty$. In addition, the Landau levels are bound even if $L \to \infty$, which violates the condition of the weak B field. We expect that the alternative setting for the periodic magnetic field on the lattice (quantized B, ω not quantized), see Ref. [38], which has not been considered in the present paper, will be more advantageous for studying the limit $\omega \to 0$. Also, this different approach will allow one to continuously scan the interval of interest in the variable q^2. We plan to address these and other issues in a forthcoming work [34].

To summarize, our final expression, Eq. (24), enables one to directly extract the subtraction function $S_1(q^2)$ from the lattice measurement of the nucleon energy levels in a periodic external magnetic field.

ACKNOWLEDGMENTS

We thank Z. Davoudi, J. Gasser, H. Leutwyler, J. A. Oller, M. Savage, G. Schierholz and N. Tantalo for useful discussions. We acknowledge the support from the DFG (CRC 110 "Symmetries and the Emergence of Structure in QCD" and Bonn-Cologne Graduate School of Physics and Astronomy). This research is supported in part by Volkswagenstiftung under Contract No. 86260 and by the Chinese Academy of Sciences (CAS) President's International Fellowship Initiative (PIFI) (Grant No. 2017VMA0025).

[1] S. Borsanyi *et al.*, Science **347**, 1452 (2015).
[2] R. Horsley *et al.*, J. Phys. G **43**, 10LT02 (2016).
[3] J. Gasser and H. Leutwyler, Nucl. Phys. **B94**, 269 (1975).
[4] J. Gasser, M. Hoferichter, H. Leutwyler, and A. Rusetsky, Eur. Phys. J. C **75**, 375 (2015).
[5] A. Walker-Loud, C. E. Carlson, and G. A. Miller, Phys. Rev. Lett. **108**, 232301 (2012).
[6] F. B. Erben, P. E. Shanahan, A. W. Thomas, and R. D. Young, Phys. Rev. C **90**, 065205 (2014).
[7] M. C. Birse and J. A. McGovern, Eur. Phys. J. A **48**, 120 (2012).
[8] K. Pachucki, Phys. Rev. A **60**, 3593 (1999).
[9] C. Peset and A. Pineda, Nucl. Phys. **B887**, 69 (2014).
[10] J. C. Collins, Nucl. Phys. **B149**, 90 (1979); **B915**, 392 (2017).
[11] R. J. Hill and G. Paz, arXiv:1611.09917.
[12] V. Bernard, N. Kaiser, and U.-G. Meißner, Nucl. Phys. **B373**, 346 (1992).
[13] V. Bernard, N. Kaiser, J. Kambor, and U.-G. Meißner, Nucl. Phys. **B388**, 315 (1992).
[14] X. D. Ji, C. W. Kao, and J. Osborne, Phys. Rev. D **61**, 074003 (2000).
[15] V. Bernard, T. R. Hemmert, and U.-G. Meißner, Phys. Rev. D **67**, 076008 (2003).
[16] R. J. Hill and G. Paz, Phys. Rev. Lett. **107**, 160402 (2011).
[17] J. M. Alarcon, V. Lensky, and V. Pascalutsa, Eur. Phys. J. C **74**, 2852 (2014).
[18] V. Lensky, J. M. Alarcon, and V. Pascalutsa, Phys. Rev. C **90**, 055202 (2014).
[19] D. Nevado and A. Pineda, Phys. Rev. C **77**, 035202 (2008).
[20] M. Gorchtein, F. J. Llanes-Estrada, and A. P. Szczepaniak, Phys. Rev. A **87**, 052501 (2013).
[21] O. Tomalak and M. Vanderhaeghen, Eur. Phys. J. C **76**, 125 (2016).
[22] S. J. Brodsky, F. J. Llanes-Estrada, and A. P. Szczepaniak, Phys. Rev. D **79**, 033012 (2009).
[23] J. Green, O. Gryniuk, G. von Hippel, H. B. Meyer, and V. Pascalutsa, Phys. Rev. Lett. **115**, 222003 (2015).
[24] N. H. Christ, X. Feng, A. Portelli, and C. T. Sachrajda (RBC and UKQCD Collaborations), Phys. Rev. D **93**, 114517 (2016).
[25] N. H. Christ, X. Feng, A. Jüttner, A. Lawson, A. Portelli, and C. T. Sachrajda, Phys. Rev. D **94**, 114516 (2016).
[26] B. C. Tiburzi and S. O. Vayl, Phys. Rev. D **87**, 054507 (2013).
[27] E. Chang, W. Detmold, K. Orginos, A. Parreño, M. J. Savage, B. C. Tiburzi, and S. R. Beane (NPLQCD Collaboration), Phys. Rev. D **92**, 114502 (2015).
[28] A. Parreno *et al.*, arXiv:1609.03985.
[29] W. Detmold, B. C. Tiburzi, and A. Walker-Loud, Phys. Rev. D **73**, 114505 (2006).
[30] Z. Davoudi and W. Detmold, Phys. Rev. D **93**, 014509 (2016).
[31] C. Kittel, *Introduction to Solid State Physics*, 7th ed. (Wiley, New York, 1996).
[32] R. Tarrach, Nuovo Cimento Soc. Ital. Fis., A **28**, 409 (1975).
[33] J. Bernabeu and R. Tarrach, Ann. Phys. (N.Y.) **102** (1976) 323.
[34] A. Agadjanov, U.-G. Meißner, and A. Rusetsky (to be published).
[35] G. Colangelo, J. Gasser, B. Kubis, and A. Rusetsky, Phys. Lett. B **638**, 187 (2006).
[36] J. Gasser, B. Kubis, and A. Rusetsky, Nucl. Phys. **B850**, 96 (2011).
[37] G. 't Hooft, Nucl. Phys. **B153**, 141 (1979).
[38] Z. Davoudi and W. Detmold, Phys. Rev. D **92**, 074506 (2015).
[39] G. Bali and G. Endrődi, Phys. Rev. D **92**, 054506 (2015).
[40] J. A. McGovern, D. R. Phillips, and H. W. Grießhammer, Eur. Phys. J. A **49**, 12 (2013).
[41] L. S. Myers *et al.* (COMPTON@MAX-lab Collaboration), Phys. Rev. Lett. **113**, 262506 (2014).

4.2 Supplement

This section provides the extended derivation of the formula for the energy shift of the nucleon ground state given by Eq. (26) in the paper. There are several approaches to arrive at the final expression, and two of them are discussed below. The open issues, which will be studied in the upcoming large paper, are summarized at the end of the supplement.

Method I

The first method is based on the application of the non-relativistic EFT in a finite volume. It follows closely the discussion of the original paper. The starting point is the quantum-mechanical Hamiltonian which acts on the single-nucleon wave function as a differential operator. It is defined as the 00-component of energy–momentum tensor:

$$\psi^\dagger H\psi = \frac{\partial\mathcal{L}_{\rm eff}}{\partial(\partial_t\psi)}\partial_t\psi - g^{00}\mathcal{L}_{\rm eff}\,. \tag{4.1}$$

First rescaling the nucleon field, $\psi \to [2W(\boldsymbol{\nabla})]^{-1/2}\,\psi$ in the non-relativistic effective Lagrangian and then applying Eq. (4.1), one gets:

$$H = H_0 + H_1 + H_2 + O(A^3), \tag{4.2}$$

where

$$\begin{aligned}
H_0 &= W(\boldsymbol{\nabla})\delta_{s's}, \\
H_1 &= -\frac{1}{\sqrt{2W(\boldsymbol{\nabla})}}\sum_{m,n=0}(-\partial_{i_1})\ldots(-\partial_{i_n})\,\Gamma^{i_1\ldots i_n,\,j_1\ldots j_m,\,\mu}_{s's}A_\mu(\mathbf{x})\partial_{j_1}\ldots\partial_{j_m}\frac{1}{\sqrt{2W(\boldsymbol{\nabla})}}, \\
H_2 &= -\frac{1}{\sqrt{2W(\boldsymbol{\nabla})}}\sum_{l,m,n=0}(-\partial_{i_1})\ldots(-\partial_{i_n})\,\Pi^{i_1\ldots i_n,\,j_1\ldots j_m,\,\mu_1\ldots\mu_l,\,\mu\nu}_{s's}[\partial_{\mu_1}\ldots\partial_{\mu_l}A_\mu(\mathbf{x})]A_\nu(\mathbf{x}) \\
&\times\ \partial_{j_1}\ldots\partial_{j_m}\frac{1}{\sqrt{2W(\boldsymbol{\nabla})}}.
\end{aligned} \tag{4.3}$$

Here, the derivatives in the square brackets act only on the function within the brackets.

At the next step, degenerate perturbation theory is applied to determine the energy shift. The total spin-averaged shift takes the form

$$\delta E = \delta E^{(1)} + \delta E^{(2)} + O(B^3)\,, \tag{4.4}$$

where $\delta E^{(1)}$ and $\delta E^{(2)}$ denote the first- and second-order term, respectively. The first-order correction reads

$$\delta E^{(1)} = \frac{1}{2}\sum_s\langle\langle\mathbf{0},s|H_1|\mathbf{0},s\rangle\rangle \equiv \frac{1}{2}\sum_s\int_0^L d^3\mathbf{x}\,\psi^{(0)^\dagger}_{0,s}(\mathbf{x})H_1\psi^{(0)}_{0,s}(\mathbf{x})\,, \tag{4.5}$$

where $|\mathbf{k}_n,s\rangle\rangle$ denotes the state vector in the non-relativistic theory that corresponds to the unperturbed solution. Accordingly, the wave function $\psi^{(0)}_{0,s}(\mathbf{x})$ takes the form

$$\psi^{(0)}_{n,s}(\mathbf{x}) = \frac{1}{L^{3/2}}e^{i\mathbf{k}_n\mathbf{x}}\chi_s\,. \tag{4.6}$$

Here, χ_s denotes the Pauli spinor. The general matrix element of the operator H_1 is given by

$$\begin{aligned}\langle\langle \mathbf{p}', s'|H_1|\mathbf{p}, s\rangle\rangle &= -\frac{1}{L^3}\int_0^L d^3\mathbf{x}\, e^{-i\mathbf{p}'\mathbf{x}}\frac{1}{\sqrt{2W(\boldsymbol{\nabla})}}\times \\ &\times \sum_{m,n=0}(-\partial_{i_1})\ldots(-\partial_{i_n})\,\Gamma_{s's}^{i_1\ldots i_n,\, j_1\ldots j_m,\,\mu}A_\mu(\mathbf{x})\partial_{j_1}\ldots\partial_{j_m}\frac{1}{\sqrt{2W(\boldsymbol{\nabla})}}e^{i\mathbf{p}\mathbf{x}}\,.\end{aligned} \tag{4.7}$$

Integrating by parts, and using the fact that the electromagnetic potential $A_\mu(x)$ vanishes at the integration limits because of the quantization condition for the ω, one obtains:

$$\langle\langle \mathbf{p}', s'|H_1|\mathbf{p}, s\rangle\rangle = -\frac{\tilde{A}_\mu(\mathbf{p}-\mathbf{p}')}{L^3\sqrt{4w(\mathbf{p}')w(\mathbf{p})}}\sum_{m,n=0}(-i\mathbf{p}')_{i_1}\ldots(-i\mathbf{p}')_{i_n}(i\mathbf{p})_{j_1}\ldots(i\mathbf{p})_{j_m}\Gamma_{s's}^{i_1\ldots i_n,\, j_1\ldots j_m,\,\mu}\,. \tag{4.8}$$

Here, $\tilde{A}_\mu(\mathbf{q})$ denotes the Fourier transform of the field $A_\mu(\mathbf{x}, 0)$,

$$\tilde{A}_\mu(\mathbf{q}) = \int_0^L d^3\mathbf{x}\, e^{i\mathbf{q}\mathbf{x}}A_\mu(\mathbf{x}, 0), \tag{4.9}$$

which explicitly reads

$$\tilde{A}_1(\mathbf{q}) = \frac{B}{2i\omega}L^3[\delta_{\mathbf{q}+\boldsymbol{\omega}} - \delta_{\mathbf{q}-\boldsymbol{\omega}}], \qquad \tilde{A}_0 = \tilde{A}_2 = \tilde{A}_3 = 0, \qquad \boldsymbol{\omega} = (0, \omega, 0) \neq 0\,. \tag{4.10}$$

In this expression, the sum is precisely the same as in the matching condition at $O(A)$,

$$\sum_{m,n=0}(-ip')_{i_1}\ldots(-ip')_{i_n}(ip)_{j_1}\ldots(ip)_{j_m}\Gamma_{s's}^{i_1\ldots i_n,\, j_1\ldots j_m,\,\mu} = \langle p', s'|j^\mu(0)|p, s\rangle. \tag{4.11}$$

Accordingly, the matrix element of the operator H_1 takes the value

$$\langle\langle \mathbf{p}', s'|H_1|\mathbf{p}, s\rangle\rangle = -\frac{\langle \mathbf{p}', s'|j^\mu(0)|\mathbf{p}, s\rangle}{\sqrt{4w(\mathbf{p}')w(\mathbf{p})}}\frac{1}{L^3}\tilde{A}_\mu(\mathbf{p}-\mathbf{p}')\,. \tag{4.12}$$

Setting $\mathbf{p} = \mathbf{p}' = 0$ and $s' = s$ in Eq. (4.12), it is seen that the first-order correction to the energy shift vanishes:

$$\delta E^{(1)} = 0. \tag{4.13}$$

As expected, this result follows from the three-momentum conservation at the vertex of the three-point function.

The second-order contribution to the energy shift consists of two parts:

$$\delta E^{(2)} = \frac{1}{2}\sum_s(\delta E_s' + \delta E_s{}'')\,, \tag{4.14}$$

The first term emerges from the second iteration of the operator H_1:

$$\delta E_s' = \sum_{\mathbf{k}_n\neq\mathbf{0}}\sum_\sigma\frac{\langle\langle \mathbf{0}, s|H_1|\mathbf{k}_n, \sigma\rangle\rangle\langle\langle \mathbf{k}_n, \sigma|H_1|\mathbf{0}, s\rangle\rangle}{w(\mathbf{0}) - w(\mathbf{k}_n)}\,. \tag{4.15}$$

It is evaluated by using Eqs. (4.12) and (4.10),

$$\delta E'_s = \frac{1}{4m}\left(\frac{B}{\omega}\right)^2 \sum_{\mathbf{k}_n\neq\mathbf{0}} \sum_{\sigma} \frac{\langle \mathbf{0}, s|j^1(0)|\mathbf{k}_n,\sigma\rangle\langle \mathbf{k}_n,\sigma|j^1(0)|\mathbf{p}, s\rangle}{4w(\mathbf{k}_n)(w(\mathbf{0})-w(\mathbf{k}_n))}\left[\delta_{\mathbf{k}_n+\omega}+\delta_{\mathbf{k}_n-\omega}\right]. \tag{4.16}$$

The second term is given by the matrix element of the operator H_2,

$$\delta E''_s = \langle\langle \mathbf{0}, s|H_2|\mathbf{0}, s\rangle\rangle\,. \tag{4.17}$$

One has:

$$\begin{aligned}\langle\langle \mathbf{p}', s'|H_2|\mathbf{p}, s\rangle\rangle &= -\frac{1}{L^3}\int_0^L d^3\mathbf{x}\, e^{-i\mathbf{p}'\mathbf{x}}\frac{1}{\sqrt{2W(\boldsymbol{\nabla})}}\times &(4.18)\\ &\times \sum_{l,m,n=0}(-\partial_{i_1})\ldots(-\partial_{i_n})\,\Pi_{s's}^{i_1\ldots i_n,\, j_1\ldots j_m,\mu_1\ldots\mu_l,\mu\nu}[\partial_{\mu_1}\ldots\partial_{\mu_l}A_\mu(\mathbf{x})]A_\nu(\mathbf{x})\times\\ &\times \partial_{j_1}\ldots\partial_{j_m}\frac{1}{\sqrt{2W(\boldsymbol{\nabla})}}e^{i\mathbf{p}\mathbf{x}}\,. &(4.19)\end{aligned}$$

The integration leads to the expression

$$\begin{aligned}\langle\langle \mathbf{p}', s'|H_2|\mathbf{p}, s\rangle\rangle &= -\frac{1}{L^3\sqrt{4w(\mathbf{p}')w(\mathbf{p})}} &(4.20)\\ &\times \sum_{l,m,n=0}(-i\mathbf{p}')_{i_1}\ldots(-i\mathbf{p}')_{i_n}(i\mathbf{p})_{j_1}\ldots(i\mathbf{p})_{j_m}\Pi_{s's}^{i_1\ldots i_n,\, j_1\ldots j_m,\mu_1\ldots\mu_l,\mu\nu}\, I_{\mu_1\ldots\mu_l,\mu\nu}\,,\end{aligned}$$

where the integral $I_{\mu_1\ldots\mu_l,\mu\nu}$ reads

$$I_{\mu_1\ldots\mu_l,\mu\nu} = \int_0^L d^3\mathbf{x}\,[\partial_{\mu_1}\ldots\partial_{\mu_l}A_\mu(\mathbf{x})]A_\nu(\mathbf{x})\,. \tag{4.21}$$

This integral has a non-zero value for $\mu_1=\cdots=\mu_l=2$, $\mu=\nu=1$ and for even l,

$$I_{2\ldots2,11} = \frac{L^3}{2}\left(\frac{B}{\omega}\right)^2(i\omega)^l, \qquad l=0,2,\ldots\,. \tag{4.22}$$

Inserting this value into Eq. (4.20), one gets

$$\begin{aligned}\langle\langle \mathbf{p}', s|H_2|\mathbf{p}, s\rangle\rangle &= -\frac{1}{2\sqrt{4w(\mathbf{p}')w(\mathbf{p})}}\left(\frac{B}{\omega}\right)^2 &(4.23)\\ &\times \sum_{l,m,n=0}(-i\mathbf{p}')_{i_1}\ldots(-i\mathbf{p}')_{i_n}(i\mathbf{p})_{j_1}\ldots(i\mathbf{p})_{j_m}\underbrace{(i\omega)\ldots(i\omega)}_{l\text{ copies}}\Pi_{ss}^{i_1\ldots i_n,\, j_1\ldots j_m,\mu_1\ldots\mu_l,\,11}\,.\end{aligned}$$

Further, using the matching condition at $O(A^2)$,

$$\begin{aligned}&\sum_{l,m,n=0}(-ip')_{i_1}\ldots(-ip')_{i_n}(ip)_{j_1}\ldots(ip)_{j_m}(iq)_{\mu_1}\ldots(iq)_{\mu_l}\Pi_{s's}^{i_1\ldots i_n,\, j_1\ldots j_m,\mu_1\ldots\mu_l,\mu\nu} =\\ &= T^{\mu\nu}(p',s';p,s;q) - U^{\mu\nu}(p',s';p,s;q)\,,\end{aligned} \tag{4.24}$$

and setting $\mathbf{p}=\mathbf{p}'=0$ and $s'=s$, the expression for the second energy correction $\delta E''_s$ takes a compact

form:

$$\delta E_s'' = -\frac{1}{4m}\left(\frac{B}{\omega}\right)^2 \left[T^{11}(0,s;0,s;\hat{q}) - U^{11}(0,s;0,s;\hat{q})\right], \tag{4.25}$$

where $\hat{q} = (0,\boldsymbol{\omega})$.

It remains to determine the quantity $U^{11}(0,s;0,s;\hat{q})$, which is a component of the Compton tensor

$$U^{11}(0,s;0,s;\hat{q}) = \frac{i}{2}\int d^4x e^{i\hat{q}\cdot x}\langle\langle \mathbf{0},s|T\, j^1(x) j^1(0)|\mathbf{0},s\rangle\rangle\,. \tag{4.26}$$

It is defined in the non-relativistic EFT, such that the completeness relation contains only the one-nucleon states:

$$\frac{1}{L^3}\sum_{\mathbf{k}_n}\sum_{\sigma}\frac{|\mathbf{k}_n,\sigma\rangle\rangle\langle\langle \mathbf{k}_n,\sigma|}{2w(\mathbf{k}_n)} = 1. \tag{4.27}$$

Inserting this expression into Eq. (4.26) and using the property of the step function

$$\int_{-\infty}^{\infty} dx_0 e^{ip_0x_0}\theta(x_0) = \frac{i}{p_0}\,, \tag{4.28}$$

one obtains

$$U^{11}(0,s;0,s;\hat{q}) = \frac{i}{2}\sum_{\mathbf{k}_n}\sum_{\sigma}\left\{i\delta_{\mathbf{k}_n-\boldsymbol{\omega}}\frac{\langle\langle \mathbf{0},s|j^1(0)|\mathbf{k}_n,\sigma\rangle\rangle\langle\langle \mathbf{k}_n,\sigma|j^1(0)|\mathbf{0},s\rangle\rangle}{2w(\mathbf{k}_n)(w(\mathbf{0})-w(\mathbf{k}_n))} + [\boldsymbol{\omega}\leftrightarrow-\boldsymbol{\omega}]\right\}. \tag{4.29}$$

In this expression, the current matrix elements are evaluated in the non-relativistic EFT. They are given precisely by the sum on the left-hand side of the matching condition in Eq. (4.11). Accordingly, the summation over $\mathbf{k}_n$ gives

$$U^{11}(0,s;0,s;\hat{q}) = F(\boldsymbol{\omega}) + F(-\boldsymbol{\omega}), \tag{4.30}$$

where

$$F(\boldsymbol{\omega}) = -\sum_{\sigma}\frac{\langle \mathbf{0},s|j^1(0)|\boldsymbol{\omega},\sigma\rangle\langle\boldsymbol{\omega},\sigma|j^1(0)|\mathbf{0},s\rangle}{4w(\boldsymbol{\omega})(w(\mathbf{0})-w(\boldsymbol{\omega}))}. \tag{4.31}$$

Finally, summing up all contributions up to $O(B^2)$, the spin-averaged total energy shift of the ground state is given by

$$\delta E = -\frac{1}{4m}\left(\frac{B}{\omega}\right)^2\frac{1}{2}\sum_s T^{11}(0,s;0,s;\hat{q}) + O(B^3) = \frac{B^2}{4m}T_1(0,-\omega^2) + O(B^3)\,. \tag{4.32}$$

This completes the derivation of the main result.

Method II

In the second approach, one works directly with the expansion of the nucleon two-point function in the external electromagnetic field, as given in Eq. (6) of the paper. To project onto the states with the zero three-momentum and a given spin component s, one performs the Fourier transformation of the

expressions in Eq. (6),

$$C = C^{(0)} + C^{(1)} + C^{(2)} + O(A^3), \tag{4.33}$$

where

$$C = \frac{1}{L^3}\int^L d^3x d^3y\, \langle 0|T\Psi_s(x)\bar{\Psi}_s(y)|0\rangle_A\,, \tag{4.34}$$

$$C^{(0)} = \frac{1}{L^3}\int^L d^3x d^3y\, \langle 0|T\Psi_s(x)\bar{\Psi}_s(y)|0\rangle\,, \tag{4.35}$$

$$C^{(1)} = \frac{i}{L^3}\int^L d^3x d^3y d^4z\, A_\mu(\mathbf{z})\langle 0|T\Psi_s(x)\bar{\Psi}_s(y) j^\mu(z)|0\rangle\,, \tag{4.36}$$

$$C^{(2)} = \frac{i^2}{2L^3}\int^L d^3x d^3y d^4z d^4v\, A_\mu(\mathbf{z})A_\nu(\mathbf{v})\langle 0|T\Psi_s(x)\bar{\Psi}_s(y) j^\mu(z) j^\nu(v)|0\rangle\,. \tag{4.37}$$

Here, $\Psi_s(x)$ denotes the nucleon interpolating field with spin component s. To simplify the discussion, the calculation will be done in Minkowski spacetime. The completeness relation takes the form

$$\frac{1}{L^3}\sum_{\mathbf{k}}\sum_{\sigma}\frac{|\mathbf{k},\sigma\rangle\langle\mathbf{k},\sigma|}{2\omega(\mathbf{k})} + \cdots = 1\,, \tag{4.38}$$

where the dots stand for the excited states contributions; they will be neglected altogether by taking the limit $x_0 - y_0 \to +\infty$ (the time extent of the lattice is assumed to be infinite).

Let us start with the matrix element $C^{(0)}$ that describes the free propagation of the nucleon. Using the translation invariance for an arbitrary operator $O(x)$,

$$O(x) = e^{-i\hat{P}x}O(0)e^{i\hat{P}x}, \qquad \hat{P} = (\hat{P}_0, \hat{\mathbf{P}})\,, \tag{4.39}$$

it takes the form

$$C^{(0)} = \frac{1}{L^6}\sum_{\mathbf{k}}\frac{1}{2w(\mathbf{k})}\int^L d^3\mathbf{x} d^3\mathbf{y}\,\theta(x_0-y_0)e^{-i\mathbf{k}(\mathbf{x}-\mathbf{y})}e^{iw(\mathbf{k})(x_0-y_0)}\langle 0|\Psi_s(0)|\mathbf{k},s\rangle\langle\mathbf{k},s|\bar{\Psi}_s(0)|0\rangle\,. \tag{4.40}$$

Integrating over all variables, one gets

$$C^{(0)} = \frac{Z_s e^{im(x_0-y_0)}}{2m}\,, \qquad Z_s = \langle 0|\Psi_s(0)|\mathbf{0},s\rangle\langle\mathbf{0},s|\bar{\Psi}_s(0)|0\rangle\,. \tag{4.41}$$

The two-point function in the presence of the external magnetic field can be written in a similar manner:

$$C = \frac{Z_s(\mathbf{B})e^{iE_s(\mathbf{B})(x_0-y_0)}}{2E_s(\mathbf{B})}, \qquad Z_s(\mathbf{B}) = \langle 0|\Psi_s(0)|E_s(\mathbf{B}),s\rangle\langle E_s(\mathbf{B}),s|\bar{\Psi}_s(0)|0\rangle\,. \tag{4.42}$$

Here, $E_s(\mathbf{B})$ is the energy of the nucleon ground state. Considering a weak periodic magnetic field

$$\mathbf{B} = (0,0,-B\cos(\omega x_2)), \qquad \omega = \frac{2\pi N}{L}, \qquad N \in \mathbb{Z}\backslash\{0\}, \tag{4.43}$$

the functions $E_s(\mathbf{B})$ and $Z_s(\mathbf{B})$ obey the polynomial expansions

$$E_s(\mathbf{B}) = m + \xi_s(\omega)B + \eta_s(\omega)B^2 + O(B^3)\,, \qquad Z_s(\mathbf{B}) = Z_s + \alpha_s(\omega)B + \beta_s(\omega)B^2 + O(B^3)\,. \tag{4.44}$$

The unknown quantities $\xi_s(\omega), \eta_s(\omega), \alpha_s(\omega)$, and $\beta_s(\omega)$ depend on the frequency ω.

The correlator $C^{(1)}$ is evaluated in a similar manner. One has

$$C^{(1)} = \frac{i}{L^9}\sum_{\mathbf{k},\mathbf{l}}\frac{1}{4w(\mathbf{k})w(\mathbf{l})}\int^L d^3\mathbf{x}d^3\mathbf{y}d^3\mathbf{z}dz_0\, A_1(\mathbf{z})\theta(x_0-z_0)\theta(z_0-y_0)$$

$$\times\; e^{-i\mathbf{k}(\mathbf{x}-\mathbf{z})}e^{iw(\mathbf{k})(x_0-z_0)}e^{-i\mathbf{l}(\mathbf{z}-\mathbf{y})}e^{iw(\mathbf{l})(z_0-y_0)}\langle 0|\Psi_s(0)|\mathbf{k},s\rangle\langle\mathbf{k},s|j^1(0)|\mathbf{l},s\rangle\langle\mathbf{l},s|\bar{\Psi}_s(0)|0\rangle\,. \quad (4.45)$$

The summation over the three-momentum simplifies the expression:

$$C^{(1)} = i\frac{e^{im(x_0-y_0)}}{4m^2L^3}\int^L d^3\mathbf{z}dz_0\, A_1(\mathbf{z})\theta(x_0-z_0)\theta(z_0-y_0)\langle 0|\Psi_s(0)|\mathbf{0},s\rangle\langle\mathbf{0},s|j^1(0)|\mathbf{0},s\rangle\langle\mathbf{0},s|\bar{\Psi}_s(0)|0\rangle\,, \quad (4.46)$$

or,

$$C^{(1)} = i\frac{Z_s e^{im(x_0-y_0)}}{4m^2L^3}(x_0-y_0)\langle\mathbf{0},s|j^1(0)|\mathbf{0},s\rangle\int^L d^3\mathbf{z}\,A_1(\mathbf{z})\,, \quad (4.47)$$

The integral over the periodic electromagnetic potential vanishes, and so

$$C^{(1)} = 0. \quad (4.48)$$

The limit of the uniform magnetic field should be handled with care, by first providing the nonzero three-momentum to the nucleons.

The calculation of the second-order matrix element $C^{(2)}$ proceeds as follows. First inserting the completeness relation and using translation invariance, one gets

$$C^{(2)} = i^2\frac{Z_s e^{im(x_0-y_0)}}{8m^2L^3}\int^L d^3\mathbf{z}d^3\mathbf{v}d\lambda_0 dv_0\, A_1(\mathbf{z})A_1(\mathbf{v})\theta(x_0-\lambda_0-v_0)\theta(v_0-y_0)\langle\mathbf{0},s|Tj^1(\lambda)j^1(0)|\mathbf{0},s\rangle, \quad (4.49)$$

where $\lambda_0 = z_0 - v_0$ is a new integration variable, while $\lambda = (\lambda_0, \mathbf{z}-\mathbf{v})$. It is then straightforward to verify the identity

$$\langle\mathbf{0},s|Tj^1(\lambda)j^1(0)|\mathbf{0},s\rangle = -\frac{2i}{L^3}\sum_{\mathbf{q}}\int_{-\infty}^{\infty}\frac{dq_0}{2\pi}e^{-iq\lambda}T^{11}(0,s;0,s;q)\,, \quad \lambda = z-v\,, \quad (4.50)$$

which holds for a sufficiently large L. The correlator $C^{(2)}$ takes the form

$$C^{(2)} = i\frac{Z_s e^{im(x_0-y_0)}}{4m^2L^6}\sum_{\mathbf{q}}\int_{-\infty}^{\infty}\frac{dq_0}{2\pi}\int^L d^3\mathbf{z}d^3\mathbf{v}d\lambda_0 dv_0$$

$$\times\; A_1(\mathbf{z})A_1(\mathbf{v})\theta(x_0-\lambda_0-v_0)\theta(v_0-y_0)e^{-iq\lambda}T^{11}(0,s;0,s;q)\,. \quad (4.51)$$

Next, the integration over v_0 gives

$$\int dv_0\,\theta(x_0-\lambda_0-v_0)\theta(v_0-y_0) = (x_0-y_0-\lambda_0)\theta(x_0-y_0-\lambda_0)\,. \quad (4.52)$$

Accordingly,

$$C^{(2)} = i\frac{Z_s e^{im(x_0-y_0)}}{4m^2L^6}\sum_{\mathbf{q}}\tilde{A}_1(\mathbf{q})\tilde{A}_1(-\mathbf{q})I(0,s;0,s;\mathbf{q})\,, \tag{4.53}$$

where $\tilde{A}_1(\mathbf{q})$ is defined in Eq. (4.9). The quantity $I(0,s;0,s;\mathbf{q})$ reads

$$I(0,s;0,s;\mathbf{q}) = \int_{-\infty}^{\infty}\frac{dq_0}{2\pi}\int_{-\infty}^{x_0-y_0} d\lambda_0\,(x_0-y_0-\lambda_0)e^{-iq_0\lambda_0}T^{11}(0,s;0,s;q)\,. \tag{4.54}$$

The shift of the variable $\lambda_0 \to x_0 - y_0 - \lambda_0$ and the partial integration over q_0 gives

$$I(0,s;0,s;\mathbf{q}) = -i\int_{-\infty}^{\infty}\frac{dq_0}{2\pi}\int_{0}^{\infty} d\lambda_0\, e^{iq_0\lambda_0}\frac{\partial}{\partial q_0}\left[e^{-iq_0(x_0-y_0)}T^{11}(0,s;0,s;q)\right]. \tag{4.55}$$

Integrating over λ_0, one obtains

$$I(0,s;0,s;\mathbf{q}) = \int_{-\infty}^{\infty}\frac{dq_0}{2\pi}\frac{e^{-iq_0(x_0-y_0)}}{q_0+i\epsilon}\left[-i(x_0-y_0)T^{11}(0,s;0,s;q)+\frac{\partial}{\partial q_0}T^{11}(0,s;0,s;q)\right], \tag{4.56}$$

where the $i\epsilon$ prescription ensures the convergence of the integral. Further, the contour integration leads to the following expression:

$$I(0,s;0,s;\mathbf{q}) = -(x_0-y_0)T^{11}(0,s;0,s;\bar{q}) - i\frac{\partial}{\partial q_0}T^{11}(0,s;0,s;q)\Big|_{q=\bar{q}}\,, \quad \bar{q}=(0,\mathbf{q})\,. \tag{4.57}$$

Finally, inserting this result into Eq. (4.53) and summing over $\mathbf{q}$, the correlator $C^{(2)}$ takes the value

$$C^{(2)} = i\frac{Z_s e^{im(x_0-y_0)}}{8m^2L^3}\left(\frac{B}{\omega}\right)^2\Big[-(x_0-y_0)T^{11}(0,s;0,s;\hat{q})- \tag{4.58}$$

$$-\frac{i}{2}\frac{\partial}{\partial q_0}T^{11}(0,s;0,s;q)\Big|_{q=\hat{q}} - \frac{i}{2}\frac{\partial}{\partial q_0}T^{11}(0,s;0,s;q)\Big|_{q=-\hat{q}}\Big], \tag{4.59}$$

where the symmetry property of the Compton tensor, $T_{11}(0,s;0,s;\hat{q}) = T_{11}(0,s;0,s;-\hat{q})$, $\hat{q}=(0,\boldsymbol{\omega})$, was used.

Next, combining Eqs. (4.44) and (4.42), one gets the Taylor expansion of the two-point function in the magnetic field strength:

$$C = \frac{Z_s e^{im(x_0-y_0)}}{2m}\left\{1+i\xi_s(\omega)B(x_0-y_0)+i\eta_s(\omega)B^2(x_0-y_0)+\cdots\right\} \tag{4.60}$$

where only the terms that are linear in $x_0 - y_0$ are explicitly shown. The unknown coefficients $\xi_s(\omega)$ and $\eta_s(\omega)$ are determined from a comparison of the left- and right-hand sides in Eq. (4.33),

$$\xi_s(\omega) = 0, \qquad \eta_s(\omega) = -\frac{1}{4m\omega^2}T_{11}(0,s;0,s;\hat{q})\,. \tag{4.61}$$

The quantities $\alpha_s(\omega)$ and $\beta_s(\omega)$ can be found in a similar fashion. In particular, $\alpha_s(\omega) = 0$, while $\beta_s(\omega)$ is given as a certain linear combination of the tensor component $T_{11}(0,s;0,s;\hat{q})$ and its derivative. As it is

seen, the first-order correction to the energy shift vanishes, while the spin-averaged second-order term reproduces the original formula.

Outlook

Let us summarize several aspects of the work that have to be studied (*in progress*):

- The limit of a constant magnetic field ($\omega \to 0$) has to be numerically investigated. In particular, one has to see, how the energy spectrum in the periodic potential transforms into the Landau levels. In practice, it is problematic to perform the zero frequency limit on the lattice because the frequency ω takes only discrete values. Accordingly, the alternative setting on the lattice (ω is arbitrary, but B is quantized) should be considered in detail.

- The finite volume corrections to the extracted quantities have to be studied. In particular, the Compton tensor in a finite volume can be estimated in the chiral EFT. However, since the rotational symmetry is broken, there is no one-to-one correspondence between the energy shift and the subtraction function. This conceptual problem has to be better understood.

- Depending on the practical lattice implementation of the external field method, there might be the Wick contractions that lead to quark-disconnected diagrams in the Compton tensor. Since the numerical evaluation of such diagrams is expensive, it is important to estimate, how large is their contribution to the correlation function. The partially quenched χPT provides a systematic framework to study the problem.

CHAPTER 5

Summary

Hadronic electroweak processes, such as pion photo(electro)production and Compton scattering, play an indispensable role in probing the structure of the hadrons. Other types of processes, such as rare B meson decays, are important in the search for physics beyond the Standard Model.

Lattice QCD is a truly first-principle method to explore the non-perturbative aspects of the strong force. Based on the path integral formulation of QCD in the Euclidean spacetime, it enables one to determine the low-energy observables, such as the masses of the stable hadrons and the matrix elements of the gauge-invariant operators. While the temporal direction of the lattice should be large enough to suppress the excited state contamination, its spatial size is always finite.

The lattice study of the processes involving hadron resonances is a more complicated matter. Due to the final state interaction, the standard techniques for the analysis of the lattice data can not be used any more. However, the finite volume formalism provides a systematic approach to extract the scattering observables in the two-body sector from the finite-volume energy spectrum. At the same time, a proper field-theoretical definition of the resonance matrix elements is called for.

Lattice simulations with background (external) fields open a possibility to study the electromagnetic structure of the nucleon and light nuclei. The external field method is also well suited to investigate some important features of low-energy nucleon Compton scattering.

The results of the thesis can be summarized as follows:

- In Chapter 2, we considered the pion photo(electro)production process in the vicinity of the $\Delta(1232)$ resonance. We provide a theoretical framework for the lattice determination of the $\Delta N\gamma^*$ transition form factors in case of the unstable Δ. After the full group-theoretical analysis of the problem, the analogue of the Lellouch-Lüscher formula for the pion production amplitude is derived. Further, we give a field-theoretical definition of the matrix elements involving resonances. The prescription for the pole extraction of the $\Delta N\gamma^*$ form factors is provided. The limit of an infinitely narrow Δ in the obtained results is also considered.

- In Chapter 3, we investigated the rare $B \to K^* l^+ l^-$ decay mode in the kinematic region of low hadron recoil. Considering a scenario with an unstable K^*, we take into account the presence of the ηK threshold. We reproduce the two-channel analogue of the Lellouch-Lüscher formula within the non-relativistic EFT. Next, we give a procedure to determine the $B \to K^*$ form factors at the complex pole position in the coupled-channel case. It is shown that the two definitions of the form factors coincide in the limit of the infinitely narrow K^*. It becomes less trivial to arrive at such a conclusion in the multi-channel problem.

- In Chapter 4, we proposed an idea on how to determine the unknown subtraction function in the

forward doubly virtual Compton scattering on the lattice. We evaluate the energy shift of the nucleon ground state in a static periodic magnetic field. The second-order term in the obtained expression is found to be proportional to the value of the subtraction function at nonzero photon virtuality. We also discuss the limits of applicability of the result. In particular, the upper bound on the magnetic field strength and the lower bound on the value of the photon virtuality are estimated.

5.1 Outlook

At present, the finite volume formalism is fully developed in the two-body sector below three-body thresholds. The method is well suited for lattice practitioners to extract the scattering observables from lattice data. Nevertheless, its application to the baryon resonances is not an easy task, and first preliminary results on the Δ should be expected in the near future.

New questions arise in the three-body sector. In principle, the finite-volume quantization condition is derived, but its form is not suitable for the analysis of the lattice data. The main problem consists in the convenient choice of the low-energy parameters (infinite-volume obesrvables). For instance, in the two-body sector, this is the phase shift that can be determined from the Lüscher formula.

Recently, the quantization condition has been derived within the non-relativistic EFT in the particle-dimer picture [164, 165]. It has been argued that the particle-dimer couplings represent a good choice of the parameters providing a simple parametrization of the three-body scattering amplitude. The idea is that one starts with a minimal set of the low-energy constants. After imposing a certain ultraviolet cutoff, they are fitted to the finite-volume energy spectrum. Adding the higher-spin dimers, the procedure is repeated until the fit does not improve any more. Once the parameters are fixed, the infinite-volume integral equations for the scattering amplitude are solved at the same cutoff value. The feasibility of the framework has been demonstrated by the numerical calculation of the three-body spectrum in a simple model.

The apparent simplicity of the proposed approach calls for several improvements and subsequent application of the framework to the real-world problems. The following open issues have to be addressed.

- *Conceptual improvements of the particle-dimer formalism*. Having in mind the lattice study of the Roper resonance $N(1440)$, the case of non-indentical particles carrying a nonzero spin has to be considered. Further, higher partial waves have to be systematically included. Accordingly, the group-theoretical aspects of the (inevitable) partial-wave mixing should be studied. The coupling of the two- and three-body channels has to be taken into account. Given the advantage of using the moving frames, the whole framework should be accordingly modified, incorporating also relativistic kinematics.

- *Three-body analogue of the Lellouch-Lüscher formula*. The important application of the developed formalism will be the study of the hadronic electroweak processes involving three-body final state interaction. One interesting example is the omega photoproduction $\gamma p \to p\omega \to p(\pi\pi\pi)$ that might help to reveal some missing baryon resonances [189]. The main goal is to obtain a certain generalization of the Lellouch-Lüscher formula.

- *Three-neutron resonances*. The experimental evidence of such systems is still lacking [190]. At the same time, a possible resonant tetraneutron state has been recently reported [191]. The quantum Monte Carlo calculations of few-neutron systems also suggest that a three-neutron resonance should exist below the tetraneutron resonance, and its energy is potentially measurable. Clearly, this topic will a subject of the future lattice simulations. From a theoretical standpoint, one should study, how the particle-dimer formalism gets modified in the presence of the long-range interactions. In case of the nucleons, the long-range part of the potential is dominated by the one-pion exchange. The inclusion of the pions in the theory, however, will not spoil the original idea of the proposal.

Bibliography

[1] S. L. Glashow, *Partial Symmetries of Weak Interactions*, Nucl. Phys. **22** (1961) 579.

[2] F. Englert and R. Brout, *Broken Symmetry and the Mass of Gauge Vector Mesons*, Phys. Rev. Lett. **13** (1964) 321.

[3] P. W. Higgs, *Broken Symmetries and the Masses of Gauge Bosons*, Phys. Rev. Lett. **13** (1964) 508.

[4] G. S. Guralnik, C. R. Hagen and T. W. B. Kibble, *Global Conservation Laws and Massless Particles*, Phys. Rev. Lett. **13** (1964) 585.

[5] A. Salam, *Weak and Electromagnetic Interactions*, Conf. Proc. **C680519** (1968) 367.

[6] S. Weinberg, *A Model of Leptons*, Phys. Rev. Lett. **19** (1967) 1264.

[7] G. Aad et al., *Observation of a new particle in the search for the Standard Model Higgs boson with the ATLAS detector at the LHC*, Phys. Lett. **B716** (2012) 1, arXiv: 1207.7214 [hep-ex].

[8] S. Chatrchyan et al., *Observation of a new boson at a mass of 125 GeV with the CMS experiment at the LHC*, Phys. Lett. **B716** (2012) 30, arXiv: 1207.7235 [hep-ex].

[9] H. Fritzsch, M. Gell-Mann and H. Leutwyler, *Advantages of the Color Octet Gluon Picture*, Phys. Lett. **B47** (1973) 365.

[10] H. Georgi and S. L. Glashow, *Gauge theories without anomalies*, Phys. Rev. **D6** (1972) 429.

[11] R. Pohl et al., *The size of the proton*, Nature **466** (2010) 213.

[12] J. J. Krauth et al., *The proton radius puzzle*, (2017), arXiv: 1706.00696 [physics.atom-ph].

[13] M. A. Belushkin, H.-W. Hammer and U.-G. Meißner, *Dispersion analysis of the nucleon form-factors including meson continua*, Phys. Rev. **C75** (2007) 035202, arXiv: hep-ph/0608337 [hep-ph].

[14] I. T. Lorenz, H.-W. Hammer and U.-G. Meißner, *The size of the proton - closing in on the radius puzzle*, Eur. Phys. J. **A48** (2012) 151, arXiv: 1205.6628 [hep-ph].

[15] G. W. Bennett et al., *Final Report of the Muon E821 Anomalous Magnetic Moment Measurement at BNL*, Phys. Rev. **D73** (2006) 072003, arXiv: hep-ex/0602035 [hep-ex].

[16] F. Jegerlehner and A. Nyffeler, *The Muon g-2*, Phys. Rept. **477** (2009) 1, arXiv: 0902.3360 [hep-ph].

[17] R. Aaij et al., *Angular analysis of the $B^0 \to K^{*0}\mu^+\mu^-$ decay using 3 fb^{-1} of integrated luminosity*, JHEP **02** (2016) 104, arXiv: 1512.04442 [hep-ex].

[18] A. Abdesselam et al., "Angular analysis of $B^0 \to K^*(892)^0 \ell^+ \ell^-$", *Proceedings, LHCSki 2016 - A First Discussion of 13 TeV Results: Obergurgl, Austria, April 10-15, 2016*, 2016, arXiv: 1604.04042 [hep-ex], URL: https://inspirehep.net/record/1446979/files/arXiv:1604.04042.pdf.

[19] J. P. Lees et al., *Evidence for an excess of $\bar{B} \to D^{(*)}\tau^-\bar{\nu}_\tau$ decays*, Phys. Rev. Lett. **109** (2012) 101802, arXiv: 1205.5442 [hep-ex].

[20] T. Blake, G. Lanfranchi and D. M. Straub, "Rare B Decays as Tests of the Standard Model", vol. 92, 2017 50, arXiv: 1606.00916 [hep-ph].

[21] URL: http://www.quantumdiaries.org/2013/08/19/a-fresh-look-for-the-standard-model/.

[22] C.-N. Yang and R. L. Mills, *Conservation of Isotopic Spin and Isotopic Gauge Invariance*, Phys. Rev. **96** (1954) 191.

[23] D. J. Gross and F. Wilczek, *Ultraviolet Behavior of Nonabelian Gauge Theories*, Phys. Rev. Lett. **30** (1973) 1343.

[24] H. D. Politzer, *Reliable Perturbative Results for Strong Interactions?*, Phys. Rev. Lett. **30** (1973) 1346.

[25] M. Gell-Mann, *A Schematic Model of Baryons and Mesons*, Phys. Lett. **8** (1964) 214.

[26] S. L. Adler, *Axial vector vertex in spinor electrodynamics*, Phys. Rev. **177** (1969) 2426.

[27] J. S. Bell and R. Jackiw, *A PCAC puzzle: pi0 –> gamma gamma in the sigma model*, Nuovo Cim. **A60** (1969) 47.

[28] K. Fujikawa, *Path Integral Measure for Gauge Invariant Fermion Theories*, Phys. Rev. Lett. **42** (1979) 1195.

[29] J. Goldstone, A. Salam and S. Weinberg, *Broken Symmetries*, Phys. Rev. **127** (1962) 965.

[30] Y. Nambu, *Quasiparticles and Gauge Invariance in the Theory of Superconductivity*, Phys. Rev. **117** (1960) 648.

[31] G. 't Hooft and M. J. G. Veltman, *Regularization and Renormalization of Gauge Fields*, Nucl. Phys. **B44** (1972) 189.

[32] L. D. Faddeev and V. N. Popov, *Feynman Diagrams for the Yang-Mills Field*, Phys. Lett. **B25** (1967) 29.

[33] D. J. Gross and F. Wilczek, *Asymptotically Free Gauge Theories. 1*, Phys. Rev. **D8** (1973) 3633.

[34] R. P. Feynman, *Very high-energy collisions of hadrons*, Phys. Rev. Lett. **23** (1969) 1415.

[35] J. D. Bjorken and E. A. Paschos, *Inelastic Electron Proton and gamma Proton Scattering, and the Structure of the Nucleon*, Phys. Rev. **185** (1969) 1975.

[36] C. Patrignani et al., *Review of Particle Physics*, Chin. Phys. **C40**.10 (2016) 100001.

[37] E. Iancu, "QCD in heavy ion collisions", *Proceedings, 2011 European School of High-Energy Physics (ESHEP 2011): Cheile Gradistei, Romania, September 7-20, 2011*, 2014 197, arXiv: 1205.0579 [hep-ph], URL: http://inspirehep.net/record/1113441/files/arXiv:1205.0579.pdf.

[38] R. Sommer, *A New way to set the energy scale in lattice gauge theories and its applications to the static force and alpha-s in SU(2) Yang-Mills theory*, Nucl. Phys. **B411** (1994) 839, arXiv: hep-lat/9310022 [hep-lat].

[39] K. G. Wilson, *Confinement of Quarks*, Phys. Rev. **D10** (1974) 2445.

[40] M. Creutz, *Monte Carlo Study of Quantized SU(2) Gauge Theory*, Phys. Rev. **D21** (1980) 2308.

[41] S. Aoki et al., *Review of lattice results concerning low-energy particle physics*, Eur. Phys. J. **C77**.2 (2017) 112, arXiv: 1607.00299 [hep-lat].

[42] S. Necco and R. Sommer, *The N(f) = 0 heavy quark potential from short to intermediate distances*, Nucl. Phys. **B622** (2002) 328, arXiv: hep-lat/0108008 [hep-lat].

[43] K. Symanzik, *Continuum Limit and Improved Action in Lattice Theories. 1. Principles and phi**4 Theory*, Nucl. Phys. **B226** (1983) 187.

[44] K. Symanzik, *Continuum Limit and Improved Action in Lattice Theories. 2. O(N) Nonlinear Sigma Model in Perturbation Theory*, Nucl. Phys. **B226** (1983) 205.

[45] M. Lüscher and P. Weisz, *On-Shell Improved Lattice Gauge Theories*, Commun. Math. Phys. **97** (1985) 59, [Erratum: Commun. Math. Phys.98,433(1985)].

[46] H. B. Nielsen and M. Ninomiya, *Absence of Neutrinos on a Lattice. 1. Proof by Homotopy Theory*, Nucl. Phys. **B185** (1981) 20, [,533(1980)].

[47] M. Lüscher et al., *Chiral symmetry and O(a) improvement in lattice QCD*, Nucl. Phys. **B478** (1996) 365, arXiv: hep-lat/9605038 [hep-lat].

[48] B. Sheikholeslami and R. Wohlert, *Improved Continuum Limit Lattice Action for QCD with Wilson Fermions*, Nucl. Phys. **B259** (1985) 572.

[49] M. Lüscher et al., *Nonperturbative O(a) improvement of lattice QCD*, Nucl. Phys. **B491** (1997) 323, arXiv: hep-lat/9609035 [hep-lat].

[50] L. Giusti et al., *Problems on lattice gauge fixing*, Int. J. Mod. Phys. **A16** (2001) 3487, arXiv: hep-lat/0104012 [hep-lat].

[51] N. Metropolis et al., *Equation of state calculations by fast computing machines*, J. Chem. Phys. **21** (1953) 1087.

[52] S. Duane et al., *Hybrid Monte Carlo*, Phys. Lett. **B195** (1987) 216.

[53] J. Bijnens and J. Relefors, *Connected, Disconnected and Strange Quark Contributions to HVP*, JHEP **11** (2016) 086, arXiv: 1609.01573 [hep-lat].

[54] URL: http://plone.jldg.org/wiki/index.php/Main_Page.

[55] M. Lüscher, *Volume Dependence of the Energy Spectrum in Massive Quantum Field Theories. 1. Stable Particle States*, Commun. Math. Phys. **104** (1986) 177.

[56] G. Colangelo, S. Dürr and C. Haefeli, *Finite volume effects for meson masses and decay constants*, Nucl. Phys. **B721** (2005) 136, arXiv: hep-lat/0503014 [hep-lat].

[57] P. F. Bedaque, *Aharonov-Bohm effect and nucleon nucleon phase shifts on the lattice*, Phys. Lett. **B593** (2004) 82, arXiv: nucl-th/0402051 [nucl-th].

[58] C. T. Sachrajda and G. Villadoro, *Twisted boundary conditions in lattice simulations*, Phys. Lett. **B609** (2005) 73, arXiv: hep-lat/0411033 [hep-lat].

[59] S. Dürr et al., *Ab-Initio Determination of Light Hadron Masses*, Science **322** (2008) 1224, arXiv: 0906.3599 [hep-lat].

[60] S. Aoki et al., *2+1 Flavor Lattice QCD toward the Physical Point*, Phys. Rev. **D79** (2009) 034503, arXiv: 0807.1661 [hep-lat].

[61] W. Bietenholz et al., *Flavour blindness and patterns of flavour symmetry breaking in lattice simulations of up, down and strange quarks*, Phys. Rev. **D84** (2011) 054509, arXiv: 1102.5300 [hep-lat].

[62] M. Lüscher and U. Wolff, *How to Calculate the Elastic Scattering Matrix in Two-dimensional Quantum Field Theories by Numerical Simulation*, Nucl. Phys. **B339** (1990) 222.

[63] J. J. Dudek et al., *Toward the excited meson spectrum of dynamical QCD*, Phys. Rev. **D82** (2010) 034508, arXiv: 1004.4930 [hep-ph].

[64] R. G. Edwards et al., *Excited state baryon spectroscopy from lattice QCD*, Phys. Rev. **D84** (2011) 074508, arXiv: 1104.5152 [hep-ph].

[65] G. P. Engel et al., *Meson and baryon spectrum for QCD with two light dynamical quarks*, Phys. Rev. **D82** (2010) 034505, arXiv: 1005.1748 [hep-lat].

[66] URL: http://gluex.org/GlueX/Home.html.

[67] URL: https://panda.gsi.de/.

[68] A. Duncan, E. Eichten and H. Thacker, *Electromagnetic splittings and light quark masses in lattice QCD*, Phys. Rev. Lett. **76** (1996) 3894, arXiv: hep-lat/9602005 [hep-lat].

[69] S. R. Coleman and S. L. Glashow, *Electrodynamic properties of baryons in the unitary symmetry scheme*, Phys. Rev. Lett. **6** (1961) 423.

[70] S. Borsanyi et al., *Ab initio calculation of the neutron-proton mass difference*, Science **347** (2015) 1452, arXiv: 1406.4088 [hep-lat].

[71] B. B. Brandt, *The electromagnetic form factor of the pion: Results from the lattice*, Int. J. Mod. Phys. **E22** (2013) 1330030, arXiv: 1310.6389 [hep-lat].

[72] A. V. Efremov and A. V. Radyushkin, *Factorization and Asymptotical Behavior of Pion Form-Factor in QCD*, Phys. Lett. **94B** (1980) 245.

[73] J. Koponen et al., *Prediction of the meson electromagnetic form factor at high Q^2 from full lattice QCD*, (2017), arXiv: 1701.04250 [hep-lat].

[74] A. J. Chambers et al., *Electromagnetic form factors at large momenta from lattice QCD*, (2017), arXiv: 1702.01513 [hep-lat].

[75] N. H. Christ et al., *First exploratory calculation of the long-distance contributions to the rare kaon decays $K \to \pi\ell^+\ell^-$*, Phys. Rev. **D94**.11 (2016) 114516, arXiv: 1608.07585 [hep-lat].

[76] Z. Bai et al., *Exploratory lattice QCD study of the rare kaon decay K + − > π + nunu − bar*, (2017), arXiv: 1701.02858 [hep-lat].

[77] T. Blake et al., *Round table: Flavour anomalies in b → sl+l- processes*, EPJ Web Conf. **137** (2017) 01001, arXiv: 1703.10005 [hep-ph].

[78] C. Bobeth et al., *Long-distance effects in $B \to K^* \ell\ell$ from Analyticity*, (2017), arXiv: 1707.07305 [hep-ph].

[79] G. Breit and E. Wigner, *Capture of Slow Neutrons*, Phys. Rev. **49** (1936) 519.

[80] A. M. Badalian et al., *Resonances in Coupled Channels in Nuclear and Particle Physics*, Phys. Rept. **82** (1982) 31.

[81] H. A. Bethe, *Theory of the Effective Range in Nuclear Scattering*, Phys. Rev. **76** (1949) 38.

[82] I. G. Aznauryan and V. D. Burkert, *Electroexcitation of nucleon resonances*, Prog. Part. Nucl. Phys. **67** (2012) 1, arXiv: 1109.1720 [hep-ph].

[83] S. Mandelstam, *Dynamical variables in the Bethe-Salpeter formalism*, Proc. Roy. Soc. Lond. **A233** (1955) 248.

[84] E. Fermi, *An attempt of a theory of beta radiation. 1.*, Z. Phys. **88** (1934) 161.

[85] W. Heisenberg and H. Euler, *Consequences of Dirac's theory of positrons*, Z. Phys. **98** (1936) 714, arXiv: physics/0605038 [physics].

[86] T. Appelquist and J. Carazzone, *Infrared Singularities and Massive Fields*, Phys. Rev. **D11** (1975) 2856.

[87] S. Weinberg, *Phenomenological Lagrangians*, Physica **A96** (1979) 327.

[88] J. S. Schwinger, *A Theory of the Fundamental Interactions*, Annals Phys. **2** (1957) 407.

[89] M. Gell-Mann and M. Levy, *The axial vector current in beta decay*, Nuovo Cim. **16** (1960) 705.

[90] S. Weinberg, *Dynamical approach to current algebra*, Phys. Rev. Lett. **18** (1967) 188.

[91] J. S. Schwinger, *Chiral dynamics*, Phys. Lett. **B24** (1967) 473.

[92] S. Weinberg, *Nonlinear realizations of chiral symmetry*, Phys. Rev. **166** (1968) 1568.

[93] S. R. Coleman, J. Wess and B. Zumino, *Structure of phenomenological Lagrangians. 1.*, Phys. Rev. **177** (1969) 2239.

[94] C. G. Callan Jr. et al., *Structure of phenomenological Lagrangians. 2.*, Phys. Rev. **177** (1969) 2247.

[95] M. Gell-Mann, R. J. Oakes and B. Renner, *Behavior of current divergences under SU(3) x SU(3)*, Phys. Rev. **175** (1968) 2195.

[96] S. Weinberg, *Pion scattering lengths*, Phys. Rev. Lett. **17** (1966) 616.

[97] M. L. Goldberger and S. B. Treiman, *Decay of the pi meson*, Phys. Rev. **110** (1958) 1178.

[98] M. Gell-Mann, *Symmetries of baryons and mesons*, Phys. Rev. **125** (1962) 1067.

[99] URL: http://www.scholarpedia.org/article/Chiral_perturbation_theory.

[100] J. Gasser and H. Leutwyler, *Chiral Perturbation Theory to One Loop*, Annals Phys. **158** (1984) 142.

[101] J. Gasser and H. Leutwyler,
Chiral Perturbation Theory: Expansions in the Mass of the Strange Quark,
Nucl. Phys. **B250** (1985) 465.

[102] S. Borsanyi et al., *SU(2) chiral perturbation theory low-energy constants from 2+1 flavor staggered lattice simulations*, Phys. Rev. **D88** (2013) 014513, arXiv: 1205.0788 [hep-lat].

[103] G. Ecker et al., *The Role of Resonances in Chiral Perturbation Theory*,
Nucl. Phys. **B321** (1989) 311.

[104] J. Bijnens et al., *Elastic pi pi scattering to two loops*, Phys. Lett. **B374** (1996) 210,
arXiv: hep-ph/9511397 [hep-ph].

[105] J. Bijnens et al., *Pion-pion scattering at low energy*,
Nucl. Phys. **B508** (1997) 263, [Erratum: Nucl. Phys.B517,639(1998)],
arXiv: hep-ph/9707291 [hep-ph].

[106] S. M. Roy,
Exact integral equation for pion pion scattering involving only physical region partial waves,
Phys. Lett. **B36** (1971) 353.

[107] G. Colangelo, J. Gasser and H. Leutwyler, *$\pi\pi$ scattering*, Nucl. Phys. **B603** (2001) 125,
arXiv: hep-ph/0103088 [hep-ph].

[108] S. Weinberg, *Nuclear forces from chiral Lagrangians*, Phys. Lett. **B251** (1990) 288.

[109] E. Epelbaum, H.-W. Hammer and U.-G. Meißner, *Modern Theory of Nuclear Forces*,
Rev. Mod. Phys. **81** (2009) 1773, arXiv: 0811.1338 [nucl-th].

[110] C. W. Bernard and M. F. L. Golterman,
Chiral perturbation theory for the quenched approximation of QCD, Phys. Rev. **D46** (1992) 853,
arXiv: hep-lat/9204007 [hep-lat].

[111] C. W. Bernard and M. F. L. Golterman,
Partially quenched gauge theories and an application to staggered fermions,
Phys. Rev. **D49** (1994) 486, arXiv: hep-lat/9306005 [hep-lat].

[112] S. R. Sharpe and N. Shoresh, *Physical results from unphysical simulations*,
Phys. Rev. **D62** (2000) 094503, arXiv: hep-lat/0006017 [hep-lat].

[113] S. R. Sharpe and R. S. Van de Water, *Unphysical operators in partially quenched QCD*,
Phys. Rev. **D69** (2004) 054027, arXiv: hep-lat/0310012 [hep-lat].

[114] C. Bernard and M. Golterman,
On the foundations of partially quenched chiral perturbation theory,
Phys. Rev. **D88**.1 (2013) 014004, arXiv: 1304.1948 [hep-lat].

[115] M. Della Morte and A. Juttner, *Quark disconnected diagrams in chiral perturbation theory*,
JHEP **11** (2010) 154, arXiv: 1009.3783 [hep-lat].

[116] T. Blum et al., *Calculation of the hadronic vacuum polarization disconnected contribution to the muon anomalous magnetic moment*, Phys. Rev. Lett. **116**.23 (2016) 232002,
arXiv: 1512.09054 [hep-lat].

[117] N. R. Acharya et al., *Connected and Disconnected Contractions in Pion-Pion Scattering*, (2017),
arXiv: 1704.06754 [hep-lat].

[118] L. Liu et al., *Isospin-0 $\pi\pi$ s-wave scattering length from twisted mass lattice QCD*, (2016),
arXiv: 1612.02061 [hep-lat].

[119] W. E. Caswell and G. P. Lepage,
Effective Lagrangians for Bound State Problems in QED, QCD, and Other Field Theories,
Phys. Lett. **167B** (1986) 437.

[120] E. E. Salpeter and H. A. Bethe, *A Relativistic equation for bound state problems*,
Phys. Rev. **84** (1951) 1232.

[121] J. S. Schwinger, *On the Green's functions of quantized fields. 1.*,
Proc. Nat. Acad. Sci. **37** (1951) 452.

[122] R. J. Hill and G. Paz,
Model independent analysis of proton structure for hydrogenic bound states,
Phys. Rev. Lett. **107** (2011) 160402, arXiv: 1103.4617 [hep-ph].

[123] J. Gasser, V. E. Lyubovitskij and A. Rusetsky, *Hadronic atoms in QCD + QED*,
Phys. Rept. **456** (2008) 167, arXiv: 0711.3522 [hep-ph].

[124] G. Colangelo et al., *Cusps in K —> 3 pi decays*, Phys. Lett. **B638** (2006) 187,
arXiv: hep-ph/0604084 [hep-ph].

[125] J. Gasser, B. Kubis and A. Rusetsky, *Cusps in K –> 3pi decays: a theoretical framework*,
Nucl. Phys. **B850** (2011) 96, arXiv: 1103.4273 [hep-ph].

[126] M. Beneke and V. A. Smirnov, *Asymptotic expansion of Feynman integrals near threshold*,
Nucl. Phys. **B522** (1998) 321, arXiv: hep-ph/9711391 [hep-ph].

[127] B. A. Lippmann and J. Schwinger, *Variational Principles for Scattering Processes. I*,
Phys. Rev. **79** (1950) 469.

[128] K. Osterwalder and R. Schrader, *Axioms for Euclidean Green's Functions*,
Commun. Math. Phys. **31** (1973) 83.

[129] K. Osterwalder and R. Schrader, *Axioms for Euclidean Green's Functions. 2.*,
Commun. Math. Phys. **42** (1975) 281.

[130] K. M. Watson, *The Effect of final state interactions on reaction cross-sections*,
Phys. Rev. **88** (1952) 1163.

[131] L. Maiani and M. Testa, *Final state interactions from Euclidean correlation functions*,
Phys. Lett. **B245** (1990) 585.

[132] K. Huang and C. N. Yang,
Quantum-mechanical many-body problem with hard-sphere interaction,
Phys. Rev. **105** (1957) 767.

[133] M. Lüscher, *Volume Dependence of the Energy Spectrum in Massive Quantum Field Theories. 2. Scattering States*, Commun. Math. Phys. **105** (1986) 153.

[134] M. Lüscher, *Two particle states on a torus and their relation to the scattering matrix*,
Nucl. Phys. **B354** (1991) 531.

[135] F.-K. Guo et al., *Hadronic molecules*, (2017), arXiv: 1705.00141 [hep-ph].

[136] D. Griffiths, *Introduction to Quantum Mechanics*, 2nd ed., Pearson Prentice Hall, 2005.

[137] V. Bernard et al., *Matrix elements of unstable states*, JHEP **09** (2012) 023,
arXiv: 1205.4642 [hep-lat].

[138] C. h. Kim, C. T. Sachrajda and S. R. Sharpe,
Finite-volume effects for two-hadron states in moving frames, Nucl. Phys. **B727** (2005) 218, arXiv: hep-lat/0507006 [hep-lat].

[139] M. Göckeler et al.,
Scattering phases for meson and baryon resonances on general moving-frame lattices, Phys. Rev. **D86** (2012) 094513, arXiv: 1206.4141 [hep-lat].

[140] T. Yamazaki et al., *Helium nuclei, deuteron and dineutron in 2+1 flavor lattice QCD*, Phys. Rev. **D86** (2012) 074514, arXiv: 1207.4277 [hep-lat].

[141] S. R. Beane et al., *Evidence for a Bound H-dibaryon from Lattice QCD*, Phys. Rev. Lett. **106** (2011) 162001, arXiv: 1012.3812 [hep-lat].

[142] T. Inoue et al., *Bound H-dibaryon in Flavor SU(3) Limit of Lattice QCD*, Phys. Rev. Lett. **106** (2011) 162002, arXiv: 1012.5928 [hep-lat].

[143] S. R. Beane et al., *The Deuteron and Exotic Two-Body Bound States from Lattice QCD*, Phys. Rev. **D85** (2012) 054511, arXiv: 1109.2889 [hep-lat].

[144] M. Lüscher, *Signatures of unstable particles in finite volume*, Nucl. Phys. **B364** (1991) 237.

[145] K. Rummukainen and S. A. Gottlieb,
Resonance scattering phase shifts on a nonrest frame lattice, Nucl. Phys. **B450** (1995) 397, arXiv: hep-lat/9503028 [hep-lat].

[146] D. J. Wilson et al., *Coupled $\pi\pi$, $K\bar{K}$ scattering in P-wave and the ρ resonance from lattice QCD*, Phys. Rev. **D92**.9 (2015) 094502, arXiv: 1507.02599 [hep-ph].

[147] Z. Fu and L. Wang, *Studying the ρ resonance parameters with staggered fermions*, Phys. Rev. **D94**.3 (2016) 034505, arXiv: 1608.07478 [hep-lat].

[148] C. Alexandrou et al., *P-wave $\pi\pi$ scattering and the ρ resonance from lattice QCD*, (2017), arXiv: 1704.05439 [hep-lat].

[149] G. S. Bali et al., *ρ and K^* resonances on the lattice at nearly physical quark masses and $N_f = 2$*, Phys. Rev. **D93**.5 (2016) 054509, arXiv: 1512.08678 [hep-lat].

[150] J. J. Dudek, R. G. Edwards and C. E. Thomas,
Energy dependence of the ρ resonance in $\pi\pi$ elastic scattering from lattice QCD, Phys. Rev. **D87**.3 (2013) 034505, [Erratum: Phys. Rev.D90,no.9,099902(2014)], arXiv: 1212.0830 [hep-ph].

[151] R. A. Briceno, *Two-particle multichannel systems in a finite volume with arbitrary spin*, Phys. Rev. **D89**.7 (2014) 074507, arXiv: 1401.3312 [hep-lat].

[152] C. Urbach, *CRC110 Workshop on Nuclear Dynamics and Threshold Phenomena: Bochum, Germany, April 5-7, 2017*, URL: http://www.tp2.rub.de/forschung/vortraege-und-workshops/ndtp2017/rest_html/program/download/2017-04-05-02-Urbach.pdf.

[153] S. R. Beane et al.,
Nucleon-Nucleon Scattering Parameters in the Limit of SU(3) Flavor Symmetry, Phys. Rev. **C88**.2 (2013) 024003, arXiv: 1301.5790 [hep-lat].

[154] S. R. Beane et al., *Hyperon-Nucleon Interactions and the Composition of Dense Nuclear Matter from Quantum Chromodynamics*, Phys. Rev. Lett. **109** (2012) 172001, arXiv: 1204.3606 [hep-lat].

[155] C. B. Lang et al., *Pion-nucleon scattering in the Roper channel from lattice QCD*, Phys. Rev. **D95**.1 (2017) 014510, arXiv: 1610.01422 [hep-lat].

[156] H.-W. Hammer, A. Nogga and A. Schwenk, *Three-body forces: From cold atoms to nuclei*, Rev. Mod. Phys. **85** (2013) 197, arXiv: 1210.4273 [nucl-th].

[157] E. Braaten and H.-W. Hammer, *Universality in few-body systems with large scattering length*, Phys. Rept. **428** (2006) 259, arXiv: cond-mat/0410417 [cond-mat].

[158] V. Efimov, *Energy levels arising form the resonant two-body forces in a three-body system*, Phys. Lett. **33B** (1970) 563.

[159] U.-G. Meißner, G. Ríos and A. Rusetsky, *Spectrum of three-body bound states in a finite volume*, Phys. Rev. Lett. **114**.9 (2015) 091602, [Erratum: Phys. Rev. Lett.117,no.6,069902(2016)], arXiv: 1412.4969 [hep-lat].

[160] M. T. Hansen and S. R. Sharpe, *Applying the relativistic quantization condition to a three-particle bound state in a periodic box*, Phys. Rev. **D95**.3 (2017) 034501, arXiv: 1609.04317 [hep-lat].

[161] K. Polejaeva and A. Rusetsky, *Three particles in a finite volume*, Eur. Phys. J. **A48** (2012) 67, arXiv: 1203.1241 [hep-lat].

[162] R. A. Briceno and Z. Davoudi, *Three-particle scattering amplitudes from a finite volume formalism*, Phys. Rev. **D87**.9 (2013) 094507, arXiv: 1212.3398 [hep-lat].

[163] R. A. Briceño, M. T. Hansen and S. R. Sharpe, *Relating the finite-volume spectrum and the two-and-three-particle S matrix for relativistic systems of identical scalar particles*, Phys. Rev. **D95**.7 (2017) 074510, arXiv: 1701.07465 [hep-lat].

[164] H.-W. Hammer, J.-Y. Pang and A. Rusetsky, *Three-particle quantization condition in a finite volume: 1. The role of the three-particle force*, (2017), arXiv: 1706.07700 [hep-lat].

[165] H.-W. Hammer, J.-Y. Pang and A. Rusetsky, *Three particle quantization condition in a finite volume: 2. general formalism and the analysis of data*, (2017), arXiv: 1707.02176 [hep-lat].

[166] H. Lehmann, K. Symanzik and W. Zimmermann, *On the formulation of quantized field theories*, Nuovo Cim. **1** (1955) 205.

[167] C. J. D. Lin et al., *K –> pi pi decays in a finite volume*, Nucl. Phys. **B619** (2001) 467, arXiv: hep-lat/0104006 [hep-lat].

[168] L. Lellouch and M. Lüscher, *Weak transition matrix elements from finite volume correlation functions*, Commun. Math. Phys. **219** (2001) 31, arXiv: hep-lat/0003023 [hep-lat].

[169] M. T. Hansen and S. R. Sharpe, *Multiple-channel generalization of Lellouch-Luscher formula*, Phys. Rev. **D86** (2012) 016007, arXiv: 1204.0826 [hep-lat].

[170] R. A. Briceno and Z. Davoudi, *Moving multichannel systems in a finite volume with application to proton-proton fusion*, Phys. Rev. **D88**.9 (2013) 094507, arXiv: 1204.1110 [hep-lat].

[171] R. A. Briceno, M. T. Hansen and A. Walker-Loud, *Multichannel $1 \to 2$ transition amplitudes in a finite volume*, Phys. Rev. **D91**.3 (2015) 034501, arXiv: 1406.5965 [hep-lat].

[172] R. A. Briceno and M. T. Hansen, *Multichannel $0 \to 2$ and $1 \to 2$ transition amplitudes for arbitrary spin particles in a finite volume*, Phys. Rev. **D92**.7 (2015) 074509, arXiv: 1502.04314 [hep-lat].

[173] Z. Bai et al., *Standard Model Prediction for Direct CP Violation in $K \to \pi\pi$ Decay*, Phys. Rev. Lett. **115**.21 (2015) 212001, arXiv: 1505.07863 [hep-lat].

[174] R. A. Briceno et al., *The $\pi\pi \to \pi\gamma^\star$ amplitude and the resonant $\rho \to \pi\gamma^\star$ transition from lattice QCD*, Phys. Rev. **D93**.11 (2016) 114508, arXiv: 1604.03530 [hep-ph].

[175] F. Hagelstein, R. Miskimen and V. Pascalutsa, *Nucleon Polarizabilities: from Compton Scattering to Hydrogen Atom*, Prog. Part. Nucl. Phys. **88** (2016) 29, arXiv: 1512.03765 [nucl-th].

[176] W. Detmold, B. C. Tiburzi and A. Walker-Loud, *Electromagnetic and spin polarisabilities in lattice QCD*, Phys. Rev. **D73** (2006) 114505, arXiv: hep-lat/0603026 [hep-lat].

[177] C. W. Bernard et al., *Lattice QCD Calculation of Some Baryon Magnetic Moments*, Phys. Rev. Lett. **49** (1982) 1076.

[178] H. R. Fiebig, W. Wilcox and R. M. Woloshyn, *A Study of Hadron Electric Polarizability in Quenched Lattice QCD*, Nucl. Phys. **B324** (1989) 47.

[179] E. Chang et al., *Magnetic structure of light nuclei from lattice QCD*, Phys. Rev. **D92**.11 (2015) 114502, arXiv: 1506.05518 [hep-lat].

[180] G. 't Hooft, *A Property of Electric and Magnetic Flux in Nonabelian Gauge Theories*, Nucl. Phys. **B153** (1979) 141.

[181] K. Pachucki, *Proton structure effects in muonic hydrogen*, Phys. Rev. **A60** (1999) 3593.

[182] W. N. Cottingham, *The neutron proton mass difference and electron scattering experiments*, Annals Phys. **25** (1963) 424.

[183] R. Tarrach, *Invariant Amplitudes for Virtual Compton Scattering Off Polarized Nucleons Free from Kinematical Singularities, Zeros and Constraints*, Nuovo Cim. **A28** (1975) 409.

[184] J. Gasser et al., *Cottingham formula and nucleon polarisabilities*, Eur. Phys. J. **C75**.8 (2015) 375, arXiv: 1506.06747 [hep-ph].

[185] A. Walker-Loud, C. E. Carlson and G. A. Miller, *The Electromagnetic Self-Energy Contribution to $M_p - M_n$ and the Isovector Nucleon Magnetic Polarizability*, Phys. Rev. Lett. **108** (2012) 232301, arXiv: 1203.0254 [nucl-th].

[186] F. B. Erben et al., *Dispersive estimate of the electromagnetic charge symmetry violation in the octet baryon masses*, Phys. Rev. **C90**.6 (2014) 065205, arXiv: 1408.6628 [nucl-th].

[187] S. J. Brodsky, F. J. Llanes-Estrada and A. P. Szczepaniak, *Local Two-Photon Couplings and the J=0 Fixed Pole in Real and Virtual Compton Scattering*, Phys. Rev. **D79** (2009) 033012, arXiv: 0812.0395 [hep-ph].

[188] S. Weinberg, *Feynman Rules for Any Spin*, Phys. Rev. **133** (1964) B1318.

[189] I. Denisenko et al., *N^* decays to $N\omega$ from new data on $\gamma p \to \omega p$*, Phys. Lett. **B755** (2016) 97, arXiv: 1601.06092 [nucl-ex].

[190] P. Truöl and J. P. Miller, *Comment on arXiv:1612.01502 'Is the Trineutron Resonance Lower in Energy than a Tetraneutron Resonance ?'*, (2017), arXiv: 1708.04459 [nucl-ex].

[191] K. Kisamori et al.,
Candidate Resonant Tetraneutron State Populated by the He4(He8,Be8) Reaction,
Phys. Rev. Lett. **116**.5 (2016) 052501.